IAEA-TECDOC-1225

Use of irradiation for chemical and microbial decontamination of water, wastewater and sludge

Final report of a co-ordinated research project
1995–1999

INTERNATIONAL ATOMIC ENERGY AGENCY

June 2001

The originating Section of this publication in the IAEA was:

Industrial Applications and Chemistry Section
International Atomic Energy Agency
Wagramer Strasse 5
P.O. Box 100
A-1400 Vienna, Austria

USE OF IRRADIATION FOR CHEMICAL AND MICROBIAL DECONTAMINATION OF WATER, WASTEWATER AND SLUDGE
IAEA, VIENNA, 2001
IAEA-TECDOC-1225
ISSN 1011–4289

Printed by the IAEA in Austria
June 2001

FOREWORD

Water resources have been and continue to be contaminated with biologically resistant pollutants from industrial, municipal and agricultural discharges.

Studies in recent years have demonstrated the effectiveness of ionizing radiation, alone or in combination with other agents such as ozone and heat, in the decomposition of refractory organic compounds in aqueous solutions and in the removal or inactivation of the pathogenic microorganisms and protozoan parasites.

The International Atomic Energy Agency (IAEA) has been active in recent years in drawing attention to the considerable potential of radiation technology for the cleanup of waste discharges from various industrial and municipal activities. The two international symposia on the use of radiation in the conservation of the environment organized by the IAEA in March 1992 in Karlsruhe, Germany, and in September 1997 in Zakopane, Poland, respectively, demonstrated the unique potential of radiation processing for the decontamination of water, wastewater and sludge. Following the recommendation of the Advisory Group Meeting on New Trends and Developments in Radiation Technology convened by the IAEA in Jerusalem in 1994, a co-ordinated research project (CRP) was initiated in 1995 to fill important knowledge gaps in this area.

This publication describes the findings of the CRP in three subject areas: groundwater remediation, decontamination of industrial and municipal wastewater and sewage sludge hygienization. It is hoped that this publication will serve as a useful reference for all those interested in using radiation for the treatment of aqueous effluents.

The IAEA wishes to thank the participants in the CRP for their valuable contributions. The IAEA officer responsible for the CRP and this publication was O. Güven of the Division of Physical and Chemical Sciences.

EDITORIAL NOTE

CONTENTS

SUMMARY 1

Advanced oxidation for groundwater remediation and for soil decontamination 5
P. Gehringer, H. Eschweiler

The application of the electron beam process in water and wastewater treatment: Fundamental and applied studies 25
W.J. Cooper, T. Tobien

Electron beam technology for purification of municipal wastewater in the aerosol flow 45
A.K. Pikaev, E.A. Podzorova, O.M. Bakhtin, S.L. Lysenko, V.A. Belyshev

Application of electron beam to industrial wastewater treatment 57
B. Han, D.K. Kim, J.Y. Boo, J.K. Kim, Y. Kim, W. Chung, J.S. Choi, H.J. Kang, A.K. Pikaev

Electron beam wastewater treatment in Brazil 65
M.H.O. Sampa, P.R. Rela, C.L. Duarte, S.I. Borrely, H. Oikawa, E.S.R. Somessari, C.G. Silveira, F.E. Costa

Gamma radiation treatment of pentachlorophenol, 2,4-dichlorophenol and 2-chlorophenol in water 87
Yongke He, Jun Liu, Jilan Wu

The destructive degradation of some organic textile dye compounds using gamma ray irradiation 97
Abdel-Gawad A.S. Emara, A.A. Abdel-Fattah, S.E. Ebraheem, Z.I. Ali, H. Gad

Effect of radiation on wastewater from textile industries in Ghana 121
S.A. Dogbe, G. Emi-Reynolds, G.K. Banini

Radiation-induced degradation of organic pollutants in wastewater 133
A.N.M. Bagyo, W.A. Lindu, S. Sadjirun, E.K. Winarno, E. Widayat, Aryanti, H. Winarno

Radiation hygienization of raw sewage sludge 147
M.R. Shah, D.S. Lavale, K.P. Rawat, P.G. Benny, A.K. Sharma, G.R. Dey, V. Bhave

Radiation technology for sewage sludge treatment: The Argentine project 163
J.G. Graiño

List of Participants 179

SUMMARY

Introduction

Environmental application of radiation processing has an advantage over other emerging processes in that a good understanding of the underlying chemistry is found in the radiation chemistry literature. In addition, industrially rugged electron beam accelerators, which are used for radiation processing of polymers, sterilization and many other applications, are available. The process is flexible because it is relatively pH insensitive, solutions to be processed may contain solids and could in fact be heterogeneous and the material throughput may be very high.

The fundamental chemistry of irradiation of water is well understood. It is this understanding that allows for the potential implementation of radiation processing to solve existing and emerging problems related to environmental pollution. In particular, application of radiation processing in water based systems has a solid foundation. The uniqueness of radiation processing results from the formation of three reactive species in irradiated solutions: oxidizing hydroxyl radical and the reducing radicals, hydrated electron and hydrogen atom, e^{-}_{aq} and H. Another unique feature is that the presence of solids does not comprise the process, thus allowing the potential application of radiation processing to sewage sludges and suspended sediments and soils. It can also be easily engineered as a unit process in a treatment system because reactions resulting in the destruction of pollutants are rapid. Another advantage of radiation processing is its capability to kill bacteria and inactivate viruses at the same time it is destroying pollutants.

The CRP on “Irradiation treatment of water, wastewater and sludge” was established in order to focus the attention of appropriate technical experts in integrating the effects of ionizing radiation on refractory organic pollutants and pathogenic microorganisms and parasites in the treatment of water, wastewater and sewage sludge. It involved research institutes from 11 countries (Argentina, Austria, Brazil, China, Egypt, Ghana, India, Indonesia, the Republic of Korea, the Russian Federation and the USA).

The objectives of the CRP were:

- to establish optimal combination treatments utilizing ionizing radiation and other agents such as oxygen, ozone, heat, etc. for decontamination of polluted water from ground and surface reservoirs and of wastewaters and sewage sludges;
- to establish the effects of dose rate on the decontamination efficiency;
- to establish technological and economic parameters.

Groundwater remediation

To better understand the application of electron beam processing to water, the group at the University of North Carolina at Wilmington conducted fundamental studies on radiation degradation of several halogenated methanes, thioanissole and methyl tert-butyl ether, a common contaminant arising from gasoline releases in the USA. The kinetic rate constants determined are used to build kinetic models to describe the destruction of target organic compounds in aqueous solutions. The work of the group at the Austrian Research Centre Seibersdorf aimed at purifying groundwater contaminated with perchloroethylene (PCE), trichloroethylene (TCE) and some genotoxic compounds. The combination of ozone and electron beam irradiation was able to mineralize trace amounts of chloroethylene in groundwater in a single stage process without formation of any by-product to be disposed of. Experiments performed with real groundwater demonstrated that the combined ozone/electron beam (EB) irradiation process is also apt to total removal of some genotoxic compounds detected in groundwater contaminated with PCE and TCE. Additional experiments further confirmed that application of UV-irradiation for disinfection of such contaminated water is not possible. Large-scale studies were conducted both in Austria and the USA to examine the practicality of using EB and ozone/EB process under different conditions, and cost figures were developed for these applications. Optimal combination treatments utilizing ionizing radiation and ozone to decontaminate polluted groundwaters in Austria were established.

Decontamination of industrial and municipal wastewater

The research groups from Brazil, China, Egypt, Ghana, Indonesia, the Republic of Korea and the Russian Federation tackled the radiation contamination of wastewaters of industrial and municipal origin. Studies involved experimental and pilot scale applications for degrading organic pollutants in municipal and industrial liquid waters as well as decolourizing of textile industry wastewaters. Two pilot plants constructed and operated in the Russian Federation and the Republic of Korea showed the technical, environmental and economic advantages of using electron accelerator to decontaminate municipal and industrial wastewaters, respectively. A pilot plant with 0.3 MeV energy and 15 kW beam power was used in the Russian Federation for the purification of real municipal wastewater at an output of 500 m^3/day. Cheaper low energy accelerator was benefited by spraying water in aerosol flow and in the presence of dissolved ozone. Another EB pilot facility constructed by Samsung Heavy Industries treated the effluents of a textile dyeing complex before the biological treatment stage. Introduction of EB treatment resulted in decolourizing and destructive oxidation of organic impurities in wastewater, subsequently giving rise to a significant reduction of chemical reagent consumption, reduction in treatment time and increase in flow rate limits of existing facility by 30–40%. A large scale demonstration plant is under construction based on the results of pilot scale application.

The scientists from Egypt, Ghana and Indonesia reported on the radiation induced destruction of deeply coloured reactive and direct dyes currently used by the textile industries in their respective countries. They have examined the potential of gamma irradiation in combination with conventional methods and with the addition of reagents, such as hydrogen peroxide, TiO_2 and ferrous ammonium sulfate on the decontamination of actual and synthesized wastewaters. A comparative study was undertaken in Egypt to evaluate the removal efficiency of three dye species by gamma irradiation and sorption. The same group also assessed exotoxicity of the dyes and their radiolysis products, using invertebrate animals. Optical absorbency and chemical oxygen demand measurements carried out by the researchers in Ghana and Indonesia showed achievement of significant reduction in these values upon irradiation to doses as low as 5–10 kGy. The group from China undertook a study to investigate the dechlorination of various chlorophenols in water. The enhancement of degradation of these organochlorides was observed when gamma irradiation was done in the presence of ozone.

The group at the Nuclear Energy Research Institute in Brazil reported on the results of experiments performed at laboratory and pilot scale to study the efficiency of using EB to remove and degrade toxic and refractory pollutants from chemical and pharmaceutical industry effluents. Scientific, technical and economic data were collected for upscaling of existing treatment facility.

Sewage sludge hygienization

The reports from Argentina and India revealed the important role that radiation processing can play in hygienization of raw sewage sludge. The technical aspects of construction of a sludge irradiation plant in Argentina were elaborated, as well as the results of preliminary field applications of irradiated sludge. A sludge hygienization research irradiator facility treating 1 m^3/min of raw sludge was constructed and put into operation in India. From the analysis of samples regularly taken from recirculation line it was found that a dose of about 2 kGy is sufficient for hygienizing the raw sewage sludge. This level of irradiation gave rise to significant reductions in total coliform, total bacteria and total salmonella shigella. The reduction was even more in aeration-irradiation than that in radiation treatment without aeration. Aeration also seemed to reduce bad odour from the sludge.

Conclusion

The CRP has generated new information that will enhance the application of radiation for decontamination of water, wastewater and sludge. It has also demonstrated the growing importance and capability of radiation as a means of removing both natural and synthetic contaminants from municipal and industrial liquid effluents. The increasing interest in using ionizing radiation for environmental clean-up is, in great part, due to very promising results recently achieved by researchers worldwide involving EB techniques. The results of the CRP also demonstrate that there is significant progress in understanding radiation degradation of refractory pollutants and in developing new approaches to combine conventional treatment techniques with radiation processing.

ADVANCED OXIDATION FOR GROUNDWATER REMEDIATION AND FOR SOIL DECONTAMINATION

P. Gehringer, H. Eschweiler
Austrian Research Center Seibersdorf,
Seibersdorf, Austria

Abstract. The advanced oxidation process (AOP) used in this paper is based on EB irradiation of water in the presence and absence of ozone. The paper describes two distinct sets of experiments, one dealing with groundwater contaminated with perchloroethylene (PCE) and some genotoxic compounds, and the other dealing with soil contaminated with polycyclic aromatic hydrocarbons (PAHs). The combination of ozone and EB irradiation has shown to be able to mineralize trace amounts of PCE contained in groundwater in a single stage process without formation of any by-product to be disposed of. Moreover, experiments performed with real groundwater have demonstrated that the combined ozone/EB irradiation process is also apt for total removal of some genotoxic compounds detected in groundwater contaminated with PCE. The design of an ozone/EB irradiation plant for treating 108 m^3/h is presented. The issue concerning both the occurrences of genotoxic compounds in oxygen containing groundwater and possible processes for their removal is discussed. In the second part soil contaminated with PAHs has been treated in aqueous suspension using ozone and EB irradiation, respectively. Experiments were performed with low contaminated soil (total PAHs about 332 mg/kg soil). With an ozone consumption of 10 g O_3/kg soil a total PAH decomposition of about 21% was recorded. EB irradiation with a reasonable radiation dose of 100 kGy results in about 7% total PAH decomposition at room temperature and about 16%, respectively at 55 – 60°C. It was recorded that almost no transfer of the PAH takes place from the soil into the water when soil is merely suspended in water. Ozone mainly attacked the high molecular fraction (i.e. consisting of 5 or 6 aromatic rings) of the PAHs investigated while EB irradiation of the aqueous soil suspension mostly decomposed the lower fraction (i.e. consisting up to 4 aromatic rings).

SECTION A: OZONE/ELECTRON BEAM IRRADIATION FOR CONTROL OF PERCHLOROETHYLENE AND SOME GENOTOXIC COMPOUNDS IN GROUNDWATER

1. INTRODUCTION

Hydroxy free radicals are the strongest oxidants known to occur in water. Processes which generate hydroxy free radicals for the subsequent use of pollutant decomposition are generally referred to as “Advanced Oxidation Processes” (AOPs).

It has been found that the addition of ozone in combination with UV radiation or hydrogen peroxide can promote the decomposition of ozone and generate hydroxy free radicals. Combining hydrogen peroxide and UV radiation alone will achieve similar results as the aforementioned ozone based processes by generating hydroxy free radicals but with a considerably lesser yield [1]. What all these AOPs have in common is that the hydroxy free radicals originate from one single source only (ozone or hydrogen peroxide, respectively), i.e. the hydroxy free radical concentration obtained is comparatively low. On the other hand, groundwater very often is contaminated by rather small amounts of highly toxic compounds. To be effective in the treatment of groundwater containing trace amounts of pollutants high hydroxy free radical concentration is necessary. Combination of ozone with EB irradiation — which represents ionizing radiation — is able to produce much higher hydroxy free radical concentrations than the AOPs mentioned before because in this combination the hydroxy free radicals originate from two different but simultaneously working sources: (1) directly from the water to be purified by the action of the EB irradiation (so-called water radiolysis), and (2) from ozone decomposition accelerated by the reducing species formed during water radiolysis [2].

Table I shows the most important steps of all ozone based AOPs including also the combination of ozone and hydrogen peroxide. It clearly illustrates that O_3/UV and O_3/H_2O_2 processes are one and the same regarding hydroxy free radical generation: in the former, one is merely forming hydrogen peroxide in situ, rather than adding it from the outside. From this table it comes out clearly that two completely different mechanisms for OH free radical generation occur. UV radiation is absorbed by ozone (and, if present, by other organics absorbing UV at 254 nm) while the energy of the fast electrons is totally absorbed by water and not by any solute. In other words, under the conditions given, UV irradiation represents the direct effect of radiation while EB irradiation stands for the indirect effect of radiation.

TABLE I. OZONE BASED AOPs WITH REGARD TO THEIR MOST ESSENTIAL REACTIONS FOR HYDROXY FREE RADICAL FORMATION IN WATER

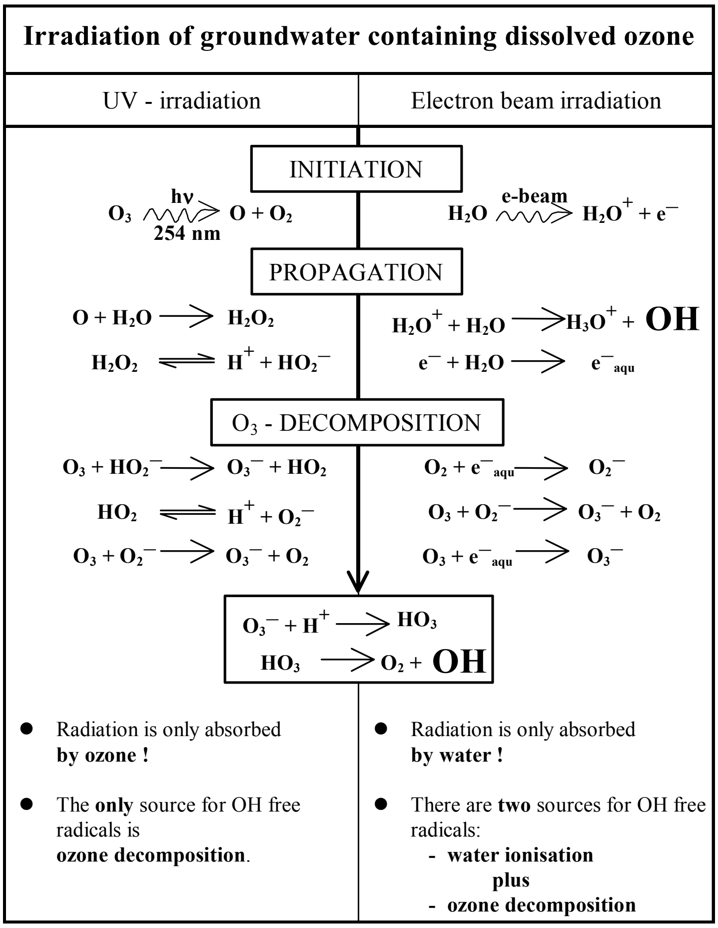

Irradiation of groundwater containing dissolved ozone

UV - irradiation	Electron beam irradiation
INITIATION	
$O_3 \xrightarrow[254\ nm]{h\nu} O + O_2$	$H_2O \xrightarrow{e\text{-beam}} H_2O^+ + e^-$
PROPAGATION	
$O + H_2O \rightarrow H_2O_2$ $H_2O_2 \rightleftharpoons H^+ + HO_2^-$	$H_2O^+ + H_2O \rightarrow H_3O^+ + OH$ $e^- + H_2O \rightarrow e^-_{aqu}$
O_3 - DECOMPOSITION	
$O_3 + HO_2^- \rightarrow O_3^- + HO_2$ $HO_2 \rightleftharpoons H^+ + O_2^-$ $O_3 + O_2^- \rightarrow O_3^- + O_2$	$O_2 + e^-_{aqu} \rightarrow O_2^-$ $O_3 + O_2^- \rightarrow O_3^- + O_2$ $O_3 + e^-_{aqu} \rightarrow O_3^-$
$O_3^- + H^+ \rightarrow HO_3$ $HO_3 \rightarrow O_2 + OH$	
● Radiation is only absorbed **by ozone !** ● The **only** source for OH free radicals is **ozone decomposition**.	● Radiation is only absorbed **by water !** ● There are **two** sources for OH free radicals: - **water ionisation** **plus** - **ozone decomposition**

The latter produces hydroxy free radicals directly from water and simultaneously the promoters for ozone decomposition (by formation of the solvated electrons e^-_{aqu}) while the former only produces the promoter for ozone decomposition (by formation of hydrogen peroxide and its deprotonated anion, respectively). Accordingly EB irradiation must be more efficient regarding hydroxy free radical generation than any other ozone based process. Since UV irradiation of hydrogen peroxide is less effective than ozone/UV [1] it is obvious that ozone/EB irradiation is the most attractive AOP for groundwater remediation.

The present paper describes the design of the plant to be constructed and reports about pilot scale experiments performed to check the finished water regarding eventual formation of genotoxic compounds. Moreover, the mechanism in which the OH free radicals are generated in the ozone/EB process is discussed and compared with the OH generation in other ozone based AOPs.

2. EXPERIMENTAL

The polluted groundwater was transported from Bad Fischau-Brunn to Seibersdorf and treated in the existing 3 m^3/h pilot plant for continuous ozone/EB irradiation treatment of water. This facility has been already described elsewhere [6]. The groundwater to be treated contained 251 mg/L bicarbonate, 8 mg/L chloride, 15 mg/L nitrate and < 0.4 mg/L DOC and was polluted with about 61 µg/L PCE. Some preliminary experiments with synthetic Bad Fischau-Brunn groundwater (prepared from Seibersdorf tap water by dilution and subsequent adjustment to the corresponding solute content of the Bad Fischau-Brunn groundwater) have been performed, too, using the same facility.

PCE was measured by gas chromatography using cold on-column injection and electron capture detection.

To test water regarding genotoxicity a combination of three bioassays based on bacteria, plants and mammalian cells has been used. This combination represents a system with different genetic endpoints and the assays selected are complementary to one another with regard to various environmental genotoxins. As bacterial assay the Salmonella/microsome in vitro test (AMES test) with the strains TA 98, TA 100 and TA 102, with and without metabolic activation was used. As plant assay the Tradescantia clone 4430 in vivo was selected measuring the induction of micronuclei in the early pollen tetrads; in the in vitro test with mammalian cells the induction of micronuclei in cultures of primary rat hepatocytes has been determined. This combination of the three bioassays has been already used earlier to search for possible genotoxic effects in the aquifer of the "Mitterndorfer Senke". For more details see Ref. [3].

3. RESULTS AND DISCUSSION

Due to the results given in Fig. 1 a radiation dose of 200 Gy was found to be sufficient to reduce the PCE content in the water from about 61 µg/L to about 1 µg/L provided the ozone concentration in water before irradiation is ≥ 6 mg/L.

The unit of the radiation dose 1 Gray (Gy) is equivalent to an absorbed energy of 1 Joule/kg. Accordingly a radiation dose of 200 Gy means a very small energy transfer into the water. Would this energy of 200 J/L be converted totally into heat, which does not take place, the temperature of the water would increase by about 0.05°C only.

According to these dose and ozone requirements a 9 kW EB accelerator and 650 g O_3/h are necessary in theory to purify 108 m^3/h of the polluted groundwater. In reality a 20 kW accelerator and a 1 kg/h ozone generator have been chosen for the treatment process.

Figure 2 shows the block diagram of the planned 108 m^3/h water treatment plant in Bad Fischau-Brunn.

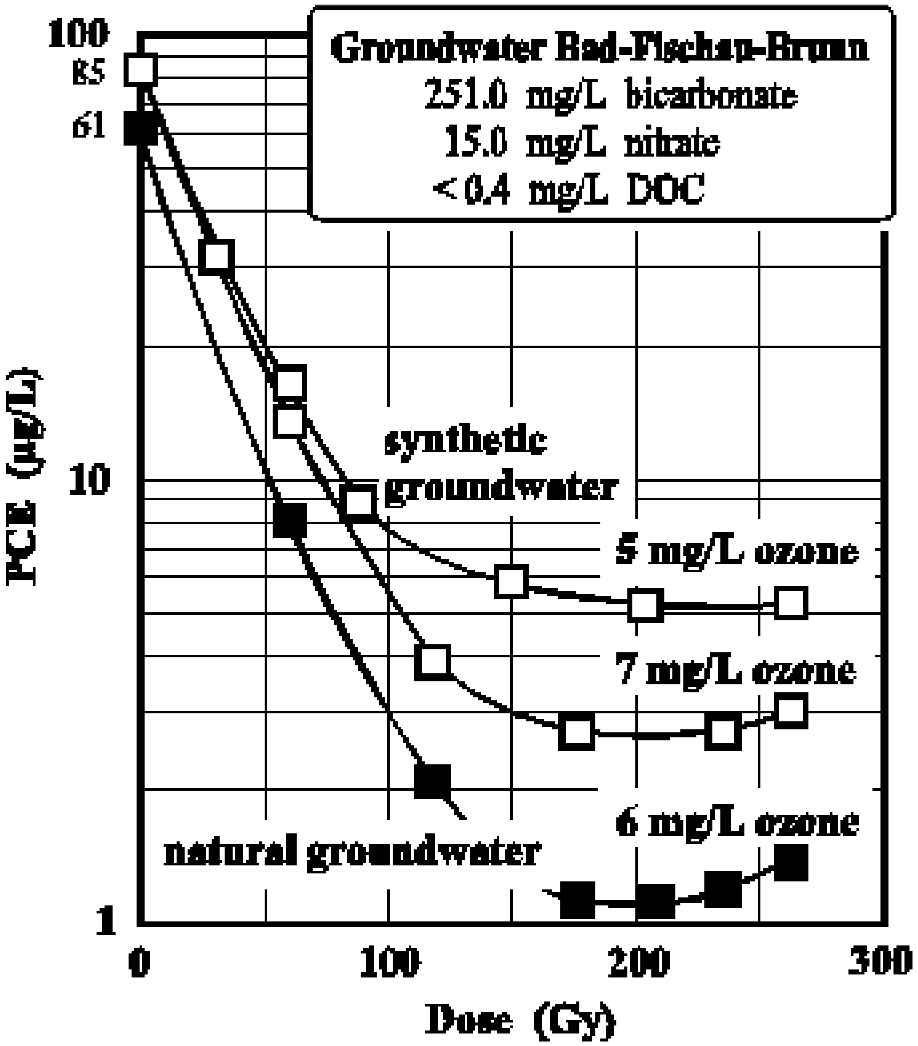

FIG. 1. Decomposition of perchloroethylene in Bad Fischau-Brunn groundwater by an ozone/EB irradiation treatment as a function of radiation dose and initial ozone concentration.

Ozone is made from pure oxygen, an ozone concentration of 13% per weight is planned. The ozone/oxygen stream is then compressed and mixed with the polluted groundwater at elevated pressure in a static mixing unit. Under the conditions given almost all ozone will be dissolved in the water but not all the oxygen. Therefore, most of the gaseous oxygen still present is released into the environment by means of a gas separator. Trace amounts of ozone are fed into an ozone destructor after the gas separator. Despite the inevitable ozone losses it is assumed that about 90% of the ozone produced remains in the water after oxygen release. The ozone containing polluted groundwater is then irradiated with 500 keV electrons in a closed irradiation chamber. The electrons penetrate into the chamber through a 30 µm thin titanium foil. Since the penetration of the 500 keV electrons in water is relatively short it is necessary to present the water to the EB in the shape of a thin, wide, fast-flowing stream. Accordingly the irradiation chamber will be 1.2 m wide but the thickness of the water stream in the chamber will be 3 mm only.

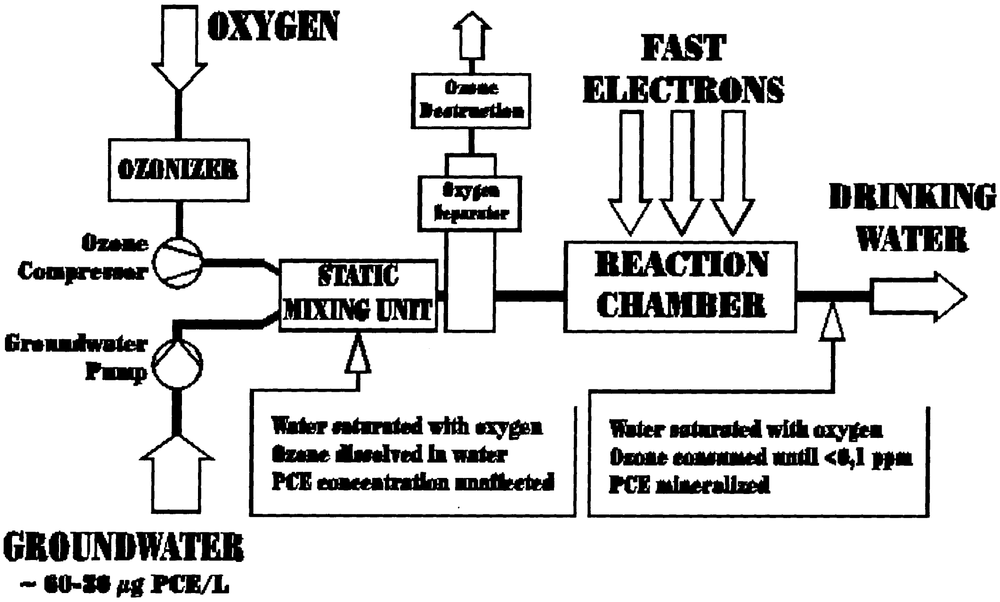

FIG. 2. Process schematic for Bad Fischau-Brunn's ozone/EB irradiation plant.

By the action of the EB irradiation in the presence of ozone, PCE is mineralized almost totally in the water [4]. The mineralization of PCE is of no influence to water quality; on the contrary, because of the ozone introduction the oxygen content of the water is increased — what can be classified as improvement of the treated water (see Table II).

TABLE II. CHANGE IN CONCENTRATION OF SOME NATURAL SOLUTES IN BAD FISCHAU-BRUNN GROUNDWATER AS A CONSEQUENCE OF THE TREATMENT PROCESS

Solute	before the treatment	Concentration in mg/L change by the treatment	after the treatment
Bicarbonate	251.0	0.06	251.06
Chloride	8.0	+ 0.068	8.068
Oxygen	8.7	+ 20.00 *	28.7 *

*can be roughly estimated only because of some degassing after treatment.

It has already been mentioned that the combination of ozone with EB irradiation is an AOP. However, compared with other ozone based AOPs the way in which the OH free radicals are generated is completely different. Groundwater can be described as a highly dilute aqueous solution of some inorganic and organic natural solutes. When dilute aqueous solutions are irradiated with fast electrons practically all the radiation energy is deposited in water molecules and the observed pollutant decomposition is brought about **indirectly** via the radicals formed from water (so-called water radiolysis). Direct action due to energy deposited directly in a solute is generally unimportant in dilute solutions, i.e. at solute concentrations below about 1 mol/L [5]. Roughly speaking the OH free radical generation in the combination of ozone with EB irradiation proceeds via 2 steps:

1. Water radiolysis:

$$H_2O \overset{\text{e-beam}}{\rightsquigarrow} OH^{\bullet};\ H^{\bullet};\ e^{-}_{aqu};\ H_2O_2$$

The action of fast electrons to water results in the direct formation of OH free radicals from the water to be purified. Beside the OH free radicals reducing species like solvated electrons and H-atoms as well as some hydrogen peroxide are formed. The reducing species and the hydrogen peroxide act now as promoter for the second step.

2. Ozone decomposition: The main reactions are:

$$\begin{aligned}
&O_2 + e^{-}_{aqu} \longrightarrow O_2^{-}\\
&O_2^{-} + O_3 \longrightarrow O_3^{-}\\
&O_3 + e^{-}_{aqu} \longrightarrow O_3^{-}\\
&O_3^{-} + H^{+} \longrightarrow HO_3^{\bullet} \longrightarrow OH^{\bullet} + O_2
\end{aligned}$$

For more details see [2, 6].

Just the opposite would take place if this groundwater is irradiated with non-ionizing UV radiation. In this case the radiation energy is deposited **directly** in ozone and not in water. The way in which the OH free radicals are formed is due to:

$$O_3 \underset{254\text{ nm}}{\overset{h\nu}{\rightsquigarrow}} O^{\bullet} + O_2$$

$$\begin{aligned}
&O^{\bullet} + H_2O \longrightarrow H_2O_2 \rightleftharpoons H^{+} + HO_2^{-}\\
&O_3 + HO_2^{-} \longrightarrow O_3^{-} + HO_2^{\bullet}\\
&O_3^{-} + H^{+} \longrightarrow HO_3^{\bullet} \longrightarrow OH^{\bullet} + O_2
\end{aligned}$$

Accordingly ozone/EB irradiation and ozone/UV irradiation represent the two ways in which radiation energy can be used. The indirect action generally is more efficient because all the radiation energy is taken by the water independent of the solutes present (as long as their concentration is < 1 mol/L). As a consequence the whole radiation energy is used for OH free radical production.

Although ozone/EB irradiation generates the OH free radicals necessary for pollutant decomposition in a total different way compared to that in the combination ozone/UV irradiation both treatment processes result in almost total mineralization of PCE. A 97% conversion of the organic chlorine into chloride for ozone/UV irradiation was reported [7], and that 96% of the organic chlorine is mineralized for the ozone/EB irradiation [4]. Moreover, it is known that PCE oxidation with OH free radicals may also produce trichloroacetic acid. Again, formation of trichloroacetic acid in trace amounts has been reported for both processes when used to decompose PCE in water [8, 4]. That means the product spectrum of PCE decomposition coincides for both AOPs even for the single organic by-product trichloroacetic acid on the ppb level. This is a clear indication that ozone/EB irradiation and ozone/UV irradiation decomposes PCE in water in exactly the same way. The only difference between both processes is the way in which the OH free radicals are formed. This includes moreover the combination ozone/hydrogen peroxide because in this process the OH free radical generation is exactly the same as in the combination ozone/UV irradiation [1]. Thus, the mechanism of PCE decomposition in water is the same for all three ozone based

AOPs. However, the ozone/EB irradiation process is able to generate more OH free radicals than any other of the ozone based AOPs. This is its crucial advantage.

The 100 m³/h demonstration plant in Bad Fischau-Brunn was expected to be the first commercial ozone/EB irradiation plant for groundwater remediation to supply drinking water worldwide. Therefore, it was decided to test the purified water with respect to formation of genotoxic compounds. AMES and micronucleus tests with primary hepatocytes gave no indication of any genotoxic effect neither in the treated nor in the untreated water but the micronucleus test with Tradescantia (Trad-MCN) showed an unexpected result (Table III).

TABLE III. RESULTS OF TRAD-MCN TEST WITH WATER FROM THE WELL IN BAD FISCHAU-BRUNN BEFORE AND AFTER TREATMENT WITH OZONE/ELECTRON BEAM IRRADIATION

Sample	Genotoxic response in micronuclei (MCN) / 100 tetrads
Groundwater before treatment	33.2 ± 20.0
Groundwater after treatment	8.7 ± 4.1
Tap water (negative control)	7.0 ± 4.1
Tap water with 0.25 mM As_2O_3/L (positive control)	20.2 ± 6.5

Due to these results it is obvious that the contaminated groundwater does not only contain PCE but also some genotoxic compounds and, moreover, that the ozone/EB irradiation treatment for PCE mineralization totally removed also these genotoxic compounds.

Origin, structure and concentration of these genotoxic compounds are not yet known. The Trad-MCN test used for its detection needs about one month to yield results. Under these conditions activated carbon filtration alone is not apt for remediation of such contaminated water.

There are some data published concerning the contamination of the aquifer "Mitterndorfer Senke". About 6 km downstream of Bad Fischau-Brunn close to a big waste disposal site an activated carbon treatment plant for PCE removal from groundwater is located. Trad-MCN tests performed gave a positive response indicating that, besides PCE, genotoxic compounds are present in the water and in some cases also in the treated water after the carbon filter [9]. Accordingly activated carbon filtration could not control the genotoxic compounds present in the water. Furthermore, when UV irradiation was applied to the water after activated carbon filtration the genotoxicity of the water treated increased in all cases exponentially with the UV irradiation dose applied. Therefore, UV disinfection of such contaminated water is not possible. Beyond that, it is even questionable whether AOPs based on UV irradiation in combination with oxidants can be applied when the water to be purified contains such genotoxic substances and/or their precursors.

4. CONCLUSIONS

It has been demonstrated that groundwater polluted with trace amounts of PCE can be successfully purified by advanced oxidation without any loss in water quality. Moreover, experiments performed have demonstrated that the ozone/EB process is also apt for total removal of some genotoxic compounds detected in groundwater contaminated with PCE. Since the combination ozone/EB irradiation may generate the highest OH free radical concentration in water it is best apt for commercialization within all ozone based AOPs. Accordingly the first commercial full scale plant based on the combination ozone/EB irradiation for treating 108 m^3/h of water polluted with about 60 µg/L PCE and some genotoxic compounds was expected to be constructed in Bad Fischau-Brunn, Austria.

The mechanism of the OH free radical generation in the combination ozone/EB irradiation is fully understood. The identical product spectrum obtained for the processes ozone/EB irradiation and ozone/UV irradiation in case of PCE decomposition in water clearly indicates that ionizing radiation can be successfully used for OH free radical production without any side effects.

5. FINAL NOTE

In 1996 the community of Bad Fischau-Brunn was approached with a proposal to install and operate an ozone/EB irradiation plant for groundwater remediation to guarantee the long term drinking water supply. The total cost of the project was about 1,6 million US dollars. The European Union (EU) funded the project with 50% of the total cost within its LIFE programme. The municipal council of Bad Fischau-Brunn unanimously voted to accept the financial support from EU. The two year approval process followed the expected path of reviews by experts and authorities. The positive result regarding the removal of genotoxic compounds by the ozone/EB irradiation treatment convinced all about the outstanding potential of the process. The process itself was never questioned or under discussion. However, a controversy between the Mayor and the opposite party regarding some other issues ended in a new election of the municipal council and of the Mayor. In the campaign started before the election by the opposite parties it was now asserted that Bad Fischau-Brunn has enough water resources and does not need the contaminated well for its water supply. The ozone/EB process itself was never attacked directly. Nevertheless, the Mayor lost the election and the new elected council — in which the opposite parties got the majority — stopped the project because of no actual need. The commercialization of the ozone/EB irradiation process was hindered by a trifling political controversy not directly related to the technology itself.

SECTION B: OXIDATIVE TREATMENT OF SOIL CONTAMINATED WITH POLYCYCLIC AROMATICS (PAHs) IN AQUEOUS SUSPENSION FOR DECONTAMINATION

1. INTRODUCTION

Soil contaminated with polycyclic aromatics (PAHs) is a serious environmental problem in many parts of the world. It is known from the literature that PAHs react very fast and effectively with hydroxy free radicals in aqueous solutions. The reactions are diffusion controlled, the reaction rate constants for the reaction of PAHs with aqueous hydroxy radicals are in the order of $1 \times 10^{10} M^{-1}s^{-1}$ [10]. However, the transfer of the PAHs from the soil into water is very difficult. Therefore, it suggested to consider a direct treatment of the contaminated soil with aqueous hydroxy radicals, i.e. to suspend the contaminated soil in water and treat the suspension with an advanced oxidation process.

Advanced oxidation processes (AOPs) are those that promote the activity of the hydroxy free radical OH in oxidation reactions. It has been found that the addition of ozone in combination with UV radiation or hydrogen peroxide can accelerate the decomposition of ozone into OH. Combining hydrogen peroxide and UV radiation alone will achieve similar results as the ozone based processes by generating OH with a considerably less OH yields [11].

The most simple method to generate OH in water is its irradiation with ionizing radiation (“water radiolysis”). However, along with the OH reducing species like solvated electrons e^{-}_{aqu} and H-atoms are formed. Since the total amount of the reducing species is even somewhat more than the OH formation they often induce undesired side reactions and may reduce, moreover, the economy of an irradiation process considerably [12, 13]. Therefore, ozone is added to the water before or during irradiation what often converts the ”hybrid” irradiation process into an almost pure AOP [6].

However, more recent investigations [14] concerning ozonation and AOP treatment of phenanthrene in aqueous solution have shown that the decomposition of this PAH is more effective by ozonation than by AOPs. This does not necessarily mean that ozonation in general is more effective for PAH destruction than AOPs are but it could be an alternative to AOPs in some cases.

The efficiency of AOPs with regard to PAH destruction obviously depends on the PAH structure. It cannot be excluded therefore that in certain cases the reducing species formed during water radiolysis may positively contribute to PAH destruction. Consequently EB irradiation of the suspended soil has also been included in the experimental programme.

Due to these considerations the following have been established:

1. EB irradiation of aqueous soil suspensions at two different temperatures (20°C and 55–60°C, resp.).
2. Ozonation of the aqueous soil suspensions at room temperature.
3. EB irradiation of aqueous soil suspensions in the presence of ozone at room temperature.

2. EXPERIMENTAL

Assessment of the results obtained with the different treatment processes applied is based on the change in the total concentration of 17 selected PAHs. The selection of the PAHs is due the NIOSH list; the compounds are given in Table IV which also contains the concentration of each individual PAH on the original soil before treatment.

TABLE IV. THE PAHs OF THE NIOSH LIST AND THEIR ORIGINAL CONCENTRATION ON THE SOIL

No.	Name	Molecular formula	Molecular weight	Structure	Concentration mg/kg soil
1	Naphthalene	$C_{10}H_8$	128	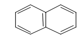	2.1
2	Acenaphtylene	$C_{12}H_8$	152	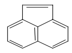	0.6
3	Acenaphtene	$C_{12}H_{10}$	154	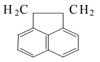	2.2
4	Fluorene	$C_{13}H_{10}$	166	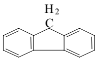	2.5
5	Phenantrene	$C_{14}H_{10}$	178	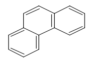	13.3
6	Anthracene	$C_{14}H_{10}$	178	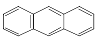	6.9
7	Fluoranthene	$C_{16}H_{10}$	202	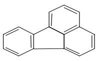	53.2
8	Pyrene	$C_{16}H_{10}$	202	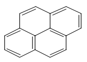	56.7
9	Benzo(a)anthracene	$C_{18}H_{12}$	228	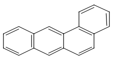	17.2
10	Chrysene	$C_{18}H_{12}$	228	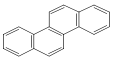	50.9
11	Benzo(b)fluoranthene	$C_{20}H_{12}$	252	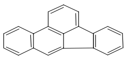	44.6
12	Benzo(k)fluoranthene	$C_{20}H_{12}$	252	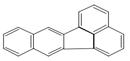	9.3
13	Benzo(e)pyrene	$C_{20}H_{12}$	252	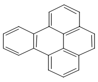	19.3
14	Benzo(a)pyrene	$C_{20}H_{12}$	252	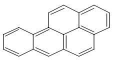	16.0
15	Dibenzo(a,h)anthracene	$C_{22}H_{14}$	278	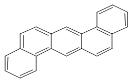	2.9
16	Benzo(g,h,i)perylene	$C_{22}H_{12}$	276	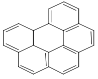	20.9
17	Indeno(1,2,3-c,d)pyrene	$C_{22}H_{12}$	276	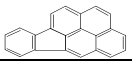	13.5

2.1. Procedure for the quantification of PAHs

2.1.1. Extraction from soil

The water suspension containing the PAH loaded soil was filtered and the filter residue extracted twice with 100 ml of acetone by ultrasonification for 1 h in each case. After additional filtering, the acetonic solution was brought to 200 ml. 200 µl internal standard solution (1 µg/ml of five deuterated PAHs in acetone: naphtalene-d8; acenaphtene-d10; phenanthrene-d10; chrysene-d12 and perylene-d12) were added to a 2 ml aliquot of the extract. After diluting this mixture by adding 1.8 ml acetone, it was ready for GC/MS analysis. The dry weight was determined by drying the extraction residue at 105°C overnight.

2.1.2. Extraction from aqueous solution

The filtered solution was extracted with 10 ml of cyclohexane twice. After adding 50 µl internal standard solution to a 1 ml aliquot, it was analysed by GC/MS.

2.1.3. Gas chromatography / mass spectrometry

Separation was performed on a DB5MS fused-silica capillary column, 30 m × 0.25 mm ID; 0,25 µm film thickness (J&W Scientific, Folsom, CA, USA), protected by a guard column DB1, 3 m × 0.32 mm ID, 0.5 µm film thickness, from the same manufacturer. Carrier gas was helium with an inlet pressure set to 100 kPa.

The mass spectrometer was operated in the electro impact mode (EI) using 70 eV ionisation voltage. The ion source temperature was 250°C, and the GC/MS-interface set to 280°C. The analyses were performed by selected ion monitoring (SIM).

3. DESCRIPTION OF THE EXPERIMENTAL SET-UP

The bench scale facility for treating the contaminated soil suspended in water consists of two storage vessels of glass S_1 and S_2 (volumes about 50 litres each) both equipped with a stirring apparatus to hold the soil in suspension. They are connected with each other via 3-way valves V_1 and V_2, respectively. V_1 also connects both vessels alternatively with a membrane pump MP made of stainless steel which pumps the suspension through the irradiation chamber and via the other valve V_2 into the corresponding vessel (for example, vessel S_1 contains the suspension to be treated, V_2 is adjusted then to conduct the suspension after treatment into the vessel S_2; when the run is finished almost all of the suspension is then in vessel S_2; now V_1 and V_2 are switched to the opposite position and another run starts pumping the suspension from S_2 via irradiation chamber into S_1). Just behind the pump is a small buffer vessel B to flatten the pulsation in the liquid which originates from the pump.

The irradiation chamber is designed for the irradiation of water layers with a thickness of 3 mm with simultaneous introduction of ozone (via frits in the bottom of the chamber) during irradiation. The window of the irradiation chamber is made of 25 µm titanium; its dimensions are 50 mm wide and 200 mm in length. The gas flow into the irradiation chamber is controlled by needle valves NV, flow meters FM and a pressure gauge P just as the flow of the aqueous suspension is controlled with regard to pressure and temperature. Heating of the suspension, when required, is provided in storage vessel S_1 by use of a heating bandage. To control the temperature in the irradiation experiments (both the room temperature and the elevated temperature) a heat exchanger HE in combination with a thermostat was used. The samples for analyses were taken using the 3-way valve V_3.

The EB accelerator is an ICT accelerator (500 kV, 25 mA, 120 cm scan width) manufactured by High Voltage Eng., USA.

Ozone was prepared from pure oxygen using a laboratory ozonizer (E. Sander Ltd., Germany). Ozone concentrations were determined routinely by measuring the UV absorption at 254 nm, calibrated against indigotrisulfonate method. The oxygen flow applied during the experiments was 140 L/h; the resulting ozone concentration was about 100 mg O_3/L O_2.

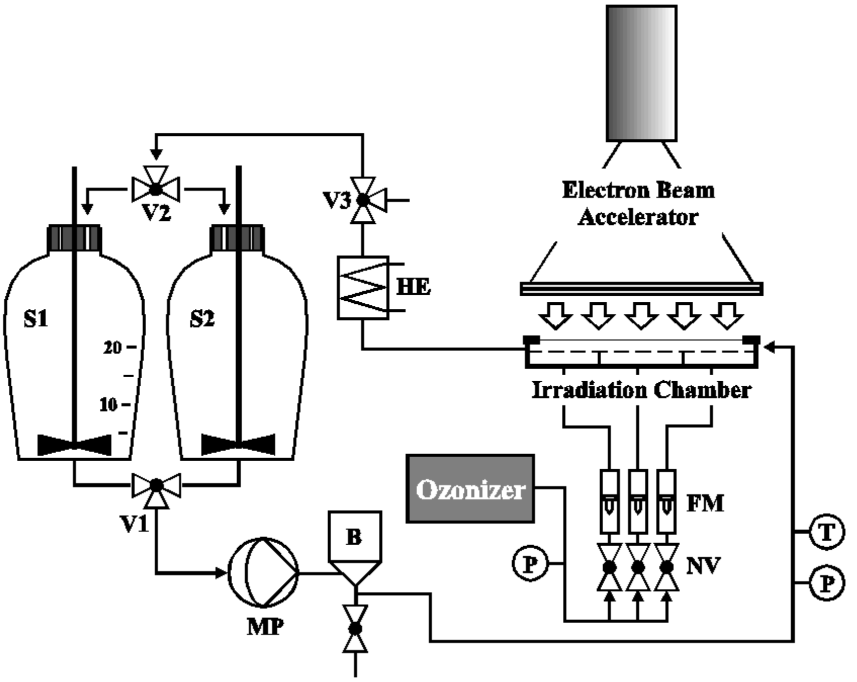

FIG. 3. Schematic view of the bench scale facility for treating soil in suspension.

This construction is very versatile and apt for the following treatment processes under complete identical conditions:

- EB irradiation
- ozonation
- combined ozone/EB irradiation (ozone introduction during irradiation)
- combination of ozonation and EB irradiation (ozone treatment before or after the irradiation, not simultaneously).

A schematic view of the experimental set-up is shown in Fig. 3.

Soil (particle diameter <1 mm) was suspended in Seibersdorf tap water and diluted with deionized water. The resulting mixture contains about 55 ppm bicarbonate. On the one hand, this is sufficient to stabilize ozone during ozonation; on the other hand, it does not scavenge too much OH radicals. The suspension contained 6% soil (per weight).

Twenty (20) litres of the suspension were used in one experiment (cycle). The flow rate was adjusted to 120 L/h what corresponds to a radiation dose of 10 kGy at 25 mA for each cycle when EB irradiation is considered. For ozonation each cycle is equivalent to an ozone dosage of 2 g O_3/kg soil. For the analyses about 150 ml of the suspension was taken for one sample.

Before starting the experiments the dead volume of the construction was determined. It was found to be about 1.5 litres. About 0.5 litres (~2.5%) of the suspension remains in the respective vessel because it is not possible to empty it totally. However, in the next cycle this non-treated part is again combined with the treated part and the effect is averaged by that due to the total of the cycles applied (at least 5 in case of the irradiation treatment processes). Moreover, there is another effect which reduced the efficiency of the process. Despite relative intense mixing by the stirring apparatus in the vessels it was not possible to hold all the soil totally in suspension. During one cycle about 10% of the total soil is precipitated on the bottom of the vessel. Again there is always an exchange of the soil precipitated and in suspension during different cycles so that the effect is averaged out. Nevertheless, these limitations resulted in a reduced efficiency of the process in the order of about 10–15% and are, moreover, most likely responsible in part for the scattering of the analytical results.

4. RESULTS AND DISCUSSION

4.1. EB irradiation at room temperature

Radiation doses of 50 kGy and 100 kGy have been applied (the unit of the absorbed radiation dose is 1 Gray (Gy). 1 Gy = 1 J/kg). However, even at the higher dose of 100 kGy, total PAH decomposition on soil did not exceed about 6.7%. Therefore, the following experiments have been performed at elevated temperature.

4.2. EB irradiation at 55–60°C

The results of these experiments are contained in Fig. 4. Radiation doses of 50, 100 and 200 kGy were applied corresponding to a total PAH decomposition of 3.5%, 15.8% and 18.4%, respectively. However, there is some inconsistency in results when the higher molecular components (above chrysene) are considered. The results obtained with 100 kGy show a much higher degree of PAH decomposition for the components above chrysene as was found for these components at the higher dose of 200 kGy. Since this is not very plausible the result obtained at 100 kGy most likely is not actual but due to the high scattering of the analytical data. This interpretation is supported by the rather high value found for the decomposition of dibenzo(a,h)anthracene which amounted to >10% at 50 kGy but only about 2% at 200 kGy. Similar results were also found for indeno(1,2,3-c,d)pyrene at these doses. Therefore, the results obtained with 200 kGy seem to be more reliable. Due to these results EB irradiation treatment seems to be more effective to PAHs of lower molecular weight (or PAHs consisting of less aromatic rings) while the PAHs with higher molecular weight (or more than 4 aromatic rings) are obviously more resistant against the attack of the free radical species formed during water radiolysis.

In the present case this is a clear disadvantage because the amount of the low molecular compounds (naphthalene until anthracene) on soil is rather small (only 8.3% of the total PAHs; see Table IV). The resulting net effect regarding total PAH decomposition must be small, therefore, although the amount of decomposition of these PAHs in general is almost 40% (at 200 kGy). However, it should be noted that doubling the radiation dose (from 100 kGy to 200 kGy) does not result in an analogous increase of the decomposition of these PAHs. The increase recorded at 200 kGy amounts to 10-20% only when compared with 100 kGy.

The more dominant PAHs on the soil to be treated are surprisingly more resistant to the irradiation process applied. The total PAH decomposition recorded is mainly due to the decomposition of fluoranthene and pyrene, which are located in the order of the PAHs

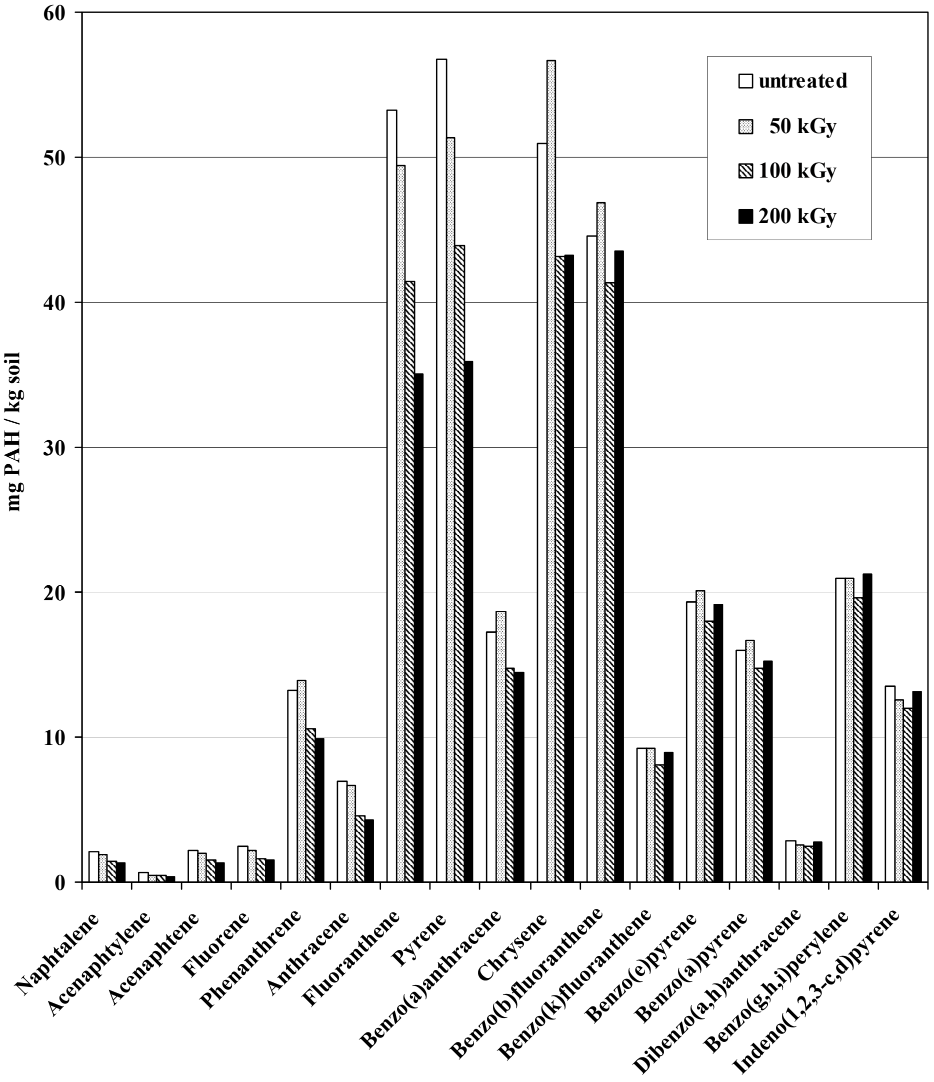

FIG. 4. Treatment of PAH contaminated soil in aqueous suspension by means of EB irradiation at 55–60°C. PAH decomposition as a function of radiation dose.

between the lower molecular weight range (until anthracene MG 178) and the higher range (above MG 228). For these two compounds also doubling of the radiation dose is more effective as it was for the compound mentioned with the lower molecular weight. However, all in all a radiation dose of 200 kGy seems to be too high to be justified with such a rather low decomposition (<20%) of the total PAHs.

It is supposed that the OH free radicals produced by the action of ionizing radiation on water play a dominant role in the decomposition of the PAHs on soil. Therefore, the next step logically is an irradiation treatment in the presence of ozone. The addition of ozone during irradiation converts the reducing species formed during water radiolysis into OH free radicals and by that the irradiation process into a pure Advanced Oxidation Process (AOP). However, before applying the AOP it was necessary to investigate the effect of ozonation alone with regard to PAH decomposition in order to determine the optimum ozone dose also for the AOP, i.e. the combination ozone/EB irradiation.

4.3. Ozonation at room temperature

The results obtained from ozonation of the PAH-containing soil in aqueous suspension are presented in Fig. 5 (except for low dose of 2 g O_3/kg soil).

At the low doses of 2 g O_3/kg soil and 6 g O_3/kg soil it is remarkable to note that mainly the high molecular PAHs are attacked by the ozone while the low and medium molecular PAHs are hardly attacked. There is an almost linear relation between the total PAH decomposition and the ozone dose applied; this is also true when the range is extended until an ozone dose of 10 g O_3/kg (corresponds to a total PAH decomposition of 20.9%). Unfortunately, above 10 g O_3/kg the linear relationship between ozone dose and total PAH decomposition considerably deviates from linearity. The corresponding value for total PAH decomposition at 20 g O_3/kg soil amounts to 27.3% only.

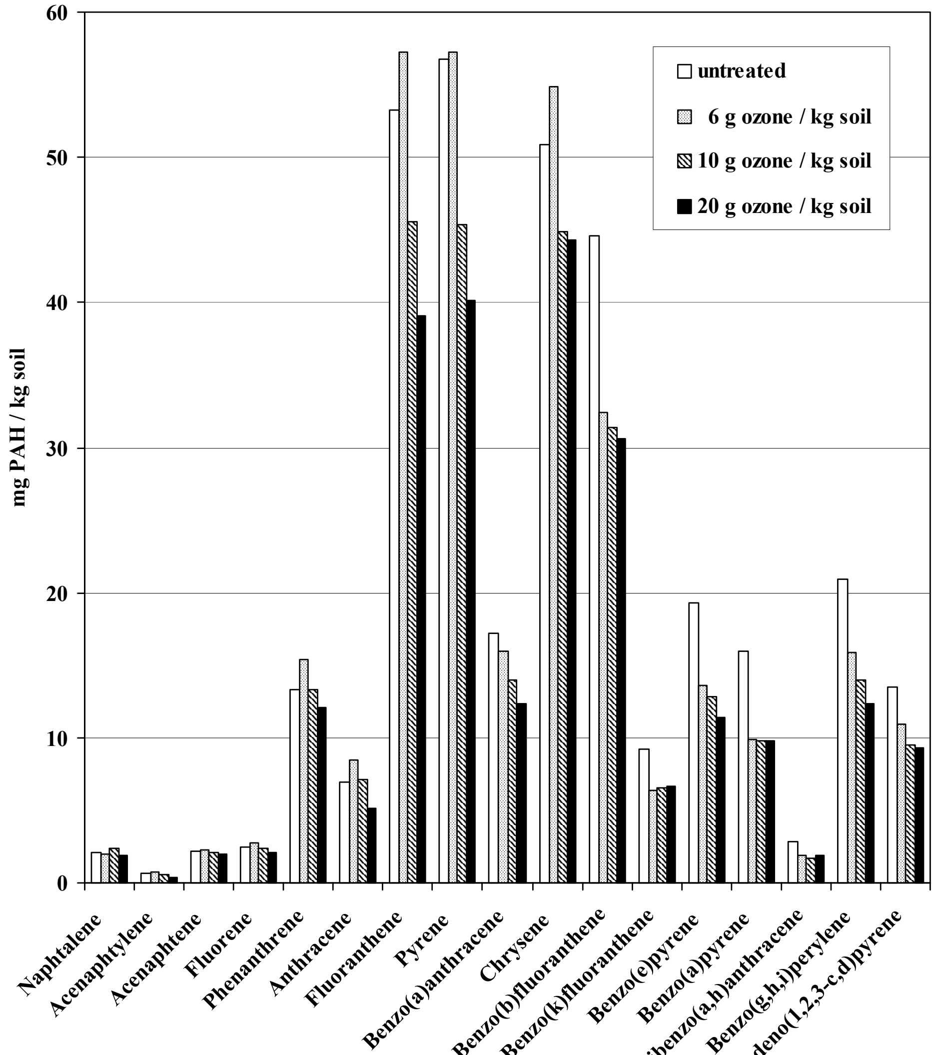

FIG. 5. Ozonation of PAH contaminated soil in aqueous suspension. PAH decomposition as a function of ozone dose applied.

Nevertheless, the results obtained from the ozonation experiments are quite expressive especially when compared with the findings from the EB irradiation experiments. At the lower ozone doses (2 g O_3/kg and 6 g O_3/kg) it was found that the high molecular PAHs were attacked by the ozone almost exclusively. In the EB irradiation treatment processes, however, it was noticed that the low molecular PAHs were essentially decomposed by that treatment.

At the higher ozone dose of 10 g O_3/kg soil the ozone obviously also attacks the PAHs in the medium molecular weight range (fluoranthene until chrysene); moreover, there is also some decomposition of the low molecular weight PAHs. At the highest ozone dose of 20 g O_3/kg all PAHs considered here are attacked. However, it is conspicuous that at the higher ozone doses the increase in the total PAH decomposition is caused by some decomposition of the low and medium molecular weight PAHs while decomposition of the higher molecular PAHs stagnated at ozone doses above 10 g O_3/kg. Since ozone itself is also a source for OH free radicals it seems possible that at higher ozone doses the soil acts as a promoter for the ozone decomposition into OH free radicals. This would mean that the decomposition of the PAHs in the low and medium molecular weight range is in reality an effect of OH free radicals originating from ozone decomposition.

It was, therefore, of interest to study the effect of the OH free radicals at higher concentrations; this can be done by using the combined ozone/EB irradiation treatment which represents as already mentioned an almost pure AOP provided that the ozone is introduced during irradiation.

4.4. Combined ozone/EB irradiation treatment

When ozone is introduced into water during irradiation most of the ozone is converted into OH free radicals. This is due to the action of the reducing species formed during water radiolysis which act as promoters for the ozone decomposition into OH free radicals. However, there is always a competition between direct ozone reactions with PAHs and ozone decomposition into OH free radicals but in this case the competition should be in favour of the ozone decomposition which means OH free radical generation.

We recorded that the combined ozone/EB irradiation treatment effected in both experiments performed better results when compared with irradiation alone but worse when compared with ozonation alone. (12.6% total PAH decomposition for the combination in comparison with 2% for the 50 kGy irradiation but 20.9% for the ozonation with 10 g O_3/kg soil ozone dose. 14.6% total PAH decomposition for the combination in comparison with 6.7% for the 100 kGy irradiation but 27.3% for ozonation with 20 g O_3/kg/soil ozone dose). It is further conspicuous that doubling both the irradiation dose and ozone dose hardly increases the total PAH decomposition (it only increases from 12.6% to 14.6%). Moreover, in both experiments total PAH decomposition obtained with the combined process is always less than the total PAH decomposition calculated by the sum of the individual processes. It is obvious, therefore, that ozone introduction during irradiation does not represent an improvement in search of a technical solution of the problem.

However, these results indicate that a combination of ozone with **subsequent** irradiation treatment could be more effective than the simultaneous treatment. On the one hand, ozonation with an ozone dose of 10 g O_3/kg soil has been found to be most efficient; on the other hand, irradiation at elevated temperature gave much better results than that obtained at room temperature. Therefore, ozonation with an ozone dose of 10 g O_3/kg soil was combined with a subsequent irradiation at 55-60°C applying radiation doses of 100 kGy and 200 kGy, respectively.

With a radiation dose of 100 kGy a total PAH decomposition of 32.8% was recorded while 43.6% was found when the irradiation dose applied was 200 kGy. Calculation of the total PAH decomposition by the sum of the individual treatment processes resulted in 36.7% (for 100 kGy) and 39.3% (for 200 kGy), respectively. Due to this result it is quite sure that the combination of ozonation with subsequent irradiation is not more than the sum of the two individual processes. In other words: **No synergistic effect exists**.

4.5. PAH decomposition in aqueous phase

It was found that there is almost no desorption of the PAHs from soil into water when soil was simply suspended (PAHs detected in water <0.1% of total PAHs on soil).

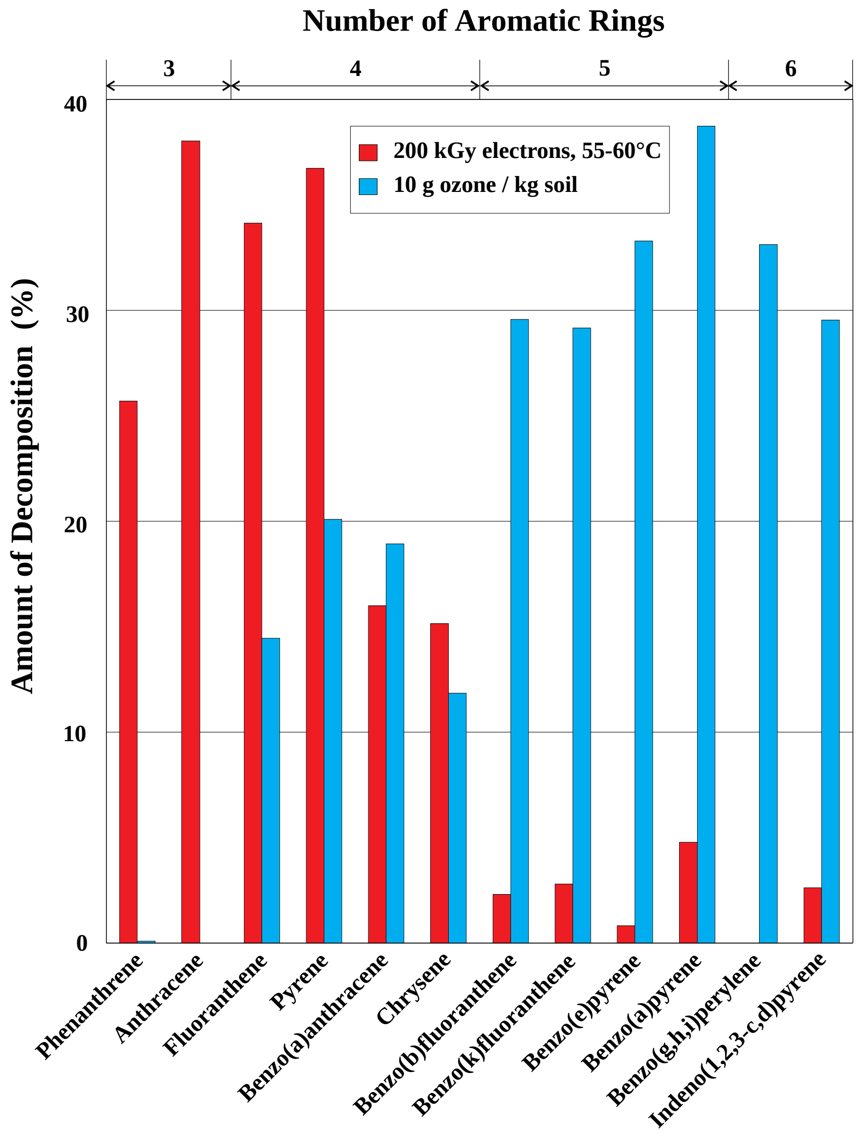

FIG. 6. Treatment of PAH contaminated soil in aqueous suspension. Effect of ozonation and EB irradiation, respectively on some selected PAHs.

5. SUMMARY

Oxidative treatment of the aqueous soil suspension reduces the total amount of the PAHs on soil but in different ways when individual PAHs are considered (see Fig. 6). It was found that ozone mainly attacked the high molecular fraction (i.e. consisting of five or six aromatic rings) of the PAHs investigated while EB irradiation of the aqueous soil suspension mostly decomposed the lower fraction (i.e. consisting up to 4 aromatic rings).

Under the conditions given irradiation of an ozonated soil suspension at 55–60°C was most effective and resulted in the highest total PAH decomposition. However, the total effect is only the sum of the effects of the two individual processes; accordingly there is no synergistic effect at all.

Using optimum conditions (10 g O_3/kg soil followed by a 100 kGy irradiation at 55–60°C) the total PAH decomposition would amount to about 33% of what corresponds to a total PAH decomposition of about 100 mg PAH/kg soil. A higher yield is hardly achievable according to the drastic yield reduction above the optimum conditions. An economic application seems to be very difficult to carry out, therefore.

REFERENCES

[1] GLAZE, W.H., KANG, J.-W., CHAPIN, D.H., The chemistry of water treatment processing involving ozone, hydrogen peroxide and ultraviolet radiation, Ozone: Sci & Eng. **9** (1987) 335–352.

[2] GEHRINGER, P., ESCHWEILER, H., The use of radiation-induced Advanced Oxidation for water reclamation, Wat. Sci. Tech. **34** (1996) 343–349.

[3] HELMA, C., ECKL, P., GOTTMANN, E., KASSIE, F., RODINGER, W., STEINKELLNER, H., WINDPASSINGER, C., SCHULTE-HERMANN, R., KNASMÜLLER, S., Genotoxic and Ecotoxic Effects of Groundwater and their Relation to Routinely Measured Chemical Parameters, Environ. Sci & Technol. **32** (1998) 1799–1805.

[4] GEHRINGER, P., PROKSCH, E., ESCHWEILER, H., SZINOVATZ, W., Remediation of groundwater polluted with chlorinated ethylenes by ozone-electron beam irradiation treatment, Appl. Radiat. Isot. **43** (1992) 1107–1115.

[5] HENGLEIN, A., Einführung in die Strahlenchemie, Weinheim/Bergstraße: Verlag Chemie, (1969) p.131.

[6] GEHRINGER, P., ESCHWEILER, H., SZINOVATZ, W., FIEDLER, H., STEINER, R., SONNECK, G., Radiation-induced OH radical generation and its use for groundwater remediation, Radiat. Phys. Chem. **42** (1993) 711–714.

[7] GLAZE, W.H., KANG, J.-W., Advanced Oxidation Processes for treating groundwater contaminated with TCE and PCE: laboratory studies, J. Am. Water Works Assoc. **80** (1988) 57–63.

[8] GLAZE, W.H., Reaction products of ozone: a review, Environ. Health Perspectives **69** (1986) 151–157.

[9] HELMA, C., SOMMER, R., SCHULTE-HERMANN, R., KNASMÜLLER, S., Enhanced clastogenicity of contaminated groundwater following UV irradiation detected by the Tradescantia micronucleus assay, Mutation Res. Letters **323** (1994) 93–98.

[10] HAAG, W.R., YAO, D.C., Rate Constants for Reaction of Hydroxyl Radicals with Several Drinking Water Contaminants, Environ. Sci. Technol. **26** (1992) 1005–1013.

[11] GLAZE, W.H., Drinking-water treatment with ozone, Environ. Sci. Technol. **21** (1987). 224–230.

[12] GEHRINGER, P., PROKSCH, E., ESCHWEILER, H., SZINOVATZ, W., Clean-up of polluted groundwater by radiation-induced oxidation (Proc. Symp. Application of Isotopes and Radiation in Conservation of Environment, Karlsruhe, 1992) 203–205.

[13] GEHRINGER, P., ESCHWEILER, H., FIEDLER, H., Ozone-electron beam treatment for groundwater remediation, Radiat. Phys. Chem. **46** (1995) 1075–1078.

[14] TRAPIDO, M., VERESSININA, J., MUNTER, R., Ozonation and Advanced Oxidation Process (AOP) Treatment of Phenanthrene in Aqueous Solutions, Ozone: Sci. & Eng. **16** (1994) 475–485.

THE APPLICATION OF THE ELECTRON BEAM PROCESS IN WATER AND WASTEWATER TREATMENT: FUNDAMENTAL AND APPLIED STUDIES

W.J. Cooper, T. Tobien
Department of Chemistry,
University of North Carolina at Wilmington,
Wilmington, North Carolina,
United States of America

Abstract. We have undertaken a three phase research project that has as the overall goal to better understand the application of the EB process to water, wastewater and sludge treatment. We have conducted studies to examine bimolecular rate constants for several halogenated methanes, several of which are common disinfection by-products when chlorination is practised. The second phase examines the ability to destroy odour causing compounds, we have selected thioanisole as the model compound, in wastewater and sludge treatment. The third phase of our study is to better understand the destruction mechanism and kinetic modelling of the fuel oxygenate, methyl tert-butyl ether, a common ground water contaminant in the US. We report here several new and re-evaluated bimolecular rate constants and the results of large scale EB treatment of water containing the compounds under study.

1. INTRODUCTION

As part of an ongoing project to better understand the application of the EB process in water treatment we have undertaken several studies. The first involves the description of the loss of halogenated methanes in drinking water by the process. To model the removal of halogenated disinfection by-products in the EB process it is necessary to have accurate bimolecular rate constants. We have evaluated several halogenated methanes that have not been previously studied, and re-evaluated several reported rate constants.

Key issues in treating wastewater and biosolids (residuals) management are not only the removal of toxic pollutants, but also the removal of odours. Several classes of compounds have been identified which are responsible for causing such odours: sulphides, dicyclopentadiene and analogs, disinfection by-products, i.e. chlorinated phenols and short-chain aldehydes, to name a few. A typical treatment procedure to remove odours involves several stripping and scrubbing stages with the addition of substantial amounts of conventional oxidizers, e.g. hypochlorous acid and/or hydrogen peroxide. Our novel approach is intended to replace the latter steps with one single treatment using an EB. The interaction of highly accelerated electrons with water generates a number of very reactive intermediates, i.e. hydrated electrons, $^{\bullet}OH$ radicals and $^{\bullet}H$-atoms, which in turn react with the odour-causing substrates. Research on the irradiation of waters containing benzene, toluene, phenol, chloroform, carbon tetrachloride, as well as several other common organic pollutants has shown excellent removal for low solute concentrations. To demonstrate the feasibility of our treatment method we chose an aromatic thioether, thioanisole (TA). Although aliphatic thioethers have been extensively studied, much less is known about their aromatic counterparts. Several recent studies investigate the oxidation of thioanisole with different pulse radiolytically generated radicals and describe the corresponding intermediates. To the best of our knowledge nothing is known so far about the reduction of thioanisole with hydrated electrons and hydrogen atoms.

The third area of this study is the kinetic modelling of methyl *tert*-butyl ether (MTBE). We have conducted several studies and believe that in the near future we will have a reasonably good understanding of the process and be able to accurately model the process.

2. EXPERIMENTAL

2.1. Pulse radiolysis

A Model TB-8/16-1S linear electron accelerator was used for the pulse radiolysis experiments, providing 5–50 nanosecond pulses of 8 MeV electrons and generating radical concentrations of 1–3 μM per pulse in all investigated systems at the electron accelerator (LINAC) facilities at the Notre Dame Radiation Laboratory. Dosimetry was based on N_2O–saturated, 10^{-2} mol dm^{-3} SCN^- solutions at $\lambda = 475$ nm, ($G\varepsilon = 5.09 \times 10^4$) where G is defined as the number of species produced or destroyed per 100 eV, and ε is in units of dm^3 mol^{-1} cm^{-1}.

2.2. Bimolecular rate constants

Rate constant measurements for the reactions of the primary water radiolysis species, the hydroxyl radical, the hydrated electron and the hydrogen atom, with the organic solutes of interest were performed in aqueous solution using established aqueous pulse radiolysis and absorption spectroscopy techniques. To isolate the hydroxyl radical reaction, the hydrated electron can be removed by using nitrous-oxide saturated solutions, where the reaction:

$$N_2O \quad + \quad e_{aq}^- \quad \longrightarrow \quad \cdot OH \quad + \quad OH^- \quad + \quad N_2 \qquad (1)$$

occurs thus nearly doubling the amount of OH-radicals present. For peroxy radical studies, solutions containing mixtures of N_2O/O_2 were employed.

To study the reaction of hydrated electrons with halocarbons, alcohols such as 2-propanol or 2-methyl-2-propanol can be used to scavenge hydroxyl radicals, according to:

$$(CH_3)_3COH + OH \longrightarrow CH_2(CH_3)_2COH + H_2O \qquad (2)$$

All rate constant measurements were conducted at room temperature (22–23°C). Typically five halomethane concentrations were used with six single rate constant estimates at each concentration and an average of ten (pulse + baseline) per estimate. Solutions were prepared immediately prior to the experiment by purging 250 ml aqueous 0.5M *tert*-butanol solutions with N_2 for 30–45 min. The inlet and outlet were immediately closed with a three way stopcock, and then the halomethane was added via syringe through a septum with stirring until everything was dissolved. (This procedure should prevent the halomethanes from evaporating during bubbling with N_2.) As soon as the halomethane was dissolved the flask was connected to the LINAC flow system (via round glassy joints) and the rate constant measured. The waste bottle was filled with N_2 prior to the experiment and connected to the flask with the halomethane solution in order to avoid N_2 bubbling through the halomethane solution during the measurement. (Both displaced volumes are the same resulting in a net pressure of "0" in both the flask and the waste bottle.) The flow system itself was filled with water in the beginning and halomethane solution later in order to avoid oxygen contamination. All measurements started out with the lowest concentration followed by measurements in the order of increasing concentration. (In order to avoid errors originating from residues of a higher concentrated solution measured beforehand.) The wavelength to monitor the hydrated electron decay was usually 650 nm with a cut-off wavelength filter for wavelengths below 500 nm.

Since the rate constant that we measured for chloroform differed considerably from the reported value, the experiment was conducted several times with chloroform from two different sources. For the peroxy radical formation reaction measurements, we used the following reaction scheme:

$$e^- + CHBr_3 \dashrightarrow CHBr_2 + Br^- \quad (3)$$

$$CHBr_2 + O_2 \dashrightarrow CHBr_2(O_2) \quad (4)$$

$$CHBr_2(O_2) + ABTS \dashrightarrow CHBr_2(O_2)^- + ABTS^+ \quad (5)$$

$ABTS^+$ (2,2'-Azinobis-(3-ethylbenzthiazoline-6-sulphonate) shows a strong absorption around 415 nm and the growth rate constant is conveniently monitored. The plot of the first order growth rate constant vs. ABTS concentrations yields two distinctive regions: a concentration dependent linear region ($k^{II}(CHBr_2(O_2)+ABTS)$ and an ABTS concentration independent region (a plateau value) for the rate determining step $CHBr_2 + O_2$. With a known O_2 concentration (air saturation = 300 μM) the bimolecular rate constant can be calculated. It is essential that *tert*-butanol be added to prevent ABTS + OH --> $ABTS^+ + OH^-$.

2.3. Large scale studies

All large scale studies were conducted at the Electron Beam Research Facility (EBRF) located at the Miami-Dade Virginia Key (Central District) Wastewater Treatment Plant. The facility consists of a 1.5 MeV electron accelerator rated at 75 kW. The electron accelerator is powered by an insulating core transformer (ICT) operating at 1.5 MeV with a continuously variable beam current from 0 to 50 mA. EB is scanned horizontally at 200 Hz and vertically at 60 Hz to give a coverage of 1.2 m width and 5 cm height. Varying the beam current changes the absorbed dose in a linear fashion, allowing for experimentation at doses from 0 to 800 krads.

The large scale research facility is designed to treat aqueous streams at 0.46 $m^3 \, min^{-1}$ (120 gpm). Influent streams at the EBRF are presented to the scanned beam in a 4 mm thick falling stream. Since the maximum penetration in water is approximately 7 mm for 1.5 MeV electrons, some electrons pass through the stream and thus not all of the beam energy is transferred to the water. The total efficiency of the system, as defined by irradiation dose divided by total electrical power in, has been determined to be 60–72%. Thus, at 50 mA (75 kW) we have recorded doses of 800 krads. Total power consumption, including pumps, chillers and other auxiliary equipment is about 125 kW.

Because the system is being used for research, and water quality is one of the main experimental variables, three influent streams are directly connected to the facility. The influent streams directly connected to the plant are potable (drinking) water, chlorinated secondary wastewater effluent and anaerobically digested sewage sludge that is 2–3% solids. In addition to the three continuous flow streams, we have the capacity to conduct large scale batch experiments (up to 22,700 L, 6000 gal) using tank trucks and/or one 9,400 L high density polypropylene tank (2,500 gallon). Batch experiments may be used for groundwater and any other source of contaminated water for which treatability studies are desired. For the batch experiments it is possible to recirculate the water and we have conducted studies where we have deposited up to 12 Mrads in one sample while it was recirculated.

The EBRF is instrumented with resistance temperature devices (RTDs) to obtain direct estimates of absorbed dose. Five RTDs are mounted in the influent (2 sensors) and effluent (3 sensors) stream immediately before and after irradiation. The RTDs are connected via an interface to a computer which continuously reads and records temperatures and the absorbed dose is estimated by converting the observed temperature differences to the energy transferred to the water.

During experiments to determine the removal efficiency of parent compounds and collect samples to determine reaction by-products, samples are taken prior to and after irradiation. These samples are obtained in the control room from continuously running sample streams.

3. RESULTS AND DISCUSSION

3.1. Halomethanes

The data presented in Tables I, II and III summarize the new bimolecular rate constants that we have evaluated over the past two years. Halogenated methanes represent a major product of disinfection (the trihalomethanes) when chlorine is used. The study we conducted herein was initiated as a result of a project completed recently [32]. In the previous study we were able to model the disappearance of CCl_4 while in the same water we were unable to model the disappearance of $CHCl_3$ using rate constants that have been published. We predicted that if the rate constant of the hydrated electron with $CHCl_3$ would be three times slower than reported then the modelled results would be very similar to the observed results that we obtained at a large scale.

They represent the bimolecular rate constants of primary water radiolysis radicals with halogenated methanes and simple halogen-substituted carbon-centred radicals with molecular oxygen. Future research will include filling-in the gaps in existing data with additional bimolecular reaction rate constants.

This study is in progress and we continue to evaluate new rate constants that will be of importance to drinking water treatment.

3.2. Thioanisole

To demonstrate the feasibility of our treatment method we chose an aromatic thioether, thioanisole (TA). Although aliphatic thioethers have been extensively studied [33–38], much less is known about their aromatic counterparts. Several recent studies [39–41] investigate the oxidation of thioanisole with different pulse radiolytically generated radicals and describe the corresponding intermediates. To the best of our knowledge nothing is known so far about the reduction of thioanisole with hydrated electrons and hydrogen atoms.

A further step is not only to report EB treatment results, but to simulate those results on the basis of reaction mechanistic models [32]. These models utilize known radiation chemical processes in pure water and account for the interference of further solutes in the sample solution. Each reaction in the model can be described by its integrated kinetic equation. In order to calculate radiation dose dependent substrate concentrations, rate constants for each reaction have to be known. The literature rate constant for thioanisole reacting with $^{\bullet}OH$ radicals failed to simulate our experimental EB treatment results. Therefore, we decided to repeat the experiment in order to obtain an $^{\bullet}OH$ rate constant for the oxidation of thioanisole. In addition, we report pulse radiolysis results for the reduction of thioanisole by hydrated electrons and hydrogen atoms. With our experimentally obtained rate constants we were able to simulate the radiation chemical processes of a large scale EB treatment of thioanisole solutions and to compare the theoretical and experimental results.

TABLE I. BIMOLECULAR RATE CONSTANTS [$M^{-1}s^{-1}$] FOR HALOGENATED METHANES

Halo-	+ e_{aq}^{-}		+ $^{\bullet}OH$		+ $^{\bullet}H$	
Methane	Experimental	Literature	Experimental	Literature	Experimental	Literature
CH_3Cl		$\sim 8 \times 10^{8}$ [1] 1.1×10^{9} [1] 4.7×10^{8} [2] 1.2×10^{9} [3]		Not Found		6×10^{4} [4]
CH_2Cl_2	5.3×10^{9}	6.3×10^{9} [5]		5.8×10^{7} [6] 9×10^{7} [7] 9×10^{7} [8]		4×10^{6} [4]
$CHCl_3$	$(1.3 \pm 0.1) \times 10^{10}$ $(1.3 \pm 0.1) \times 10^{10}$	3×10^{10} [9]		$\sim 5 \times 10^{6}$ [10] 1.5×10^{7} [11] 7.4×10^{6} [12] 5.4×10^{7} [7] 5.0×10^{7} [7]	$(7.3 \pm 1.3) \times 10^{7}$	1.1×10^{7} [4]
CCl_4	±	1.3×10^{10} [13] 1.9×10^{10} [14] 2.4×10^{10} [15]		Not Found		4.4×10^{7} [4] 3.2×10^{7} [16]
CH_3Br		Not Found		Not Found		Not Found
CH_2Br_2		2×10^{10} [17]		9.9×10^{7} [7] 9.0×10^{7} [7]		4.1×10^{8} [17]
$CHBr_3$	$(2.2 \pm 0.2) \times 10^{10}$	1×10^{10} [18]		1.3×10^{8} [7] 1.1×10^{8} [18]	1.9×10^{9} [19]	Not Found
$CHBr_2Cl$	$(2.0 \pm 0.2) \times 10^{10}$	Not Found		Not Found		Not Found
$CHBrCl_2$	$(1.6 \pm 0.2) \times 10^{10}$	Not Found		Not Found		Not Found

TABLE II. BIMOLECULAR RATE CONSTANTS [$M^{-1}s^{-1}$] FOR HALOGENATED METHANES CONTAINING FLUORINE AND IODINE

Halo-	+ e_{aq}^{-}		$^{\bullet}$OH-		+ $^{\bullet}$H	
Methane	Experimental	Literature	Experimental	Literature	Experimental	Literature
CCl_3F		1.6×10^{10} [19]				1.6×10^{6} [20]
CCl_2F_2		1.4×10^{10} [19]				$<1.0 \times 10^{6}$ [20]
$CClF_3$		4.4×10^{9} [21]				$<1.0 \times 10^{6}$ [20]
CH_3I		1.6×10^{10}[22] 1.6×10^{10}[23]				1.1×10^{10} [24]
CH_2I_2		3.4×10^{10} [25] 3.4×10^{10}[26]		6.3×10^{9}[27] 2.1×10^{9}[27]		1.2×10^{10}[25]
CH_2ClI				4.0×10^{9}[28]		
CF_3I						

TABLE III. BIMOLECULAR RATE CONSTANTS [$M^{-1}s^{-1}$] FOR CARBON CENTRED RADICALS OF HALOGENATED METHANES

Halomethane Radicals	+O_2	
	Experimental	Literature
$^{\bullet}CH_2Cl$		1.9×10^{9} [29] 6.3×10^{9} [30]
$^{\bullet}CHCl_2$		4.7×10^{9} [30]
$^{\bullet}CCl_3$		3.3×10^{9} [31]
$^{\bullet}CH_2Br$		2×10^{9} [29]
$^{\bullet}CHBr_2$	2.1×10^{9} [32]	Not Found
$^{\bullet}CHBrCl$		Not Found

3.2.1. The reaction of thioanisole with $^{\bullet}$OH-radicals

The pulse radiolysis of aqueous, nitrous oxide-saturated thioanisole $CH_3S\text{-}C_6H_5$ (TA) solutions in the concentration range of 1×10^{-4}M to 1×10^{-3}M yields a complex spectrum of intermediates with absorption maxima at 310 nm, 365 nm and 530 nm. Ioele and co-workers [39] as well as Mohan and Mittal [40] assigned these absorptions to a radical cation $TA^{\bullet+}$ absorbing at 310 nm and 530 nm (reaction 6):

$$CH_3S\text{-}C_6H_5 + {}^{\bullet}OH \longrightarrow \underset{310\ \&\ 530\ \text{nm}}{[CH_3S\text{-}C_6H_5]^{\bullet+}} + OH^{-} \qquad (6)$$

and an $^{\bullet}OH$ radical addition product $TA(OH)^{\bullet}$ absorbing at 365 nm (reaction 7)

$$CH_3S\text{-}C_6H_5 \quad + \quad {}^{\bullet}OH \longrightarrow \quad \underset{365\ \text{nm}}{CH_3S\text{-}C_6H_5(OH)^{\bullet}} \qquad (7)$$

Another possible reaction pathway for $^{\bullet}OH$-radicals attacking thioanisole is an H-atom abstraction at the methyl site:

$$CH_3S\text{-}C_6H_5 \quad + \quad {}^{\bullet}OH \longrightarrow \quad \underset{260\ \text{nm}}{{}^{\bullet}CH_2S\text{-}C_6H_5} \quad + \quad H_2O \qquad (8)$$

Results of Ioele and co-workers [39] regarding a reaction of $SO_4^{\bullet-}$ with thioanisole suggest the possibility of this reaction pathway. In addition, hydrogen abstraction products from carbon atoms adjacent to sulphur normally exhibit an absorption maximum at around 280 nm. Data from our absorption spectrum cannot positively identify such a product because only a weak absorption at around 260 nm is observable. However, a comparison of the time traces at 260 nm and for the radical cation $TA^{\bullet+}$ absorbing at 310 nm reveals a significant difference regarding the growth kinetics, i.e. the growth at 310 nm is twice as fast as at 260 nm. On this basis, we suggest a hydrogen abstraction by $^{\bullet}OH$-radicals as a third and minor reaction pathway.

Bimolecular rate constants for the reaction of $^{\bullet}OH$-radicals with thioanisole were determined using two methods:

1) directly: by plotting of pseudo-first order rate constants at 310, 365 and 530 nm versus different thioanisole concentrations (range 1×10^{-4}M to 1×10^{-3}M) and 2) indirectly: via a competition for the $^{\bullet}OH$-radical between the scavenger *tert*-Butanol and thioanisole and plotting of the resulting absorption ratios A_0/A at 310, 365 and 530 nm versus the corresponding concentration ratio [t-ButOH]/[TA]. A_0 is the absorption value of the generated intermediate at the respective wavelength without scavenger, whereas A is a decreased absorption of this intermediate due to increased amounts of the competing scavenger. The slopes of the resulting lines and the bimolecular rate constant for a reaction of *tert*-butanol with $^{\bullet}OH$ radicals [25] ($k_3 = 6 \times 10^8\ M^{-1}s^{-1}$) are used to calculate bimolecular rate constants for the reaction of thioanisole with $^{\bullet}OH$-radicals (Table IV).

Since the 310 nm and 365 nm absorptions are in close vicinity to each other, an overlap of the two absorptions can be assumed. We corrected the values by only considering the influence of the strong radical cation absorption with a maximum at 310 nm on the weaker absorption at 365 nm. From the work of Ioele and co-workers [15] an absorption ratio for the radical cation absorption at 310 nm versus the absorption of the same radical cation species at 365 nm was estimated at 9200:500. Our 310 nm absorption value was multiplied by this factor and then subtracted from the 365 nm absorption value. Furthermore, an H-atom adduct to the benzene ring, which we will describe in a later section, also absorbs at exactly the same wavelength (365 nm). In order to account for this absorption, a residue value at 365 nm was obtained with an excess of *tert*-butanol (0.5 mol L^{-1} *tert*-butanol vs. 1 mmol L^{-1} thioanisole), assuming that all $^{\bullet}OH$-radicals reacted with *tert*-butanol and the resulting residue absorption value was due to the hydrogen addition product. This value was also subtracted from each 365 nm absorption maxima.

TABLE IV. BIMOLECULAR RATE CONSTANTS DETERMINED AT 310, 365 AND 530 nm AND MAXIMUM ABSORPTIONS AT THESE WAVELENGTHS

Wavelength λ (nm)	Rate Constant ($M^{-1}s^{-1}$) (Direct Method)	Rate Constant ($M^{-1}s^{-1}$) (Indirect Method)	Maximum Absorption, Gxε (Molecules $(100\ eV)^{-1}M^{-1}cm^{-1}$)
310	$(1.20\pm0.1) \times 10^{10}$	$(1.0\pm0.1) \times 10^{10}$	3.44×10^{4}
365	$(6.40\pm0.65) \times 10^{9}$	$(7.90\pm0.75) \times 10^{9}$	1.38×10^{4} [a]
530	$(1.10\pm0.1) \times 10^{10}$	$(1.0\pm0.1) \times 10^{10}$	1.48×10^{4}

[a] Corrected value (correction – see below).

The rate constants (Table IV) obtained at 310 nm and 530 nm by two different experimental methods are nearly identical. Their average is:

$$k(TA+{}^{\bullet}OH) = (1.10\pm0.1) \times 10^{10}\ M^{-1}s^{-1}$$

This value indicates a practically diffusion controlled reaction of $^{\bullet}$OH-radicals with thioanisole. Thus, we assume this value to be the observed or overall rate constant $k_{obs}(TA+{}^{\bullet}OH)$ to be used in all subsequent calculations.

One can compare our rate constant $(1.10\pm0.1) \times 10^{10}\ M^{-1}s^{-1}$ for the TA radical cation formation with those of other one-electron oxidizing agents either reacting with thioanisole, e.g. $3.9 \times 10^{9}\ M^{-1}s^{-1}$ for $SO_4^{\bullet-}$ [39], $>1.5 \times 10^{9}\ M^{-1}s^{-1}$ for Tl^{2+} [39], and $3.0 \times 10^{9}\ M^{-1}s^{-1}$ for $CH_3I^{\bullet+}$ [42], or reacting with anisole, e.g. $5.0 \times 10^{9}\ M^{-1}s^{-1}$ for $SO_4^{\bullet-}$ [43] and $5.0 \times 10^{8}\ M^{-1}s^{-1}$ for Tl^{2+} [43]. Although most of these rate constants are in the same order of magnitude, our rate constant is at least twice as high as any other value. We attribute this difference to the nature of the oxidants themselves.

Our rate constant for the $^{\bullet}$OH adduct formation on thioanisole $(7.90\pm0.75) \times 10^{9}\ M^{-1}s^{-1}$ can be compared to a similar reaction of anisole CH_3O-C_6H_5 with $^{\bullet}$OH-radicals. A value of $5.4 \times 10^{9}\ M^{-1}s^{-1}$ was reported by O'Neill and co-workers [43], which is slightly lower than the one for the thioanisole $^{\bullet}$OH adduct. The electron density at the benzene ring should have a great influence on the reaction rate of the $^{\bullet}$OH addition. Sulphur compared with oxygen has filled d-orbitals and the exchange of CH_3O- by CH_3S- in thioanisole induces an increase in electron density at the benzene ring. As observed, the rate constant of the $^{\bullet}$OH addition on thioanisole is increased versus the same reaction with anisole. To further illustrate the impact of the electron density at the benzene ring, one can compare the $^{\bullet}$OH-addition rate constants of phenol and phenoxide ions. The phenol rate constant $6.6 \times 10^{9}\ M^{-1}s^{-1}$ is higher than the one for anisole due to an increased mesomeric induction of electron density in the benzene ring [44]. Deprotonation of phenol leads to phenoxide ions with an even more increased electron density induction and a respective rate increase to $9.6 \times 10^{9}\ M^{-1}s^{-1}$ [45].

In contrast to our results, Mohan and Mittal [40] reported one rate constant for a reaction of thioanisole with $^{\bullet}$OH radicals of $3.5 \times 10^{9}\ M^{-1}s^{-1}$ measured directly by fitting their experimental data with exponential first order growth curves for all absorptions (310 nm, 365 nm, 530 nm and 740 nm). Unfortunately they did not account for absorption overlaps nor the influence of an H-atom adduct on thioanisole.

Further experiments were carried out to investigate the influence of oxygen on the growth and decay characteristics of the different absorptions, and to observe a growth of possible additional reaction products. Even at the highest O_2-concentration (O_2-saturation) we could not detect any influence on the growth or decay kinetics at 310 nm, 365 nm and 530 nm nor did any new intermediates appear. The only observable change was a slight decrease in the 365 nm absorption due to an H-atom scavenging competition between oxygen and thioanisole (see next section for the reaction of H-atoms with thioanisole).

3.2.2. The reaction of thioanisole with hydrogen atoms

These experiments were carried out in N_2-saturated, oxygen-free thioanisole solutions at pH1, where most of the hydrated electrons are converted into hydrogen atoms according to reaction (4). Additionally, the solutions contained 0.5 mol L^{-1} *tert*-butanol to scavenge $^{\bullet}$OH-radicals. An intermediate spectrum was obtained 3.5μs after the electron pulse, which exhibits a strong absorption with a maximum also at 365 nm (similar to the previously described $^{\bullet}$OH-radical adduct). In addition, weak absorptions were present at 260, 310 and 530 nm. The latter two absorptions were due to the reaction of thioanisole with $^{\bullet}$OH-radicals, since *tert*-butanol is not able to scavenge all $^{\bullet}$OH-radicals under the applied conditions (0.5 mol L^{-1} *tert*-butanol vs. 1 mmol L^{-1} thioanisole, approximately 3.2% of all $^{\bullet}$OH-radicals are reacting with thioanisole. This minor reaction pathway cannot account for the observed strong absorption at 365 nm.).

We attribute the observed absorption at 365 nm to an adduct of hydrogen atoms at the benzene ring. This addition reaction is very similar to the previously described reaction of $^{\bullet}$OH-radicals, which is mainly due to the similarities between $^{\bullet}$OH-radicals and H-atoms in their electrophilic reactions.

$$CH_3S\text{-}C_6H_5 \;+\; {}^{\bullet}H \;\longrightarrow\; \underset{365\ \text{nm}}{CH_3S\text{-}C_6H_5(H)^{\bullet}} \qquad (9)$$

In general, the predominant pathway of a reaction between aromatic compounds and hydrogen atoms is by addition to the aromatic ring [46–53]. Several pulse radiolytic studies have been carried out in which formation of the cyclohexadienyl type radical was directly observed [47, 48, 50, 53]. In order to determine the rate constant of the adduct formation, we directly fitted the actual absorption time traces for different substrate concentrations with first order exponential curves obtaining pseudo-first order growth rate constants. A plot of these rate constants versus different thioanisole concentrations yields a straight line with a bimolecular growth rate constant of $(1.20 \pm 0.07) \times 10^9\ M^{-1}s^{-1}$ as the slope. Our estimated rate constant for the $^{\bullet}$H-adduct formation compares favourably to a number of similar reactions, e.g. the $^{\bullet}$H-addition to benzene ($1.1 \times 10^9\ M^{-1}s^{-1}$) [53], phenol ($1.4 \times 10^9\ M^{-1}s^{-1}$) [54], anisole ($1.2 \times 10^9\ M^{-1}s^{-1}$) [54] and nitrobenzene ($1.04 \times 10^9\ M^{-1}s^{-1}$) [50].

As well as $^{\bullet}$OH-radicals in reaction (7) hydrogen atoms by itself are able to abstract a hydrogen atom from the thiomethyl group:

$$TA \;+\; {}^{\bullet}H \;\longrightarrow\; \underset{260\ \text{nm}}{{}^{\bullet}CH_2S\text{-}C_6H_5} \;+\; H_2 \qquad (10)$$

A comparable weak absorption between 250 and 300 nm of a possible hydrogen abstraction product is observed in the spectrum. Unfortunately this absorption is too weak to be characterized quantitatively and therefore we cannot exclude a reaction pathway according to reaction (9). On this basis we have to assume the above estimated rate constant for a reaction of thioanisole with hydrogen atoms to be an overall rate constant.

3.2.3. The reaction of thioanisole with hydrated electrons

To study hydrated electron reactions, pulse radiolytic experiments were carried out in N_2-saturated, oxygen free thioanisole solutions with an addition of 0.5 mol L^{-1} *tert*-butanol to scavenge $^{\bullet}OH$-radicals. In the UV/visible range the spectra at various times after the electron pulse show only the very strong absorption of hydrated electrons. Their decay under the above stated conditions is dependent on the thioanisole concentrations (concentration range 0.1–1 mM). A plot of the pseudo-first order decay rate constants for the decay of the hydrated electrons versus different thioanisole concentrations yields a straight line with a slope of $k(TA+e_{aq}^{-})=(3.10\pm0.3) \times 10^{8}\ M^{-1}s^{-1}$.

Our rate constant was significantly higher than those of other benzene containing compounds reacting with hydrated electrons, e.g. benzene $1.2 \times 10^{7}\ M^{-1}s^{-1}$ [55], toluene $1.2 \times 10^{7}\ M^{-1}s^{-1}$ [55], phenol $1.8 \times 10^{7}\ M^{-1}s^{-1}$ [55], anisole $<3 \times 10^{5}\ M^{-1}s^{-1}$ [56], and aniline $2.6 \times 10^{7}\ M^{-1}s^{-1}$ [55]. The determined value is also higher than comparable aliphatic sulphides undergoing the same reaction [57]. We concluded from these comparisons that an aromatic ring coupled with a thioether moiety as in thioanisole offers a unique enhancement towards reductions by hydrated electrons.

3.2.4. Large scale EB treatment

Figures 1 and 2 summarize the results of large scale EB treatments at pH5 and pH9. In both cases a distinctive relationship between the applied radiation dose and a resulting thioanisole concentration in the irradiated samples was observed, i.e. the thioanisole concentration decreased exponentially with increasing radiation dose. This behaviour was similar to that observed in similar EB treatment of other low molecular weight organic pollutants [58]. The amount of substrate removed (removal efficiency) though differs depending on the pH. At the lower pH of 5 the thioanisole removal is more efficient than at pH9. As an example, a radiation dose of 200 krad at pH5 is sufficient to remove 99+% of thioanisole compared to 300 krad at pH9. This takes into account overall low influent thioanisole concentrations with equal or similar values at both pH, e.g. 80.0 μmol L^{-1} (9.40 ppm) at pH5 and 87.0 μmol L^{-1} (10.20 ppm) at pH9, respectively. Differences in alkalinity are believed to be one probable reason for a lower removal efficiency at pH9 when compared to the results at pH5 [32]. Experimentally we found the alkalinity varied between 40 and 60 mg L^{-1}. At pH9 one should expect a carbonate/bicarbonate ratio of about 1:4. Since these ions themselves scavenge $^{\bullet}OH$ radicals [59, 60] and hydrated electrons [61, 62] this interaction will have a negative influence on the thioanisole removal. At a pH of 5, carbonate and bicarbonate ion concentrations are very negligible because of their transformation into CO_2, which in turn dissipates to the atmosphere in the stirring process. This removal of additional scavenger in the substrate solution should lead to the observed higher thioanisole removal efficiency at pH5.

It should be noted that the actual non-irradiated influent concentrations differed considerably from our initial estimate of 170.40 μmol L^{-1} (20.0 ppm) which was calculated for an addition of 340 ml thioanisole to 17 m^3 water. This concentration decrease is consistent in all influent samples as well as in the blank effluent samples. We attribute this to an incomplete dissolution and mixing process, evaporation losses and absorption of the thioether substrate by the metal piping system.

3.2.5. Removal simulation and kinetic modelling

On the basis of known radiation chemical reactions in pure water and considering the interference from additional radical scavengers in drinking water — like oxygen, carbonate ion, bicarbonate ion, DOC, etc. — one is able to derive a simplified reaction mechanistic model for EB irradiated water [32]. The computer code MAKSIMA-CHEMIST uses this model along with our experimentally estimated rate constants for reactions of thioanisole with $^{\bullet}OH$ and $^{\bullet}H$ radicals and hydrated electrons (reactions 11–13) in addition to all other rate constants known from literature.

$$CH_3S\text{-}C_6H_5 + {}^{\bullet}OH \longrightarrow \text{Products}; \quad k_{obs}=1.10 \times 10^{10}\ M^{-1}s^{-1} \qquad (11)$$

$$CH_3S\text{-}C_6H_5 + {}^{\bullet}H \longrightarrow \text{Products}; \quad k_{obs}=1.20 \times 10^{9}\ M^{-1}s^{-1} \qquad (12)$$

$$CH_3S\text{-}C_6H_5 + e^{-}_{aq} \longrightarrow \text{Products}; \quad k_{obs}=3.10 \times 10^{8}\ M^{-1}s^{-1} \qquad (13)$$

The removal simulation results for thioanisole under the experimental conditions at pH5 and 9 are plotted in Figures 1 and 2 together with the actual experimental destruction curves. At pH5 we find good agreement between experimental and simulated thioanisole concentration values. The same model overestimates the removal efficiency at pH9. We have observed this discrepancy in removal prediction at lower pH versus an overestimation at a higher pH in several different classes of compounds [63]. We therefore attribute this discrepancy to a pH dependent process in the potable water itself. One possibility for an additional scavenger at pH9 compared to pH5 is monochloramine. So far, our simulations are not able to account for an interaction of this solute due to lack of rate constant information in the literature. Chloramines, a common disinfectant, are stable in a pH range of 8 to 9 and decompose in an irreversible reaction into nitrogen, chloride and nitrite/nitrate at a pH below 8 [64, 65]. Experimentally we were able to determine the presence of chloramines at the higher pH, but not at pH5. Currently experiments are under way to estimate rate constants of the different chloramines with $^{\bullet}OH$ and $^{\bullet}H$ radicals and hydrated electrons in order to quantify their scavenging influence in an EB treatment.

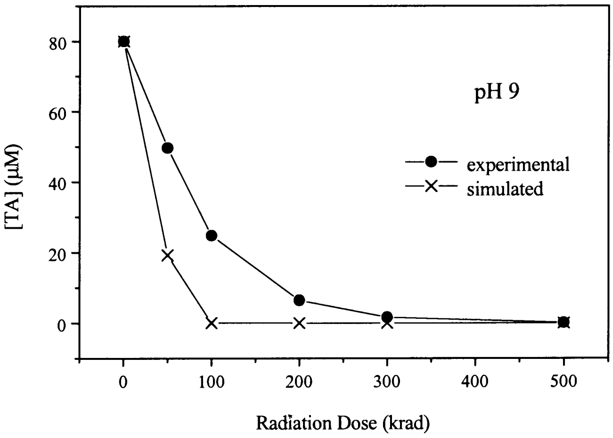

FIG. 1. Experimental (.) and simulated (x) thioanisole concentration changes in potable water upon radiation with an EB at different radiation doses at pH9.

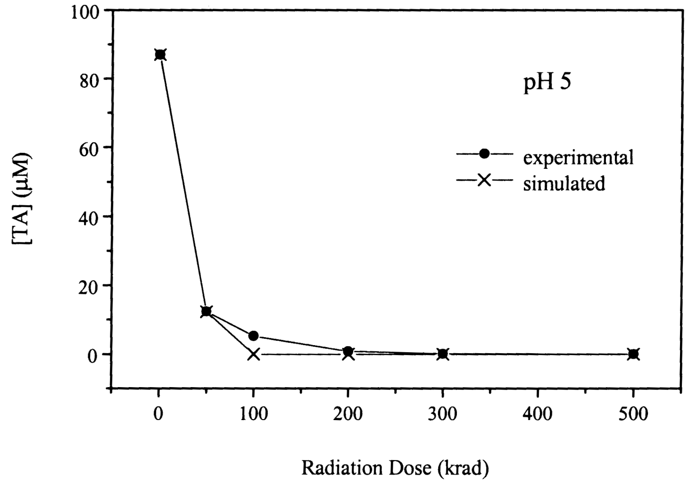

FIG. 2. Experimental (.) and simulated (X) thioanisole concentration changes in potable water upon radiation with an EB at different radiation doses at pH5.

3.3. Methyl tert-butyl ether

3.3.1. The reaction of MTBE with ${}^{\bullet}$OH-radicals

The Pulse Radiolysis of aqueous, nitrous oxide-saturated MTBE solutions yields a radical spectrum which exhibits only a single absorption with a maximum at 260 nm. This absorption is very long-lived and shows a dose rate dependent decay.

$$(CH_3)_3COCH_3 \quad + \quad {}^{\bullet}OH \xrightarrow[-H_2O]{} \underset{\mathbf{A}}{(CH_3)_3COC^{\bullet}H_2} \tag{14}$$

$$(CH_3)_3COCH_3 \quad + \quad {}^{\bullet}OH \xrightarrow[-H_2O]{} \underset{\mathbf{B}}{{}^{\bullet}CH_2(CH_3)_2COCH_3} \tag{15}$$

$$\mathbf{A/B} \quad + \quad TNM \longrightarrow NF^- \quad + \quad \text{products} \tag{16}$$

We attribute this absorption to the carbon-centred radicals A and B, which are formed in a mechanism suggested by Eibenberger et al. [66]. Since it is only a very weak absorption we determined the bimolecular rate constant for the reaction between ${}^{\bullet}$OH-radicals and MTBE in competition with thiocyanate anions (SCN^-). From the slope of the straight line obtained from plotting the absorption ratio $A_0[(SCN)_2^{\bullet-}]/A[(SCN)_2^{\bullet-}]$ versus the concentration ratio $[MTBE]/[SCN^-]$ and the bimolecular rate constant for the reaction of thiocyanate with ${}^{\bullet}$OH of $k^{II}(SCN^- + {}^{\bullet}OH) = 1.1 \times 10^{10}$ $M^{-1}s^{-1}$ we obtained a bimolecular rate constant of $k^{II}(MTBE + {}^{\bullet}OH) = 2.0 \times 10^9$ $M^{-1}s^{-1}$. Our rate constant is in good agreement with 1.6×10^9 $M^{-1}s^{-1}$ for this reaction reported by Eibenberger [66].

In the presence of oxygen the absorption at 260 nm is increased by a factor of 3. In contrast to an anticipated accelerated decay of the carbon-centred radicals in a reaction with oxygen a growth of an absorption is observable. This growth depends on the oxygen concentration. A plot of the pseudo-first order growth rate versus different O_2^- concentrations yields a straight line (Fig. 3) with a slope of 1.2×10^9 $M^{-1}s^{-1}$. We attribute this absorption to a formation of alkylperoxy radicals according to

$$\mathbf{A} + O_2 \longrightarrow (CH_3)_3COC(OO^{\bullet})H_2 \quad (17)$$

and

$$\mathbf{B} + O_2 \longrightarrow {}^{\bullet}OOCH_2(CH_3)_2COCH_3 \quad (18)$$

and the slope gives the overall rate constant of these two processes. To the best of our knowledge there exists no account describing the absorption of such alkylperoxy radicals in water. Eibenberger [66] suggests a ratio of **A**:**B** = 71:29 for aqueous solutions and since we used aqueous solutions in all our experiments we took the results of Eibenberger as the basis for further calculations.

3.3.2. The reaction of MTBE with hydrated electrons

The Pulse Radiolytic experiments were carried out in N_2-saturated, oxygen free MTBE solutions with an addition of 0.5 mol/l *tert*-butanol to scavenge $^{\bullet}$OH-radicals. The decay of the hydrated electron signal in these solutions depends on the MTBE concentration. A plot of the pseudo-first order decay rate constants at different substrate concentrations versus these concentrations yields a straight line with a slope of $k^{II}(\text{MTBE}+e^-_{aq}) = 1.75 \times 10^7\ M^{-1}s^{-1}$ (Fig. 4). Our rate constant can be compared with a limiting rate constant value for diethyl ether of $k^{II}(\text{diethyl ether}+e^-_{aq}) < 1.0 \times 10^7\ M^{-1}s^{-1}$ and is therefore in the same order of magnitude.

The respective spectrum shows only a very weak absorption with a maximum also around 260 nm besides the very strong absorption of the hydrated electrons. A very high concentration of MTBE was chosen to compete with the “normal” electron decay in water (approximate first order decay rate constant of hydrated electrons: $2 \times 10^5\ s^{-1}$). Under these conditions a substantial amount of $^{\bullet}$OH-radicals are also scavenged by MTBE and therefore lead to the previously described absorption at 260 nm, accounting for our observations.

Since we are attributing an absorption to carbon-centred radicals, the possibility of radicals coming from *tert*-butanol and contributing to this absorption has to be eliminated, since those radicals only differ in a replacement of a methyl group by hydrogen compared to radical **B**. Spectra of *tert*-butanol solutions alone under various pH conditions and at various times after the electron pulse did not yield an absorption maximum around 260 nm, though one could observe a steady rise of an absorption towards the lower wavelength region. This last finding could serve as further evidence that the H-atom abstraction takes place mostly at the methoxy-site of MTBE.

A possible mechanism for the reaction between MTBE and hydrated electrons could be a dissociative electron capture according to

$$(CH_3)_3COCH_3 + e^-_{aq} \longrightarrow (CH_3)_3C^{\bullet} + {}^-OCH_3 \quad (19)$$

with a subsequent protonation of methanolate

$${}^-OCH_3 + H_2O \longrightarrow HOCH_3 + OH^- \quad (20)$$

3.3.3. The reaction of MTBE with hydrogen atoms

These experiments were carried out with N_2-saturated, oxygen free substrate solutions at pH1, where most of the hydrated electrons are converted into hydrogen atoms according to reaction (7). In addition, these solutions contain 0.5mol/l *tert*-butanol to scavenge ${}^{\bullet}OH$-radicals. During Pulse Radiolysis we could only observe the 260 nm absorption, which was due to partial scavenging of ${}^{\bullet}OH$-radicals by MTBE. One would expect an additional increase of the 260 nm-absorption, because H-atoms can also abstract hydrogen according to

$$(CH_3)_3COCH_3 \quad + \quad {}^{\bullet}H \quad \xrightarrow[-H_2]{} \quad \underset{\mathbf{A}}{(CH_3)_3COC^{\bullet}H_2} \qquad (21)$$

$$(CH_3)_3COCH_3 \quad + \quad {}^{\bullet}H \quad \xrightarrow[-H_2]{} \quad \underset{\mathbf{B}}{{}^{\bullet}CH_2(CH_3)_2COCH_3} \qquad (22)$$

Unfortunately we could not observe this increase. Furthermore we were not able to determine a rate constant value for a reaction between hydrogen atoms and MTBE. In a competition reaction we monitored absorption changes at 410 nm of an H-atom adduct on p-benzoquinone depending on the MTBE concentration. We did not observe any decrease of this absorption with increasing MTBE concentrations. On the contrary, at high substrate concentrations the absorption at 410 nm started to increase due to a scavenging of ${}^{\bullet}OH$ radicals by MTBE and a subsequent reaction of those carbon-centred radicals with p-benzoquinone to form an absorption at 430 nm. This type of reaction is known for C-centred radicals obtained from methanol, ethanol and isopropanol, but carbon-centred radicals from *tert*-butanol react only very slowly or not at all with p-benzoquinone. The absoption at 430 nm is further evidence for the reaction site of ${}^{\bullet}OH$-radicals at the methoxy group of MTBE.

Assuming that the expected decrease in the 410 nm absorption of p-benzoquinone, which is competing with MTBE for hydrogen atoms, is not compensated by the absorption increase around 430 nm for MTBE(–H) + p-benzoquinone, we can calculate a limiting rate constant value for a reaction between MTBE and H-atoms. We did not see any change in the 410 nm absorption up to an MTBE concentration of 50 times the p-benzoquinone concentration. Furthermore, assuming that we would be able to observe an absorption change around 410 nm if 10% of the hydrogen atoms would react with MTBE, we can calculate a limiting value as follows:

$$k^{II}(\text{MTBE}+{}^{\bullet}H) = 0.1 \times (1/50) \times k^{II}(\text{p-benzoquinone}+{}^{\bullet}H)$$

With an experimentally estimated value of $k^{II}(\text{p-benzoquinone}+{}^{\bullet}H) = 4.0 \times 10^{9}\ M^{-1}s^{-1}$ (same experimental conditions as applied in the competition kinetics measurements) we calculated a limiting value of:

$$k^{II}(\text{MTBE}+{}^{\bullet}H) = 8.0 \times 10^{6}\ M^{-1}s^{-1}$$

This result is only a very rough estimate mainly because of the competition with p-benzoquinone and its interfering reaction as described above.

These data have been incorporated into a kinetic model that describes the removal of MTBE in aqueous solution. The reactions that we have used and the kinetic model that has been developed is summarized in Table V, in 81 equations:

TABLE V. KINETIC MODEL FOR THE DESCRIPTION OF THE RADIOLYTIC DESTRUCTION OF METHYL *TERT*-BUTYL ETHER IN AQUEOUS SOLUTION

No.	Reactants	Products	k ($M^{-1}\ s^{-1}$)	
1	$\cdot OH + H_2$	$H\cdot + H_2O$	4.000e+07	Pure Water Reactions
2	$\cdot OH + H_2O_2$	$O_2^{-}\cdot + H_2O$	2.700e+07	
3	$\cdot OH + HO_2^{-}$	$H_2O + O_2^{-}\cdot$	7.500e+09	
4	$\cdot OH + O_2^{-}\cdot$	$O_2 + OH^{-}$	1.100e+10	
5	$\cdot OH + H_2O_2^{+}$	$O_2 + H_3O^{+}$	1.200e+10	
6	$\cdot OH + HO_2\cdot$	$O_2 + H_2O$	1.000e+10	
7	$\cdot OH + \cdot OH$	H_2O_2	5.500e+09	
8	$\cdot OH + OH^{-}$	$H_2O + O^{-}\cdot$	1.300e+10	
9	$\cdot OH + O^{-}\cdot$	HO_2^{-}	2.000e+10	
10	$O^{-}\cdot + H_2O$	$\cdot OH + OH^{-}$	9.300e+07	
11	$O^{-}\cdot + HO_2^{-}$	$O_2^{-}\cdot + OH^{-}$	4.000e+08	
12	$O^{-}\cdot + H_2$	$e^{-}_{aq} + H_2O$	1.200e+08	
13	$O^{-}\cdot + H_2O_2$	$O_2^{-}\cdot + H_2O$	2.700e+07	
14	$O^{-}\cdot + O^{-}\cdot$	$2OH^{-} + O_2$	6.000e+08	
15	$e^{-}_{aq} + H\cdot$	$H_2 + OH^{-}$	2.500e+10	
16	$E^{-}_{aq} + e^{-}_{aq}$	$2OH^{-} + H_2$	5.500e+09	
17	$e^{-}_{aq} + O_2$	$O^{-}\cdot$	1.900e+10	
18	$e^{-}_{aq} + H_2O_2$	$\cdot OH + OH^{-}$	1.200e+10	
19	$E^{-}_{aq} + O_2^{-}\cdot$	O_2^{2-}	1.300e+10	
20	$e^{-}_{aq} + H^{+}$	$H\cdot$	2.300e+10	
21	$e^{-}_{aq} + H_2O$	$H\cdot + OH^{-}$	8.900e+02	
22	$e^{-}_{aq} + HO_2^{-}$	$\cdot OH + 2OH^{-}$	3.500e+09	
23	$e^{-}_{aq} + \cdot OH$	OH^{-}	3.000e+10	
24	$e^{-}_{aq} + O^{-}\cdot$	$2OH^{-}$	2.200e+10	
25	$H\cdot + O_2$	$HO_2\cdot$	2.100e+10	
26	$H\cdot + O_2^{-}\cdot$	$HO_2^{-}\cdot$	2.000e+10	
27	$H\cdot + H\cdot$	H_2	5.000e+09	
28	$H\cdot + \cdot OH$	H_2O	7.000e+09	
29	$H\cdot + HO_2\cdot$	H_2O_2	1.000e+10	
30	$H\cdot + H_2O_2$	$H_2O + \cdot OH$	9.000e+07	
31	$H\cdot + OH^{-}$	$e^{-}_{aq} + H_2O$	2.200e+07	
32	$H\cdot + H_2O$	$H_2 + \cdot OH$	1.000e+01	
33	$HO_2\cdot + O_2^{-}\cdot$	$O_2 + H_2O_2 + OH^{-}$	9.700e+07	
34	$HO_2\cdot + HO_2\cdot$	$H_2O_2 + O_2$	8.300e+05	
35	$HO_2\cdot$	$H^{+} + O_2^{-}\cdot$	8.000e+05	
36	$H^{+} + O_2^{-}\cdot$	$HO_2\cdot$	4.500e+10	
37	$H^{+} + HO_2^{-}\cdot$	H_2O_2	2.000e+10	
38	$H^{+} + OH^{-}$	H_2O	1.430e+11	
39	H_2O_2	$H^{+} + HO_2^{-}$	3.560e-02	

No.	Reactants	Products	k (M^{-1} s^{-1})	
40	H_2O	$OH^- + H^+$	2.600e-05	
41	$HCO_3^- + \cdot OH$	$CO_3^-\cdot + H_2O$	8.500e+06	Alkalinity Reactions
42	$HCO_3^- + e^-_{aq}$	PDTS	1.000e+06	
43	$HCO_3^- + H\cdot$	PDTS	4.400e+04	
44	$CO_3^{2-} + \cdot OH$	$CO_3^-\cdot + OH^-$	3.900e+08	
45	$CO_3^{2-} + e^-_{aq}$	PDTS	3.900e+05	
46	$CO_3^-\cdot + \cdot OH$	PDTS	3.000e+09	
47	$CO_3^-\cdot + O_2^-\cdot$	$O_2 + CO_3^{2-}$	6.500e+08	
48	$CO_3^-\cdot + H_2O_2$	$HCO_3^- + HO_2\cdot$	8.000e+05	
49	$CO_3^-\cdot + HO_2^-$	$HCO_3^- + O_2^-\cdot$	5.600e+07	
50	$CO_3^-\cdot + CO_3^-\cdot$	PDTS	2.000e+07	
51	$DOC + e^-_{aq}$	PDTS	1.000e+07	DOC Reactions
52	$DOC + H\cdot$	PDTS	1.000e+07	
53	$DOC + \cdot OH$	PDTS	2.000e+08	
54	$NO_3^- + e^-_{aq}$	NO_3^{2-}	9.700e+09	Nitrate Ion Reactions
55	$NO_3^- + H\cdot$	PDTS	1.400e+06	
56	$NO_3^{2-} + O_2$	$O_2^- + NO_3^-$	2.200e+08	
57	$Br^- + H\cdot$	PDTS	2.800e+07	Bromide Ion Reactions
58	$Br^- + \cdot OH$	PDTS	1.100e+10	
59	$NH_2Cl + e^-_{aq}$	PDTS	1.000e+08	Chloramine Reactions
60	$NH_2Cl + \cdot OH$	PDTS	1.000e+08	
61	$MTBE + \cdot OH$	$MTBE\cdot + H_2O$	2.000e+09	MTBE Reactions
62	$MTBE + H\cdot$	$MTBE\cdot + H_2$	1.000e+05	
63	$MTBE + e^-_{aq}$	$MTBE^-$	1.750e+07	
64	$MTBE\cdot + DOC$	MTBE + PDTS	0.000e+00	(MTBE Reformation)
65	$MTBE\cdot + O_2$	$MTBO_2\cdot$	1.240e+09	
66	$MTBO_2\cdot$	TBA + F	1.000e+05	
67	$TBA + \cdot OH$	$TBA\cdot + H_2O$	6.000e+08	
68	$TBA + H\cdot$	$TBA\cdot + H_2$	1.700e+05	
69	$TBA + e^-_{aq}$	PDTS	4.000e+05	
70	$TBA + CO_3^-\cdot$	PDTS	1.600e+02	
71	$TBA\cdot + O_2$	$TBAO_2\cdot$	1.500e+09	
72	$TBAO_2\cdot + H_2O$	$TB(OH)_2$	4.500e+10	
73	$F + \cdot OH$	FA	1.000e+09	
74	$F + H\cdot$	$\cdot CHO + H_2$	5.000e+06	
75	$F + e^-_{aq}$	$\cdot CH_2OH + OH^-$	1.000e+07	
76	$FA + \cdot OH$	CO_2	1.300e+08	
77	$FA + H\cdot$	$CO_2 + H_2 + H\cdot$	4.400e+05	
78	$FA + e^-_{aq}$	FA^-	1.400e+08	
79	$\cdot CH_2OH + O_2$	$HOCH_2OO\cdot$	4.900e+09	
80	$HOCH_2OO\cdot$	$F + H_3O^+ + O_2^-$	3.000e+00	
81	$HOCH_2OO\cdot + OH^-$	${}^-OCH_2OO\cdot + H_2O$	1.800e+10	

Using this model we have accurately predicted the destruction of MTBE in aqueous solutions at 0.45 m^3/min. There are improvements that we need to make; however, it appears that this will be completed within the next year. Once this model is completed we should be able to predict removal of the MTBE, formation and destruction of the reaction by-products in waters from any source.

4. CONCLUSIONS

We have reported several new and re-evaluated rate constants for halogenated methanes. In particular, the one reported for $CHCl_3$ was found to be the rate constant predicted from large scale studies. We continue to evaluate more rate constants as we continue to develop the EB process for the destruction of organic pollutants and, in drinking water, for drinking water disinfection by-products.

We have shown that the EB treatment can remove thioanisole from drinking water. In order to predict a removal efficiency, the respective rate constants for a reaction of thioanisole with $^{\bullet}OH$ and $^{\bullet}H$ radicals and hydrated electrons were estimated via pulse radiolysis and used in a kinetic model. This model is able to describe the experimental EB treatment results at the lower pH5, but overestimates the thioanisole removal at pH9. Monochloramine, which is present at pH9 but not at pH5, may scavenge $^{\bullet}OH$ and $^{\bullet}H$ radicals and hydrated electrons. This could therefore lead to the observed decreased removal efficiency of thioanisole at pH9.

We have also evaluated several new rate constants for the e^-_{aq} attachment to halogenated methanes. These should be helpful in studies we shall undertake in the near future. We have also shown that an EB treatment can remove thioanisole and MTBE from drinking water. In order to predict a removal efficiency the respective rate constants for a reaction of thioanisole and MTBE with $^{\bullet}OH$ and $^{\bullet}H$ radicals and hydrated electrons were estimated via pulse radiolysis and used in a kinetic model. This model is able to describe the experimental EB treatment results at the lower pH5, but overestimates the thioanisole and MTBE removal at pH9. Monochloramine, which is present at pH9 but not at pH5 may scavenge $^{\bullet}OH$ and $^{\bullet}H$ radicals and hydrated electrons. This could therefore lead to the observed decreased removal efficiency of thioanisole at pH9.

ACKNOWLEDGEMENTS

We thank the US National Science Foundation for partial support of this project. Two projects supported portions of this research, the most recent one of which was BES 97-29965. Large scale studies could not have been possible without the support of the Miami-Dade Water and Sewer Department.

REFERENCES

[1] BALKAS, T.I., FENDLER, J.H., SCHULER, R.H., Radiolysis of aqueous solutions of methyl chloride. The concentration dependence for scavenging electrons within spurs. J. Phys. Chem. **74** (1970) 4497–505.

[2] SCHMIDT, K.H., HAN, P., BARTELS, D.M., Radiolytic yields of the hydrated electron from transient conductivity: Improved calculation of the hydrated electron diffusion coefficient and analysis of some diffusion-limited (e-)aq reaction rates. J. Phys. Chem. **4** (1972) 199–208.

[3] GETOFF, N., Advancement of radiation induced degradation of pollutants in drinking and waste water, Appl. Radiat. Isot. **40** (1989) 585–94.

[4] NETA, P., FESSENDEN, R.W., SCHULER, R.H., An electron spin resonance study of the rate constants for reaction of hydrogen atoms with organic compounds in aqueous solution. J. Phys. Chem.**4** (1973) 199–208.

[5] BALKAS, T.I.,, The radiolysis of aqueous solutions of methylene chloride, Int. J. Radiat. Phys. Chem. **4** (1972) 199–208.

[6] EMMI, S.S., BEGGIATO, G., CASALBORE-MICELI, G., FUOCHI, P.G., OH radical reaction with SH2C12: Direct spectrophotometric observation of CHC12 radical formation, Radioanal. Nucl. Chem., Lett. **93** (1985) 189–197.

[7] HAAG, W.R., YAO, C.C.D., Rate constants for reaction of hydroxyl radicals with several drinking water contaminants. Environ. Sci. Technol., **26**(5) (1992) 1005–13.

[8] GETOFF, N., Radiation- and photo-induced degradation of pollutants in water. A comparative study, Radiat. Phys. Chem. **37** (1991) 673–380.

[9] HAR, E.J., GORDON, S., THOMAS, J.K., Rate constants of hydrated electron reactions with organic compounds, J. Phys. Chem. **68** (1964) 1271–1274.

[10] REZANSOFF, B.J., McCallum, K.J., WOODS, R.J., Radiolysis of aqueous chloroform solutions, Can. J. Chem. **48** (1970) 271–276.

[11] ANBAR, M., MEYERSTEIN, D., NETA, P., Reactivity of aliphatic compounds towards hydroxyl radicals, J. Chem. Soc., Pt. B. (1966) 742–747.

[12] CHUTNY, B., Contribution to the oxidation mechanism of ferrous ions by hydroxy radicals in the presence of organic compounds, Collect. Czech. Chem. Commun. **31** (1966) 358–361.

[13] AFANASSIEV, A.M., OKAZAKI, K., FREEMAN, G.R., Effect of solvation energy on electron reaction rates in hydroxylic solvents, J. Phys. Chem. **83** (1979) 1244–1249.

[14] MEISEL, D., MATHESON, M.S., MULAC, W.A., RABININ, J., Transients in the flash photolysis of aqueous solutions of tris(2,2-bipyridine)ruthenium(II) ion. J. Phys. Chem. **81** (1977) 1449–1455.

[15] MICIC, O.I., CERCEK, B., Diffusion-controlled reactions in mixed solvents, J. Phys. Chem. **81** (1977) 833–837.

[16] KOESTER, R., ASMUS, K.-D., Die Reduktion von Tetrachlorkohlenstoff durch hydratisierte Elektronen, H-Atome und reduzierende Radikale, Z. Naturforsch. Teil B. **26** (1971) 1104–1108.

[17] HAYES, D., SCHMIDT, K.H., MEISEL, D., Growth mechanisms of silver halide clusters from the molecule to the colloidal particle, J. Phys. Chem. **93** (1989) 6100–6109.

[18] LAL, M., MAHAL, H.S., Reactions of alkylbromides with free radicals in aqueous solutions, Radiat. Phys. Chem. **40** (1992) 23–26.

[19] BALKAS, T.I., FENDLE, J.H., SCHULER, R.H., The radiation chemistry of aqueous solutions of CFC13, CF2C12 and CF3C1, J. Phys. Chem. **75** (1971) 455–466.

[20] NETA, P., FESSENDEN, R.W., SCHULER, R.H., An electron spin resonance study of the rate constants for reaction of hydrogen atoms with organic compounds in aqueous solution, J. Phys. Chem. **75** (1971) 1654–1666.

[21] BULLOCK, G., COOPER, R., Reactions of aqueous trifluoromethyl radicals, Trans. Faraday Soc. **66** (1970) 2055–64.

[22] BULLOCK, G., COOPER, R., Reactions of aqueous trifluoromethyl radicals, Trans. Faraday Soc. **66** (1970) 2055–64.

[23] THOMAS, J.K., Pulse radiolysis of aqueous solutions of methyl iodide and methyl bromide. The reactions of iodine atoms and methyl radicals in water, J. Phys. Chem. **71** (1967) 1919–1925.

[24] MEZYK, S.P. and BARTELS, D.M., J. Phys. Chem. **98** (1994) 10578 pp.

[25] HAYES, D., SCHMIDT, K.H., MEISEL, D., Growth mechanisms of silver halide clusters from the molecule to the colloidal particle, J. Phys. Chem. **93** 6100–6109.

[26] INFELTA, P.P., GRAETZEL, M., THOMAS, J.K., Luminescence decay of hydrophobic molecules solubilized in aqueous micellar systems. A kinetic model, J. Phys. Chem. **78** 90–95.

[27] MOHAN, H., MOORTHY, P.N., Formation of radical cations of polyiodomethanes: A pulse radiolysis study, J. Chem. Soc., Perking Trans. **2** 277–282.

[28] MOHAN, H., MITTAL, J.P., Structure -reactivity studies on the nature of transients formed on reaction of OH radicals with chloroiodoalkanes in aqueous solution, J. Chem. So., Perkin Trans. **2** 1731–1736.

[29] MARCHAJ, A., KELLY, D.G., BAKAC, A., ESPENSON, J.H., Kinetics of the reactions between alkyl radicals and molecular oxygen in aqueous solution. J. Phys. Chem. **95** (1991) 4440–4441.

[30] EMMI, S.S., Haloalkyl radicals: Formation and reactivity of mono- and dichloromethylperoxy radicals (Proc. Fifth Tihany Symposium on Radiation Chemistry, Budapest, 1982), Akad. Kiado, Budapest (1982).

[31] MOENIG, J., BAHMNEMANN, D., ASMUS, K.-D., One electron reduction of carbon tetrachloride in oxygenated aqueous solutions: a trichloromethyldioxy-free radical mediated formation of chloride and carbon dioxide. Chem. Biol. Interact. **47** (1983) 15–27.

[32] MAK, F.T., ZELE, S.R., COOPER, W.J., KURUCZ, C.N., WAITE, T.D., NICKELSEN, M.G., Wat Res., **31** (1997) 219–228.

[33] GILBERT, B.C., HODGEMANN, D.K.C., NORMAN, R.O.C., J. Chem. Soc., Perkin Trans. **2** (1973) 1748 pp.

[34] BONIFACIC, M., ASMUS, K.-D., J. Chem. Soc., Perkin Trans. **2** (1980) 758 pp.

[35] BONIFACIC, M., MOECKEL, H., BAHNEMANN, D., ASMUS, K.-D., J. Chem. Soc., Perkin Trans. **2** (1975) 675 pp.

[36] GOEBL, M., BONIFACIC, M., ASMUS, K.-D., J. Am. Chem. Soc. **106** (1984) 5984 pp.

[37] ASMUS, K.-D., Sulphur Centered Reactive Intermediates in Chemistry and Biology (CHATGILIAOGLU, K.-D., Ed.), Plenum Press, New York (1990).

[38] ASMUS, K.-D., Acc. Chem. Res. **12** (1974) 436 pp.

[39] IOELE, M., STEENKEN, S., BACIOCCHI, E., J. Phys. Chem. A **101** (1997) 2979–2987.

[40] MOHAN, H., MITTAL, J.P., J. Phys. Chem. A **101** (1997) 10012–10017.

[41] JONSSON, M., LIND, J., MERENYI, G., ERIKSEN, T.E. J. Chem. Soc. Perkin Trans. **2** (1995) 67–70.

[42] MOHAN, H., ASMUS, K.-D., J. Phys. Chem. **92** (1988) 118–122.

[43] O'NEILL, P., STEENKEN, S., SCHULTE-FROHLINDE, D., J. Phys. Chem. **79** (1975) 2773–2779.

[44] FIELD, R.J., RAGHAVAN, N.V., BRUMMER, J.G., J. Phys. Chem. **86** (1982) 2443–2449.

[45] MATTHEWS, R.W., SANGSTER, D.F., J. Phys. Chem. **69** (1965) 1938–1946.

[46] ANBAR, M., MEYERSTEIN, D., NETA, P., Nature **209**, London (1966) 1348 pp.

[47] ASMUS, K.-D., CERECK, B., EBERT, J., HENGLEIN, A., WIGGER, A., Trans. Faraday Soc. **63** (197) 2435 pp.

[48] LAND, E.J., EBERT, M., Trans. Faraday Soc., **63** (1967) 1181 pp.

[49] MICHAEL, B.D., HART, E.J. J. Phys. Chem. **74** (1970) 2878 pp.

[50] NETA, P., DORFMAN, L.M., J. Phys. Chem. **73** (1969) 413 pp.

[51] NETA, P.,, SCHULER, R.H., Radiat. Res. **47** (1971) 612 pp.

[52] NETA, P., FESSENDEN, R.W., SCHULER, R.H. J. Phys. Chem. **75** (1971) 1654 pp.

[53] SAUER, J.M.C., WARD, B. J. Phys. Chem **71 (**1967) 3971 pp.

[54] NETA, P., SCHULER, R.H., J. Am. Chem. Soc. **94** (1971), 1056–1059.

[55] ANBAR, M., BAMBENEK, M., ROSS, A.B., Natl. Stand. Ref. Data Ser., Natl. Bur. Stand., **43**, USA (1973).

[56] RAZEM, D., HAMILL, W.H., J. Phys. Chem., **81** (1977) 1625–1631.

[57] TOBIEN, T., ASMUS, K.-D., unpublished work.

[58] KURUCZ,C.N., WAITE, T.D., COOPER, W.J., NICKELSEN, M.G., Rad. Phys. Chem. **45** (1995) 805–816.

[59] BUXTON, G.V., WOOD, N.D., Radiation Chemistry of High Temperature Water, Cookridge Radiat. Res. Center, USA (1986).

[60] BUSTON, G.V., ELLIOT, A.J., Radiat. Phys. Chem. **27** (1986), 241–243.

[61] NASH, K., MULAC, W., NOON, M., FRIED, S., SULLIVAN, J.C., J. Inorg. Nucl. Chem. **43** (1981) 897–899.

[62] THOMAS, J.K., GORDAON, S., HART, E.J., J. Physics Chem. **68** (1964) 1524–1527.

[63] TOBIEN, T., COOPER, W.J., unpublished data.

[64] JAFVERT, C.T., VALENTINE, R.L., Environ. Sci. Technol. **26** (1992) 577–586.

[65] VALENTINE, R.J., JAFVERT, C.T., Environ. Sci. Technol. **22** (1988) 691–696.

[66] EIBENBERGER, J., SCHULTE-FROHLINDE, D., STEENKEN, S.J., J. Phys. Chem. **84** (1980) 704–710.

ELECTRON BEAM TECHNOLOGY FOR PURIFICATION OF MUNICIPAL WASTEWATER IN THE AEROSOL FLOW

A.K. Pikaev, E.A. Podzorova
Institute of Physical Chemistry of Russian Academy of Sciences,
Moscow, Russian Federation

O.M. Bakhtin, S.L. Lysenko, V.A. Belyshev
State Scientific Research Laser Center 'Raduga',
Raduzhnyi, Vladimirskaya Oblast',
Russian Federation

Abstract. The paper summarizes the results from the study on EB and ozone treatment of wastewater in the aerosol flow. It includes the description of the respective pilot plant with output 500 m^3/day (it is equipped with electron accelerator with electron energy 0.3 MeV and beam power 15 kW), the results of the study on the effects of electron irradiation on various group parameters (colour, COD, BOD_5, total number of microbes, odour and so on) and content of inorganic and organic pollutants of municipal wastewater in the aerosol flow and the preliminary data on economic feasibility of the purification method.

1. INTRODUCTION

EB methods for purification and disinfection of water and wastewater are being developed comparatively widely (see, for example, Refs [1, 2]). The most important of them are combined methods (in particular, EB and ozone treatment; see, for instance, Refs [3–5]). However, the respective facilities are based on electron accelerators with electron energy of ~1 MeV and higher. Such accelerators are expensive that restricts wide application of the mentioned methods. We developed the technology of combined EB and ozone treatment of wastewater with the use of cheaper low-energy electron accelerator. With this purpose the liquid wastewater is sprayed and irradiated in the aerosol flow (sometimes in the presence of ozone).

This report summarizes the results obtained on the study of combined EB and ozone treatment of municipal wastewater (mainly from small town Raduzhnyi, Vladimirskaya oblast', Russia) in the aerosol flow. The data were partially published earlier [6–8].

2. EQUIPMENT AND MATERIALS

2.1. Pilot plant

Figure 1 shows the scheme of pilot plant constructed and used for the study on purification of municipal wastewater. In the figure, (1) is reservoir of wastewater intake, (2) is electric pump unit for wastewater moving, (3) is sprayer unit (it contains four sprayers) for production of the aerosol, (4) is irradiation chamber, (5) is electron accelerator, (6) is turboblower, (7) is power supply, (8) is control desk, (9) is electric pump unit for purified wastewater removal, and (10) is biological shielding. In the plant, irradiated air containing ozone can circulate through the irradiation chamber.

In the plant, the accelerator of 'Astra' type is used. Some details of its construction and operation principles were described earlier [9]. Its parameters are presented in Table I. The parameters of the pilot plant are shown in Table II.

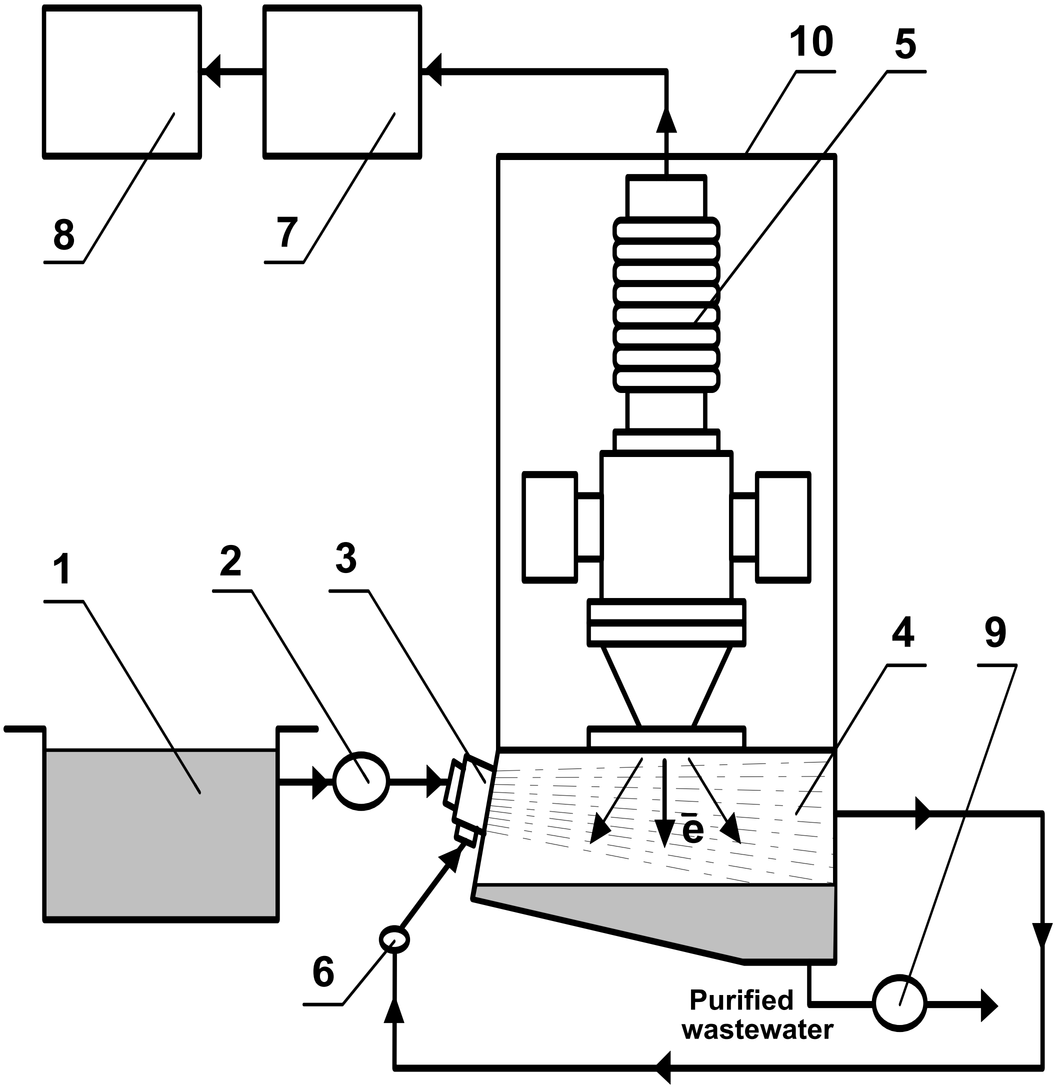

FIG.1. Scheme of pilot plant for combined EB and ozone treatment of municipal wastewater in the aerosol flow.

TABLE I. PARAMETERS OF ELECTRON ACCELERATOR

Parameter	Value
Energy	0.3 MeV
Maximum beam power	15 kW
Maximum pulse frequency	100 Hz
Beam cross-section	700 × 600 mm
Accelerator size	1200 × 800 × 170 mm

TABLE II. PARAMETERS OF PILOT PLANT FOR WASTEWATER PURIFICATION IN THE AEROSOL FLOW

Parameter	Value
Output	500 m^3/day
Power consumption	58 kW
Occupied area	40 m^2
Speed of air feed	288 dm^3/s
Speed of wastewater flow	9.65 m/s
Flow thickness in irradiation chamber	9 cm

Density of the aerosol formed by the sprayer is equal to 0.02–0.05 g/cm^3. Because of it the range of electrons increased by 20–50 times in comparison with liquid wastewater. This gives rise to the use of low energy EB for the treatment of wastewater in the aerosol flow. Since the density of the aerosol is considerably higher than that of air, electron energy is predominantly absorbed by water droplets. For example, if the aerosol density is 0.02 g/cm^3, the water droplets absorb over 90% of electron energy. The size of the droplets depends on the diameter of the sprayer nozzle and the rates of wastewater and air feed. The diameter of droplets was from 50 to 180 μm.

2.2. Dosimetry

Dosimetry was conducted with cellulose triacetate films. The absorbed dose was also calculated on the base of the distribution of absorbed electron energy in a multilayer medium.

2.3. Materials and reagents

As it was mentioned, municipal wastewater from the small town of Raduzhnyi (Vladimirskaya oblast, Russia) was treated by EB in the aerosol flow. The used reagents were reagent grade and utilized without special purification. Wastewater was preliminarily purified from large solid particles by sedimentation and filtration.

3. ANALYTICAL PROCEDURES

The various parameters of water quality before and after EB treatment at different doses were measured.

3.1. Group parameters

The values of COD, BOD5, colour, odour, transparency, contents of inorganic pollutants and total number of microbes were determined according to the well-known procedures [10, 11]. Figure 2 shows the dependence of COD value for municipal wastewater on dose as a result of EB treatment in the aerosol flow. The results of the study on various parameters of unirradiated and irradiated wastewater are listed in Table III.

Note that upon EB treatment the aggregation of disperse particles occurs and the precipitate is formed; it is collected at the bottom part of the irradiation chamber. The analysis of precipitate and water over it was conducted separately. The water was taken for analysis by decantation. The weights of dry residues were equal to 880, 450 and 280 mg/dm^3 at room temperature, 103–1050°C and 178–1820°C, respectively. The formation of precipitate is continued for 20–24 h after irradiation. This post-effect causes additional (~50%) decrease in the COD values of irradiated water.

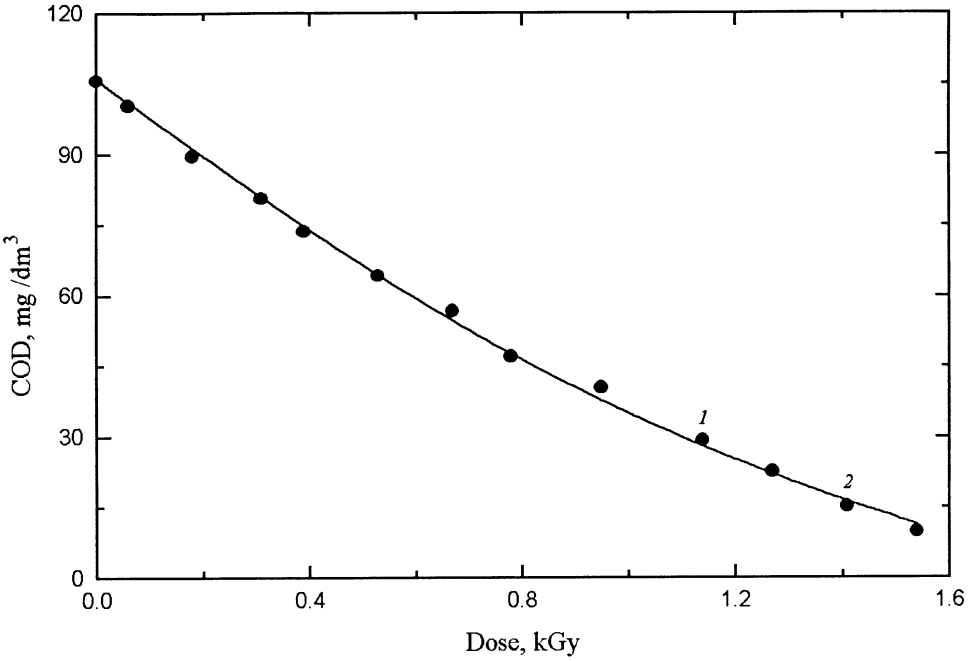

FIG.2. Decrease in COD value of municipal wastewater as a result of EB treatment (1 and 2 are COD values approved by Russian State Standard for service water and water basins for fish farming, respectively).

TABLE III. PARAMETERS OF UNIRRADIATED AND IRRADIATED MUNICIPAL WASTEWATER IN THE AEROSOL FLOW

Parameter	Before irradiation	Dose, kGy	After irradiation	Requirements of Russian State Standard for service water, not more
Colour (units)	160	1.3	20	20
Transparency (cm)	1.3	1.3	20	–
Suspended solids (mg/dm^3)	156	1.3	5	–
Odour (force)	4.5	1.4	0	–
COD (mg/dm^3)	40–100	0.9–1.4	4–12	30(15*)
	100–150	0.9–1.3	21–34	
	150–450	1.0–1.4	40–100	
	412	2.5–4.6	4–12	
BOD$_5$ (mg/dm^3)	18–24	0.8–1.3	7.9–9.2	9.8
Sulphates (mg/dm^3)	283	0.8–1.3	160	260
Phosphates (mg/dm^3)	8.8	0.8–1.3	4.3	8.7
Chlorides (mg/dm^3)	48	0.8–1.3	23	300
Nitrites (mg/dm^3)	Not detected	1.0–1.4	Not detected	0.02
Nitrates (mg/dm^3)	Not detected	1.0–1.4	3.0	9.1
Total number of microbes (cell/cm^3)	10^5	1.3	< 1	–

* The permitted limit for water basins for fish farming.

The initial wastewater has a dark grey colour. After irradiation (dose 1.3 kGy), it became colourless.

3.2. Removal of synthetic surfactants

The special experiments on radiation-induced removal of synthetic surfactants present in wastewater were carried out. The analysis of surfactants was performed via standard procedure [12]. The study was caused by the fact that these pollutants are non-biodegradable. The data obtained are shown in Fig. 3. It is seen that dose required for the removal of synthetic surfactants from 13.25 to 0.2 mg/dm^3 (the latter is a concentration permitted for service water by Russian State Standard) is equal to 4–5 kGy.

3.3. Determination of metal ions

The emission spectrometer «Plasma-40» (Perkin-Elmer) was used for determination of metal ions in unirradiated and irradiated wastewater and in formed precipitate. The content of metal ions in the precipitate was determined after its dissolution in acidic water. The data obtained are shown in Table IV.

3.4. Determination of organic pollutants

Chromatograph-mass spectrometer «Saturn-4D-GC/MS» (Varian) was utilized for the determination of the origin of organic pollutants and their contents in unirradiated and irradiated wastewater, and also in the precipitate. The procedure No 8270 of E.P.A. of the U.S.A. [13] was used with this purpose. To analyse the pollutants present in the precipitate the sample was extracted for 8 h by a benzene-ethanol aseotropic mixture in Soxhlet apparatus.

Over 120 organic compounds were analysed, and in the case of over 70 of them, they were identified and their concentrations measured. The sensitivity of the procedure was 10–50 ng/dm^3. The data on concentrations of organic pollutants are shown in Table V.

Among the organic pollutants which were analysed but not identified because of their absence or very low concentration were bis-(2-chloroethyl) ether, 1,2-dichlorobenzene, 1,3-dichlorobenzene, 1,4-dichlorobenzene, bis-(2-chloroisopropyl) ether, N-nitroso-di-N-propylamine, hexachloroethane, nitrobenzene, isophorone, bis-(2-chloroethoxy)methane, 1,2,4-trichlorobenzene, 2-chloronaphthalene, 4-chloroaniline, hexachlorobutadiene, hexachlorocyclopentadiene, 2-nitroaniline, acenaphthalene, 2,4-dinitrotoluene, 2,6-dinitrotoluene, benzofluorantenes, benzo[e]pyrene, perylene, benzo[g,h,i]perylene, indeno[1,2,3-cd]pyrene, dibenzo [a,h]anthracene, hexachlorobenzene, di-n-butyl phthalate, di-n-octyl phthalate, butyl benzyl phthalate, bis-(2-ethyl hexyl) ether, 4-chlorophenyl ether, 4-bromodiphenyl ether, N-nitrosodiphenylamine, chlordane, dieldrin, aldrin, 2-chlorophenol, 2,4-dimethylphenol, 2,6-dimethylphenol, 3,4-dimethylphenol, 3,4-dichlorophenol, 2,3,6-trichlorophenol, 2,4,5-trichlorophenol, pentachlorophenol, 2-nitrophenol, and 4-nitrophenol.

The analysis of volatile organic compounds was also carried out — via the procedure No. 624 of E.P.A. of the USA [14]. With this purpose, the mentioned chromatograph mass spectrometer in combination with equilibrium sampler «Head Space Genesis» was used. The samples for analysis were taken from vapour phase at 850C. The detection limit of this procedure was 0.01-0.3 μg/dm^3. The data obtained are presented in Table VI. Among the pollutants which were analysed but not identified because of their absence or very low concentrations were dimethyl trisulfide, dimethyl tetrasulfide, sulphur S6, sulphur S8, 2-cyclohexanol, and bicyclo[2,2,1]-heptan-2-ol.

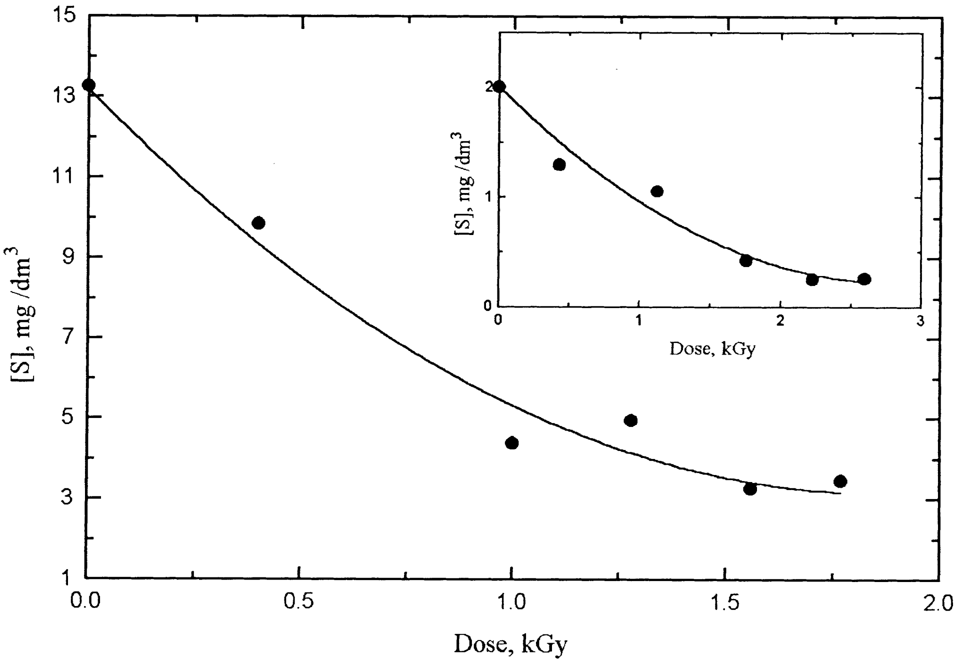

FIG.3. Dependence of concentration [S] of synthetic surfactants on dose upon EB treatment of municipal wastewater in the aerosol flow.

TABLE IV. CONTENTS OF METALS IN UNIRRADIATED AND IRRADIATED (DOSE 1.3 kGy) WASTEWATER AND IN PRECIPITATE SEPARATED FROM IRRADIATED WASTEWATER

Metal	Content in		
	Unirradiated wastewater, mg/dm^3	Irradiated wastewater, mg/dm^3	Precipitate, mg/g
Cr	<0.006	<0.006	2.5*
Zn	<0.002	<0.002	0.15*
Fe	1.7	0.12	29.0*
Mn	0.63	<0.001	0.039
Mg	74.5	19.8	2.3
Cu	<0.005	<0.005	0.028
Ca	219.9	70.7	5.28
Na	39.3	13.1	1.42
K	24.6	6.3	2.85

* Obviously, considerable part of iron, chromium and zinc in precipitate consists of corrosion products from irradiation chamber.

TABLE V. THE CONCENTRATIONS OF ORGANIC POLLUTANTS IN UNIRRADIATED AND IRRADIATED (1.3 kGy) MUNICIPAL WASTEWATER AND IN THE PRECIPITATE SEPARATED FROM IRRADIATED WASTEWATER

Pollutant	Concentration in		
	Unirradiated wastewater, µg/dm^3	Irradiated wastewater, µg/dm^3	Precipitate, µg/g*
Naphthalene	1.35	0.036	7.85
1-Methylnaphthalene	0.34	0.033	3.73
2-Methylnaphthalene	1.09	0.88	6.32
Dimethylnaphthalenes, total	0.37	Not detected	7.10
Trimethylnaphthalenes, total	0.04	Not detected	2.0
Acenaphthene	Not detected	Not detected	0.20
Fluorene	0.32	Not detected	5.10
Dibenzofuran	Not detected	Not detected	0.12
Phenathrene	0.50	0.10	2.15
Anthracene	Not detected	Not detected	0.15
Fluoranthene	0.20	Not detected	0.45
Pyrene	0.15	Not detected	0.22
Benzo[a]anthracene	Not detected	Not detected	0.15
Chrysene	0.05	0.02	0.50
Benzo[a]pyrene	Not detected	Not detected	0.25
DDE	0.16	0.02	0.84
DDD	Not detected	Not detected	0.07
DDT	0.06	Not detected	0.11
Lindane	0.09	Not detected	0.26
Carbazole	0.04	Not detected	0.21
Phenol	6.68	0.26	Not analysed
2-Methylphenol	19.15	0.18	Not analysed
3-Methylphenol	16.45	0.21	Not analysed
4-Methylphenol	0.32	0.13	Not analysed
4-Chlorophenol	1.32	Not detected	Not analysed
2,4-Dichlorophenol	1.20	Not detected	Not analysed
2,3-Dichlorophenol	0.42	Not detected	Not analysed
Trichlorobiphenyls, total	0.06	Not detected	5.45
Hexachlorobiphenyls, total	Not detected	Not detected	1.85
Ethylbenzene	1.56	0.17	0.53
p-Xylene + *m*-xylene	4.54	0.35	1.10
1-Ethyl-2-methylbenzene	2.66	0.11	1.21
Propylbenzene	0.26	Not detected	2.86
1,2,4-Trimethylbenzene	1.80	0.23	4.15
1,3,5-Trimethylbenzene	2.65	0.20	6.77

Pollutant	Concentration in		
	Unirradiated wastewater, $\mu g/dm^3$	Irradiated wastewater, $\mu g/dm^3$	Precipitate, $\mu g/g$*
1,2,3-Trimethylbenzene	4.20	0.07	6.65
Indan	1.74	Not detected	5.32
1-Ethyl-1,4-dimethylbenzene	0.18	Not detected	3.90
4-Ethyl-1,2-dimethylbenzene	0.06	Not detected	1.85
1-Methyl-4-isopropylbenzene	0.16	Not detected	4.80
2-Ethenyl-1,4-dimethylbenzene	1.23	Not detected	11.4
1,2,3,4-Tetramethylbenzene	0.20	0.05	6.30
Pentamethylbenzene	0.33	Not detected	5.90
Cyclopentanone	0.11	Not detected	0.62
2-Isopropylbenzaldehyde	0.09	Not detected	1.44
4,4'-Dimethylbiphenyl	0.14	Not detected	0.83
3,4-Diethyl-1,1'-biphenyl	0.21	Not detected	1.66
4-Methyl-9H-fluorene	0.30	Not detected	2.30
3-Hexadecanone**	Not detected	0.08	Not detected
Dimethyl disulphide	18.9	Not detected	2.25
Dimethyl trisulfide	32.06	Not detected	8.23
Dimethyl tetrasulfide	11.23	Not detected	11.16
Sulphur S_8	1186.5	Not detected	2446.0
9-Octadecanone	2.87	0.14	18.9
9-Octadecanol	12.6	0.09	17.7
2-Hexyl-1-decanol	0.56	Not detected	8.50
4-Hydroxy-2,5-dimethyl-3(2-H)-furanone**	Not detected	0.11	Not detected
Benzothiazole**	Not detected	0.95	Not detected
N-Ethyl-2-benzothiazolamine**	0.08	0.18	Not detected
Benzyl alcohol**	Not detected	0.03	0.26
Cyclobutyl phenyl ketone	1.69	Not detected	4.18
Trihydroxyphenyl butanone	0.60	Not detected	1.90
2,5-bis-(Isopropyl)thiophene	8.58	Not detected	56.9
Hexanedicarboxylic acid**	Not detected	0.23	Not detected
Cholest-5-ene-3-ol	124.8	Not detected	643.6
Cholest-8(14)-ene	85.53	Not detected	2876.5
Cholestane-3-ol, acetate (3β,5α)	14.50	Not detected	132.8
Cholest-8(14)-ene-7,15-diol (5α)	45.90	Not detected	456.3
3-Methoxycholest-5-ene (3β)	6.26	Not detected	54.9
2,4-Ethylcoprostanol	23.8	Not detected	346.3

* The content of the precipitate from 1 dm^3 of irradiated wastewater is about 20 mg.

** This compound is a product of radiolysis.

TABLE VI. THE CONCENTRATIONS OF VOLATILE ORGANIC POLLUTANTS SEPARATED FROM IRRADIATED (1.3 kGy) MUNICIPAL WASTEWATER

Pollutant	Concentration, µg/dm^3	
	Unirradiated wastewater	Irradiated wastewater
Dimethyl disulphide	56.5	Not detected
p-Xylene + m-xylene	9.2	5.2
o-Xylene	4.0	2.0
Isopropylbenzene	2.9	0.25
2-(2-Propenyl)phenol	11.8	Not detected
3,4-Dihydro-2-methylbenzofuran	6.8	Not detected
N-Ethylaniline	0.13	Not detected
Hydrocarbons C_6–C_{14}	4–34	4–22
Methyl octanate	7.3	Not detected

TABLE VII. PRELIMINARY ECONOMIC EVALUATION OF COMBINED EB AND OZONE TREATMENT OF MUNICIPAL WASTEWATER IN THE AEROSOL FLOW (by 1 January 1999)*

Process	Cost (roubles/m^3)
Conventional purification (total)	195
Chlorination + use of biopond	49
EB treatment (after removal of mechanical admixtures by sand filter) to decrease COD value from 500 to 30 mg/dm^3	56
The same to decrease the COD value from 150 to 30 mg/dm^3	32

* US dollar = 25 roubles.

From Tables V and VI it follows that initial municipal wastewater contains naphthalene and its derivatives, phenol and its derivatives, alkylbenzenes, derivatives of biphenyls and so on. The considerable part of pollutants in unirradiated wastewater consisted of sulphur-containing compounds (their concentrations are from several dozens up to about one thousand micrograms per litre) and cholesterol derivatives (their concentrations are up to several hundred micrograms per litre).

The main part of the organic pollutants are removed with the formed precipitate (see Table V) which is separated by filtration. Note that irradiation gives rise to the formation of several new compounds such as benzyl alcohol, 3-hexadecanone, hexadicarboxylic acid. As a result of irradiation of wastewater, the formation of hydrogen peroxide is observed. Its concentration at dose 1.3 kGy is 1.5 × 10-6 mol/dm3 (~0.05 mg/dm^3). Note that in irradiated wastewater nitrate ions were detected (they were absent in unirradiated wastewater). It is caused by the fact that nitrogen oxides are formed upon irradiation of air. The oxides reacting with water give nitrite and nitrate ions; upon further irradiation, nitrite ions are oxidized to nitrate ions.

The precipitate also captures inorganic pollutants. It was found that the concentrations of phosphates, sulphates, chlorides and carbonates in the precipitate after separation from wastewater irradiated to dose 1.3 kGy are 20, 500, 85 and 50 mg/g, respectively.

The results obtained show that the content of pollutants in irradiated wastewater decreased by 2–3 orders of magnitude or the pollutants were absent at all. From the comparison of the concentrations of pollutants (their amount is about two dozens) not removed completely with the concentrations approved for service water by respective standards (see Refs [15–17]), it follows that the first of them are noticeable lower than the second. Therefore, EB treatment of municipal wastewater in the aerosol flow at several kilograys in combination with circulation of irradiated air containing ozone through irradiation chamber leads to the required purification of wastewater.

4. MECHANISM OF PURIFICATION

The purification is due to the reactions of pollutants with products of radiolysis of water droplets and air (including single oxygen). The removal of pollutants also occurs as a result of their capture by a precipitate which is formed because of the aggregation of disperse particles upon EB treatment. Ozone facilitates the purification via reactions with some organic pollutants and formation of the additional amount of high-reactive species (for example, $^{\bullet}$OH and RO$^{\bullet}$ radicals).

5. ECONOMIC FEASIBILITY

Table VII shows the results of preliminary evaluation of economic feasibility for the method under consideration. It is seen that from economic viewpoint the method can compete successfully with the conventional purification (chlorination and use of biological ponds).

The municipal wastewater flow of the town of Raduzhnyi is about 7,000 m^3/day. Hence, in order to purify such level of wastewater it is necessary to construct the plant with 14 above-mentioned low-energy electron accelerators with beam power 15 kW or two accelerators with beam power 105 kW.

6. CONCLUSION

From the results obtained one can deduce the following:

(1) The comparatively cheap low energy electron accelerators can be used for combined EB and ozone treatment of municipal wastewater, if it is irradiated in the aerosol flow.
(2) The method is suitable, for example, for purification and disinfection of municipal wastewater of small towns.
(3) Even in the case of high polluted wastewater, the doses required for the purification are comparatively low (not over 4–5 kGy).
(4) The purification is due to the reactions of pollutants with products of radiolysis of water droplets and air, to the capture of pollutants by the precipitate formed upon irradiation, and to reactions of ozone leading to the formation of additional amount of high-reactive species.

REFERENCES

[1] WAITE, T.D., et al., “Full scale EB systems for treatment of water, wastewater and medical waste”, Radiation Technology for Conservation of the Environment (Proc. Symp. Zakopane, 1997), IAEA, Vienna (1998) 187–202.

[2] PIKAEV, A.K. “New environmental applications of radiation technology”, ibid., 243–254.

[3] WOODS, R.J., PIKAEV, A.K., Applied Radiation Chemistry: Radiation Processing, Wiley, New York (1994) 535 pp.

[4] GEHRINGER, P., ESCHWEILER, H., FIEDLER, H., Ozone electron beam treatment for groundwater remediation, Radiat. Phys. Chem. **25** (1995) 1075–1078.

[5] BUSLAEVA, S.P., et al., Removal of non-biodegradable surfactants in aqueous solutions upon the action of accelerated electrons, Khim. Prom. 6 (1991) 47–50.

[6] PIKAEV, A.K., PODZOROVA, E.A., BAKHTIN, O.M., Combined electron beam treatment of wastewater in the aerosol flow, Radiat. Phys. Chem. **49** (1997) 155–157.

[7] PODZOROVA, E.A., et al., New data on electron beam treatment of municipal wastewater in the aerosol flow, Radiat. Phys. Chem. **52** (1998) 361–364.

[8] PODZOROVA, E.A., et al., “Removal of pollutants from municipal wastewater by electron beam treatment in the aerosol flow”, Khim.Vys. Energ. **33** (submitted).

[9] LYAKISHEV, V.G. Electron accelerator with wide beam for radiation technologies, Vestnik ADS ‘RadTekh-Evrazia’, No.1(3), (1992) 49–52.

[10] LABINSKAYA, A.S. Microbiology with the Technique of Microbiological Examinations. Moscow, Meditsina (1978), 105 pp (in Russian).

[11] LUR'E, Yu.Yu., RYBNIKOVA A.I., Chemical Analysis of Industrial Wastewater. Khimiya, Moscow (1974) 335 pp (in Russian).

[12] LUR'E, Yu.Yu. Analytical Chemistry of Industrial Wastewater. Khimiya, Moscow (1984), 447 pp (in Russian).

[13] Federal Register. Vol.48, No.208. Rules and Regulations. Semivolatile Organic Compounds by Isotope Dilution. Procedure No.8270, GC/MC. U.S.A. Environmental Protection Agency, Washington, D.C. (1994).

[14] Federal Register. Vol. 48, No. 208. Rules and Regulations. Volatile Organic Compounds. Procedure No.624. U.S.A. Environmental Protection Agency, Washington, D.C. (1994).

[15] BELOUSOVA, M.YA., et. al., Main Properties of Organic Compounds Controlled in Water. Nauka, Moscow (1987) 392 pp (in Russian).

[16] BESPAMYATNOV, G.P., et al., Permitted Concentrations of Hazardous Substances in Air and Water . Khimiya, Leningrad (1975) 455 pp (in Russian).

[17] Drinking Water. Sanitary Requirements and Control of Quality. Russian State Standard 2874–82. State Committee of Standards, Moscow (1982) (in Russian).

APPLICATION OF ELECTRON BEAM TO INDUSTRIAL WASTEWATER TREATMENT

B. Han, D.K Kim, J.Y. Boo, J.K. Kim, Y. Kim, W. Chung
Central Research Institute, Samsung Heavy Industries Co., Ltd,
Taejon, Republic of Korea

J.S. Choi, H.J. Kang
Institute of Dyeing Technology
Taegu, Republic of Korea

A.K. Pikaev
Institute of Physical Chemistry of Russian Academy of Sciences,
Moscow, Russian Federation

Abstract. Global withdrawals of water to satisfy human demands have grown dramatically in this century. Between 1900 and 1995, water consumption increased by over six times, more than double the rate of population growth. This rapid growth in water demand is due to the increasing reliance on irrigation to achieve food security, the growth of industrial uses, and the increasing use per capita for domestic purposes. Given the seriousness of the situation and future risk of crises, there is an urgent need to develop the water efficient technologies including economical treatment methods of wastewater and polluted water.

In the Central Research Institute of Samsung Heavy Industries (SHI), many industrial wastewater including leachate from landfill area, wastewater from papermill, dyeing complex, petrochemical processes, etc. are under investigation with EB irradiation. For the study of treating dyeing wastewater combined with conventional facilities, an EB pilot plant for treating 1,000m^3/day of wastewater from 60,000m^3/day of total dyeing wastewater has constructed and operated in Taegu Dyeing Industrial Complex. A commercial plant for re-circulation of wastewater from Papermill Company is also designed for S-paper Co. in Cheongwon City, and after the successful installation, up to 80% of wastewater could be re-used in paper producing process.

1. INTRODUCTION

Samsung Heavy Industries (SHI) was established in 1974 and has managed to enter into a wide range of successful business ventures. These include plant engineering, industrial machinery, shipbuilding, and construction. The volume of annual sales is over 3 billion dollars with 10,000 employees. The Central Research Institute of SHI is located in Daeduk Science Town, which is at the central part of Korea. The Accelerator Laboratory in this institute is devoted for the development of accelerator technologies and applications.

The research activities for the applications of accelerator include wastewater treatment, combustion flue gas purification, semi-conductor treatment, and other radiochemical processing. The treatment of industrial wastewater with EB for environmental application is one of the actively studied subjects in the Central Research Institute. The method for the removal of heavy metals from wastewater and other technologies [1, 2] are developed with the joint works of Central Research Institute of SHI and Institute of Physical Chemistry (IPC) of the Russian Academy of Sciences.

2. INCREASE OF WORLD WATER CONSUMPTION

Actually 70% of the world is covered with water, however, the reality is that 97.5% of all water on earth is salt water, leaving only 2.5% as fresh water. Nearly 70% of that fresh water is frozen in the icecaps of Antarctica and Greenland, and most of the remainder is present as soil moisture, or lies in deep underground aquifers as groundwater not accessible for human use. As a result, less than one per cent of the world's fresh water, or about 0.007 per cent of all water on earth, is readily accessible for direct human uses [3]. This is the water found in lakes, rivers, reservoirs and those underground sources that are shallow enough to be tapped at an affordable cost. Only this amount is regularly renewed by rain and snowfall, and is therefore available on a sustainable basis.

It has been estimated that the amount of the fresh water that is readily accessible for human use at about 9,000 cubic kilometres a year, and another 3,500 cubic kilometres of water that is captured and stored by dams and reservoirs could be added. Harnessing the remaining water resources for human needs becomes increasingly costly, because of topography, distance and environmental impacts. Currently, humans are using about half the 12,500 cubic kilometres of water that is readily available. Given an expected population increase of about 50% in the next 25 years, coupled with expected increases in demand as a result of economic growth and life-style changes, this does not leave a great room for increased consumption [3]. Water needs to be left in rivers to maintain healthy ecosystems, including fisheries. When global water picture is examined at a country level, some countries still have large amounts of water per capita, but others, however, are already facing serious difficulties. Future increases in demand due to population growth and increased economic activities will inevitably impinge further on the available water resources.

Despite improvement in the efficiency of water use in many developed countries, the demand for fresh water has continued to climb as the world's population and economic activities have expanded. From 1900 to 1995, withdrawals of fresh water from rivers, lakes, reservoirs, underground aquifers, and other sources increased by more than a factor of six. Increases in irrigation and, to a lesser extent, industrial uses of water have been the largest sources of this growing demand. At the same time, contamination by pollutants has seriously degraded water quality, effectively decreasing the supply of fresh water.

The results have been increased pressure on fresh water resources in most regions of the world and a lack of adequate supplies in some localities. Water experts and international institutions warn that water shortages could become critical in some regions.

In Korea, the annual average rainfall is 1.3 times greater than that of the world, but it varies too much with season and area to control for withdrawal. Only 24% of rainfall could be accessible for human uses. If in the absence of far more effective management of water resources, this could pose a serious long term obstacle to the sustainable development of Korea.

TABLE I. SUPPLY AND DEMAND OF FRESH WATER IN KOREA (in billion tons)

Year	1994	2001	2006	2011
Demand	2,990	3,364	3,499	3,665
Supply	3,222	3,429	3,454	3,465
Shortage	-	-	45	200

3. ELECTRON BEAM TREATMENT OF WASTEWATER

People have used water as a convenient sink into which to dump wastes. The pollution comes from many sources, including untreated sewage, chemical discharges, petroleum leaks and spills, agricultural chemicals, etc. The wastewater discharged has outstripped nature's ability to break them into less harmful elements. Pollution spoils large quantities of water, which then cannot be used. Virtually all pollutants can be removed from water, especially in the case of toxic substances, but would be very expensive and require sophisticated techniques.

Treatment of municipal and industrial wastewater becomes a more important subject in the field of environment engineering. Treatment of the industrial wastewater containing refractory pollutant with EB is actively studied in SHI. EB treatment of wastewater often leads to their purification from various pollutants. It is caused by the decomposition of pollutants as a result of their reactions with highly reactive species formed from water radiolysis (hydrated electron, OH free radical and H-atom). Sometimes such reactions are accompanied by the other processes, and the synergistic effect upon the use of combined methods such as EB treatment with ozonation, EB and adsorption and others improves the effect of EB treatment of the wastewater purification.

In Korea, the industries are concentrated in near urban areas resulting in severe water pollution problems in most large cities. Major sources of water pollution include chemical-intensive industries such as textiles, metal plating, electronics, papermill and refineries. Typical contaminants include non-biodegradable substances, grease and oils, acids and caustics, heavy metals such as cadmium and lead, sludge and a long list of synthetic organic compounds. The amounts of wastewater generated and discharged in Korea are summarized in Table II.

TABLE II. THE AMOUNT OF WASTEWATER GENERATED AND DISCHARGED IN KOREA [4] (in 1,000m^3/day)

	Number of companies (%)	Amount of waste-water generated (%)	Amount of waste-water discharged (%)
Textile	1,423 (5.6)	473 (5.4)	457 (19.2)
Papermill	268 (1.1)	711 (8.1)	364 (15.3)
Light Ind.	511 (2.0)	390 (4.5)	243 (10.2)
Processing Ind.	3,376 (13.3)	439 (5.0)	200 (8.4)
Metal fabrication	437 (1.7)	5,346 (61.1)	169 (7.1)
Others	9,284 (76.2)	1,382 (15.8)	942 (39.7)
Total:	25,299 (100)	8,741 (100)	2,375 (100)

The wastewater under current investigation at SHI are from dyeing companies, petrochemical processes, papermill and leachate from sanitary landfill area, etc. Those are also summarized in Table III. Two electron accelerators of energy 1 MeV each in continuous mode at Daeduk (SHI) and one accelerator of 5 MeV in pulsed mode at Moscow (IPC) are used in experiments. Applied sets of dose for the experiments were measured with an ordinary or modified Fricke dosimeter and dichromatic dosimeter.

TABLE III. WASTEWATER UNDER INVESTIGATION AT SHI

Source of wastewater	Purpose of investigation	Results
Dyeing company	Removal of colour and organic impurities	Pilot plant constructed Improve removal efficiencies
Papermill	Decrease COD, colour Increase re-use rate	Reduction in impurities Commercial plant designed
Petrochemical co.	Removal of organic residues after processing	Removal of TCE, PCE, PVA, HEC and other substances
Leachate from landfill area	Removal of organic impurities Improvement of Bio-treatment	Bio-treatment efficiency improved
Heavy metals	Decrease the content of heavy metal ions in water	Removal of Cd,Cr^{+6},Hg up to 98% (95% in Pb)
Power plant clean-up	Decrease the content of organic acid and detergent	Decrease the content of organic substance

4. PILOT PLANT FOR WASTEWATER FROM DYEING PROCESS

An EB pilot plant for treating 1,000m^3/day of dyeing wastewater from 60,000m^3/day of total wastewater was constructed in the Taegu Dyeing Industrial Complex (TDIC). TDIC now includes more than a hundred factories occupying an area of 600,000m^2 with 13,000 employees in total. Majority of the factories has equipment used for dip dyeing, printing, and yarn dyeing. Production requires high consumption of water (90,000m^3/day), steam, and electric power, being characterized by a large amount of highly coloured industrial wastewater. Therefore, intensive and effective purification of the wastewater is one of the most complicated and actual problems of TDIC's current activities.

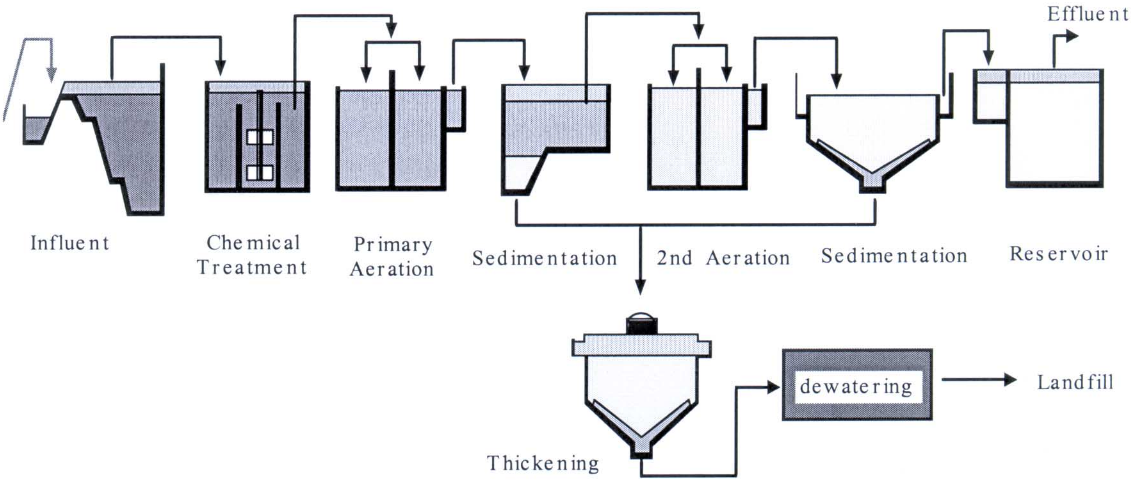

FIG. 1. Process flow in dyeing wastewater.

TABLE IV. TYPICAL CHARACTERISTICS OF WASTEWATER

Parameter	pH	BOD_5 (mg/l)	COD_{Mn} (mg/l)	Suspended solids (mg/l)	Colour units
Raw wastewater	12	2,000	900	100	1,000
After chemical treat	6.8-7.5	1,700	450	50	500
After 1st Bio-treat	7.0-8.0	1,300	250	50	400
After 2nd Bio-treat	7.0-8.0	30	60	50	250

Purification of the wastewater is performed by Union wastewater treatment facilities using conventional methods schematically described in Fig. 1. Current facility treats up to 8,000m^3 of wastewater per day, thereby extracting up to 730 m^3 of sludge. Rather high cost of purification results from high contamination of water with various dyes and ultra-dispersed solids. Because of increase in productivity of factories and increased assortment of dyes and other chemicals, substantial necessity appears in re-equipment of purification facilities by application of efficient methods of wastewater treatment. The existing purification system is close to its limit ability in treatment of incoming wastewater. Some characteristics of raw wastewater and of treated water after several treatment stages and effluence are listed in the Table IV.

Studies have been carried out regarding the possibility of EB application for purification of wastewater. With the collaboration of SHI Central Research Institute and IPC, the experiments on irradiation of model dye solutions and real wastewater samples (from various stages of current treatment process) have been performed [4]. The results of laboratory investigations of representative sets of samples showed the application of EB treatment of wastewater to be perspective for its purification (Fig. 2). The most significant improvements result in decolourizing and destructive oxidation of organic impurities in wastewater. Installation of the radiation treatment on the stage of chemical treatment or immediately before biological treatment may result in appreciable reduction of chemical reagent consumption, reduction of treatment time, and increase in flow rate limit of existing facilities by 30–40%.

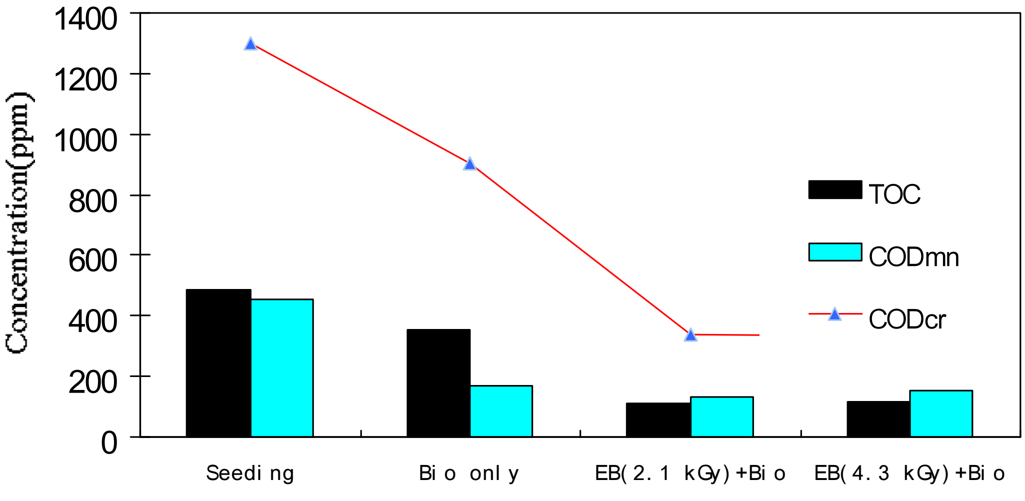

FIG. 2. Combined effect of e-beam and biological treatment.

A pilot plant for a large scale test (flow rate of 1,000 m^3 per day) of wastewater starts operation with the electron accelerator of 1 MeV, 40 kW (Fig. 3). The accelerator was installed in Feb. 1998 and the technical lines are finished in May. The Tower Style Biological treatment facility (TSB) which could treat up to 1,000 m^3 per day was also installed in October. The wastewater from various stages of the existing purification process can be treated with EB in this plant to investigate the experimental possibilities of the pilot plant, and it will give rise to elaborate the optimal technology of the EB treatment of wastewater with increased reliability at instant changes in the composition of wastewater. The wastewater is injected under the e-beam irradiation area through the nozzle type injector to obtain the adequate penetration depth. The speed of injection could be varied upon the dose and dose rate.

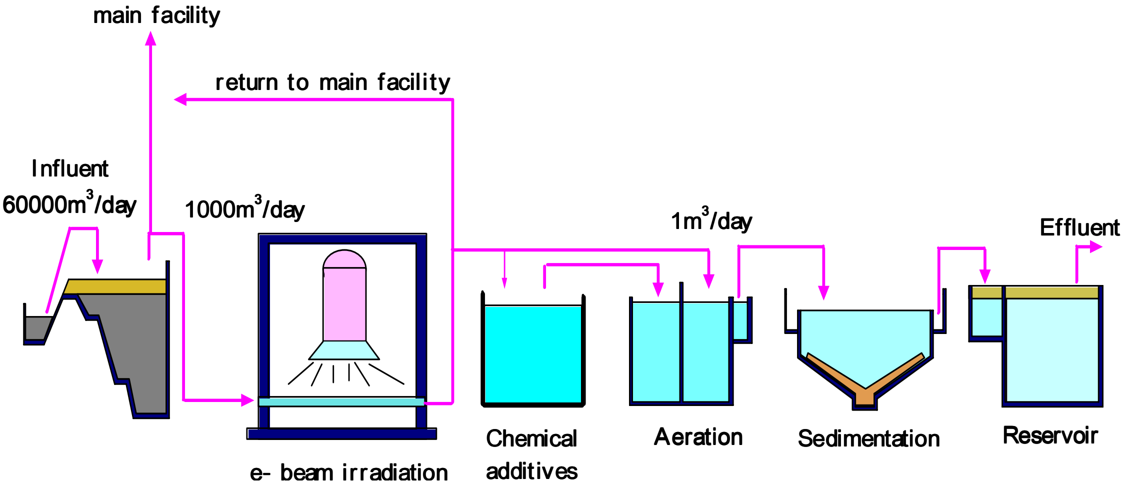

km

FIG. 3. Schematic diagram of pilot plant at Taegu dyeing complex.

5. COMMERCIAL PLANT DESIGN FOR WASTEWATER FROM PAPERMILL

A commercial plant for re-circulation of wastewater with EB from Papermill Company is also under planning in S-paper Co. and SHI. S-paper Co. is located in Cheongwon City, 120 south of Seoul, and consumes 18,000 m^3 of water per day. The major products of this company are papers for newsprint (450t/day) and are mainly made of recycled paper (91%) and pulps. Purification of wastewater is now performed by two stages of chemical and biological treatment facilities.

For the economical point of view, this company tried to recycle the treated water to production lines, but used only 20-30% at total water since the amount of organic impurities after treatment are high and some of them are accumulated during re-circulation. In order to develop the most efficient method for re-circulation of wastewater, the experiments were conducted with samples in various stages of treatment. The best result obtained is irradiation of water after biological treatment combined with coagulation and filtration (Fig. 4). Irradiation in this stage, the additional removal of impurities, is up to 80% in TOC (Total Organic Carbon) values.

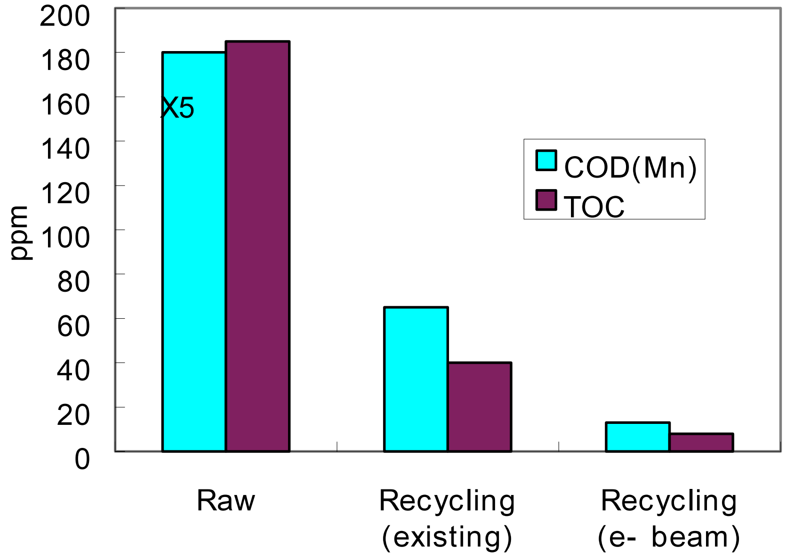

FIG. 4. Treatment of wastewater from papermill.

On the base of data obtained by SHI and IPC the suitable doses in this case are determined as around 1 kGy for the flow rate of 15,000 m^3 wastewater per day (since the 3,000m^3 of wastewater is returned to initial stage with sludge). Therefore, four accelerators with the total power of 320kW and treating systems are designed. After the successful installation of EB treatment facilities, up to 80% of wastewater could be re-used in paper production process (Fig. 5).

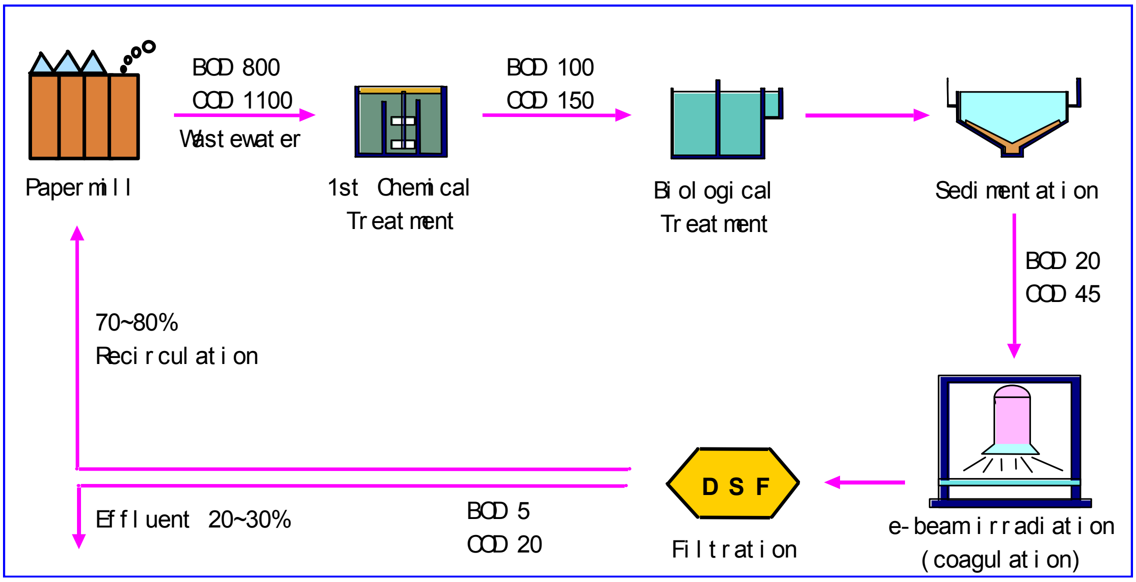

FIG. 5. Process flow of e-beam facility for wastewater from papermill.

6. SUMMARY AND CONCLUSIONS

6.1. General

- EB treatment of industrial wastewater is under development in SHI for the removal of non-degradable wastes, and also for the re-use of wastewater for production process.

- For industrial wastewater with low impurity levels such as contaminated ground water, cleaning water and etc., purification only with EB is possible, but requires high amount of irradiation doses.

- For industrial wastewater with high impurity levels such as dyeing wastewater, leachate and etc., purification only with EB requires high amount of doses and far beyond economies.

- EB treatment combined with conventional purification methods such as coagulation, biological treatment etc. is suitable for reduction of non-biodegradable impurities in wastewater and will extend the application area of EB.

6.2. Experimental

- A pilot plant with EB for treating 1,000m^3/day of wastewater from dyeing industries has constructed and operated continuously since Oct 1998. EB irradiation instead of chemical treatment shows much improvement in removing impurities and increases the efficiency of biological treatment. Actual plant is under consideration based upon the experimental results.

- Commercial plant for re-circulation of 15,000m^3/day of wastewater from papermill is also investigated, and after the successful installation, up to 80% of wastewater could be re-used in paper producing process.

ACKNOWLEDGEMENTS

The authors wish to acknowledge the support of the International Atomic Energy Agency and the Ministry of Foreign Affairs and Trade of the Korean Government.

REFERENCES

[1] PONOMAREV, A.V., et. al., Radiation Physics and Chemistry **49** (1997) 473 pp.
[2] PIKAEV, A.K., et. al., Mendeleev Communication (1997) 52 pp.
[3] UN report "Comprehensive Assessment of the Freshwater Resources of the World", April (1997) http//www.un.org/dpcsd/dsd/freshwat.htm.
[4] Annual Report of the Ministry of Environmental Affairs of Korea (1996).
[5] PIKAEV, A.K, et al., Mendeleev Communication (1997) 176 pp.
[6] HAN, B., KIM, D.K., IAEA report - IAEA-SM-350/32 (1997) 339 pp.

ELECTRON BEAM WASTEWATER TREATMENT IN BRAZIL

M.H.O. Sampa, P.R. Rela, C.L. Duarte, S.I. Borrely, H. Oikawa,
E.S.R. Somessari, C.G. Silveira, F.E. Costa
Instituto de Pesquisas Energéticas e Nucleares – IPEN-CNEN/SP,
São Paulo, Brazil

Abstract. Experiments were performed at laboratory scale and at pilot plant scale to study the efficiency on using EB to remove and degrade toxic and refractory pollutants mainly from industrial origins. An upflow stream hydraulic system that governs the efficiency of the EB energy transferred to the stream was developed. Two different sources of samples were used to treat industrial effluents from a pharmaceutical chemical industry located in São Paulo and from a Governmental Wastewater Treatment Plant (WWTP) in São Paulo State, which receives the major quantity of industrial wastewater. Using samples from this WWTP, studies to combine EB irradiation process with conventional treatment were carried out with experimentation doses of 5 kGy, 10 kGy and 20 kGy and the irradiation effects were evaluated in the following parameters: COD, BOD, solids, TOC, THMs, PCE, TCE, BTX and concentration of organic acids by-products. Toxicity studies were also carried out for different sites and industrial activities showing significant removal of acute toxicity by increasing values of the EC-50 for most of the experiments. The economic aspects of this technology were evaluated and the estimated processing costs for some values of delivered doses and operation are reported here.

1. INTRODUCTION

Environmental pollution has recently become a significant world concern. The main sources of this contamination are industries which generate and deliver to the environment injurious effluents often without any previous treatment. Most of these contaminants biodegrade very slowly, becoming dangerous to humans, plants and animals.

The variables involved in the environment's recuperation are numerous, mainly due to great variety of chemical compounds and raw material used by industry. The most complicated industrial effluents are organic compounds, especially the synthetic ones the removal and degradation of which would be difficult with conventional methods.

The quality and quantity of industrial wastes vary depending on the type of used materials and industrial process. The aim of the conventional techniques employed is to reduce the volume and toxicity of the effluents. Some of these available techniques are co-precipitation, adsorption on charcoal and resins, oxidation, flotation, biodegradation, incineration, radiation and recycling.

One of the most widely used methods to treat organic compounds is adsorption on charcoal. However, this process only transfers the contaminant from liquid to solid phase. In this treatment the organic compounds are not degraded and used charcoal has to be decontaminated or properly stored.

The oxidation process has attracted many researchers due to the capacity to mineralize organic compounds. The most efficient oxidation is the use of OH radicals. There are various methods for generating OH radicals: use of ozone, hydrogen peroxide and ultra-violet (AOP – Advanced Oxidation Process). The most simple and efficient method for generating OH radicals in situ is the interaction of ionizing radiation with water [1].

The use of ionizing radiation has great ecological and technological advantages, especially when compared to physical-chemical and biological methods. Ionizing radiation degrades organic compounds, generating substances that are easily biodegraded, and making it not necessary to add chemical compounds.

Another aspect to be considered is the recent survey of pollutant agents in the rivers of São Paulo State which reported widespread contamination due to industrial waste, mainly organochloride compounds. As the conventional and available technologies to treat such wastewater have low efficiency and high cost, the Government through the São Paulo State Sanitation Company (SABESP) and some industries are searching for alternative technologies to degrade these chemical compounds to obtain better quality water and consequently improve sanitary conditions and preserve the environment.

The industries that contribute most to the pollution of the São Paulo Metropolitan Region are metallurgical (including mechanical and automobile), followed by the textile, food, chemical, electrical and cellulose and paper industries. The metallurgical and chemical industries produce 87% of inorganic load, while the chemical, food and textile industries produce 79% of organic load discharged into the Tietê River without any treatment [2,3]. The Environmental Protection Agency of São Paulo State (CETESB) resolved that the industrial enterprises need to control and treat liquid effluents before delivery to the rivers or to the Public Wastewater Treatment System.

Considering these aspects the Government of São Paulo State and the industries are concentrating a major effort in a programme on decontamination of the main rivers and water reservoirs located close to industrial areas through the implementation of new Wastewater Treatment Plants. As these plants have a low efficiency for the removal of refractory pollutants, mainly organochloride compounds, there is a need for an alternative technology to be used in conjunction with the conventional treatment to improve the reduction of pollutants.

Probably, the best way in some cases would be the treatment at industrial sites before disposal to the wastewater treatment plant and eventually to the environment. The main development to be achieved will be a technique reliable and economically available to greatly reduce the emission of industrial pollutants.

Considering these aspects, the specific solution is to develop and introduce in Brazil an alternative technology for wastewater and industrial effluent treatment, mainly for the degradation of refractory pollutants, using ionization radiation by submitting the pollutant material to high-energy EB.

In this direction, the Institute for Energetic and Nuclear Research, in São Paulo, Brazil (IPEN) started the development of an alternative technology for wastewater and industrial effluent treatment, mainly for the degradation of pollutants, using radiation from a high-energy EB. This technology has been extensively studied by many research centres [4–9].

A wastewater treatment pilot plant set up in an EB facility was used in order to study the removing and degrading efficiency of toxic and refractory pollutants, mainly from industrial origins (organic compounds), to destroy pathogenic microorganisms in wastewater and sludge. This pilot plant can be used to scale up the design of commercial plants. The main goal of this research is to optimize the irradiation system to get high efficiency with low EB energy in order to reduce the costs of the facility including the EB machine, utilities and irradiation vault (investments costs).

2. IPEN'S PILOT PLANT

A pilot plant was set up to treat wastewater and industrial effluents at IPEN's EB Facility. The EB Accelerator is a 1.5 MeV Dynamitron type from Radiation Dynamics Inc. USA. The accelerating voltage ranges from 500 keV to 1.5 MeV and the beam current from 1mA to 25 mA. The beam with a frequency of 100Hz was adjusted to scan an area of 60cm length and 2 cm width [10].

The pilot plant (Fig. 1) can process up to 70 L/min with an average dose rate of 5 kGy. Two tanks with 1,200 L capacity is used for storage and collection of liquid, and two pumps are used to homogenize and pump the liquid through the irradiation device. A sample system allows collecting the samples before and after irradiation. A real time calorimetric system was developed to control the dose rate delivered to the stream.

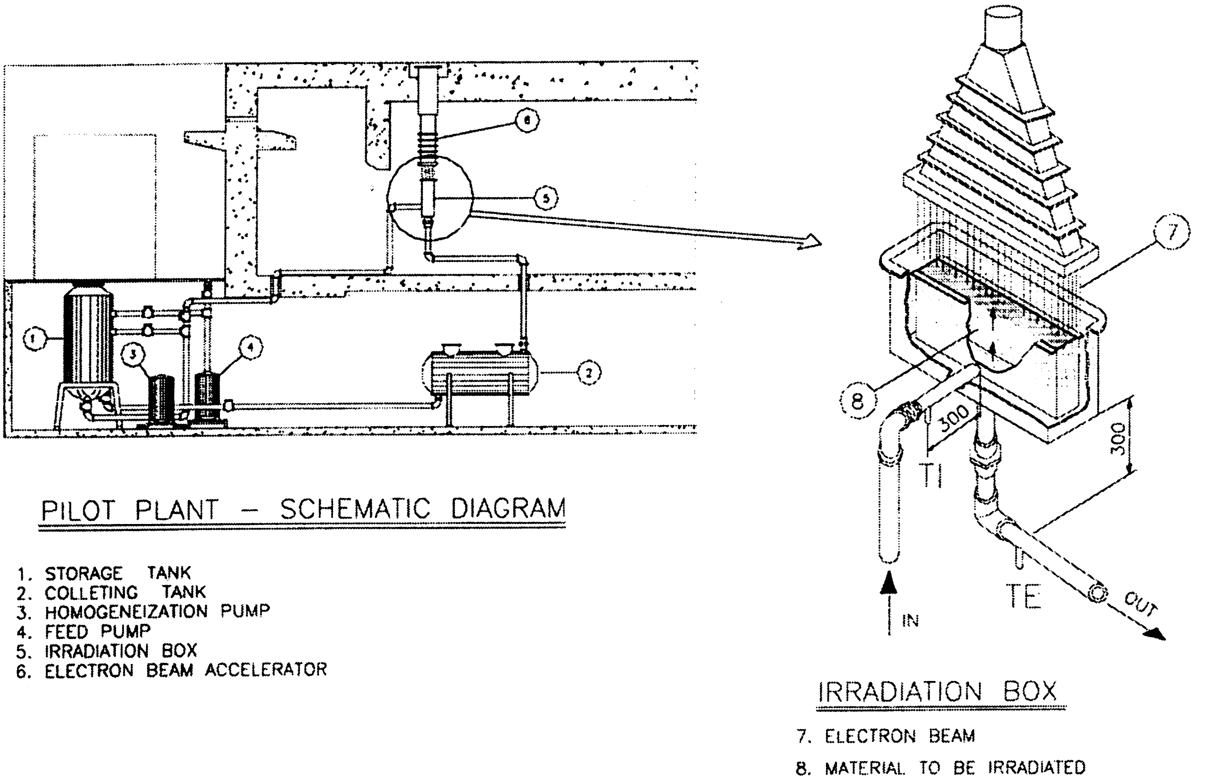

FIG. 1. Schematic diagram of pilot plant.

2.1. Hydraulic system

The hydraulic system, where the water is presented to the EB, governs the efficiency of this technology. The present work included the ***development of an upflow irradiation device*** that, by its configuration, theoretically alleviate the dependence of energy transfer to the stream with the beam accelerating voltage (penetration capability).

Three models of upflow stream irradiation device were tested; the models are represented in Fig. 2. The sequence of the development started with the model 1 that was upgraded to models 2 and 3. The model 3 fitted with a titanium foil window allows the irradiation device to work as a closed system where, in this configuration, hazardous liquids can be processed in a safe condition, avoiding the spread of gaseous by-products to the environment and allowing to sample the gas formed during the irradiation process and also re-inject the gas in the influent stream to be submitted to the EB treatment. Figure 3 shows the placement of the irradiation device under de EB machine [11].

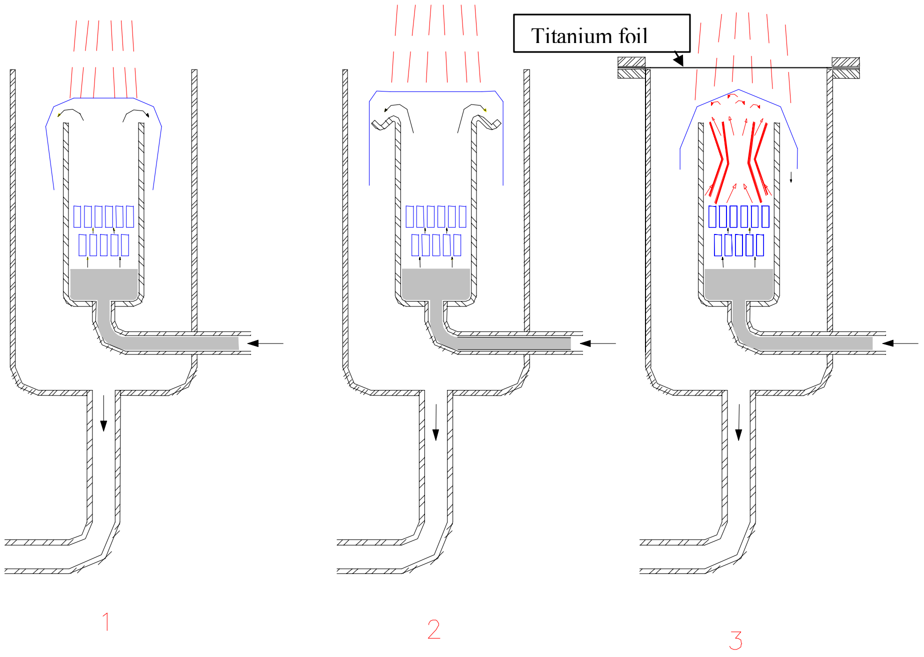

FIG. 2. Models of upflow stream irradiation devices.

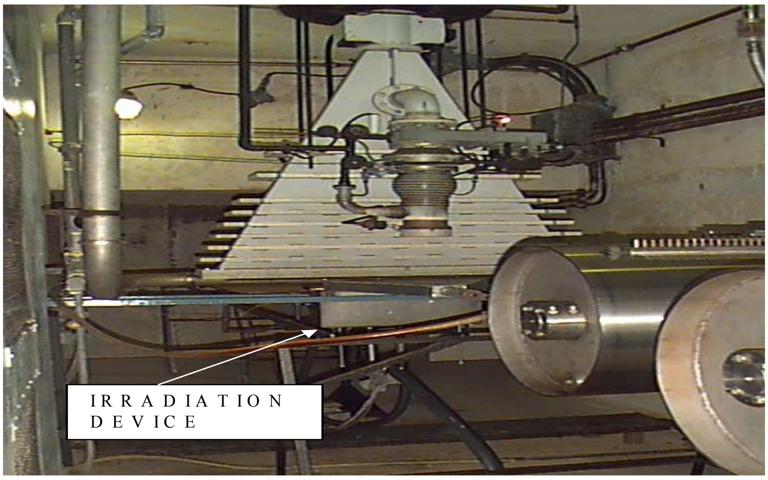

FIG. 3. External view of the irradiation device.

2.2. Dosimetric system

For a better control of parameters involved during the liquid waste radiation processing, an on line calorimetric system was developed [12] where the absorbed dose is obtained by measuring the temperature difference of the water stream before and after the irradiation device.

The dosimetric system is based on two Wire Current Output Temperature Transducers, WCOTT, model, GE-ADJ590J, from Intersil, located in the influent and in the effluent pipes 35 cm before and after the irradiation device. The temperature transducers are connected via an interface to a PC computer that continuously reads and records the temperatures and transforms the values to the equivalent dose delivered to the stream. Figure 4 shows the electric circuit diagram.

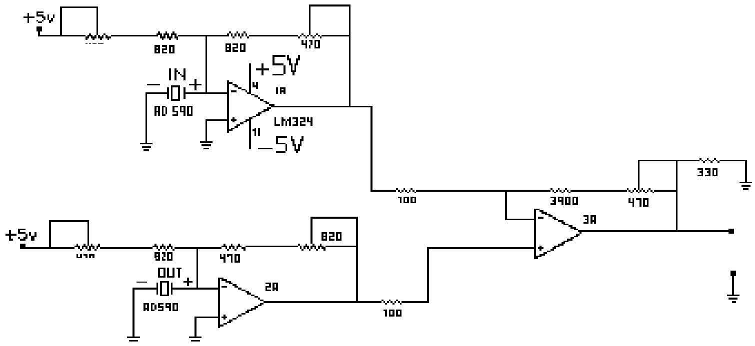

FIG. 4. Dosimetric system electric circuit diagram.

To evaluate the consistency of the dose registered by the calorimetric system, experiments were been performed using an aqueous chemical dosimeters, where the colour degradation of a commercial textile dye named "Duacouro" similar to Acid Red 265 was measured by the UV-Visible spectrophotometer at 500 nm [13].

2.3. Hydraulic system efficiency studies

For each irradiation device a series of tests were carried out in different operating conditions with the purpose to determine the maximum efficiency of the system. The efficiency was determined by the relation between the absorbed dose of the stream registered in the calorimeter and the delivered dose from EB accelerator (without losses). Using the amount of 200 hours of the IPEN's pilot plant the best results of the efficiency for the developed irradiation prototypes are shown in Table I.

TABLE I. EFFICIENCY OF THE PROTOTYPES

	Model 1	Model 2	Model 3	
			Open system	Self-cont. system
EB energy (MeV)	1.5	1.5	1.5	1.5
Flow (L/min)	45	45	54	54
Efficiency (%)	33	72	76	67

Besides getting the best efficiency results, Model 3 becomes a versatile device where different kinds of effluents can be processed, specially the hazardous wastes. The tests were performed in two configurations: (a) without the titanium foil window becoming the hydraulic circuit opened to the environment, and (b) fitted with the foil becoming a self-contained system.

All the efficiency tests were done simultaneously with dye degradation tests and the Figure 5 shows the efficiency of the irradiation device and the colour dye degradation in function of EB energy under the same radiation processing condition for the self-contained configuration.

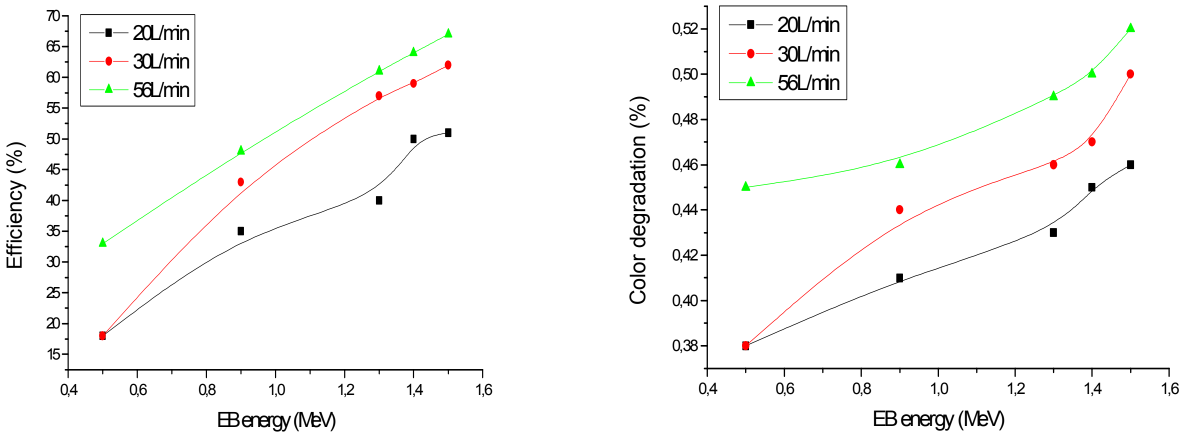

FIG. 5. Efficiency of the irradiation device & colour dye degradation as a function of EB energy.

3. INDUSTRIAL WASTEWATER TREATMENT

To conduct all the experiments, two different sources of samples were used: (a) from a pharmaceutical chemical industry located in São Paulo, and (b) from a Public Wastewater Treatment Plant in São Paulo State where reception of industrial wastewater is predominant.

3.1. EB irradiation of samples from industry

One of the most important chemical and pharmaceutical industry in Brazil was approached. A special transport truck was used to load 1,000 L of liquid waste from industry to the EB Pilot Plant.

The industrial wastewater was irradiated with air mixing and delivering the following doses: 2 kGy, 5 kGy, 10 kGy, 15 kGy and 20 kGy; and without air mixing at doses 2 kGy, 15 kGy and 20 kGy. The effectiveness of the treatment was evaluated by chemical analyses of the samples before and after irradiation. The parameters analysed were COD (chemical oxygen demand), absorption spectrum (300 nm a 700 nm) chloroform, perchloroetilene (PCE), trichloroetilene (TCE), carbon tetrachloride and dichloroethane by gas chromatography. All chemical analyses were performed according the Standard Methods for the Examination of Water and Wastewater published by American Public Health Association [14].

It is important to point out that the degradation rate was above 80% for the majority of the compounds in air mixing at a 2 kGy dose. When the samples were irradiated without air mixing the degradation was higher. Table II shows these results.

TABLE II. DEGRADATION OF ORGANIC COMPOUNDS FROM INDUSTRIAL EFFLUENT AFTER EB IRRADIATION

Dose (kGy)	Chloroform (ppm)		PCE (ppm)		TCE (ppm)		Carbon tetrachloride (ppm)		Dichloro ethane (ppm)	
	no air	air	no air	air	no air	air	no air	air	no air	air
0.0	0,83	0.83	0.87	0.87	3.57	3.57	9.74	9.75	87.93	87.93
2.0	nd	0.02	nd	0.10	0.36	0.61	2.36	3.37	nd	4.05
5.0	-	0.33	-	0.50	-	2.06	-	8.28	-	69.32
10.0	-	0.09	-	0.24	-	1.09	-	3.76	-	56.37
15.0	nd	0.04	-	0.09	0.32	0.54	1.68	2.17	nd	43.50

Table III presents the effects on COD values. A decrease close to 30% for the samples irradiated with air mixing at 2 kGy dose was observed and in the case of irradiation without air mixing the COD did not show significant changes for doses until 15 kGy, at 20 kGy dose the value decreased about 30%. The decreasing of the colour was more significant in the samples submitted to high doses, greater than 10 kGy and without air mixing. These results were not expected because in the literature dye degradation is always greater for air mixing condition.

TABLE III. COD VALUES OF SAMPLES FROM INDUSTRIAL EFFLUENT IRRADIATED AT DIFFERENT DOSES

Dose (kGy)	COD (mgO_2/L)	COD (mgO_2/L)
	no air	air
0.0	952.0	952.0
2.0	1048.1	682.7
5.0	1040.0	702.0
10.0	1000.0	1009.7
15.0	971.2	1028.9
20.0	548.1	625.1

3.2. EB irradiation process combined to conventional treatment

These experiments were performed with the objective to use the EB technology combined with the biological treatment in order to get a better performance of the Public Wastewater Treatment Plant in São Paulo State [15]. In order to verify in which stage of the plant EB processing could be more efficient, five points were selected for sampling: from main industrial receiver unit influent (RUI), coarse bar screens effluent (CB), medium bar screens effluent (MB), primary sedimentation effluent (PS) and final effluent (FE). EB irradiation was performed in a batch system using a Dynamitron II EB Accelerator with a conveyor velocity of 6.7m/min. The beam with 2 cm width was scanned in 120 cm length. The samples were placed in a Pyrex vessel with each layer 4 mm thick. Eight composed samples (four sampling collected each two hours during 12 hours) were collected from each selected point. The samples were irradiated at IPEN's EB Facility and the delivered doses were 5 kGy, 10 kGy and 20 kGy. The following analyses were performed: Total Organic Carbon (TOC), Chemical Oxygen Demand (COD), Biochemical Oxygen Demand (BOD), dissolved and volatile solids dried at 550°C and total solids dried at 103–105°C, Trihalomethanes (THMs), tetrachloroethylene (PCE), trichloroethylene (TCE), benzene, toluene, xylene, phenol, organic acids. Evaluation of the irradiation treatment efficiency was verified by the chemical analysis of the duplicate samples before and after irradiation.

The average concentration of the eight samplings of main organic compounds present in different steps of the WWTP before and after EB irradiation are shown in Table IV, and the variation between the sampling is about 50%. The receiver unit (RUI) and the coarse bar screen (CB) points receive, exclusively, industrial effluent; before the medium bar screens (MB) point, the plant receives about 20% in volume of domestic effluent. As such the average of all organic compounds analysed was higher in the first two steps, requiring high doses for degradation; besides that, the other contaminants present, such as solids, metals and dyes contributed to the necessity of higher doses.

These experiments showed that for RUI and CB it was necessary for 20 kGy dose to degrade about 99% of all organic compounds present, but for the others steps like MB and PS, 99% degradation was obtained at 10 kGy dose. For the final effluent (FE), a low dose (2 kGy) is enough to degrade the remaining organic compounds and dyes after biological treatment; colouration still remains in the effluent and the radiation processing contribute to colour degradation (Fig. 6).

The average concentrations of conventional parameters are shown in the Table V. It was verified that there were no significant changes in these values after irradiation. Most of the pH values decreased after irradiation, this is an expected result considering that the degradation of organic compounds generates smaller molecules of organic acids. The COD values were divided by BOD values to evaluate the biodegradability improvement and these results are shown in Fig. 7.

To evaluate the by-products from radiation processing, mass spectrometry and organic acid analyses were made. Results of the mass spectrometry analysis showed that no by-products were formed after irradiation, but it was detected, using a high performance liquid chromatography, that there was an increase of ppm concentration of the organic acids oxalic, tartaric, ascorbic and formic, mainly in the RUI and CB points. The results obtained of organic acids from different samplings after EB irradiation in case of RUI, CB and final effluent points are shown in the Figs 8, 9 and 10, respectively.

EB irradiation showed efficiency in destroying aromatic organic compounds trihalomethanes, PCE and TCE present in industrial effluent and the necessary irradiation dose depends on the concentration of the pollutant in the effluent.

These studies showed that in this WWTP, there are two possibilities to utilize the EB irradiation process: in the reception of industrial effluent — delivering high dose (20 kGy) in order to maintain the good performance of the wastewater treatment plant, and in the final effluent — delivering a low dose (5 kGy) to enhance the clarification, making possible the reuse of treated wastewater to industrial applications.

TABLE IV. AVERAGE CONCENTRATION OF THE MAIN ORGANIC COMPOUNDS PRESENT AT DIFFERENT STEPS OF WWTP, WITH EB IRRADIATION

Dose (kGy)	Chlorof. (ppb)	Bromof. (ppb)	Dichlorobromomethane (ppb)	DibromochloroMethane (ppb)	TCE (ppb)	PCE (ppb)	Benzene (ppb)	Toluene (ppb)	Xylene (ppb)	Phenol (ppb)
RUI										
0	925±425	154±75	206±125	665±324	178±95	402±187	1750±824	2689±823	6444±2590	2800±1250
10	490±225	49±25	75±26	193±95	56±25	132±74	654±296	1675±785	3076±1459	3143±2503
20	199±20	<20	<20	53±25	43±15	43±25	<50	568±259	387±65	1987±657
CB Effluent										
0	647±145	176±98	159±65	617±321	120±56	24±10	2012±1251	7750±2799	3398±1654	2237±1167
10	126±78	38±21	32±18	338±154	63±31	<10	631±259	4635±1787	2043±987	2765±1345
20	69±25	<20	<20	92±25	36±14	<10	131±31	1262±678	893±323	1893±987
MB Effluent										
0	992±453	132±78	296±134	904±421	235±123	80±31	860±245	1990±765	1310±567	1500 ±678
5	152±79	41±21	118±76	613±311	111±25	12±5	493±198	453±251	152±34	2210 ±998
10	<10	32±9	59±9	161±98	<20	<10	<50	<50	<50	<200
PS Effluent										
0	3331±1250	<20	<20	<20	460±156	100±67	767±321	556±125	890±342	990±432
5	470±251				40±25	<10	<50	254±112	132±67	1256±521
10	156±32				<20			<50	<50	<200
Final Effluent										
0	815±123	<20	<20	<20	76 ±21	80±34	325±99	<50	<50	<200
5	<10				<20	<10	<50			<200
10	<10									<200

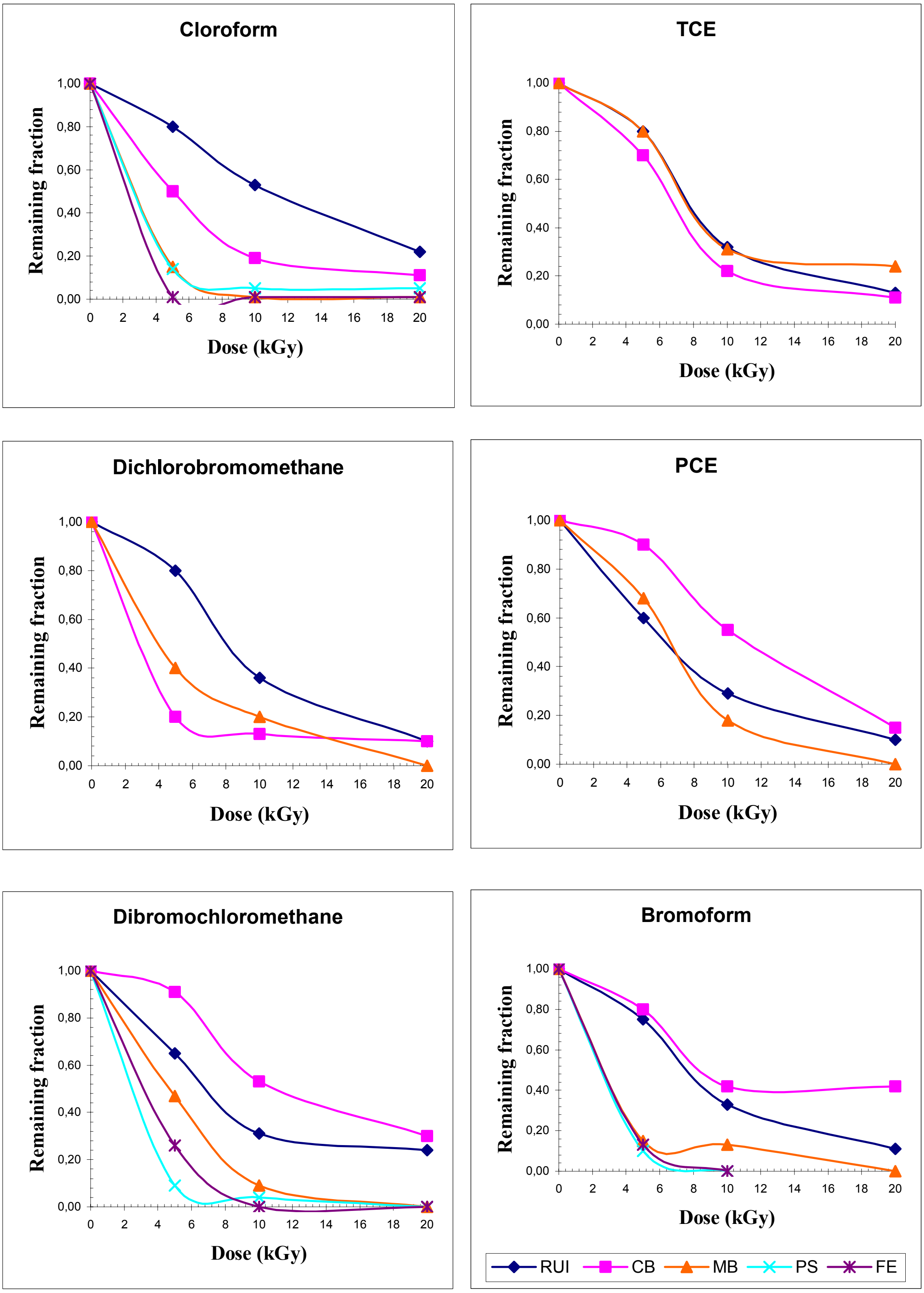

FIG. 6. Degradation of the organic compounds present at the different steps of WWTP after EB irradiation.

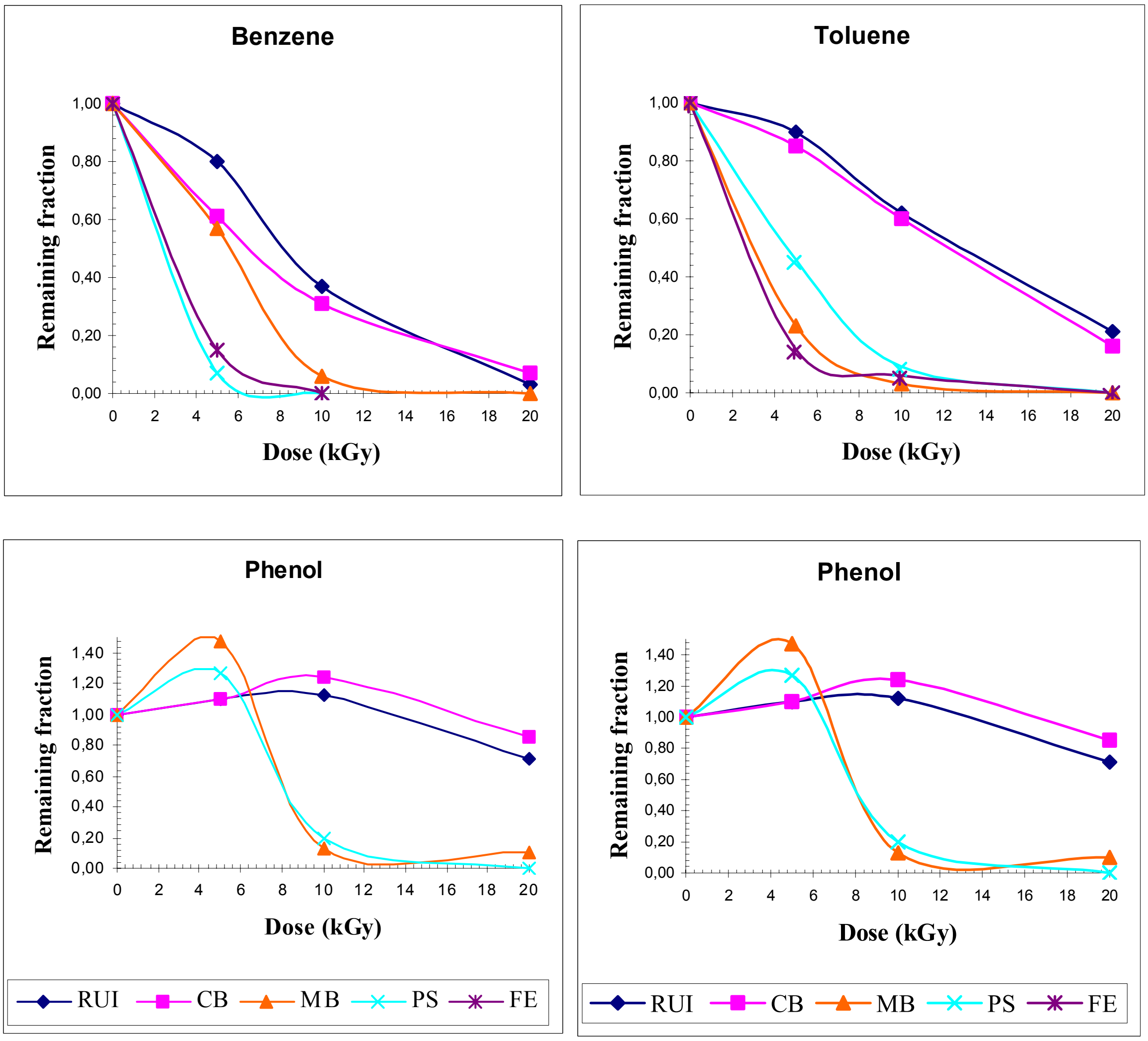
Benzene
Toluene
Phenol
Phenol
Remaining fraction
Dose (kGy)
1,00
0,80
0,60
0,40
0,20
0,00
1,40
1,20
0
2
4
6
8
10
12
14
16
18
20
RUI
CB
MB
PS
FE

FIG. 6. (cont.).

TABLE V. VARIATION OF THE CONVENTIONAL PARAMETERS IN DIFFERENT STEPS OF WWTP WITH EB IRRADIATION

Dose (kgy)	COD (mgo$_2$/l)	BOD (mgo$_2$/l)	TOC (mg/l)	Total Solid (mg/l)	Total Volatile Solid (mg/l)	pH
RUI						
0	1482 ±525	895 ±322	330 ±74	3599 ±982	624± 237	8.3 ±0.3
10	1383 ±483	708 ±352	341 ±74	3720 ±968	700± 206	8.0 ±0.3
20	1380 ±453	547 ±285	351 ±82	3813 ±933	844± 206	7.7 ±0.4
CB Effluent						
0	1044 ±547	544 ±183	212±79	1648 ±1025	352±224	7.4 ±0.2
10	891 ±444	538 ±350	207 ±78	1634 ±941	413± 257	7.4 ±0.3
20	898 ±468	401 ±347	187 ±81	1834 ±1001	518± 251	7.3 ±0.4
MB Effluent						
0	635 ±118	291 ±52	465 ±278	1691 ±690	583 ±328	7.5 ±0,4
10	683 ±93	259 ±72	469 ±286	1544 ±596	492 ±258	7.4 ±0,3
20	674 ±109	307 ±96	498 ±312	1434 ±552	513 ±173	7.3 ±0,3
PS Effluent						
0	696 ± 396	409 ±266	428 ±245	1333 ±377	450 ±284	7.8 ± 0,5
5	584 ±204	244 ±70	454 ±233	1448 ±525	581 ±448	7.8 ± 0,4
10	550 ±152	288 ±106	494 ±207	1533 ±600	294 ±151	7.6 ± 0,5
Final Effluent						
0	177 ±65	32 ±14	185 ±133	1263 ±372	203 ±109	7.8 ±0,4
5	183 ±68	37 ±18	180 ±125	1146 ±284	236 ±95	7.5 ±0,4
10	174 ±55	37 ±10	187 ±105	1384 ±507	321 ±174	7.4 ±0,5

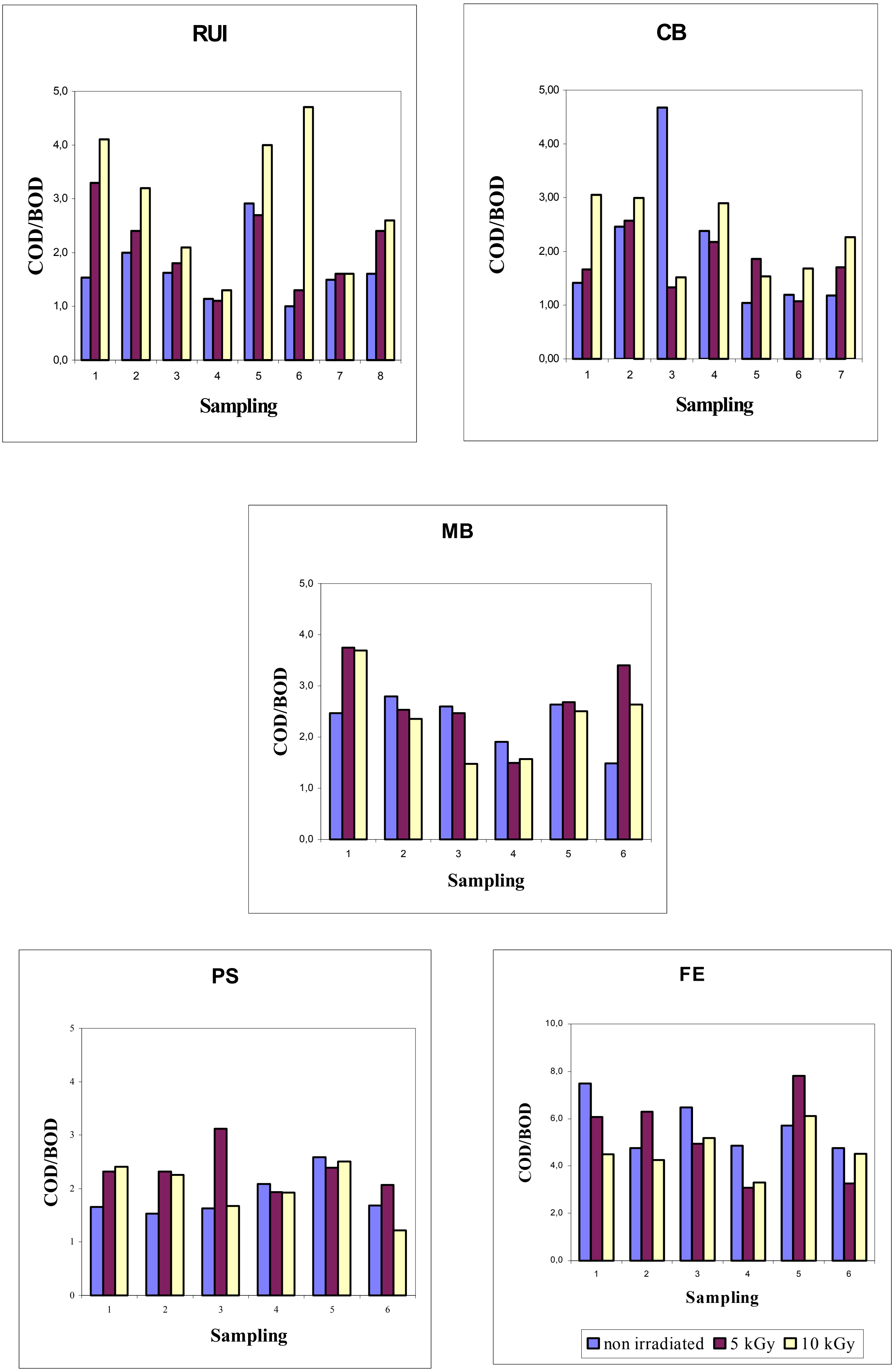

FIG. 7. Biodegradability variation of samples from different steps of the WWTP.

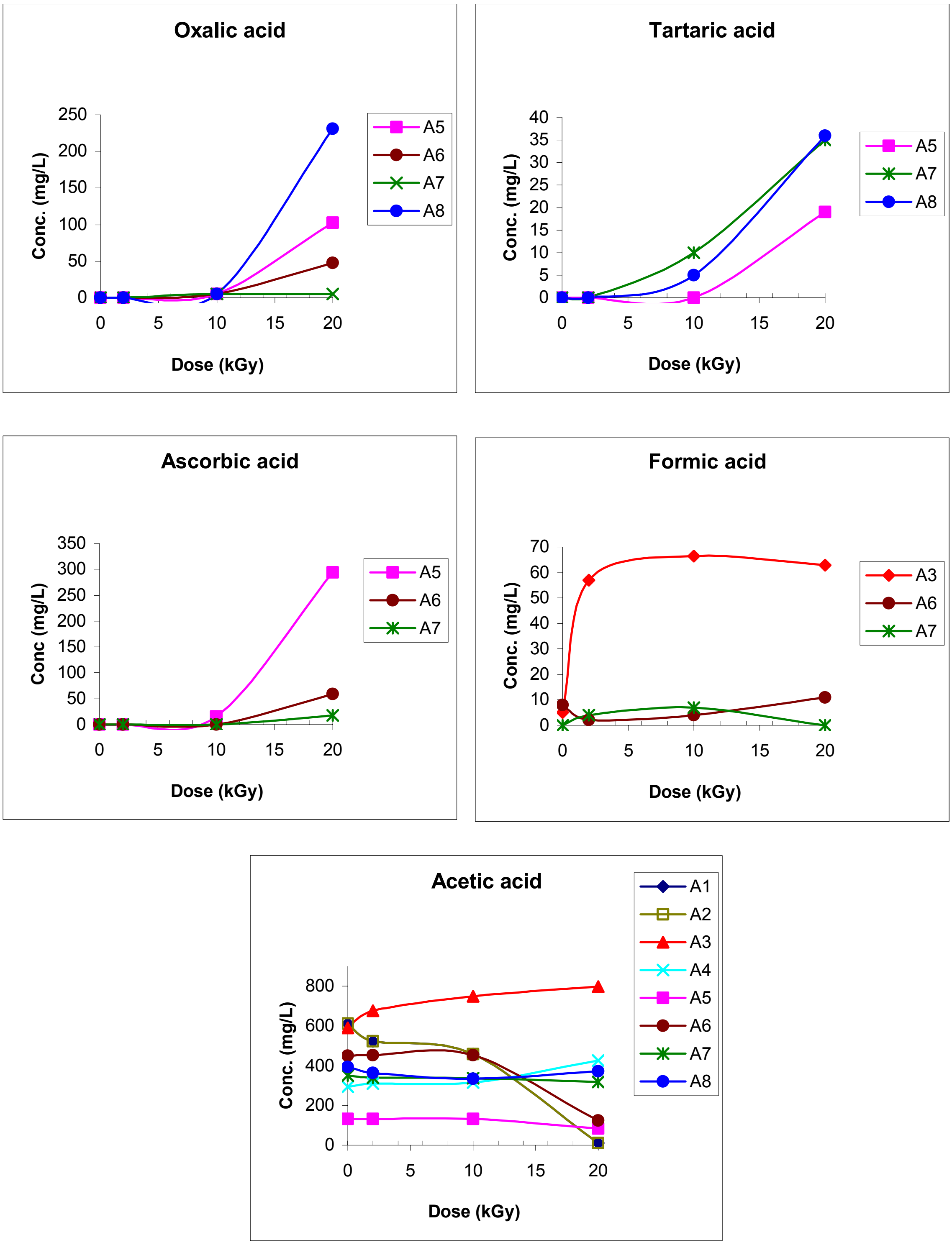

FIG. 8. Variation of organic acids concentration in the different samplings (A) of Receiver Unit Initial (RUI) after EB irradiation.

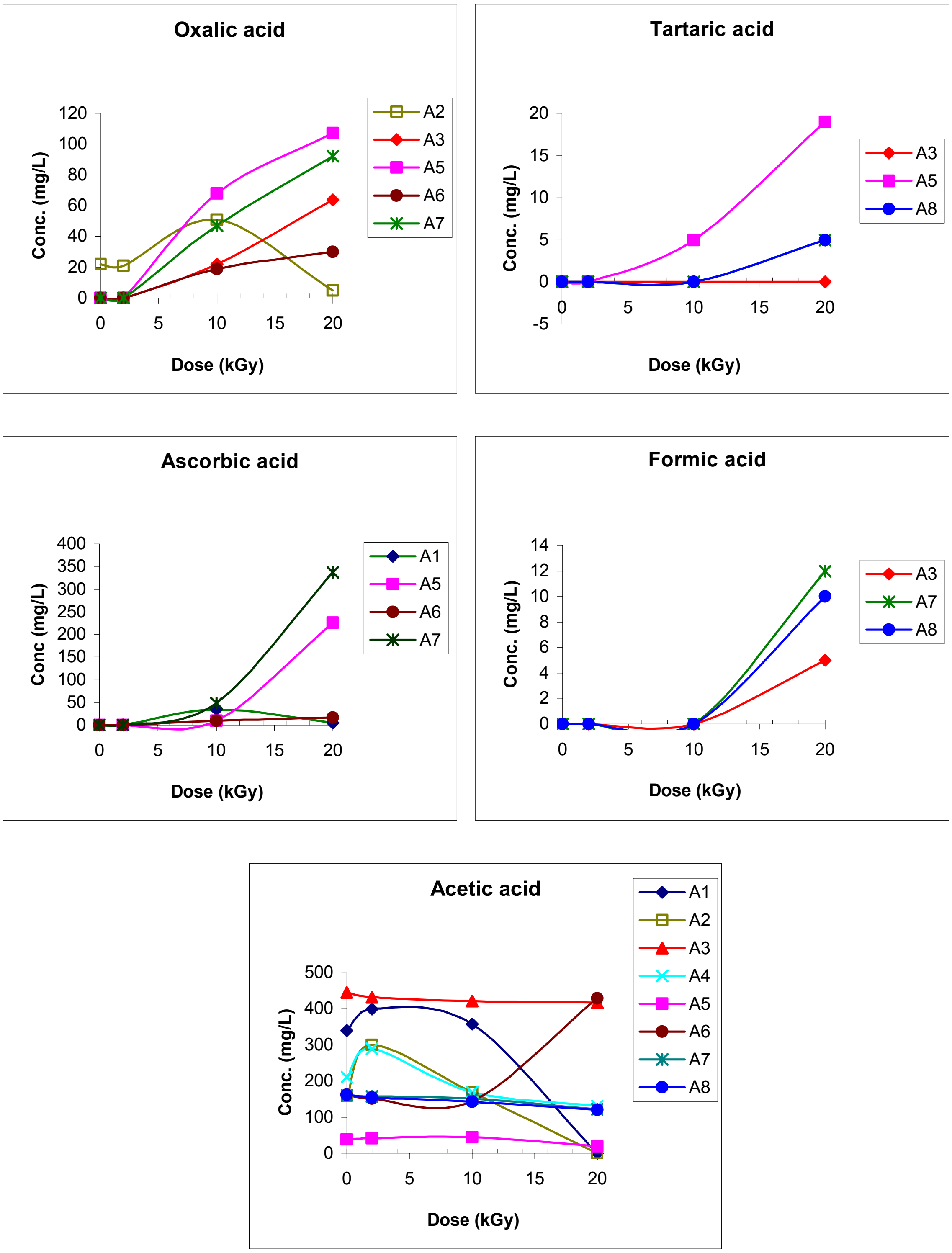

FIG. 9. Variation of organic acids concentration in the different samplings (A) of Coarse Bar Screen (CB) after EB irradiation.

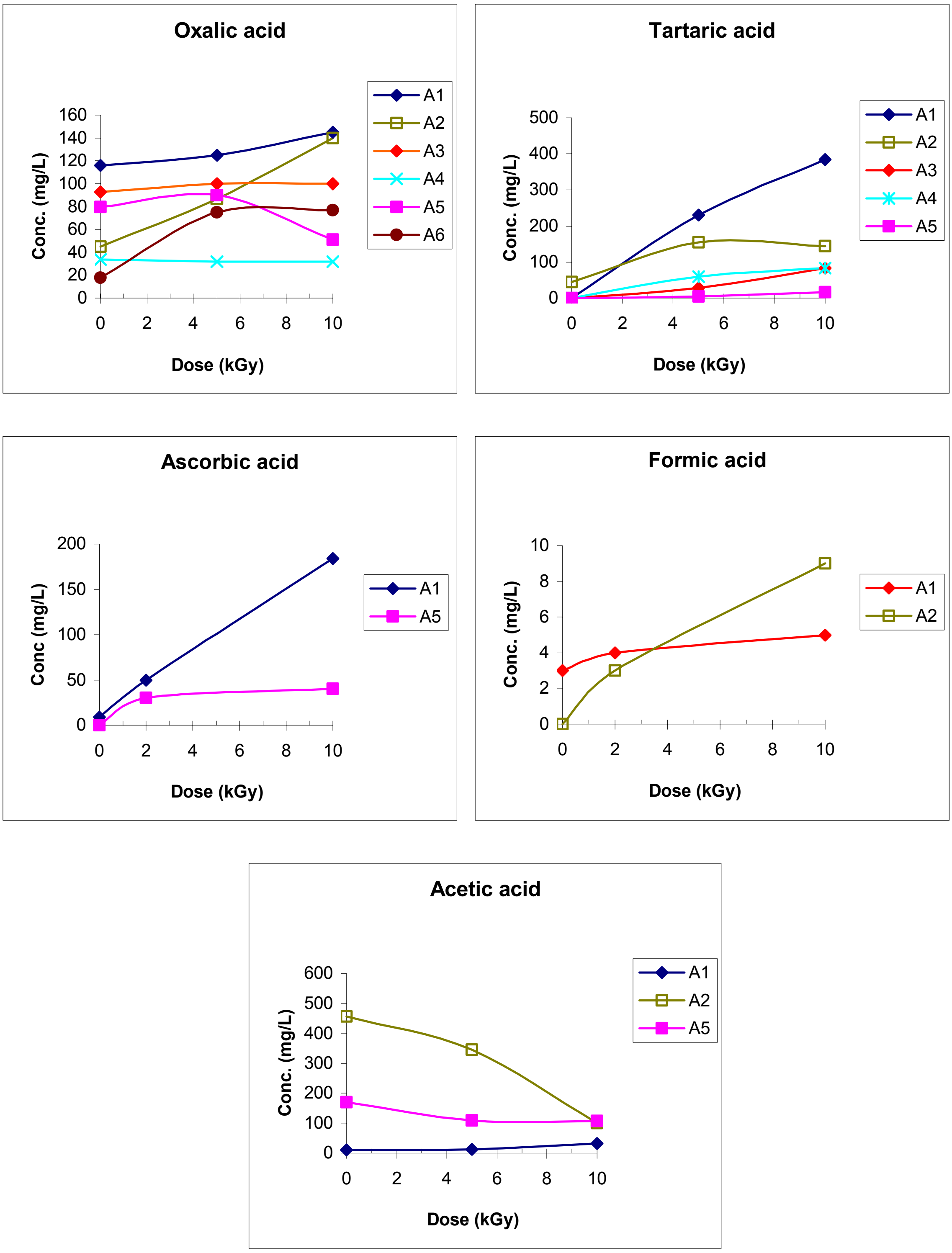

FIG. 10. Variation of organic acids concentration in the different samplings (A) from final effluent after EB irradiation.

4. TOXICITY STUDIES

Toxicity studies were carried out with the objective to evaluate the efficiency of radiation for acute toxicity removal. Acute toxicity response was expressed as EC-50 value, which means the sample concentration reduces the measured effect by 50%. *Daphnia similis* tests measure the mobility of the organisms, an EC-50 value of 7.2% means that at 7.2% of sample concentration, 50% of the exposed organisms are affected (immobile or dead). The tested organisms and standard methods were the following: (a) Bacteria *Vibrio fischeri*, Microtox System® – Basic Test Protocol – 15 minutes exposure, (b) Sea urchin *Lytechinus variegatus* (Fertilization test): 80 minutes exposure, measuring acute sublethal effects, for samples discharged into the sea [16]. (c) Microcrustacean *Daphnia similis*, acute test for 48 hours exposure, all of them in standard conditions [17]. All effluent and influent samples were tested with the Microtox System and some of them confirmed with the two others toxicity tests. The data were discussed according to the toxicity rank established by Bulich [18].

Thirty wastewater samples were collected from different sites and industrial activities. The sampling included different WWTP influents and effluents from different industrial activities (petrol extraction, chemical pharmaceutical, textile and a complex mixture of industrial effluents), as presented in Table VI. The acute toxicity evaluation was carried out for irradiated and unirradiated samples with different radiation doses using an EB accelerator in a batch system. Few samples were irradiated by gamma rays with a ^{60}Co, gamma cell – 10.000 Ci activity.

TABLE VI. RANGE OF TOXICITY ACCORDING TO THE SAMPLING SITES AND RELATED INDUSTRIAL ACTIVITIES AND RADIATION DOSE EFFECTS (PRELIMINARY RESULTS)

Site number and industrial activity	Range of toxicity for raw sample EC-50, Microtox (V. fischeri) (concentration %)	Dose (kGy) and EC-50 (%) (Benefits by dose)
01. WWTP A Sewage prevalence Site 1	6.52 (4.98 - 7.23) - 20.28 (14.5-28.3) n = 3; Average: 11.33 ± 7.75	3.0 kGy ⇒ 45.45% for Microtox (V.fischeri)
02. WWTP B Industrial effluent prevalence Site 2	2.24(1.87–2.67)-15.81 (13.49 – 18.62); n = 10;Average: 9.28 ± 5.27	6.0 kGy ⇒ 45.45%; for V.fischeri , except when EC50 was < 5.0% for unirradiated sewage, it required higher doses
03. Industry 1 Produced Water – Petrol extraction activities Site 3	2.59 (1.77–3.80)- 14.64 (12.76 – 16.90); n = 4; Average: 2.10 ± 0.31, for V.fischeriAverage: 2.95 ± 3.35, for Lytechnus variegatus	9.0 kGy ⇒ 1.74% for V.fischeri and 1.56% for L. variegatusNo improvement, except for the first experiment with gamma rad. (9.0 kGy ⇒ from 2.59% to 26.03%)
04. Industry 2 Chemical Pharmaceutical Site 4	0.10(0.08-0.14) - 0.61 (0.29-1.31); n = 2	9.0 kGy ⇒ 0.30%40.0 kGy ⇒ 0.83%. No improvement
05. Industry 3 Textile Site 5	1.65 (1.52- 1.78)- 12.71 (7.30 – 23.10); n = 2	10.0 kGy ⇒ 45.45% for V.fischeri 10.0 kGy ⇒ 66.20% (D.similis)
06. Complex Mixture of Industrial Effluents Site 6	0.71 (0.51 – 0.99) – 10.27(9.85-16.11); n = 9Average:2.24 ± 1.43, for V.fischeri BacteriaAverage: 2.42 ± 1.95, for D. similis	20.0 kGy ⇒ 20.33% No improvement for doses up to 20.0 kGy

Note: WWTP – Wastewater Treatment Plant; n – number of samplings.

Two different statistical analyses were applied for the EC-50 calculations. For Microtox Tests the statistical method was a linear regression, using the sample concentrations versus the gamma effect. Note that this gamma effect is the ratio of light lost to light remaining after exposure of the reagent to a sample and, in this case, EC-50 is the concentration at which gamma is equal to 1, that is, the light lost equals the light remaining [19]. For Fertilization tests (*L. variegatus*) and Mobility tests (*D. similis*), the EC-50 values were determined by Trimmed Spearman-Karber method, American Public Health Association [14].

All samples submitted to radiation presented originally a very high level of toxicity according to the range showed in Table VI. Significant removal of acute toxicity was obtained for most of the experiments, and the toxicity removal efficiency depended on its initial concentration as well as on the origin of the sample.

Figures 11 and 12 present toxicity data from two different wastewater treatment plants. These data demonstrated that for toxicity removal, radiation effect was more efficient for sewage samples compared to raw industrial effluents. At the plant where the sewage was prevalent the required doses were lower than 3.0 kGy, and at the plant where industrial effluent was prevalent the required doses were higher, i.e. from 9.0 kGy to 15.0 kGy. Otherwise, complex mixture of industrial effluents required doses from 30.0 kGy to 100.0 kGy, especially when raw samples were extremely toxic with EC-50 values lower than 1.0% (and up to 4.0%), as shown in Fig. 13.

The effluents from the petrol extraction activities or produced water did not present toxicity removal by irradiation for most experiments. A previous experiment was carried out using gamma and EB radiation and, only for the first sampling, the gamma radiation increased the EC-50 value from 2.59% to 26.03% for Microtox Test, as shown in Fig. 14 and Table VI. It is important to note that the lower the EC-50, the higher the toxicity is. No improvement was obtained for the effluents from industries 1 and 2 although only a few, preliminary experiments were carried out (see Table VI).

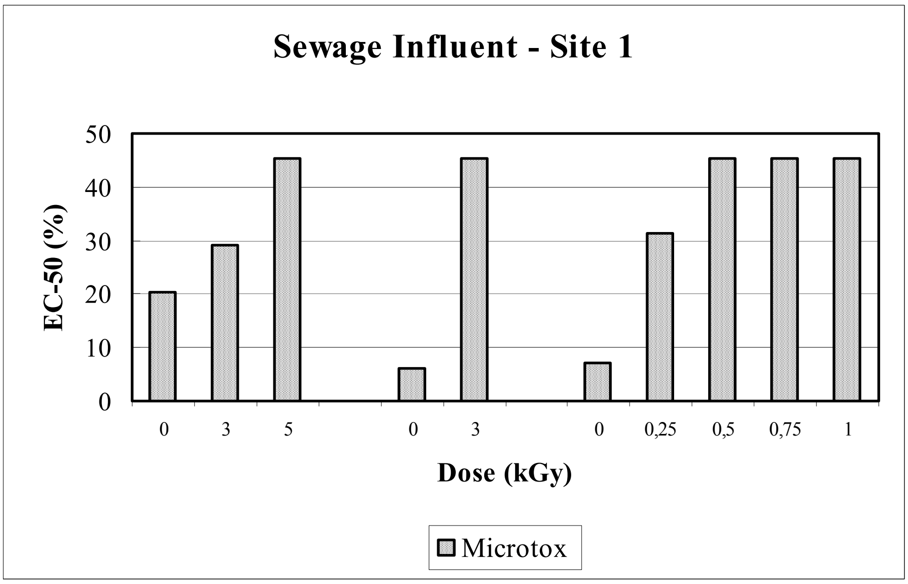

FIG. 11. Radiation effects on acute toxicity evaluated by Microtox tests applied to untreated and irradiated sewage influent from Site 1.

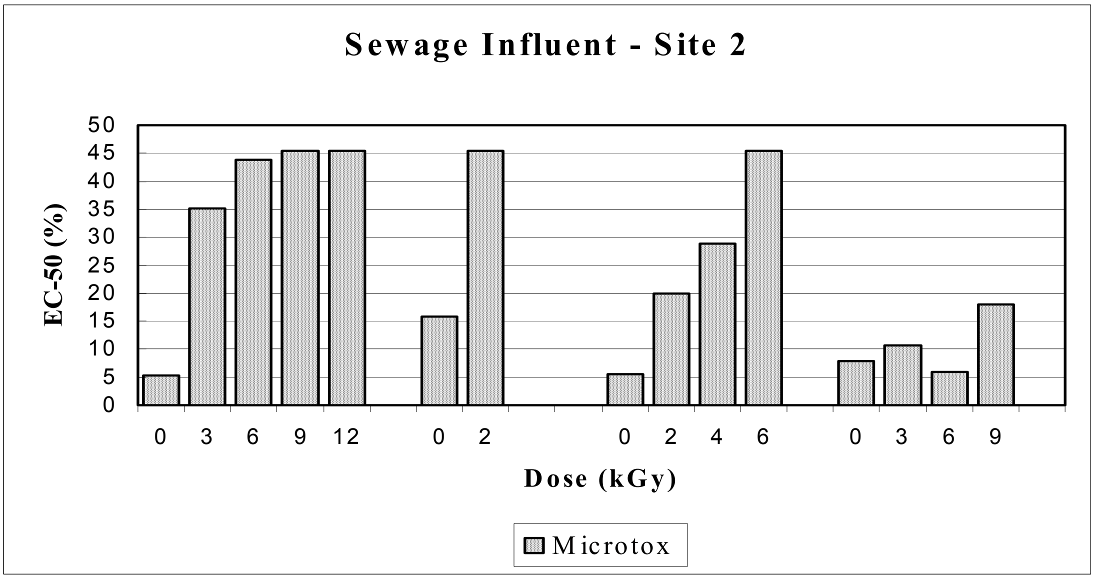

FIG. 12. Radiation effects on acute toxicity evaluated by Microtox tests applied to untreated and irradiated sewage influent from Site 2.

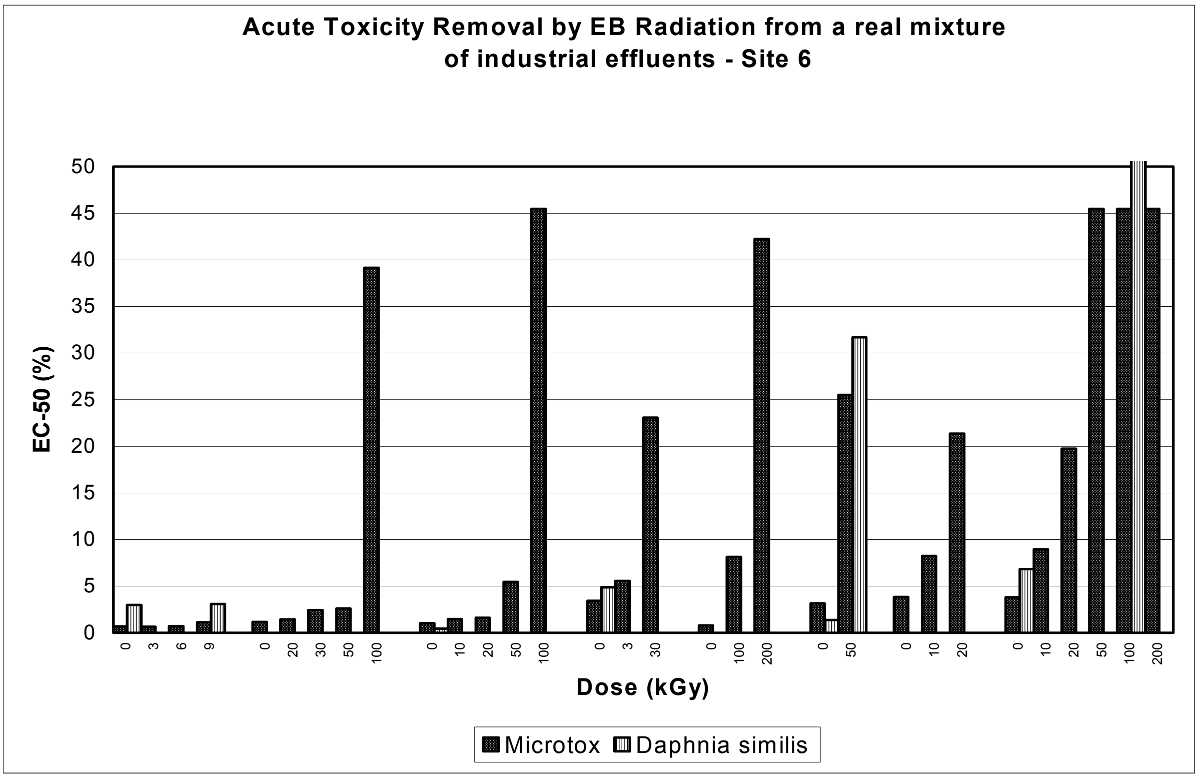

FIG. 13. Radiation effects on acute toxicity evaluated by Microtox and D.similis tests applied to untreated and irradiated complex mixture of industrial effluents from Site 6.

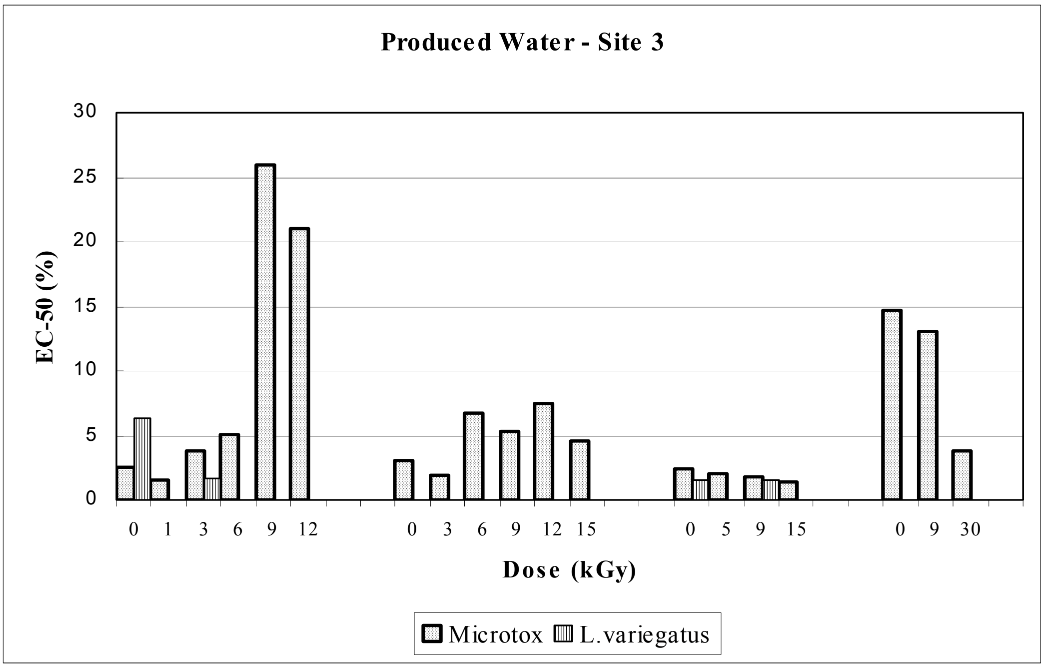

FIG. 14. Radiation effects on acute toxicity evaluated by Microtox and fertilization tests applied to untreated and irradiated complex mixture of industrial effluents from Site 3.

5. ECONOMIC ASPECTS

If the technology aspect of the process is well known, it has been demonstrated that the economic aspect and cost benefit remain the key issues to transfer the technology to the industry. Below are some process costs so far identified during these experiments.

5.1. Capital and amortization costs

The costs for EB and shielding depend on the specification of the equipment. Being conservative in this preliminary cost analysis the considered machine is an EB Accelerator 1.5 V, 60 A Dynamitron from Radiation Dynamics, Inc. (USA). For cost estimation purposes, accelerator cost was assumed at US $1.1 million and the installation (shielding), at US $400,000. The operating schedule was assumed to be three shifts, seven days per week and 8,000 hours per year (uptime).

Investment cost was assumed at an interest rate of 10% per year, with the cost equivalent per hour of US $18.7. Amortization of the whole facility was assumed for 15 years, with equivalent amortization cost per hour at US $12.5. The capital cost (investment plus amortization) is about US $31.2 per hour.

5.2. Variable costs

Labour cost for one operator and one material handler per shift would be equivalent to US $22.5 per hour (including administrative cost). Electricity cost is based on an average rate of US$0.08 per kilowatt. Equivalent cost for 120 kWh is US $9.5. Maintenance cost would be equivalent to US $10.0 per hour. Total of operating costs would be about US $42.0 per operating hour.

5.3. Total cost

The sum of fixed and variable costs would be about US $73.2 per operating hour. The unit cost for treatment cost process depended on delivered dose, unit processing cost. Table VII shows the processing costs for some values of delivered doses and operation.

TABLE VII. ESTIMATED PROCESSING COSTS FOR SOME VALUES OF DELIVERED DOSES AND OPERATION

Energy(MeV)	Dose(kGy)	EB Current(mA)	Flow(m^3/h)	Efficiency(%)	Cost(US\$/m^3)
1.5	2.0	60	113	70	0.65
1.5	3.0	60	75	70	1.00
1.5	5.0	60	45	70	1.62
1.5	10.0	60	22	70	3.32

6. CONCLUSIONS

Concerning the development of hydraulic system where water is presented to the EB that governs the efficiency of the radiation processing, the results are promising, allowing processing of liquids with a competitive price. The hydraulic system can still be improved to be used with low accelerating voltage EB in order to reduce processing costs. The improvement of real industrial effluents related to the radiation process can be also shown by the toxicity removal obtained for 87.7% of the irradiated samples, which changed from very toxic to slightly toxic, except for produced water. This toxicity removal could significantly improve the efficiency of a post-biological treatment, after the radiation process. The performed research in the laboratory and in the pilot plant show that high energy electrons are an effective treatment for many pollutants. However there is a lack of information concerning the use of this technology by the environmental engineers. Extra effort must be done to promote this technology to the engineering community to understand the benefits of aqueous chemistry associated with radiation of water.

ACKNOWLEDGEMENTS

The authors wish to thank the support of the International Atomic Energy Agency and the strong collaboration of São Paulo State Sanitation Company (SABESP), Hoechst do Brasil S.A. and Petrobras – Petroleo Brasileiro S.A.

REFERENCES

[1] GEHRINGER, P., PROKSCH, E., ESCHWEILER, H., SZINOVATZ, W. Appl. Radiat. Isot. **43** (1992).

[2] SÃO PAULO STATE SANITATION COMPANY – SABESP – Bulletin, São Paulo, Brazil, July 1991.

[3] ALONSO, L.R., SERPA, E.L. Ambiente-Revista CETESB de Tecnología **8** (1994) 12 pp.

[4] COOPER, W.J., MEACHAM, D.E., LIN, K., NICKELSEN, M.G., FORD, D.B., KURUCZ, C.N., WAITE, T.D., J. Air Waste Manag. Assoc. **43** (1993).

[5] WAITE, T.D., KURUCZ, C.N., COOPER, W.J. NARBAITZ, R., GREENFIELD J. (Proc. National Conference on Environmental Engineering, Austin, Texas, 1989).

[6] SWINWOOD, J.F., WAITE, T.D., KRUGER, P., RAO, S.M., IAEA Bulletin **1** (1994).

[7] PIKAEV, A.K., Russian Chem. Rew. **64** (1995).

[8] GETOFF, N., Radiat. Phys. Chem. **47** (1996).

[9] TATA, A., MANNI, S., Radiat.Phys.Chem. **42** (1993) 4–6.

[10] SAMPA, M.H.O., BORRELY, S.I., VIEIRA, J.M., RELA, P.R., CALVO, W.A.P. NIETO, R.C., DUARTE, C.L. PEREZ, H.E.B., SOMESSARI, E.S., LUGÃO, A.B. Radiat.Phys.Chem. **46** (1995).

[11] RELA, P.R., SAMPA, M.H.O., DUARTE, C.L., COSTA, F.E., SCIANI, V. in XI International Meeting on Radiation Processing–IMRP, March 15–19, 1999, Australia.

[12] COSTA, F.E., RELA, P.R. (Proc. 4th Meeting on Nuclear Applications, Brazil) (1997) 122 pp.

[13] DUARTE, C.L., SAMPA, M.H.O., RELA, P.R., OIKAWA, H., SOMESSARI, E.S. (Proc. XI International Meeting on Radiation Processing – IMRP, 15–19 March 1999, Australia).

[14] AMERICAN PUBLIC HEALTH ASSOCIATION, Standard Methods for the Examination of Water and Wastewater, 17 ed., Washington, DC, APWA, AWWA, WPCF (1997).

[15] DUARTE, C.L., SAMPA, M.H.O., RELA, P.R., OIKAWA, H., CHERBAKIAN, E.H., SENA, H.C., ABE, H. (Proc. XI International Meeting on Radiation Processing – IMRP, Australia, 15–19 March 1999).

[16] NIPPER, M.G., PROSPERI, V.A., ZAMBONI, A.J. Bull. Environ. Contam. Toxicol. **50** (1993) 646 pp.

[17] ASSOCIAÇÃO BRASILEIRA DE NORMAS TÉCNICAS, ABNT, Standard NBR 12713 (1993).

[18] BULICH, A.A., Biochem. **22** (1982) 45 pp.

[19] MICROBICS CORPORATION, Microtox® M500 Operating Manual, A Toxicity Testing Handbook, Version 3 (1994).

GAMMA RADIATION TREATMENT OF PENTACHLOROPHENOL, 2,4-DICHLOROPHENO AND 2-CHLOROPHENOL IN WATER

Yongke He, Jun Liu, Jilan Wu
Department of Technical Physics,
Beijing University,
Beijing, China

Abstract. The aim of this work was to investigate γ radiation treatment of pentachlorophenol (PCP), 2,4-dichlorophenol (DCP) and o-chlorophenol (o-CP) in water. The dechlorination of PCP, DCP and o-CP has been studied using γ radiation as well as ozonization. G(Cl-) is always much higher than the corresponding G(-PCP),this means that some primary radiolytic products are unstable during post irradiation. PCP is much easier to be decomposed under irradiation than that of simple chlorophenol. Some stable radiolytic intermediates were be detected. Primary analysis reveals some quinones among the final products with toxicity that remains unclear. In the pulse radiolytic experiment, it was determined that about 53% of radicals undergo electrotransfer and others undergo addition when OH radicals react with PCP. The values of COD(Mn) after irradiating PCP in dosage were determined. It is recommended to bubble ozone simultaneously when radiation (or electron beam) treat CPs contaminating water.

1. INTRODUCTION

Chlorination is widely used in drinking water treatment for disinfection and often seriously increase the level of toxic chlorinated organic by-products, and it is not surprising to find chlorophenols (CPs) among them [1]. Therefore research is needed in the applicability of radiation in water treatment.

Pentachlorophenol(PCP) and its salts, primarily the sodium salt have gained wide applications both in industry and agriculture and they are among the common environmental pollutants. In the seventies PCP was used in China in the fight against snail fever and as a herbicide. Its biodegradation is slow, and hence it is not surprising that it is still observed in many drinking water resources. CPs are toxic at concentrations of few μg/L and are also persistent, thus are listed in the US-EPA list of priority pollutants and in the European Community Directive 76/464/EEC as dangerous substances discharged into the aquatic environment [2, 3]. Since 1996, an IAEA project on the treatment of PCP in drinking water has been implemented.

OH radical is a very strong oxidant and react with most organic compounds at a diffusion control rate with little selection, and as a result, the concerned hazardous compound remains undestroyed at rather high absorbed dose applied. Model systems should be studied to obtain necessary data required for figuring out the radiolytic processes and making a practical estimation upon pertinent G values and rate constants. Pulse radiolysis is of quite help for kinetic studies. OH-radical-induced dechlorination of PCP, DCP and o-CP has been studied. To reduce the absorbed dose required, other methods like ozonation might be used in combination. Our works focus on the remediation of drinking water polluted with PCP and other CPs by the methods of γ radiation as well as ozonization. From the time of drinking water treatment prior to ensuring promising methods, one must confirm its reasonableness carefully. In this case, accompanying the degradation of PCP DCP and o-CP under irradiation, some stable intermediates have been detected, with potential toxicity considered. In the present paper, we report some latest results concerning to the radiation treatment of PCP, DCP and o-CP.

2. EXPERIMENTAL

Chemicals of the highest purity were commercially available and used without further purification. Prior to irradiation the solutions were saturated with air or N_2O. The pH of solutions were adjusted by 0.1M NaOH. Irradiation was carried out in ^{60}Co facilities in Beijing University and dose rates were determined with a Fricke dosimeter.

The decomposition of CPs were measured by HPLC on C_{18} columns. The mixture of methanol and water was used as fluent, where proportions and flow rates changed with different objects. PCP was detected at 320 nm and o-CP and DCP were detected at 280 nm. MS was performed with APCI (atmosphere pressure chemical ionization) source, negative mode, referring to Puig [4] with modification.

The yield of chloride ion was measured by ion selective electrode (Orion 9417B type), spectrophotometry (according to Florence) [5] and HPLC (Dionex 2010i), respectively.

Chemical Oxygen Demand (COD) was determined as described by Yu [6].

3. RESULTS AND DISCUSSION

3.1. Gamma radiolysis of PCP

Table I compiles G values of PCP consumption and Cl^- formation in different atmospheres.

TABLE I. COMPILATION OF G VALUES OF PCP CONSUMPTION AND CHLORIDE IONS FORMATION UNDER TIRRADIATION

	Air		N_2O [a]			N_2O+NaN_3 [b]	N_2
$[PCP]_0$ ($mol \cdot l^{-1}$)	1.3×10^{-4}	1.5×10^{-5}	1×10^{-4}	1×10^{-4}	1×10^{-4}	1×10^{-4}	1.6×10^{-5}
pH	9.7	5	5	9	10	9	9
G(-PCP) ($10^{-7} mol \cdot J^{-1}$)	0.90	0.55	2.9	2.9	2.9	1.9	1.2
G(Cl^-) ($10^{-7} mol \cdot J^{-1}$)	6.0	ND	4.4(7.9)[c]	6.0(9.9)[c]	8.2(9.9)[c]	6.5(7.5)[c]	4.8
Dose range (Gy)	0~140	0~32	0~150	0~150	0~150	0~150	0~500

[a]: N_2O saturated solution; [b]: N_2O saturated solution with $[NaN_3]$ = 210^{-3} M; [c] post-irradiation storage.

From the above, G(-PCP) is always much lower than G(OH), indicating that the phenoxy radicals formed may regenerate some PCP during their decay. G(Cl^-) is always much higher than the corresponding G(-PCP). We confirmed this by different ways including ion selective electrode, spectrophotometry and sometimes HPLC. This means that some primary irradiation products are unstable during post-irradiation storage, which release Cl^- continuously and meanwhile consume no further PCP.

From Fig. 1, both the G(-PCP) and G(Cl^-) were strongly dependent on doses. It reveals that when higher doses were applied, the intermediates would compete with PCP in capturing OH or e^-_{aq}.

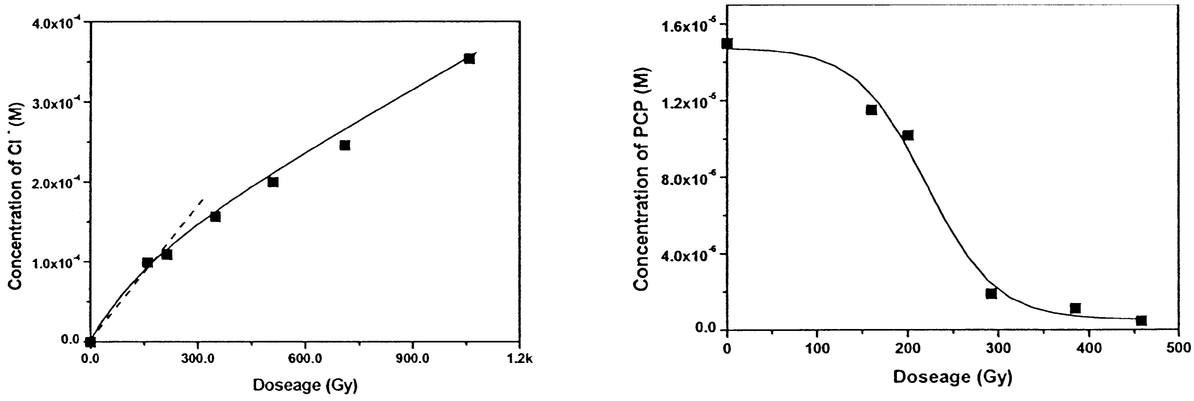

(a) *(b)*

FIG. 1. (a) Dependence of G(Cl^-) on dose, 1.6×10^{-4}M PCP, pH9.6, air saturated solution; (b) Dependence of G(-PCP) on dose, 1.5×10^{-5}M PCP, pH5, air saturated solution.

3.2. Pulse radiolysis and mechanism of PCP degradation

When radiolytically generated OH radical reacts with PCP at the beginning stage two pathways compete with each other: electron transfer and radical addition [7].

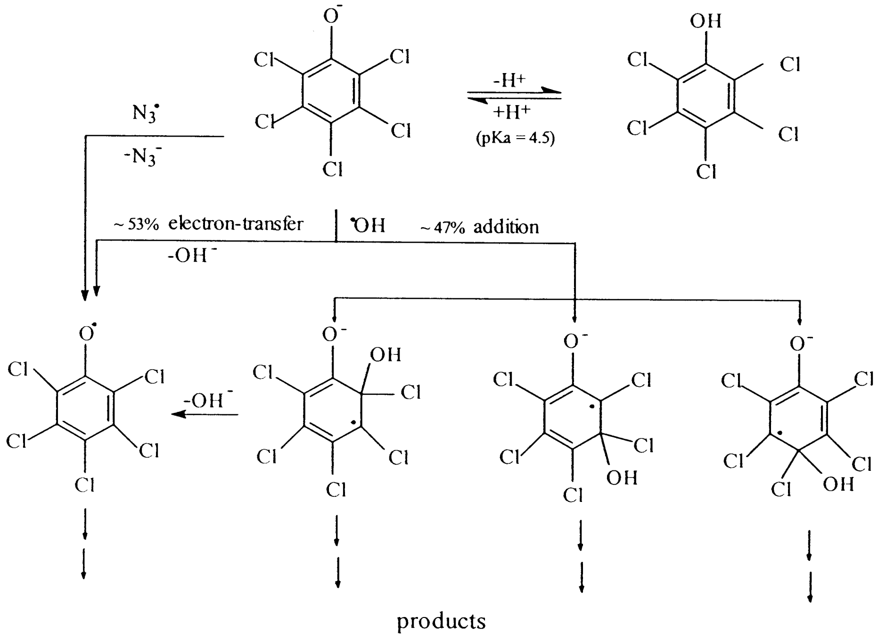

In a pulse radiolysis experiment, using optical and conductivity detection alternatively, Fang determined [8] that about 53% OH radicals undergo electron transfer and the others undergo addition when OH radicals react with PCP. Though further detailed mechanism relating to the release of Cl^- from pentachlorophenoxyl radical and depronated hydroxytetrachlorophenoxyl radical still leaves to be found. Based on Table I, we can properly draw out that in both ways only a part of PCP is eventually consumed and more than one Cl^- is released from a destroyed PCP molecule.

Comparing rate constants of OH and e^-_{aq} reacting on chlorophenols, quinones and chloranils with that on pentachlorophenol ($k(Cl_5C_6O^- + {}^{\cdot}OH) = 8.610^9 dm^3 \cdot mol^{-1} \cdot s^{-1}$) [7], it is easy to understand that both the G(-PCP) and G(Cl^-) are strongly dependant on the dose. The consumption of PCP and the release of Cl^- are reduced evidently as dose increases. Thus, some unexpected situations might take place. For example, if dose applied is insufficient, the water still retains undesirable chloranils.

3.3. γ Radiolysis of o-CP and DCP

Table II shows the compilation of G values of 2,4-dichlorophenol and 2-chlorophenol.

TABLE II. G VALUES OF O-CP AND DCP; PH5, AIR SATURATED SOLUTION

	o-CP			DCP	
$[CP]_0$ M	110^{-3}	410^{-4}	110^{-5}	4.410^{-4}	110^{-5}
G(-CP) 10^{-7}mol·J^{-1}	4.2	1.8	1.2	2.0	0.3
G(Cl^-) 10^{-7}mol·J^{-1}	0.3	0.2	ND	1.2	ND
Dose range (Gy)	0~432	0~420	0~32	0~420	0~300

With increasing concentration, the G value of decomposition is increased. It reveals that there existed competition reaction of OH radicals with radiolytic products. From Table II, it can be seen that the elimination of Cl from PCP is much easier than that from o-CP and DCP. The reason is very clear that as the chlorine atom attracts electron, the benzene ring in PCP is in a more stress.

Approaching to more practical case, the experiments of degradation of DCP and o-CP on dose were done. The results are shown in Figs 2 and 3.

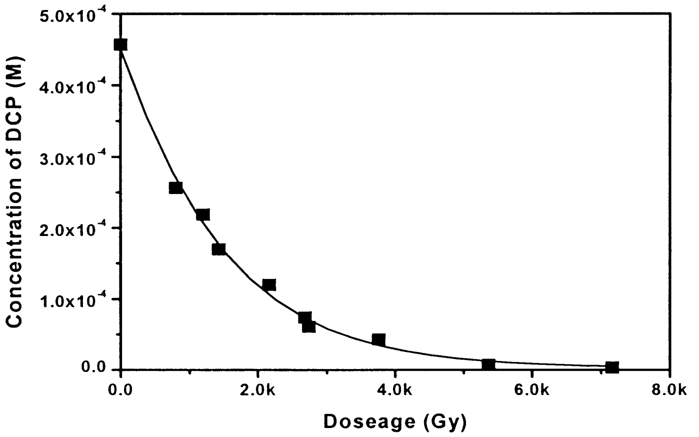

FIG. 2. The dependence of degradation of DCP on dose; pH5, air saturated 4.4×10^{-4}M DCP solution.

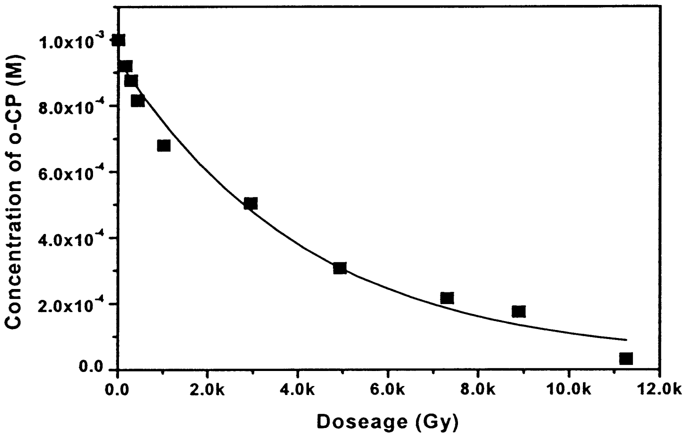

FIG. 3. The dependence of degradation of o-CP on dose; pH5, air saturated 1×10^{-3}M o-CP solution.

The dose used to decompose the parent compound is higher than that calculated from corresponding G values. It displays once again that the intermediates compete to scavenge OH radical against parent compound.

3.4. Intermediate radiolytic products

From the view of drinking water treatment, prior to ensuring a promising methods, one must confirm its reasonableness carefully. In this case, accompanying the degradation of PCP under irradiation, we detected some stable intermediates:

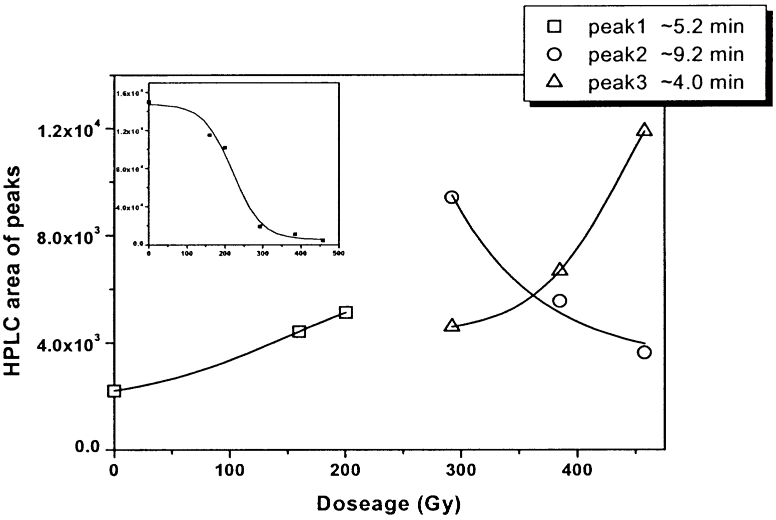

FIG. 4. Growth and decay of intermediate radiolytic products of PCP (1.5×10^{-5}M, pH5, air saturated solution). Peak 1 disappeared when absorbed dose is higher than 300 Gy; There is no signal of peak 2 and peak 3 when dose is lower than 200 Gy. Insert is corresponding degradation of PCP, c.f. Fig. 1(b).

It can be seen that, even in the case of γ radiolysis of 1.5×10^{-5} M PCP, when dose applied was about 500 Gy, the accumulation of a second radiolytic product was still going on. Measuring chemical oxygen demand (COD_{Mn}) after irradiating PCP in different dosages supports the result above.

TABLE III. DEPENDENCE OF COD ON DOSE FOR pH5, AIR SATURATED 6.3×10^{-5}M PCP SOLUTION

Dose (Gy)	0	530	1600	2800
COD_{Mn} (mg/L)	10.5	10.5	9.4	3.4

At absorbed dose of 530 Gy about half of PCP is consumed, yet the COD value doesn't change. The COD value decreased markedly only when the dose was high enough to consume almost all PCP. We suggest that at the early stage the benzene ring open is negligible in the consumption of PCP induced by OH radicals though O_2 is present, which agrees to the low reactivity of phenoxy radicals towards O_2.

Therefore, it is necessary to separate these compounds, determine their structure and evaluate their toxicity. The unknown compound may be 2-chloro-p-benzoquinone; its UV spectrum is shown in Fig. 5.

In model systems where water was contaminated by o-CP and DCP, more intermediates were produced which underwent more complex change than those contaminated by PCP during irradiation. This may be due to the difference of primary degradation mechanism between PCP and o-CP and DCP.

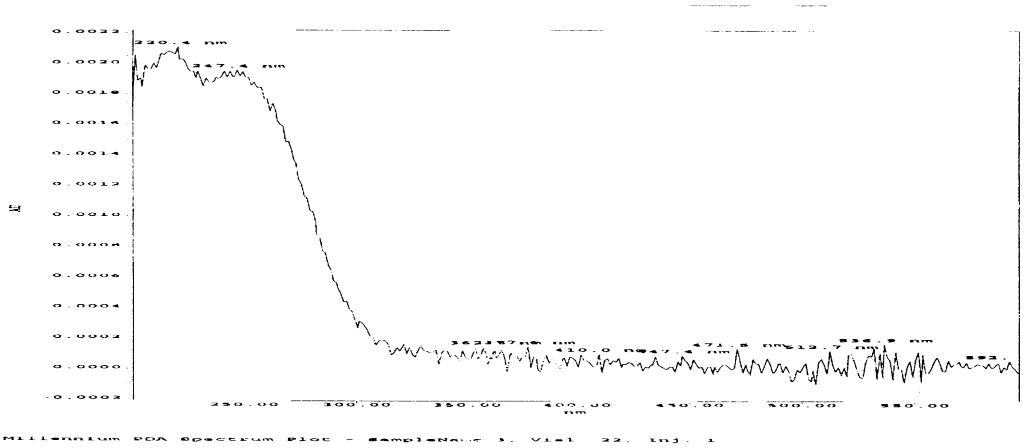

FIG. 5. *UV Spectrum of unknown compound taken from the HPLC-DAD of γ irradiated pH5, air saturated 1.5 ×10^{-5}M PCP solution.*

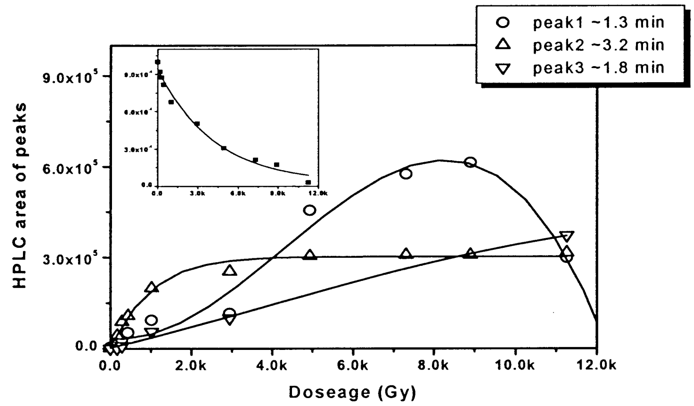

FIG. 6. *Growth and decay of intermediate radiolytic products of o-CP (1.010^{-3}M, pH5, air saturated solution); insert is the corresponding degradation of o-CP, c.f. Fig. 3.*

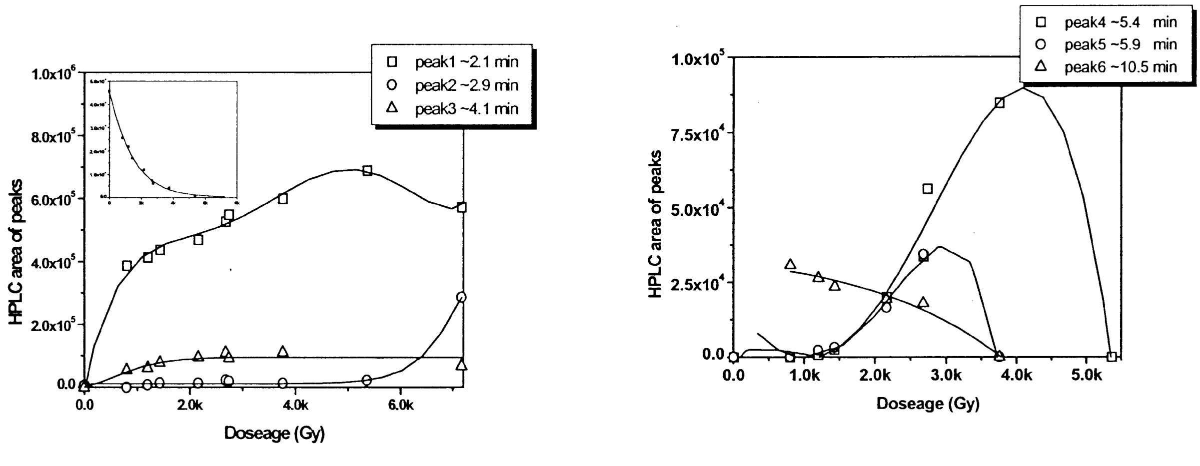

FIG. 7. *(a) and (b) Growth and decay of intermediate radiolytic products of DCP (4.42 × 10^{-4}M, pH5, air saturated solution); insert is the corresponding degradation of DCP, c.f. Fig. 2.*

3.4. Combination of ozonization and γ irradiation

It is believed that O_3 can breakdown unsaturated carbon-carbon bonds and therefore destroy the benzene ring of aromatic compounds, whereas radiation treatment alone usually requires relatively high dose to achieve the same effects, even in the presence of O_2.

We tried ozonization and obtained MS spectra of ozonization products as well as that of irradiation products. The two series of MS spectra are so similar in the case of o-CP and DCP. Combined with information obtained from HPLC analysis, we propose that during ozonization CPs were degraded in similar way as irradiation, i.e. OH radical attacks rather than through predicted C=C cleavage.

Ozone treatment of o-CP:

M/e: 127 $\xrightarrow{O_3}$ 143, 145

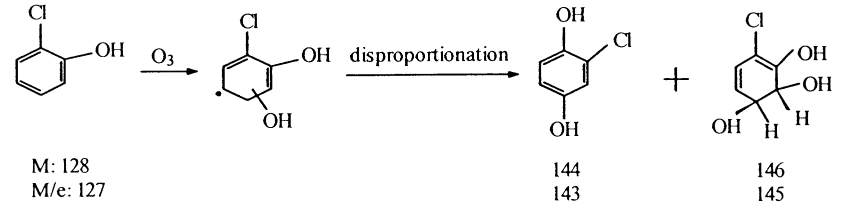

γ radiolysis of o-CP:

M/e: 127 $\xrightarrow{1kGy}$ 108 , 127 , 143, 159 , 161

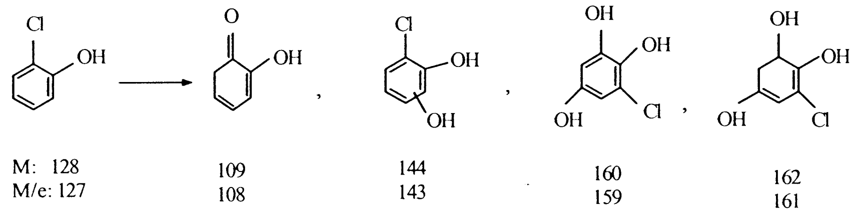

Ozone treatment of DCP:

M/e: 161 $\xrightarrow{O_3}$ 177, 142, 127

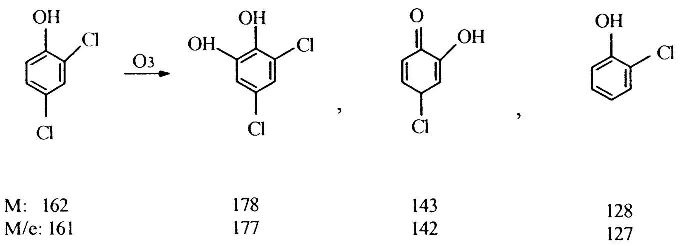

γ radiolysis of DCP:

M/e: 161 $\xrightarrow{1kGy}$ 143 , 177, (low peak: 127 , 123 , 111)

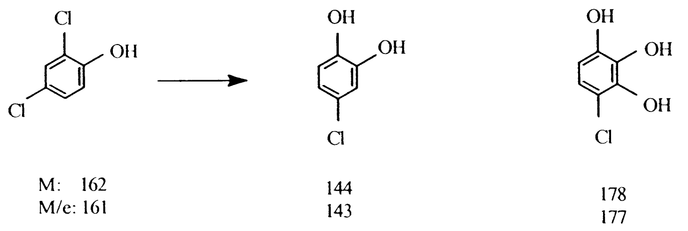

This agrees with Weiss's chain decomposition mechanism of ozone in water [9, 10]:

$$\begin{array}{lllll} \text{Initiation} & O_3 + OH^- & \longrightarrow & HO_2(O_2^-) & + \; O_2^- \\ \text{Propagation} & O_2^- + O_3 & \xrightarrow{+H+} & 2O_2 & + \; OH \\ & OH + O_3 & \longrightarrow & HO_2(O_2^-) & + \; O_2 \\ \text{Termination} & \multicolumn{4}{l}{\text{consumption of } O_2^-,\ HO_2 \text{ and } OH} \end{array}$$

The peroxyl radicals (HO2·or·O2-) may perform similar manner on CPs like OH radicals [11].

However, O3 can convert radiolytically generated reducing species (hydrated electron and H atom in the absence of O2, or .O2- under aeration) to oxidizing OH radicals and thus can improve the efficiency of radiation-induced oxidation. Therefore, ozone may be considered a good partner of ionizing radiation in some water treatment [10].

$$e_{aq}^- + O_3 \longrightarrow O_3^- \qquad k = 3.6 \times 10^{10}\ M^{-1} \cdot s^{-1}$$

$$H + O_3 \longrightarrow HO_3 \qquad k = 3.6 \times 10^{10}\ M^{-1} \cdot s^{-1}$$

$$\text{or } O_2^- + O_3 \longrightarrow O_3^- + O_2$$

$$O_3^- + H^+ \rightleftharpoons HO_3$$

$$HO_3 \longrightarrow OH + O_2$$

Moreover, PCP exhibited its specialty among CPs towards ozonization. PCP degraded quickly during ozonization and left far less by-products.

4.CONCLUSION

If γ irradiation method is used to treat city water (drinking water), potential toxicity of radiolytic intermediates must be considered. Though the chronic toxicity equivalency factors (TEFS) of pentachlorophenol is greater than that of monochlorophenol (1:0.04) [12], the content of chlorophenol is 35 times greater than that of PCP in some city drinking waters. In addition, PCP is much easier to be decomposed under γ irradiation than that of simple chlorophenol; however, we should pay more attention to the radiolytic intermediates of simple chlorophenols. Future work should be done such as separation and identification of intermediates, its formation and decay kinetics, evaluation of the toxicity of intermediates and so on.

Evaluation of treatment efficiency by final product analysis is necessary. COD and TOC are common indices of the qualities of water and wastewater, as for the evolution of their qualities after radiation treatment. The fact is that some simple organic compounds such as formic acid and acetic acid are non-toxic, yet they are included in COD and TOC values. While formic acid can easily be oxidized to CO_2 by OH radical in the presence of O_2, it requires very high doses to further oxidize acetic acid to CO_2. Therefore, basic research to obtain detailed mechanistic information, especially detailed product spectra, is needed for both designing and optimizing the treatment process.

It is recommended to bubble ozone simultaneously when γ radiation (or EB) treats CPs contaminating water. Ozone itself, in water can, react on CPs through OH and HO_2 radicals, and it can also convert radiolytically generated reducing species into oxidizing OH radicals and therefore enhance the efficiency of radiation-induced decomposition.

REFERENCES

[1] YUE, S.L., Study on by-products generated in running water of Shanghai during the chlorination disinfection, Zhongguo Geishui Paishui (Chinese journal of water supply and drainage) **8** (1992) 8-11.

[2] HENNION, M.C., PICHON, V., BARCELO, D., Trends Anal. Chem. **13** (1994) 361 pp.

[3] EPA Method 604, Phenols, Federal Register, Environmental Protection Agency, Part 3, 40 CFR Part 136 (1984) 58 pp.

[4] PUIG, D., BARCELO, D. et al., J. Mass Spectr. **31** (1996) 1297 pp.

[5] FLORENCE, T.M., FARRAR, Y.J., Spectrophotometric determination of chloride at the parts-per-billion level by the mercury (5) thiocyanate method, Anal. Chimi. Acta. **54** (1971) 373 pp.

[6] YU, R.B., LU, Z.R. (Eds.), Analytical methods and instruments applied to water pollution, Shanghai Science and Technology Press, Shanghai (985) 109 pp.

[7] FANG, X., HE, Y., WU, J., VON SONNTAG, C., Hydroxyl-radical induced dechlorination of pentachlorophenol in water (Proc. Symp. Zakopane, Poland, 1997) IAEA, Vienna (1998).

[8] FANG, X., HE, Y., LIU, J., WU, J., Oxidative decomposition of pentachlorophenol in aqueous solution, Rad. Phys. Chem. **53** (1998) 411-415.

[9] WEISS, J., Trans. Faraday Sco. **31** (1935) 668 pp.

[10] STAEHELIN, J., HOIGNE, J., Ozone decomposition in water studied by pulse radiolysis, Part I, J. Phys. Chem. **88** (1988) 2560–2564.

[11] GETOFF, N., Radiation induced decomposition of biological resistant pollutants in water, Appl. Radiat. Isot. **37** (1986) 1103–1109.

[12] KOVACS, T.G., MARTEL, P.H., et al., Aquatic toxicity equivalency factors for chlorinated phenolic compounds present in pulp mill effluents, Environ. Toxic. Chem. **12** (1993) 281–289.

THE DESTRUCTIVE DEGRADATION OF SOME ORGANIC TEXTILE DYE COMPOUNDS USING GAMMA RAY IRRADIATION

Abdel-Gawad A.S. Emara*, A.A. Abdel-Fattah, S.E. Ebraheem,
Z.I. Ali, H. Gad
National Center for Radiation Research and Technology,
Cairo, Egypt
*National Nuclear Regulatory and Radiation Control Centre,
Cairo, Egypt

Abstract. The destructive degradation of 8 coloured reactive and direct dye compounds currently used in the textile industry has been investigated. These dyes are: Levafix Blue ERA (LB), Levafix Brilliant Red E4BA (LBR), Levafix Brilliant Yellow EGA (LBY), Drimarene Scarlet F3G (DS), Drimarene Brilliant Green X3G (DBG), Fast Yellow RL (FY), Fast Violet 2RL (FV) and Fast Orange 3R (FO). The process of degradation of the respective dye has been followed spectrophotometrically at the characteristic lmax. The variation of the colour intensity of aerated aqueous solution of the investigated dyes has been measured as a function of gamma irradiation dose. In all cases, the amplitude of the absorption bands of the dye compound was found to decrease with the increase of the gamma dose. Irradiation was carried out for actual waste and distilled water. By comparing the heights of the absorption maxima in both the visible and ultraviolet ranges, it was found that complete decolouration is attained at lower doses than that needed for the process of degradation of the dye. The kinetics of the degradation process has been traced and the kinetic constant, k_1, was calculated and found to be concentration dependent indicating a first order reaction in all cases. The radiation-chemical yield (G-value) as a measure of the efficiency of gamma ray to degrade the respective dye was calculated for all dye compounds and it was found that the G-value in all cases increases exponentially for low radiation doses and changes linearly for high radiation doses. Also the K* value (the efficiency coefficient of dye radiolysis) was calculated and compared for the different dye compounds e.g. for FO, FY and FV dyes, the K* values were found to range from 5.5×10^{-9} to 1.92×10^{-7} $\text{mol}\cdot\text{L}^{-1}\cdot\text{cm}^{-1}$. In addition to the study of a single dye compound in solution, mixtures of different dyes (3 dyes) were also subjected to g-ray irradiation simulating more closely actual waste effluents. Also the effect of some other chemicals used in the textile industry such as H_2O_2 and NaOCl on the degradation process was investigated. The specific bimolecular rate constants of the reaction of dyes with the hydroxyl radical (OH) were determined by studying the effect of ethanol concentration on G-value using competition kinetics. The effect of pH, NaOCl and H_2O_2 on the degradation process was studied. In addition to the main objective of the use of gamma rays to achieve the destruction of the dye compounds, the eco-toxicity of the dyes and their irradiation products was assessed using some invertebrate animals (snails) for the three FO, FY and FV dyes. The FV dye and its degradation products were found to be toxic (results of hemocyte count, hemagglutination titter, total protein content and accumulation levels) and should be completely degraded and removed from the wastewater streams using high irradiation doses. Also, and for the purpose of comparison, the sorption of the FV, FY and FO dyes on conventional sorbents such as charcoal was tested. gamma ray irradiation, as compared with conventional sorption techniques, was found to be very rapid and the removal of organic pollutants from wastewaters can be achieved nearly instantaneously. It appears that, for the complete destruction and full removal of organic pollutants from waste effluents, the sequential adsorption using chemical techniques followed by gamma irradiation treatment may prove to be more effective and advantageous.

1. INTRODUCTION

In the last few decades the worldwide rapid industrial growth and population increase, has resulted in the release and accumulation of different pollutant materials in the environment with their subsequent adverse effect to the ecosystem and its natural habitat. Industrial wastes in the form of solid, gas or liquid effluents represent one of the most serious problems of environmental pollution and necessitate strict control and appropriate treatment processes. These processes vary according to the nature of the pollutant material, its concentration, its interaction and behaviour in the environment. Several treatment methods and techniques have been developed and are known for the treatment and ultimate disposal of the relevant pollutants [1–3].

Extensive investigations on the degradation of a number of dye stuff materials using gamma rays have been carried out in our laboratory [4–5]. In the early seventies the use of high level radiation in waste treatment has been discussed in a symposium held in Munich in 1975 [6]. Of special importance in this context is the work carried out at Sandia Laboratory (USA) which has demonstrated the technical feasibility of the process of the gamma ray irradiation of wastewater and sludge. In 1992, the IAEA organized an international symposium where different problems and prospects for the use of radiation in the preservation of the environment were discussed [7].

This work is part of a co-ordinated research project dealing with the use of gamma ray irradiation technique for the destruction and subsequent elimination of some organic dye stuff materials commonly released from the textile industry in Egypt. These dyestuff materials are known to be highly structured polymers which are non-biodegradable and toxic in many cases.

In this work the data obtained in a three year co-ordinated research project on the use of gamma radiation for achieving the destruction of a number of dye stuff materials (8 dyes) are reported. Both water dye solutions and actual dye waste effluents were tested. Several parameters were measured to determine the optimum conditions for gamma ray irradiation. The kinetics and degradation reaction order for every dye were studied.

In addition, the eco-toxicity of the three dye materials (FY, FO, and FV) with respect to some of the bio-organisms (snails) present in the effluent release canal of the textile processing complex was tested using appropriate biological investigations and methods. Also, the adsorption of the above mentioned three dye materials on conventional adsorbents such as charcoal, under varying experimental conditions, was investigated and the results are compared with those obtained with the gamma ray irradiation technique.

2. EXPERIMENTAL

2.1. Reagents

The following dye materials were used in the respective investigations:

(1) Levafix Blue ERA, (LB) reactive dye, product of Bayer
(2) Levafix Brilliant Red E4BA, (LBR) reactive dye, product of Bayer
(3) Levafix Brilliant Yellow EGA, (LBY) reactive dye, product of Bayer.
(4) Drimarene Scarlet F3G, (DS) reactive dye, product of Sandoz.
(5) Drimarene Brilliant Green X3G, (DBG) reactive dye, product of Sandoz
(6) Fast Yellow RL, (FY) Direct dye, M. Wt. 956, product of ISMA dye – Egypt.
(7) Fast Violet 2RL, (FV) Direct dye, M. Wt. 703, product of ISMA dye – Egypt.
(8) Fast Orange 3R, (FO) Direct dye, M. Wt. 327.5, product of ISMA dye – Egypt.

These dyes are of a commercial grade and are mainly used in the textile industry in Egypt.

The chemical structure of the first five dyes is unknown while the structure of the other three dyes is as follows:

Fast Yellow RL

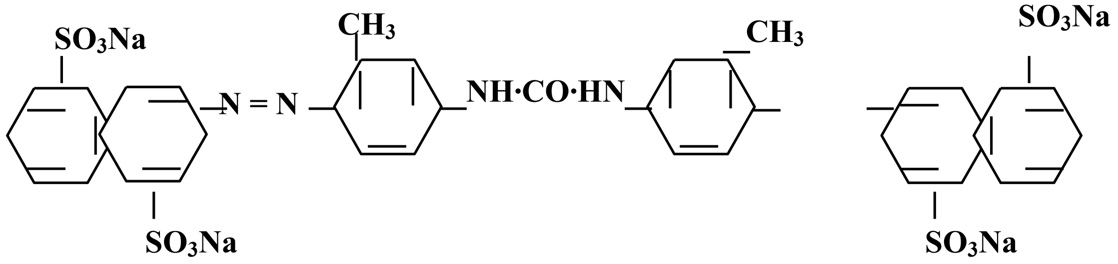

Fast Violet 2RL

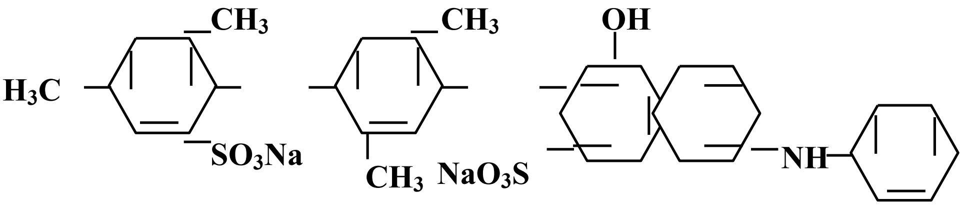

Fast Orange 3R

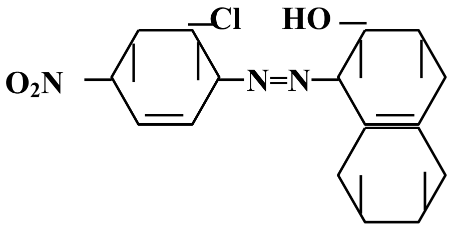

Double distilled water was used in all preparations, except if otherwise stated. All other reagents were of an analytical grade.

2.2. Apparatus and methods

A Unicam UV4 double beam spectrophotometer (product of Unicam Co. Ltd., England) was used to measure absorption spectra of the irradiated and unirradiated dye solutions. HANNA HI-931401 pH meter was used for adjusting and measuring the pH of the dye solutions under investigation.

Irradiations were carried out with gamma rays in the ^{60}Co gamma chamber 4000A (product of India) using Pyrex tubes (15 mm diameter and 60 mm height). The absorbed dose rate in the irradiation facility through the time of this contract was measured to range from 2.75 to 1.92 kGy/h, using Fricke dosimetry, [G(Fe^{3+}) = 1.62 μmol/J] [8]. Sample tubes were irradiated at the calibrated positions in the sample chamber using a specially designed wooden holder. The temperature during irradiations was ca. 30°C.

For the three dyes (FV, FO and FY), the eco-toxicity of the dye was measured using known biological assessment techniques (Hemocyte count, Hemagglutination assay, total protein content and accumulation level). The invertebrate *Biomphalaria. alexandria* was used as test animal [9–12].

3. RESULTS AND DISCUSSION

3.1. Irradiation of organic dyestuff materials using γ rays

3.1.1. Absorption spectra and determination of extinction coefficients

The absorption spectra of different concentrations of aqueous solutions of the investigated dyes were displayed and the absorption maxima were determined for each dye. Figure 1, the absorption spectra of Drimarene Scarlet, is an example of the several absorption spectra measured for the different dye solutions. The wavelengths at maximum absorption (λ_{max}) for each dye and the concentration range used are given in Table I. It was found that all dyes have main absorption bands in the visible region and some absorption bands in the UV region of the spectrum, which are attributed to the skeleton of the dye molecule. The peaks at about 220 nm wavelength are attributable to substituted aromatic rings and those at about 270±10 nm may be attributed to carbonyl groups. The absorption bands in the visible region of the spectrum are attributed to the chromophore group and its auxochromic substituents [12]. The structures of FO, FY and FV are given in the experimental part. FO is a monoazo dye while FY and FV are diazo dyes. The absorption bands at 416, 390 and 520 nm for FO, FY and FV, respectively, are attributable to the azo group and its auxochromic substituents [13]. For all dyes tested a concentration range with the corresponding λ_{max} was determined where Beer's law is obeyed.

The absorption spectra of different concentrations of DS dye in actual wastewater are plotted (Fig. 2) and compared with those obtained by using distilled water (Fig. 1). The absorption spectrum of DS in distilled water has two peaks in the visible region of the spectrum at 400 and 504 nm (Fig. 1). In case of DS in wastewater, the peak at 400 nm disappears and the peak at 504 is shifted to lower wavelengths (496 nm).

TABLE I. λ_{max} AND THE CORRESPONDING CONCENTRATION RANGE OF THE DYE

Dye	λ_{max}, nm	Concentration range
LB	220, 275, 612	0.025 – 0.15 g/L
LBR	278, 330, 514, 542	0.025 – 0.15 g/L
LBY	220, 280, 320, 414	0.0125 – 0.075 g/L
DS DS*	220, 300, 400, 504 220, 290, 315, 496	0.00625 – 0.0375 g/L
DBS DBS*	220, 285, 348, 620, 660 220, 285, 348, 620, 660	0.0125 – 0.05 g/L
FO	416	5×10^{-5} - 3×10^{-4}
FY	220, 260, 390	1×10^{-5} - 6×10^{-5} mol/L
1.1.2. FV	240, 520	5×10^{-5} - 2×10^{-4}

* Dye dissolved in actual wastewater.

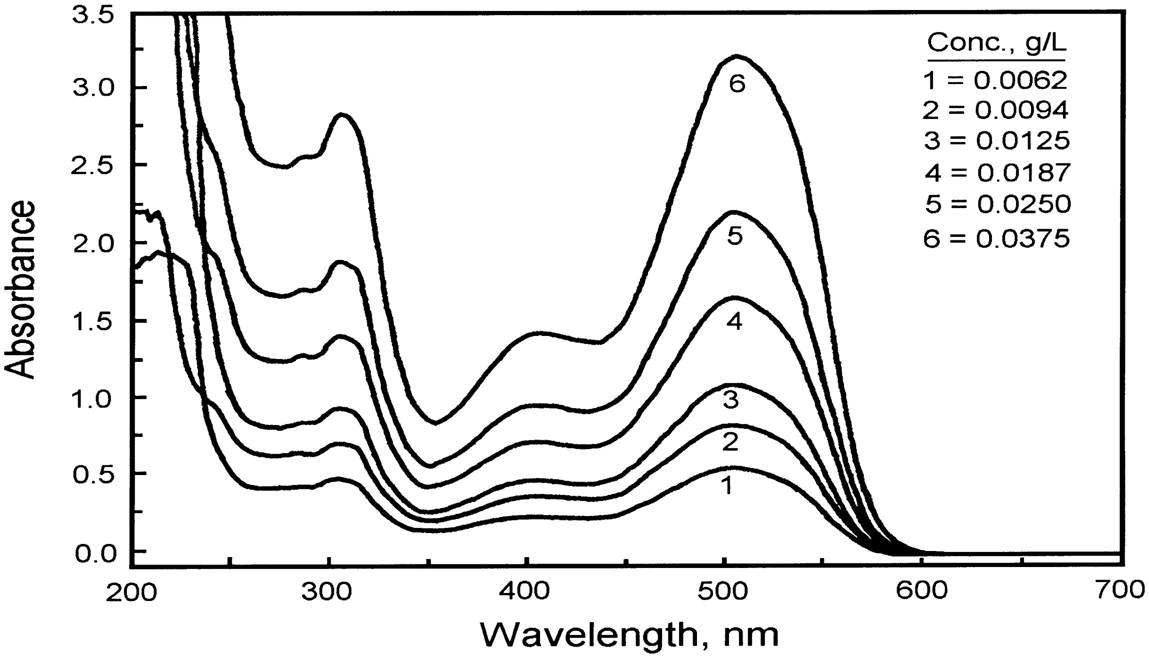

FIG. 1. Absorption spectra for different concentrations of Drimarene scarlet F3G (DS) dye dissolved in distilled water.

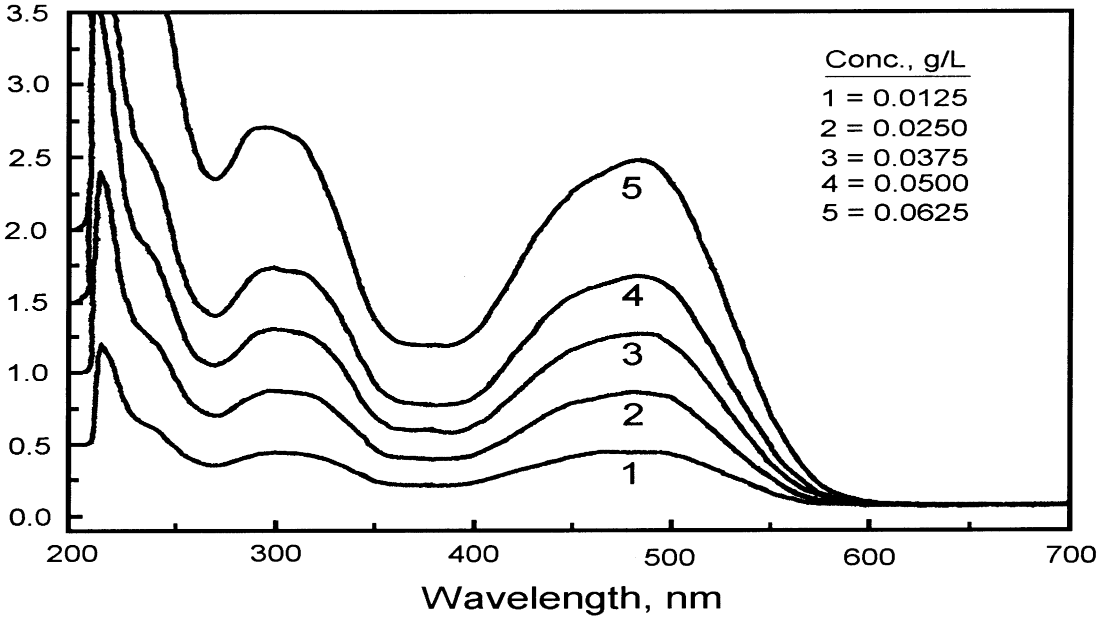

FIG. 2. Absorption spectra for different concentrations of Drimarene scarlet F3G (DS) dye dissolved in actual wastewater.

Similarly, the absorption spectra of the DBG dye in distilled and wastewater have two adjacent peaks in the visible region at 620 and 660 nm. The absorption peak at 660 nm is prominent in the presence of distilled water while that peak at 620 nm is prominent in the presence of wastewater. These variations appear to be due to the presence of other ingredients in the wastewater effluents. For all dyes studied, the optical densities at the different absorption maxima of dyes were plotted as a function of dye concentration (Fig. 3). Linear relationships were obtained, indicating that Beer's law is obeyed in the used range of concentrations. The extinction coefficients, ε, at each wavelength were determined as the slopes of the straight lines given in Fig. 3 and the values are given in Table II.

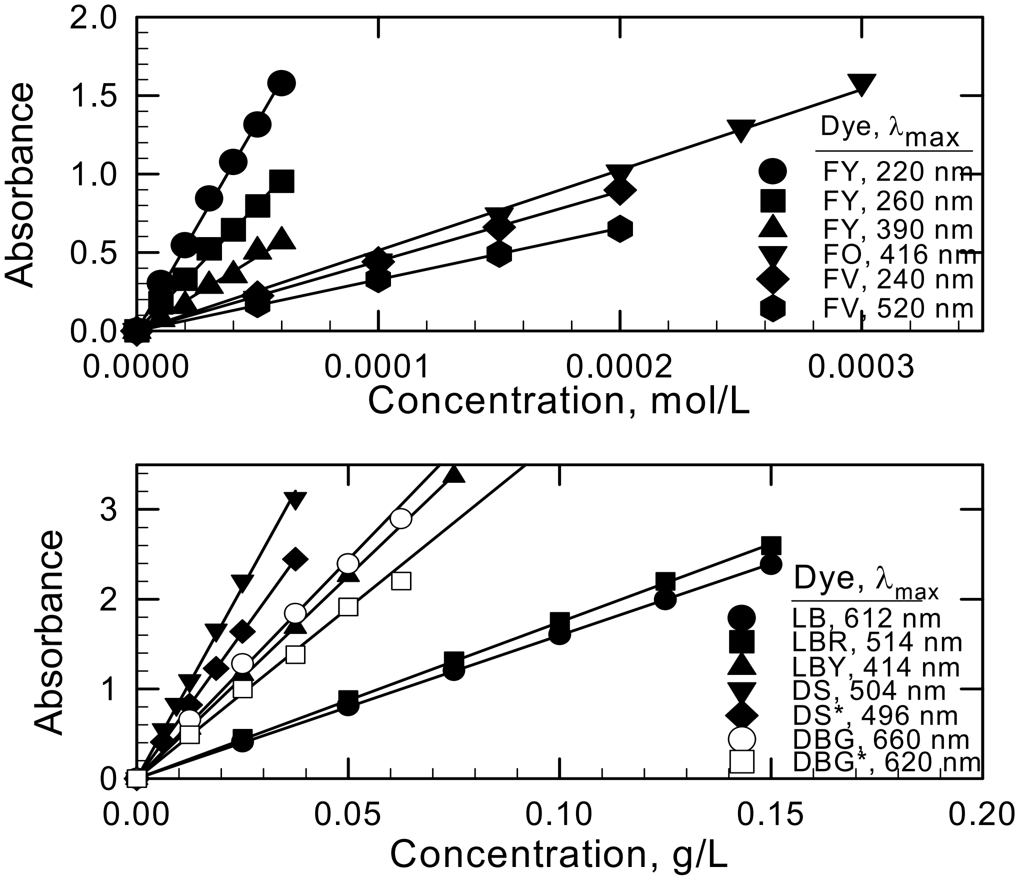

FIG. 3. Variation of optical absorbency as a function of concentration of LB, LBR, LBY, DS, DBG, FY, FO and FV dyes. (*) dye dissolved in actual wastewater. Analysis wavelength is indicated.

TABLE II. EXTINCTION COEFFICIENTS FOR DIFFERENT DYES AT DIFFERENT WAVELENGTHS

Dye	λ_{max}, nm	Extinction coefficient, (ε)
LB	612	15.89 $L \cdot g^{-1} \cdot cm^{-1}$
LBR	514	17.37 $L \cdot g^{-1} \cdot cm^{-1}$
LBY	414	44.94 $L \cdot g^{-1} \cdot cm^{-1}$
DS	504, 496♣	85.6, 65.4* $L \cdot g^{-1} \cdot cm^{-1}$
DBG	662, 620♣	48.84, 38.06* $L \cdot g^{-1} \cdot cm^{-1}$
FO	416	5128.35 $L \cdot mol^{-1} \cdot cm^{-1}$
FY	220, 260, 390	26643.96, 16114.29, 9473.63 $L \cdot mol^{-1} \cdot cm^{-1}$
FV	240, 520	4446.67, 3267.33 $L \cdot mol^{-1} \cdot cm^{-1}$

♣ Dye dissolved in actual wastewater.

3.1.2. The radiation-induced reduction of dye concentration

Aqueous solutions of different dye concentrations were irradiated for different absorbed doses and the absorption spectra of the unirradiated and irradiated dye solutions were recorded. An example of the several spectra recorded is shown in Fig. 4. It can be observed that the amplitude of all absorption bands decreases gradually with the increase of the absorbed dose. The rate of decrease of the amplitude of the absorption band in the visible region (decolouration) is higher than that for the peaks in UV region (degradation). In other words, complete decolouration (indicated by complete disappearance of the absorption band in the visible region) can be attained at doses lower than that needed for complete degradation of the respective dye. Similar absorption spectra for other concentrations of all used dyes were obtained indicating the same behaviour with varying responses to gamma irradiation.

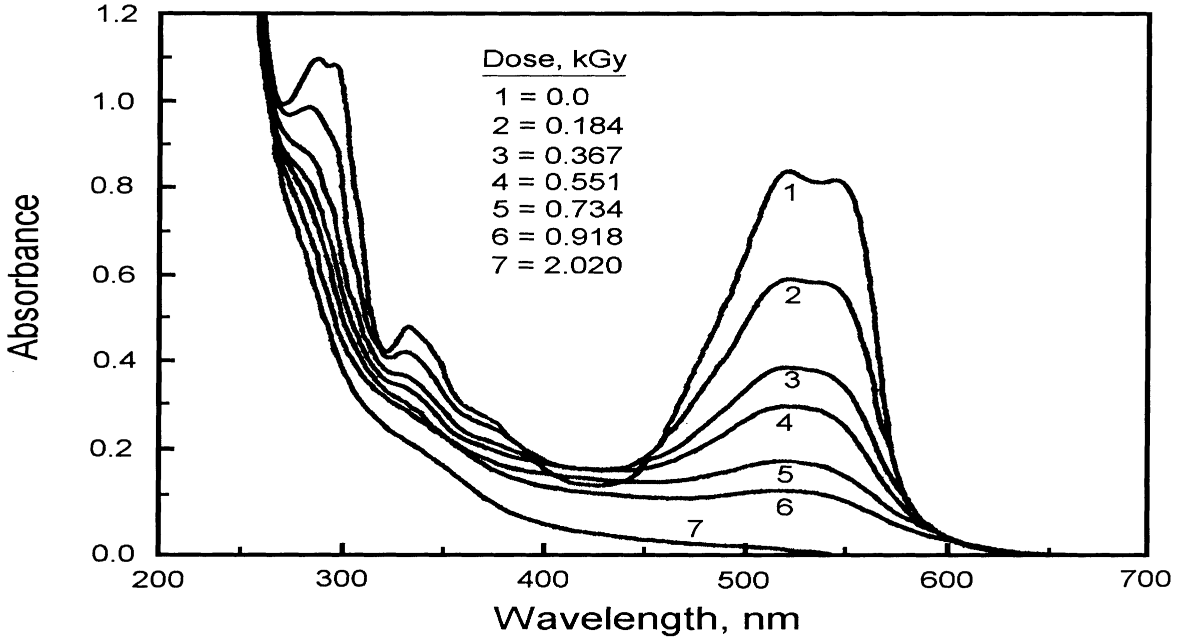

FIG. 4. Absorption spectra of aqueous Levafix Brilliant Red E4BA dye solution, unirradiated and irradiated to different absorbed doses. [dye] = 0.05 g/L.

Figure 5 shows the percentage radiation-induced reduction in absorbency at different wavelengths for 5 × 10^{-5} mol/L solutions of the FY, FO and FV dyes as a function of absorbed dose. As already mentioned, it can be seen that complete decolouration is attained at lower doses than that needed for degradation. For example complete decolouration of FY dye solution is attained at about 2.5 kGy while the degradation (reduction in absorbency at 220 nm) at this dose is only about 60%. This indicates that decolouration of solution is not an indication of the complete destruction of the organic dye. The results obtained for different concentrations of LB, DS and FY dyes are tabulated in Table III. It can be seen that, for the same initial dye concentration, the degree of decolouration as well as degradation (reduction in optical density of peaks in the UV region of the spectrum) increases with the increase of the absorbed dose. Also, at the same dose, the increase of the initial dye concentration results in a decrease of the percentage of degradation. From Table III it can be also noticed that, for the same dye concentration, the extent of decolouration in wastewater media is lower than that in distilled water.

TABLE III. REDUCTION PERCENT IN OPTICAL DENSITY, $(\Delta A/A_O)_\lambda$, FOR DS DYE IN DISTILLED AND WASTEWATER TOGETHER WITH LB AND FY DYES AT DIFFERENT INITIAL DYE CONCENTRATIONS (C_O) AND RADIATION DOSES

Reduction percent in optical density, $(\Delta A/A_o)_\lambda$, %											
C_o, g/L	Dose, kGy	LB at 612 nm	C_o, g/L	Dose, kGy	DS at 504 nm	DS♣ at 496 nm	C_o, mol/L	Dose, kGy	FY at 220 nm	FY at 260 nm	FY at 390 nm
0.03	0.2	19	0.0125	0.2	27	n	2×10^{-5}	0.32	18	29	44
	0.8	47		0.8	59	50		0.64	33	51	85
	3.0	89		3.0	94	82		1.28	56	83	99
	10.0	a		10.0	a	n		4.0	93	a	a
0.05	0.2	9	0.025	0.2	21	n	4×10^{-5}	0.32	21	25	31
	0.8	28		0.8	53	43		0.64	28	37	58
	3.0	70		3.0	84	80		1.28	42	57	87
	10.0	97		10.0	a	n		4.0	82	93	a
0.15	0.2	6	0.0375	0.2	7	n	6×10^{-5}	0.32	17	19	20
	0.8	17		0.8	30	29		0.64	23	28	44
	3.0	45		3.0	66	65		1.28	39	47	73
	10.0	76		10.0	93	n		4.0	71	84	98

♣ Dye dissolved in actual wastewater.
a Complete decolouration is reached at lower doses.
n Not analysed.

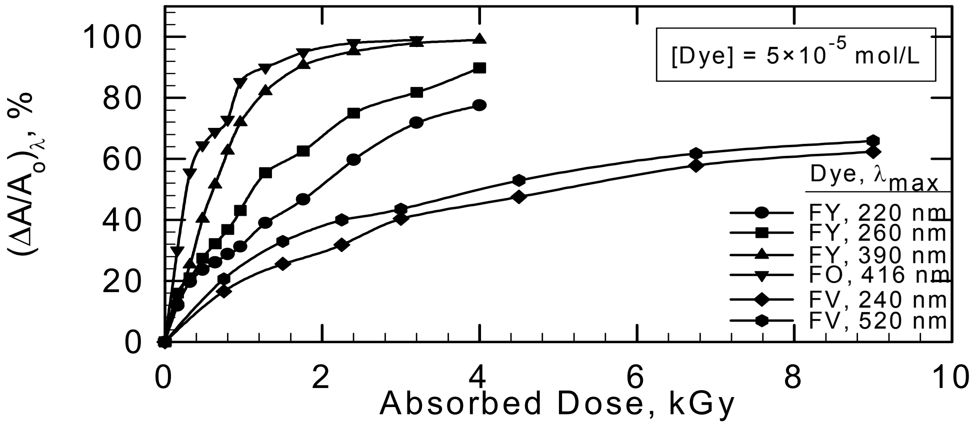

FIG. 5. Variation of $(\Delta A/A_o)$ % of 5 × 10^{-5} mol/L FY, FO and FV dye solutions as a function of absorbed dose. Analysis wavelength is indicated.

3.1.3. The kinetics of degradation

The study of the decolouration kinetics of aqueous solutions of the dyes under investigation was carried out by following the reduction in dye concentration, spectrophotometrically, at absorption maxima in the visible region whereas the study of degradation kinetics was carried out by following the absorption maxima in the UV region of the spectrum. Figure 6 shows the relationship between the residual concentration for different initial dye concentrations (determined spectrophotometrically at λ_{max}) and the absorbed dose. It is seen that the radiation-induced decrease in dye concentration for all different concentrations, as plotted on a logarithmic scale, shows a linear relation with the absorbed dose in accordance with a first order radiolytic effect as expressed by the following equation:

$$-dC = k_1 C \cdot dD \qquad (1)$$

which when integrated gives,

$$\ln C = \ln C_o - k_1 D \qquad (2)$$

where

C is the dye concentration (g/L or mol/L)*
C_o is the initial dye concentration (g/L or mol/L),
D is absorbed dose (Gy),
k_1 is the reaction rate constant (Gy^{-1}).

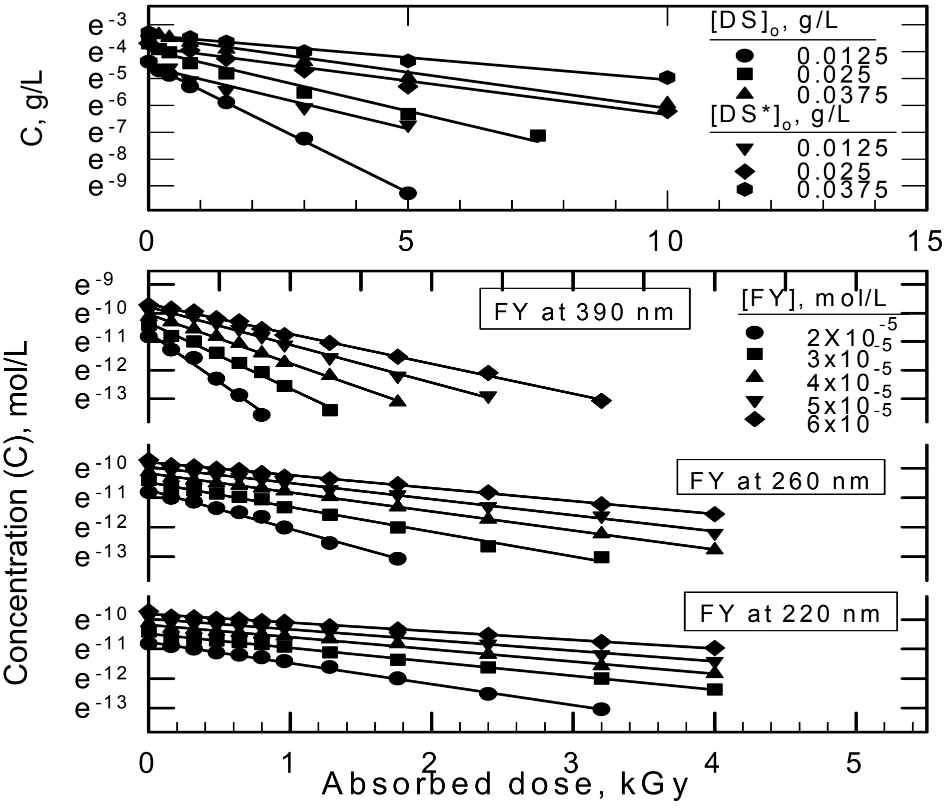

FIG. 6. Residual concentration of DS and LBY dyes vs. the absorbed dose. Initial concentration is indicated (*) dye dissolved in actual wastewater.

---

* For investigated dyes of unknown structure, the concentration of the dye was expressed in g/L.

The kinetic constants are obtained as the slopes of the straight lines mentioned above. The values of k_1 for the different concentrations of different dyes are shown on Table IV. It can be seen that k_1 is dependent on the initial concentration of dye and decreases as the concentration increases, i.e.

$$k_1 \propto \frac{1}{C_o}$$

$$k_1 = \frac{\text{constant}}{C_o} \tag{3}$$

The plot of k_1 versus $1/C_o$ gives straight lines passing through the origin (Fig. 7) showing a good agreement with the proposed degradation scheme of Piccinini and Ferrero, 1975 [14] and relating the kinetic rate constant, k_1, to the initial concentration by the following equation:

$$k_1 = \frac{K^*}{C_o} \tag{4}$$

where

K^* is the efficiency coefficient of dye radiolysis.

K^* values of the dyes under investigation are obtained as the slopes of the straight lines plotted in Fig. 7 and given in Table V.

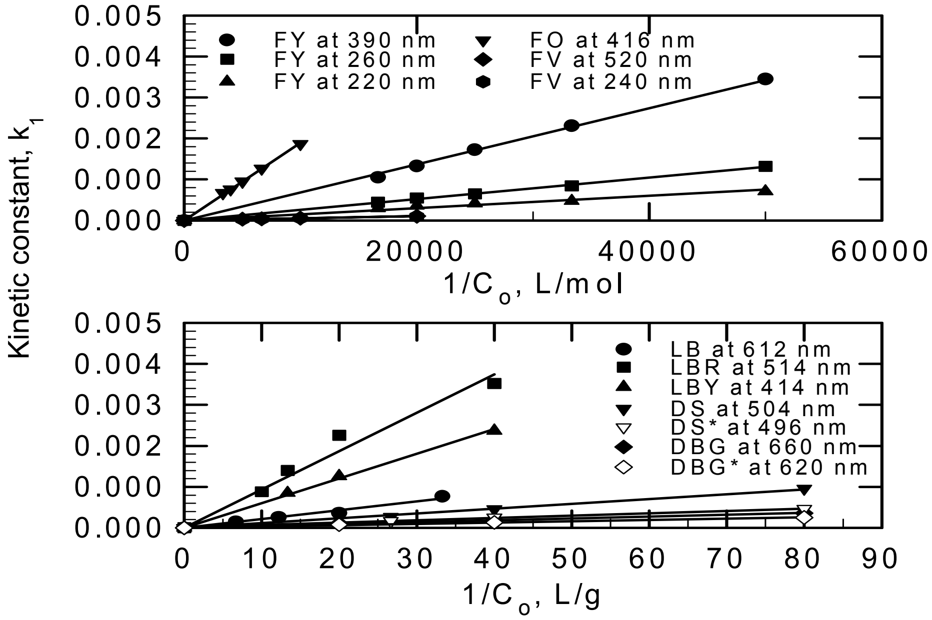

FIG. 7. The relation between k_1 and $1/C_o$ for different dyes. The different dyes and analyses wavelengths are indicated. (*) dye dissolved in actual wastewater.

TABLE IV. KINETIC RATE CONSTANT, K_1, FOR DIFFERENT INITIAL CONCENTRATIONS OF THE DIFFERENT DYES AT DIFFERENT λ_{MAX}

Dye	C_o, g/L	l_{max}, nm	k_1, Gy^{-1}	Dye	C_o, mol/L	l_{max}, nm	k_1, Gy^{-1}
LB	0.030	612	7.63×10^{-4}	FO	1×10^{-4}	416	1.87×10^{-3}
	0.050	“	3.55×10^{-4}		1.5×10^{-4}	“	1.27×10^{-3}
	0.082	“	2.50×10^{-4}		2×10^{-4}	“	9.53×10^{-4}
	0.150	“	1.46×10^{-4}		2.5×10^{-4}	“	7.59×10^{-4}
LBR	0.025	514	3.52×10^{-3}		3×10^{-4}	“	6.73×10^{-4}
	0.050	“	2.06×10^{-3}	FY	2×10^{-5}	220	7.1×10^{-4}
	0.075	“	1.17×10^{-3}		“	260	1.32×10^{-4}
	0.100	“	0.88×10^{-3}		“	390	3.45×10^{-3}
LBY	0.026	414	2.37×10^{-3}		3×10^{-5}	220	4.77×10^{-4}
	0.050	“	1.26×10^{-3}		“	260	8.41×10^{-4}
	0.075	“	0.85×10^{-3}		“	390	2.31×10^{-3}
DS	0.0125	504	0.27×10^{-3}		4×10^{-5}	220	4.17×10^{-4}
	“	496♣	0.17×10^{-3}		“	260	6.46×10^{-4}
	0.025	504	0.46×10^{-3}		“	390	1.72×10^{-3}
	“	496♣	0.25×10^{-3}		5×10^{-5}	220	3.6×10^{-4}
	0.0375	504	0.96×10^{-3}		“	260	5.46×10^{-4}
	“	496♣	0.46×10^{-3}		“	390	1.33×10^{-3}
DBG	0.0125	660	0.1×10^{-3}		6×10^{-5}	220	2.94×10^{-4}
	“	620♣	0.07×10^{-3}		“	260	4.41×10^{-4}
	0.025	660	0.19×10^{-3}		“	390	1.05×10^{-3}
	“	620♣	0.13×10^{-3}	FV	5×10^{-5}	240	9.95×10^{-5}
	0.050	660	0.36×10^{-3}		“	520	1.05×10^{-4}
	“	620♣	0.25×10^{-3}		1×10^{-4}	240	5.58×10^{-5}
					“	520	5.8×10^{-5}
					1.5×10^{-4}	240	3.7×10^{-5}
					“	520	4.05×10^{-5}
					2×10^{-4}	240	2.6×10^{-5}
					“	520	3.26×10^{-5}

♣ Dye dissolved in actual wastewater

TABLE V. EFFICIENCY COEFFICIENTS OF RADIOLYSIS OF DIFFERENT DYES

Dye	λ_{max}, nm	K^*, $g \cdot L^{-1} \cdot Gy^{-1}$	Dye	λ_{max}, nm	K^*, $mol \cdot L^{-1} \cdot Gy^{-1}$
LB	612	2.2×10^{-5}	FO	416 nm	1.9×10^{-7}
LBR	514	8.9×10^{-5}	FY	390	6.8×10^{-8}
LBY	414	5.9×10^{-5}		260	2.6×10^{-8}
DS	504	1.2×10^{-5}		220	1.5×10^{-8}
	496♣	5.9×10^{-6}	FV	520	5.5×10^{-9}
DBG	660	4.5×10^{-6}		240	5.1×10^{-9}
	620♣	3.2×10^{-6}			

♣ Dye dissolved in actual wastewater.

3.1.4. The radiation-chemical yield (G-value)

The radiation-chemical yield (G-value) for the degradation of different dyes is calculated using the general formula [15]:

$$G(-\text{dye}) = \frac{\Delta \text{C}}{\rho D} \qquad \text{mol/J} \qquad (5)$$

where

ΔC is the change in dye concentration, mol/L,
ρ is the density of dye solution, kg/L,
D is the absorbed dose in Gy.

From the experimental results, the kinetic behaviour was found to be of first order, substituting for C from equation (1) in equation (5):

$$G(-\text{dye}) = \frac{\text{C}_\text{o} - \text{C}}{\rho D} = \text{C}_\text{o}\frac{(1 - e^{-\text{k}_1 D})}{\rho D} \qquad (6)$$

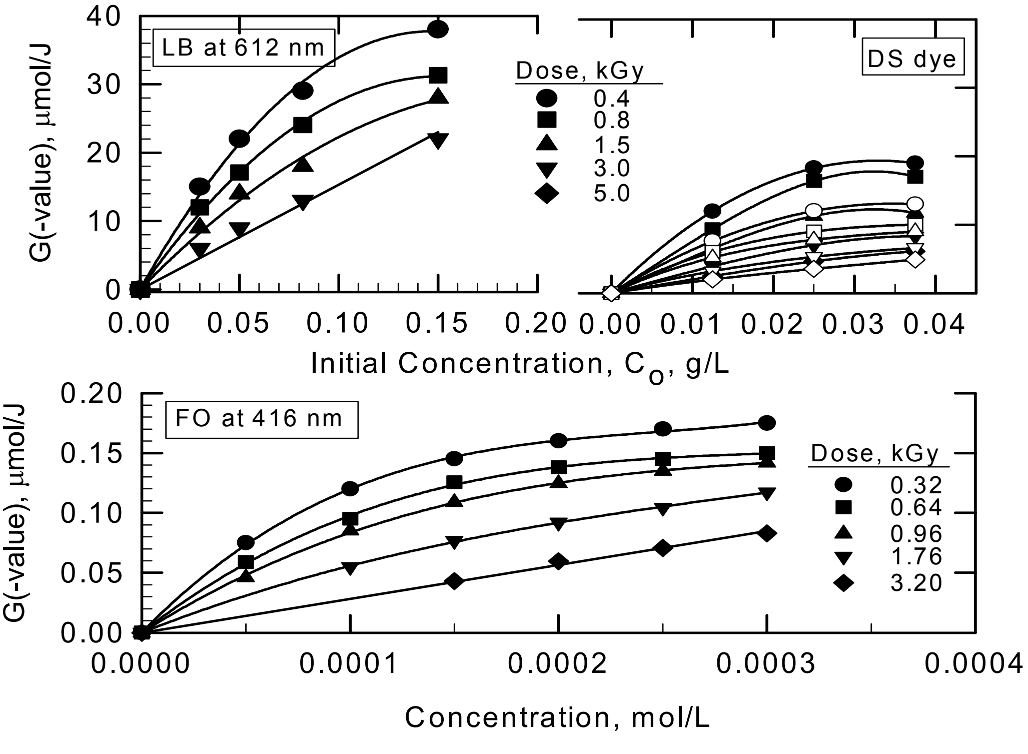

FIG. 8. Behaviour of G(-value) versus initial concentration, C_o, of different dyes at different doses. Solid symbols for dyes dissolved in distilled water and open symbols for dyes dissolved in wastewater.

Figure 8 shows the change in radiation-chemical yield, G-value, versus initial concentration, C_0, at different doses. It can be seen that at low doses G-value increases exponentially with the increase of Co, and at high doses G-value increases nearly linearly with the increase of Co. Also, the change from exponential increase at low doses to linear increase at high doses is a gradual change as shown in Fig. 8. These experimental results are in good agreement with the mathematical derivation given above. At high doses, the term e^{-klD}, in equation (6) tends to be zero, this explains the linear increase of G-value with Co which is experimentally obtained at high doses.

3.1.5. Irradiation of a mixture of dyes

The presence of a mixture of different dyes in solution is expected to affect the position of the absorption bands characteristic of each dye. Figure 9 shows the absorption spectra of different concentrations of the mixture (the mixture consists of equal concentrations of three dyes). It can be seen that there is no shift for the position of the peaks in the visible region except for the two characteristic peaks of LBR dye where the amplitude of the peak at 540 nm is higher than that of the other peak at 514 nm.

The extinction coefficients of the three dyes in the mixture were determined using the optical density at the maximum of the characteristic peak for each dye in the mixture (612 nm for LB, 540 nm for LBR and 414 nm for LBY) and were found to be 13.33, 20.8 and 36.6 $L\cdot g^{-1}\cdot cm^{-1}$, respectively.

The presence of different dyes in a waste solution during irradiation is expected to affect the efficiency of the radiolysis process and the kinetics of decolouration. In this study a mixture of LB, LBR and LBY dyes with equal concentrations (0.05 g/L for each dye in the mixture, prepared by mixing equal volumes from solutions containing 0.15 g/L of each dye) is irradiated to different doses and the absorption spectra of mixture solutions were recorded before and after irradiation (Fig. 10).

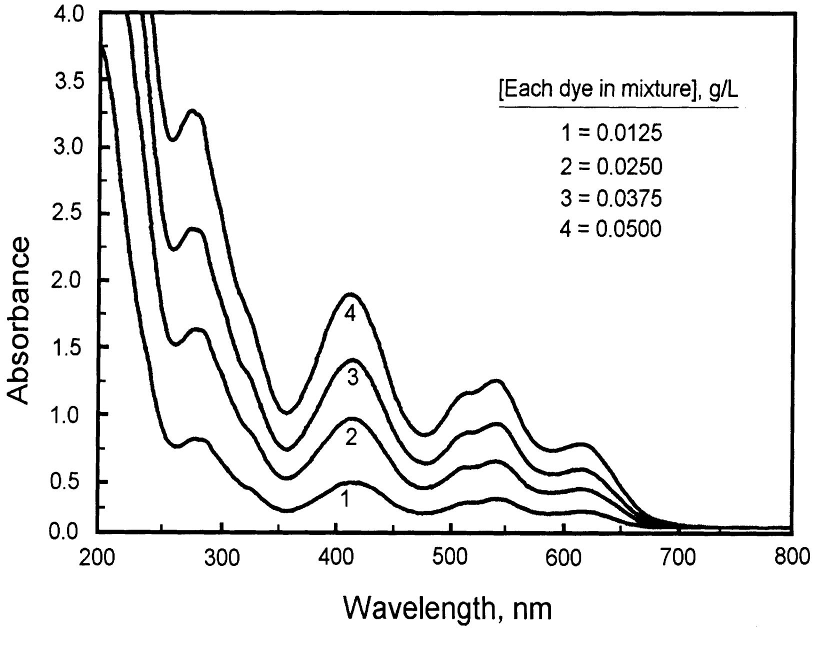

FIG. 9. Absorption spectra of different solutions of mixed LB, LBR and LBY dyes (each solution contains equal concentration of each dye).

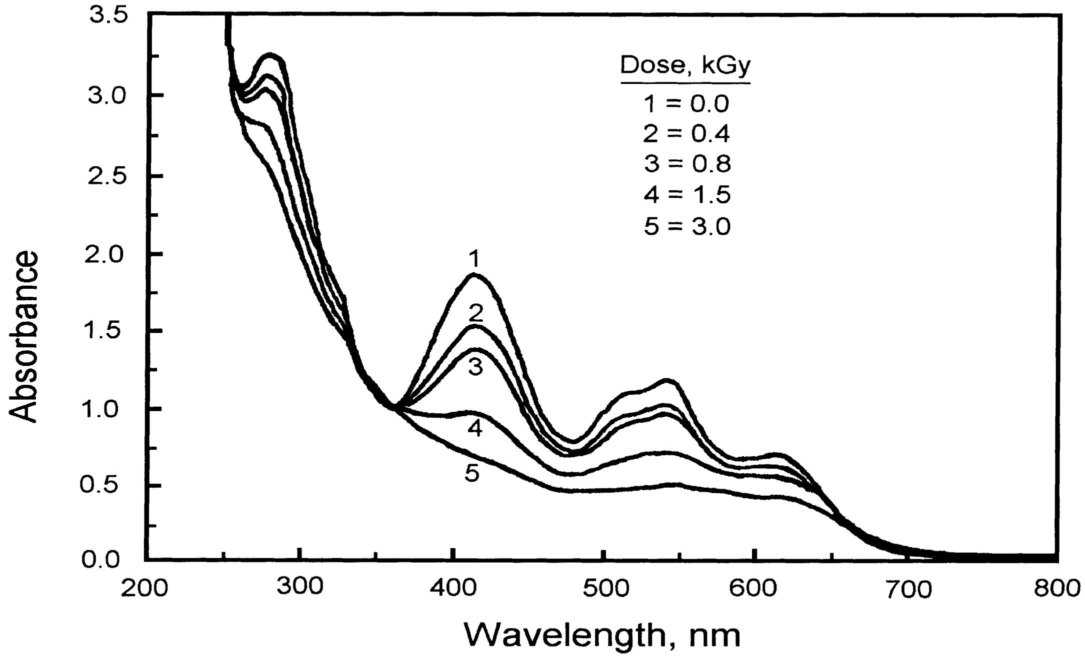

FIG. 10. Absorption spectra of aqueous solutions of mixed Levafix dyes, unirradiated and irradiated to different doses. [each dye]=0.05 g/L.

The kinetics of the competing decolouration reaction of the three dyes in the mixture was studied by irradiating, to different doses, a mixture of the three dyes having equal concentrations (0.05 g/L of each dye in the mixture). The results reveal that the decolouration process follows a first order kinetics for all dyes with different rate constants. Figure 11 shows the relation between the natural logarithm of the residual concentration of the three dyes (0.05 g/L of each dye) and the absorbed dose. The linearity of the relationships reflects the first order radiolytic effect for these dyes. The reaction rate constants, k_1, of decolouration of LB, LBR and LBY dyes were determined as the slope of the straight lines cited before and given in Table VI and are compared with values for single dye solution. It can be seen that the rate of the decolouration process of the three dyes decreases in the mixture for different irradiation conditions (0.46 for LB, 0.13 for LBR and 0.32 for LBY). The decrease of the kinetic constant may be attributed to the increase of the total concentration of dyes in solution. The difference in the percentage decrease may be due to the different competing reactions taking place between the different dye molecules, with different chemical structure, and the primary radiolysis products of water.

TABLE VI. THE KINETIC RATE CONSTANTS OF DECOLOURATION OF THE THREE DYES SEPARATELY AND IN MIXTURE

	Kinetic rate constant, k1, Gy^{-1}		
	LB	LBR	LBY
0.05 g/L single dye	0.355×10^{-3}	2.057×10^{-3}	1.26×10^{-3}
0.05 g/L dye in mixture	0.162×10^{-3}	0.267×10^{-3}	0.403×10^{-3}

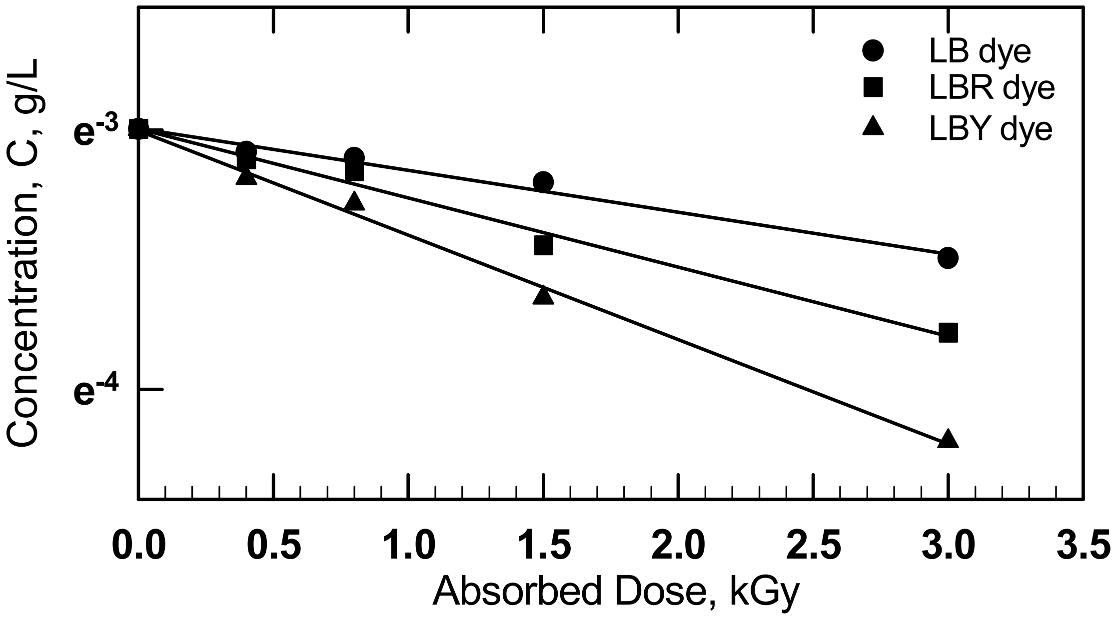

FIG. 11. Residual concentration of Levafix dyes (C) vs. the absorbed dose. lmax in the mixture (612 nm for LB, 540 nm for LBR and 414 nm for LBY. [Each dye in the mixture] = 0.05 g/L.

3.1.6. Effect of pH

The degradation behaviour at different pH values for some representative dyes (LBR, FY, FO and FV) was studied by irradiating different aqueous dye solutions to a dose of 0.8 kGy for LBR (0.075 g/L), FY (4×10^{-5} mol/L), FO (2×10^{-4} mol/L) or 2.25 kGy for FV (1×10^{-4} mol/L). The dependence of the degradation process on pH is shown in Fig. 12. It can be seen that FO, FY and FV dyes are destroyed in the pH range from 4 to 9 with a reduced sensitivity at lower and higher pH range. LBR molecules are destroyed most effectively in acid media while the degradation percent is about constant in the pH range 4-8. It decreases sharply at pH higher than 9. On the other hand the decolouration of FV dye (reduction in absorbency at 520 nm) shows a different behaviour in acidic medium where it increases sharply at pH >3.

The observed behaviour of the effect of the pH change on the degree of decolouration or degradation is not quite clear. A possible explanation might be based on the acid-base properties of the $^{\bullet}OH$ radicals. In strong basic solution, the $^{\bullet}OH$ radicals dissociate to the less reactive $^{\bullet}O^-$ radical [16], i.e.

$$^{\bullet}OH \longleftrightarrow H^+ + {}^{\bullet}O^- \quad (pK = 11.9) \qquad (11)$$

In fact the degradation scheme depends on the relative reactivity of the various species, availability of oxygen, dose, pH of solution and temperature [17].

In acidic solution ($e^-_{aq} + H^+ \longrightarrow H^{\bullet}$, $k = 2.3 \times 10^{10}$ L·mol^{-1}·s^{-1}), the reducing H atoms are scavenged by oxygen leading to a formation of $HO_2^{\bullet}$ which can be involved in the degradation process. The $O^{\bullet -}_2$ species are not very reactive, hence, at pH>7 the $^{\bullet}OH$ radicals are the major primary attacking transients. The sharp decrease in the degree of degradation over pH>9 may be a result of the low reactivity of $^{\bullet}O^-$ and $O^{\bullet -}_2$ species to the attack of the dyes [16].

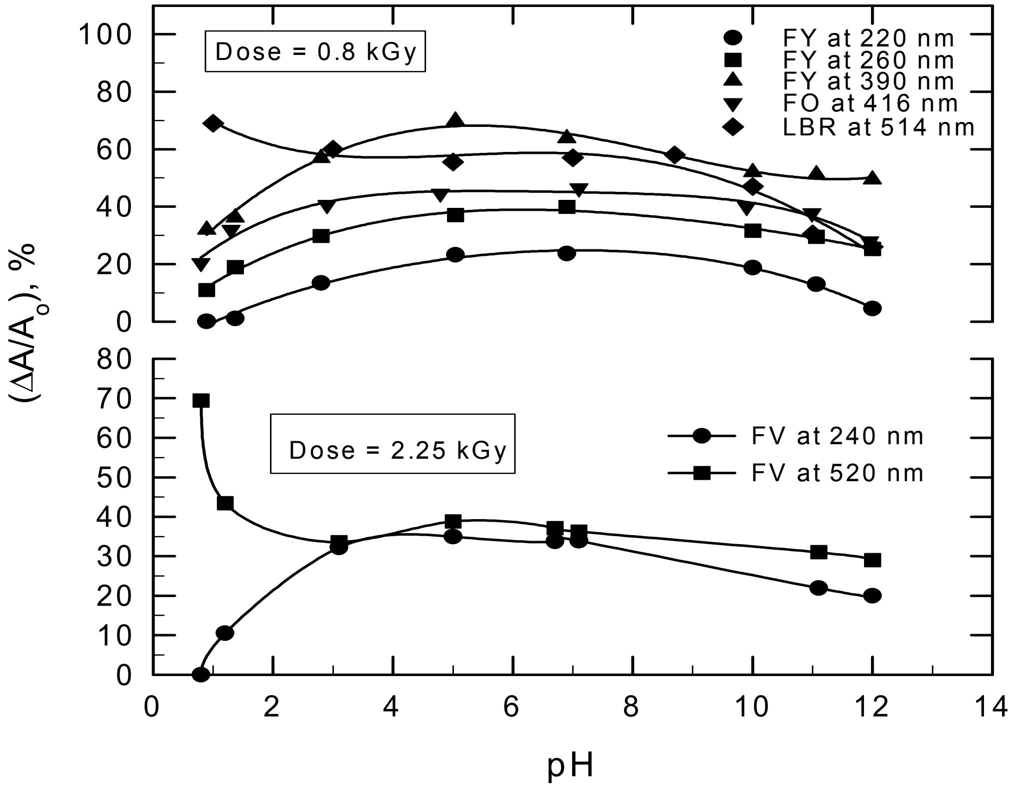

FIG. 12. Variation of $\Delta A/A_o$, % of LBR, FY, FO and FV dye as a function of pH. Dose and wavelength of analysis are indicated.

3.1.7. Effect of some additives on the decomposition of dye solution

3.1.7.1. Effect of ethanol

$^{\bullet}OH$ radicals effectively oxidize organic pollutants such as organic dyes. For the dyes LBR, FY, FO and FV, the role of $^{\bullet}OH$ radicals in degradation of the respective dye is examined by adding ethanol which acts as a good scavenger to $^{\bullet}OH$ radicals [18]. Fig. 13a shows the influence of ethanol concentration on the radiation-chemical yield, G(-dye), of LBR (0.075 g/L), FY (4×10^{-5} mol/L), FO (2×10^{-4} mol/L) and FV (1×10^{-4} mol/L) aqueous dye solutions at pH = 4. From this figure, it is seen that G(-dye) decreases sharply with increase of ethanol concentration up to 1×10^{-3} mol/L. The decrease in G(-dye) on addition of ethanol can lead to the suggestion that $^{\bullet}$OH radical destroys the dye more efficiently than does the ethanol radical. This effect may be attributed to the very fast reaction of $^{\bullet}$OH radical with ethanol [19, 20] according to the reaction:

$$^{\bullet}OH + CH_3CH_2OH \xrightarrow{k_2} CH_3{}^{\bullet}CHOH + H_2O \qquad (7)$$

where

rate constant $k_2 = 1.1\times10^9$ L·mol^{-1}·s^{-1}.

On the basis of the results given above, the degradation reaction of dyes by $^{\bullet}$OH radical may be written as follows:

$$\text{Dye} + {}^{\bullet}OH \xrightarrow{k} \text{degradation product} \qquad (8)$$

The rate constant for the reaction (8) can be determined by the use of competition kinetic [20]. Considering the yield of those radicals that react with the dye and ethanol as G_r, then

$$G(\text{-dye}) = G_r \frac{kC_{o,d}}{kC_{o,d} + k_2C_{o,e}} \qquad (9)$$

where

$C_{o,d}$ is the initial concentration of dye,
$C_{o,e}$ is the initial concentration of ethanol.

The reciprocal of equation (9) is

$$\frac{1}{G(-\text{dye})} = \frac{1}{G_r}\left[1 + \frac{k_2}{k}\cdot\frac{C_{o,e}}{C_{o,d}}\right] \qquad (10)$$

It is obvious, from equation (10), that the relation between 1/G(-dye) and the ethanol concentration, $C_{o,e}$, is a linear relation with slope of $\frac{k_2}{k}\cdot\frac{1}{C_{o,d}G_r}$ and the intercept is $1/G_r$. The plots of 1/G(-dye) versus $C_{o,e}$ for LBR, FY, FO and FV dyes are shown in Fig. 13b which are in good agreement with equation (10). The slopes of the straight lines were obtained and by using the value 1.1×10^9 L·mol^{-1}·s^{-1} for k_2 [21], the rate constants for the reaction of $^{\bullet}$OH radical with the different dyes, k, are calculated. Table VII shows the values of the slopes of the straight lines and k for LBR, FY, FO and FV dyes (Fig. 13b).

The estimation of the rates with which the dyes and ethanol compete for the $^{\bullet}$OH radical (in s^{-1}) can be carried out by multiplying the rate constants (in L·mol^{-1}·s^{-1}) and solute concentration (in mol/L) [22]. For example:

$– d\ (\text{ethanol})/dt = 1.1\times10^{9}\ \text{L}\cdot\text{mol}^{-1}\cdot\text{s}^{-1} \times 5\times10^{-4}\ \text{mol}\cdot\text{L}^{-1} = 5.5\times10^{5}\ \text{s}^{-1}$.
$– d\ (\text{ethanol})/dt = 1.1\times10^{9}\ \text{L}\cdot\text{mol}^{-1}\cdot\text{s}^{-1} \times 1\times10^{-3}\ \text{mol}\cdot\text{L}^{-1} = 1.1\times10^{6}\ \text{s}^{-1}$.
$– d\ (\text{ethanol})/dt = 1.1\times10^{9}\ \text{L}\cdot\text{mol}^{-1}\cdot\text{s}^{-1} \times 5\times10^{-3}\ \text{mol}\cdot\text{L}^{-1} = 5.5\times10^{6}\ \text{s}^{-1}$.

$– d\ (\text{FO at 416 nm})/dt = 1.43\times10^{9}\ \text{L}\cdot\text{mol}^{-1}\cdot\text{s}^{-1} \times 2\times10^{-4}\ \text{mol}\cdot\text{L}^{-1} = 2.86\times10^{5}\ \text{s}^{-1}$.
$– d\ (\text{FY at 390 nm})/dt = 2.89\times10^{9}\ \text{L}\cdot\text{mol}^{-1}\cdot\text{s}^{-1} \times 4\times10^{-5}\ \text{mol}\cdot\text{L}^{-1} = 1.156\times10^{5}\ \text{s}^{-1}$.
$– d\ (\text{FY at 260 nm})/dt = 2.95\times10^{9}\ \text{L}\cdot\text{mol}^{-1}\cdot\text{s}^{-1} \times 4\times10^{-5}\ \text{mol}\cdot\text{L}^{-1} = 1.18\times10^{5}\ \text{s}^{-1}$.
$– d\ (\text{FY at 220 nm})/dt = 3.24\times10^{9}\ \text{L}\cdot\text{mol}^{-1}\cdot\text{s}^{-1} \times 4\times10^{-5}\ \text{mol}\cdot\text{L}^{-1} = 1.3\ \times10^{5}\ \text{s}^{-1}$.
$– d\ (\text{FV at 520 nm})/dt = 2.22\times10^{9}\ \text{L}\cdot\text{mol}^{-1}\cdot\text{s}^{-1} \times 1\times10^{-4}\ \text{mol}\cdot\text{L}^{-1} = 2.22\times10^{5}\ \text{s}^{-1}$.
$– d\ (\text{FV at 240 nm})/dt = 4.0\times10^{10}\ \text{L}\cdot\text{mol}^{-1}\cdot\text{s}^{-1} \times 1\times10^{-4}\ \text{mol}\cdot\text{L}^{-1} = 4\times10^{6}\ \text{s}^{-1}$.

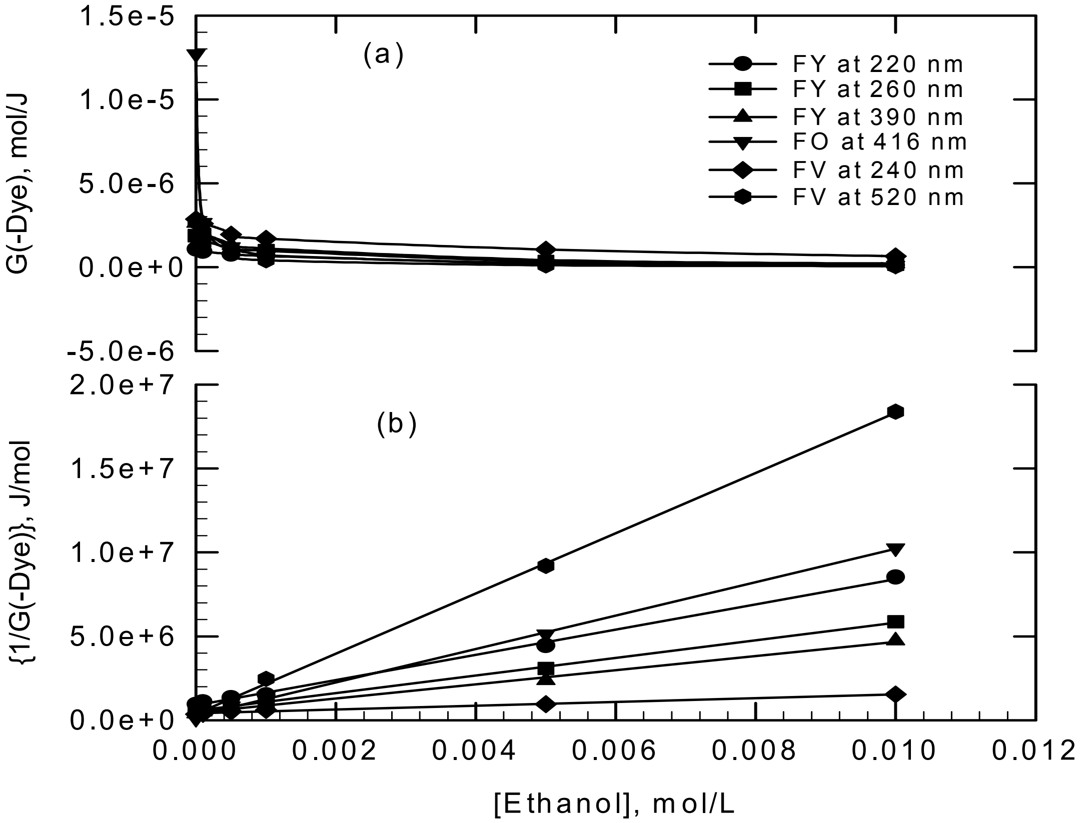

FIG. 13. (a) Effect of ethanol concentration on G(-Dye) of FY, FO and FV aqueous solutions; pH = 4.
(b) Variation of 1/G(-Dye) as a function of ethanol concentration; pH = 4.

TABLE VII. THE VALUES OF k AND THE CONSTANTS OF THE LINEAR RELATIONS

Dye	l_{max}, nm	Intercept, J·mol^{-1}	Slope, J·L·mol^{-2}	k, L·mol^{-1}·s^{-1}
FO	416	2.59×10^5	9.96×10^8	1.43×10^9
FY	390	4.43×10^5	4.21×10^8	2.89×10^{10}
	260	5.63×10^5	5.24×10^8	2.95×10^{10}
	220	8.87×10^5	7.52×10^8	3.24×10^{10}
FV	520	3.62×10^5	1.796×10^9	2.22×10^9
	240	4.10×10^5	1.127×10^8	4.00×10^{10}
LBR♣	514	1.63×10^4 J·g^{-1}	6.14×10^6 J·L·g^{-1}·mol^{-1}	3.89×10^7 L·g^{-1}·s^{-1}

♣ Dye concentration in g/L.

From these results, it is evident that for ethanol concentrations higher than 5×10^{-4} mol/L, how ethanol can protect the dye from destruction by $^{\bullet}$OH radical attack except for FV at 240 nm. This conclusion is of course true only for dye concentrations equal to or lower than the concentrations used in this estimation. In the case of FV at 240 nm, ethanol should be higher than 5×10^{-5} mol/L. These data are an example showing the importance of kinetic studies, which help in the evaluation of the competing effect of different pollutant species that may be present in an actual wastewater steam.

3.1.7.2. Effect of NaOCl and H_2O_2

In the textile treatment processes, chemicals such as NaOCl and H_2O_2 are used. The degradation behaviour at different NaOCl or H_2O_2 concentrations for FY, FO and FV dyes was studied by irradiating different aqueous dye solutions to a dose of 0.8 kGy for FY (4×10^{-5} mol/L) and FO (2×10^{-4} mol/L) or 2.25 kGy for FV (1×10^{-4} mol/L). The degradation behaviour versus NaOCl and H_2O_2 concentration is shown in Figs. 14 and 15, respectively. It can be seen that, for FV dye, the degradation percent increases as the concentration of NaOCl and H_2O_2 increases and reaches maximum at 0.002 mol/L of H_2O_2 and 0.006 mol/L of NaOCl. At higher concentrations of both NaOCl and H_2O_2 the degradation extent decreases. On the other hand, for FY and FO dyes the extent of degradation decreases as a result of the addition of NaOCl or H_2O_2. The exact explanation of these results is not clear at this stage but it should be related to the chemical structure of the dyes and the oxidizing properties of both NaOCl and H_2O_2.

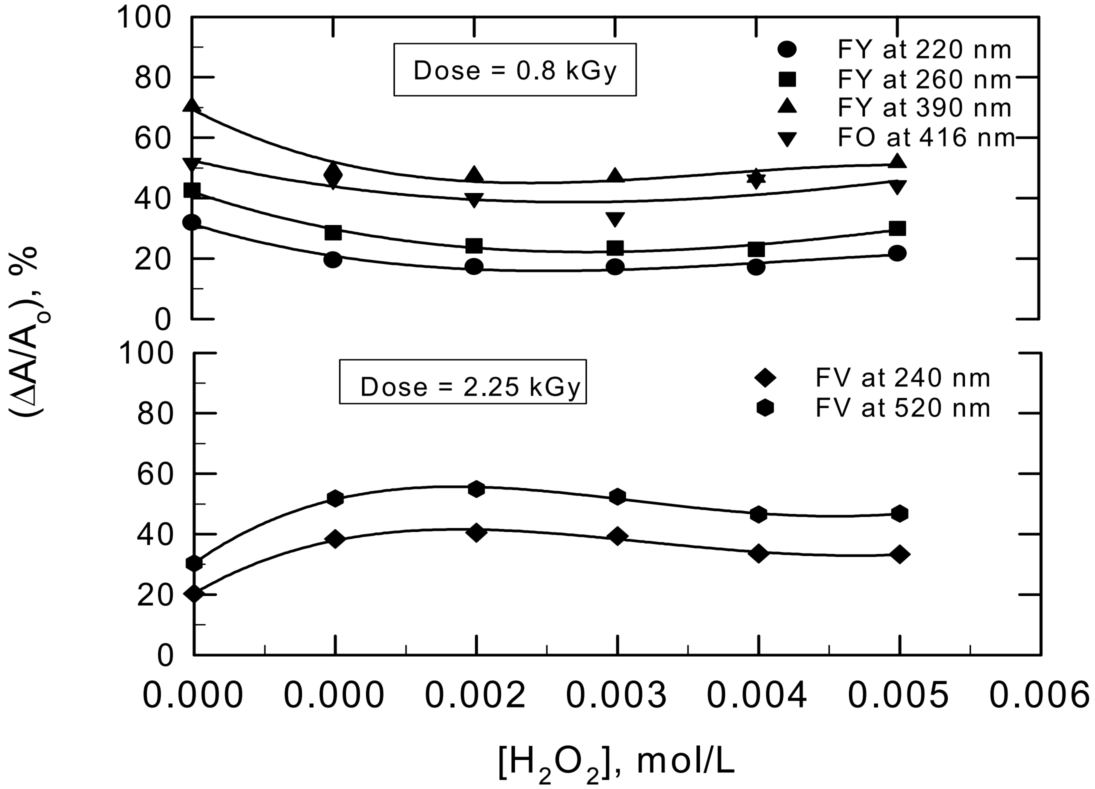

FIG. 14. Effect of H_2O_2 concentration on the degradation of FY, FO and FV dyes. Doses and analysis wavelengths are indicated.

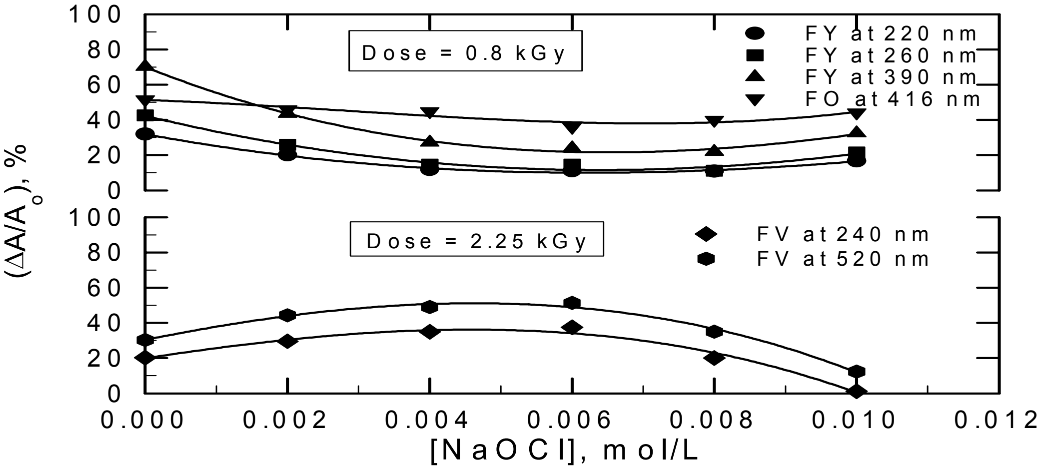

FIG. 15. Effect of NaOCl concentration on the degradation of FY, FO and FV dyes. Doses and analyses wavelengths are indicated.

3.2. Assessment of the biological eco-toxicity of the dye stuff compounds

The data for the eco-toxicity assessment of the three dyes (FV, FO and FY) are presented in Tables VIII and IX and in Fig. 16. Table VIII shows the percentage survival of snails exposed to different dye solutions of different concentrations for 24, 48 and 72 hours. It is clear that FV dye has a clear toxic effect on the snails studied. The 50% lethal dye concentration (Lc_{50}) was determined using Fig. 16 and was found to be 300 ppm. Concentrations lower than 100 ppm did not show any lethal effect after 72 hour exposure time.

TABLE VIII. PERCENTAGE OF SURVIVAL OF SNAILS EXPOSED TO DIFFERENT TEXTILE DYES AT DIFFERENT CONCENTRATIONS FOR 24, 48, AND 72 HOURS

		Concentration, ppm						
Dye	Time, h	100	200	300	400	500	600	700
Control	24	100	100	100	100	100	100	100
	48	100	100	100	100	100	100	100
	72	100	100	100	100	100	100	100
FV	24	92	72	50	40	40	30	20
	48	88	70	48	30	30	10	05
	72	75	70	48	30	20	10	05
FO	24	100	100	100	100	100	100	90
	48	100	100	100	100	100	100	90
	72	100	100	100	100	100	100	90
FY	24	100	100	100	100	100	100	100
	48	100	100	100	100	100	100	100
	72	100	100	100	100	100	100	100

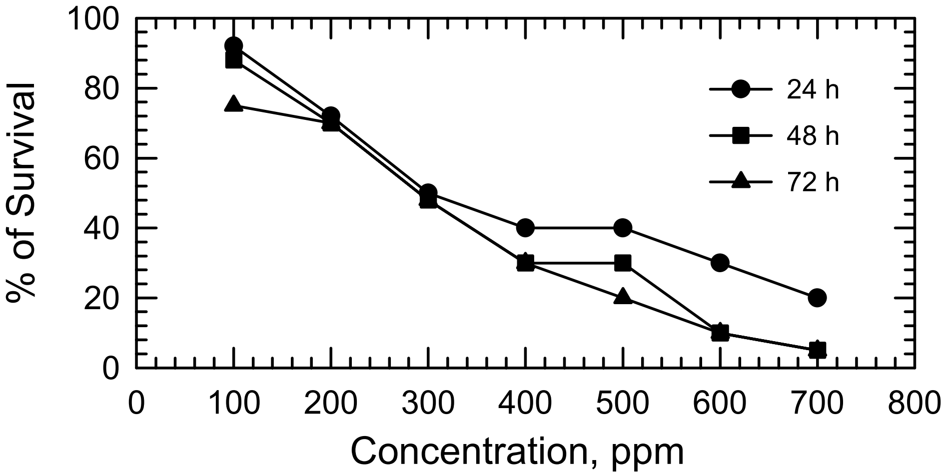

FIG. 16. The variation of percent survival of snail with dye concentration (ppm).

Table IX summarizes the effect of the FV toxic dye as shown by the values of the respective indicators of the snails viability (agglutination test, mean number of hemocytes, hemagglutination titer, total protein content and dye accumulation level) for both the cases of irradiated and unirradiated dye solution at concentrations of 50 ppm. The tabulated results for the agglutination test and mean number of hemocyte count indicate that high radiation doses are needed to achieve complete detoxication of the dye solution. High irradiation doses are therefore needed for the complete elimination of toxic dyes such as the tested FV dye under the experimental condition studied. Also, the dye concentration in water should not exceed 50 ppm.

TABLE IX. BIOLOGICAL CHANGES IN B*iomophlaria alexandrina* SNAILS EXPOSED TO NON-IRRADIATED AND IRRADIATED (7.5 AND 22.5 KGY) FV DYE (50 ppm) FOR 72 HOURS

Dye treatment Parameter	Mean No. of hemocyte count X ± S.D.	Hemagglutinationtiter	Total protein content mg/g tissue	Dye accumulation level µg/g tissue
Control	349.0 ± 47.9	1 : 64	86.7 ± 3.4	------
Unirradiated	452.0 ± 72.2*	1 : 128	79.5 ± 4.4**	223.5 ± 20.7
Irradiated (7.5 kGy)	419.0 ± 60.6*	1 : 128	84.8 ± 4.9*	84.8 ± 17.2**
Irradiated (22.5 kGy)	364.0 ± 4.4$^{\#}$	1 : 64	85.4 ± 5.5$^{\#}$	51.8 ± 15.1**

** Significant at (P<0.001)
* Significant at (P< 0.05)
# Non significant.

3.3. Adsorption of the dye stuff materials using conventional adsorbents

The removal of organic pollutants from waste solution has been widely practised using conventional sorbents such as charcoal, peat, Al2O3, etc. The sorption of the three dyes FV, FO and FY on granular charcoal has been studied under varying conditions of dye concentration and pH. The equilibrium time has been determined (Fig. 17) and was found to be about six hours. The sorption data for different dye concentrations and pH are presented in Table X. These data show that granular charcoal is a good sorbent material for the dyes investigated. The regeneration of the sorption capacity of the charcoal can be achieved by washing with dilute acid or with water. It is seen in this respect that both g-ray irradiation and sorption processes can affect the removal of dye material from waste solutions. The economics of the two techniques has to be studied and compared. In this context it should be mentioned that equilibrium sorption studies need much longer time to achieve dye removal from waste solutions. Also, the capacity of the sorbent material cannot be fully regained after use.

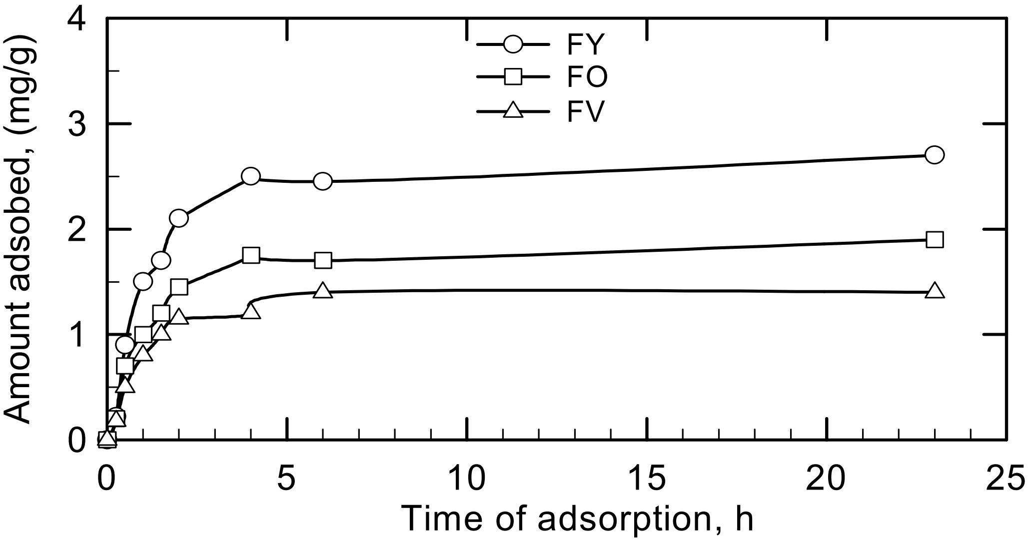

FIG. 17. The amount adsorbed (mg/g) on granular activated carbon as a function of time of adsorption (h) for different dyes. Initial concentration = 50 mg/L.

TABLE X. THE SORPTION VALUES OF FY, FO AND FV DYES (C_O = 100 MG/L) AT DIFFERENT pH VALUES

Dye	λ_{max}, nm	PH	% of removal
FY	390	4	93.80
		7	81.42
		9	74.20
FO	416	4	66.70
		7	51.30
		9	56.50
FV	520	4	93.03
		7	68.10
		9	57.50

♣ Dye concentration in g/L.

REFERENCES

[1] GETOFF, N., Purification of drinking water by irradiation. A review, Proc., Indian Acad. Sci., (Chem. Sci.) **105** (1993) 373 pp.

[2] McKAY, G., Use of Adsorbents for The Removal of Pollutants from Wastewaters, CRC Press Inc., London (1996).

[3] SHENG, H.L., CHI, M.L., Treatment of textile waste effluents by ozonation and chemical coagulation, Water Res. **27** (1993) 1743 pp.

[4] EL ASSY, N.B., ABDEL-REHIM, F., ABDEL-GAWAD, A.S., ABDEL-FATTAH, A.A., J. Radioanal. Nucl. Chem. **148** (1991) 235 pp.

[5] EL ASSY, N.B., ABDEL-REHIM, F., ABDEL-GAWAD, A.S., ABDEL-FATTAH, A.A., J. Radioanal. Nucl. Chem. **157** (1991) 133 pp.

[6] Radiation for Clean Environment, Proc. Int. Symp., IAEA-SM 194/407, (1975).

[7] Symposium on “Application of Isotopes and Radiation In Conservation of Environment”, Karlsruhe, 9-13 March (1992).

[8] SEHESTED, K., In “Manual on Radiation Dosimetry”, (Holm, N.W., Berry, R.J., Dekker, M., Eds.] New York (1970) 313 pp.

[9] FAIRHUST, S., J. Soc. Dyestuff Colour **105** (1989) 315 pp.

[10] HOBBS, S.J., J Soc. Dyestuff Colour **105** (1989) 326 pp.

[11] RIVA, M., FLOS, R., CRESPI, M., PEPIO, M., Arch. Environ. Contam. Toxicol. **23** (1992) 206 pp.

[12] ANLIKER, R., Recent development concerning the ecotoxicology of dyestuffs (12th Congress of the International Federation of Associations of Textile Chemists and Colourists, Budapest, 1981) 1 pp.

[13] SUZUKI, N., NAGAI, T., HOTTA, H., WASHINO, M., Int. J. Appl. Radiat. and Isot. **26** (1975) 726 pp.

[14] PICCININI, N., FERRERO, F., Effect of gamma irradiation on the degradation of dyes, Radiat. Clean Environ.(Proc. Int. Symp.) IAEA-SM 194/407 (1975) 249 pp.

[15] McLAUGHLIN, W.L., BOYD, A.W., CHADWICK, K.H., MCDONALD, J.C., MILLER, A., Dosimetry for Radiation Processing, Taylor & Francis, London (1989).

[16] DORFMAN, L.M., ADMAS, G.E., Reactivity of Hydrogen in Aqueous Solutions, National Reference Data System, US Dep. of Commerce, National Bureau of Standards, Reports NSRDS-NBS, (1973) 46 pp.

[17] GETOFF N., Peroxyl Radicals (Alfassi, Z. B., Ed.) John Wiley & Sons Ltd. (1997).

[18] ABDEL-REHIM, F., EID, S.A., SOUKA, N., McLAUGHLIN, W.L., Radiat. Phys. Chem. **27** (1986) 211 pp.

[19] GUPTA, B., HART, J., Radiat. Res. **48** (1971) 819 pp.

[20] SPINKS, J.W.T., WOOD, R.J., An Introduction to Radiation Chemistry, 3rd Ed, Wiley and Sons, New York (1994).

[21] ANBAR, M., NETA, P., Int. J. Appl. Radiat. Isotop. **18** (1967) 493 pp.

[22] HOIGNE J., Radiation for clean environment (Proc. Int. Symp., IAEA-SM 194/407 (1975).

EFFECTS OF RADIATION ON WASTEWATER FROM TEXTILE INDUSTRIES IN GHANA

S.A. Dogbe, G. Emi-Reynolds, G.K. Banini
National Nuclear Research Institute (GAEC),
Legon, Ghana

Abstract. Wastewater samples from three textile industries in Ghana were progressively irradiated in a gamma irradiator of dose rate 7.8 kGy/h. Gamma irradiation alone was done, and also in combination with hydrogen peroxide, sodium peroxide and ferrous ammonium sulphate. Preliminary work involved irradiation of model aqueous solutions of six textile dyes commonly used in Ghana. The dyes were Cibacron Yellow 6G, Cibacron Violet 2R, Basilen Blue P 5R, Basilen Brown P 2R, Solidazol Red RB, Acramin Green FB. Colour and pH of the wastewater and dye solutions were found to decrease with irradiation. Decolouration of the wastewater improved further when irradiation was carried out in combination with the chemical agents. Ferrous ammonium sulphate showed the most improved decolouration. Values of chemical oxygen demand (COD) of the wastewater were found to decrease with irradiation.

1. INTRODUCTION

Indiscriminate discharges of untreated wastewater into the environment by industries in Ghana are now a great concern. It was estimated that textile industries alone discharge about 72.5×10^6 litres of wastewater daily containing high levels of toxic and non-biodegradable dyestuffs and other chemicals [1]. This situation has caused destruction of life in some lagoons, and reduced soil fertility of potential farmland in other areas of the country.

To avert this environmental problem the Environmental Protection Agency of Ghana came out with sector specific effluent quality guidelines for discharge into the environment. Industries are, therefore, under obligation not only to treat their wastewater but also adopt efficient treatment methods. Wastewater treatment methods such as, filtration, sedimentation and chlorinating, which are practised by some textile industries, are reported to be ineffective and environmentally dangerous [2, 3]. It has, therefore, become expedient to study alternate methods that are efficient and environmentally friendly. Earlier studies [4–7] have shown that coloured materials undergo bleaching or decrease in colour when exposed to ionizing radiation. In principle, therefore, gamma and e-beam irradiation can be considered as alternate method of treatment of wastewater from textile industries. This work, therefore, examines the potential of gamma irradiation, and in combination with some chemical agents for decolouration and decomposition of dyestuffs and other organic pollutants in wastewaters from textile industries in Ghana.

2. EXPERIMENTAL

2.1. Materials

Five soluble dyes — Cibacron Yellow 6G, Cibacron Violet 2R, Basilen Blue P 5R, Basilen Brown P 2R, Solidazol Red P RB, and a disperse dye, Acramin Green, were obtained from three major textile industries in Ghana. The dyes were manufactured in Germany. Untreated wastewaters labelled GT.1, GT. 2, and GT. 3 were collected from the same three industries. Analytical grade chemicals: 30% Hydrogen peroxide, 30% Sodium peroxide solution and 30% ferrous ammonium sulphate solution were used.

2.2. Methods

Model aqueous solutions of concentrations 50, 100, 150, and 200 ppm that are close to the content of dyes in industrial wastewater were prepared with each dye. The pH of the dye solutions was measured using WTW pH meter model 523. A Unicam SP 1800 UV/vis-spectrophotometer was used to scan the absorption spectra of each dye solution over the wave length range 200-800 nm, and the optical densities at the characteristic wave lengths were measured.

200 ml of each dye solution was transferred separately into 250 ml leak-proof polypropylene bottles. The bottles were then irradiated progressively to a maximum dose of 6 kGy in a gamma irradiator of dose rate 7.8 kGy/h available at the Ghana Atomic Energy Commission. Twenty-four hours after every irradiation interval, the pH and optical absorption at the characteristic wavelengths of the dye solutions were measured. The wastewaters were similarly irradiated progressively to a maximum dose of 20 kGy by gamma irradiation alone and in combination with each chemical. The parameters, pH and optical absorption at the characteristic wavelength, were measured after every irradiation interval. Chemical oxygen demand (COD) of the wastewaters was determined before and after each irradiation interval by a standard procedure [8].

3. RESULTS AND DISCUSSION

3.1. Absorption spectra

The optical absorption spectra of the unirradiated dye solutions showed strong absorption at the following wavelengths: Cibacron Yellow 6G, 432 nm; Basilen Brown P 2R, 460 nm; Solidazol Red P RB, 530 nm; Cibacron Violet 2R, 560; Basilen Blue P 5R, 570 nm; Acramin Green FB, 650 nm. Each dye solution showed a second absorption band at about 230 nm. On irradiation the absorption band at 230 was not affected even at 6 kGy. The absorption bands at 430, 460, 530, 560 and 570 nm were found to decrease rapidly with increasing irradiation dose. The decrease was more rapid for the lower concentration (50 ppm) dye solutions than the high concentration solutions. The maximum absorption band of the lowest concentration solution disappeared almost completely at a dose of 2 kGy. For the highest concentration (200 ppm) dye solution, the maximum absorption bands disappeared after 4-kGy irradiation dose. From other studies [9, 10], the absorption band at 230 nm was attributed to substituted aromatic rings of the dye molecule. Similarly, the absorption bands at 430, 460, 530, 560 and 570 nm were attributed to azo groups and their auxochromic substitutes. The observed changes in the absorption bands in the visible region with irradiation dose, therefore, suggest destruction of only the chromophoric groups with little or no effect on the substituted aromatic rings of the dye molecule [4].

The optical absorption spectra of the pigment (Acramin Green FB) solution, with strong absorption bands at 230 nm and 650 nm, was totally unaffected by irradiation even after 6 kGy dose. This would imply that irradiation could not promote any breakdown of the pigment.

Text cont. on p. 131.

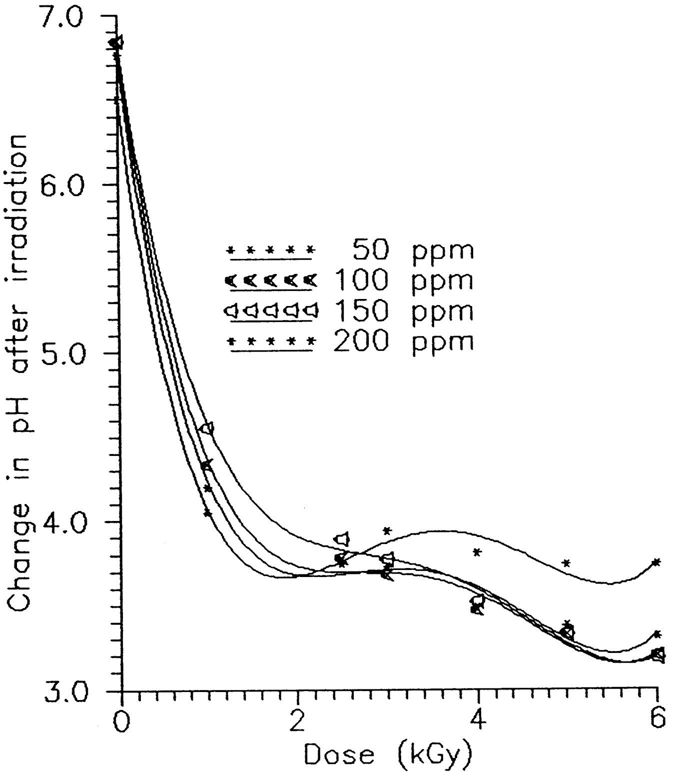

FIG. 1. Change of pH with irradiation doses (kGy) of various concentrations (ppm) of Cibacron Yellow 6G.

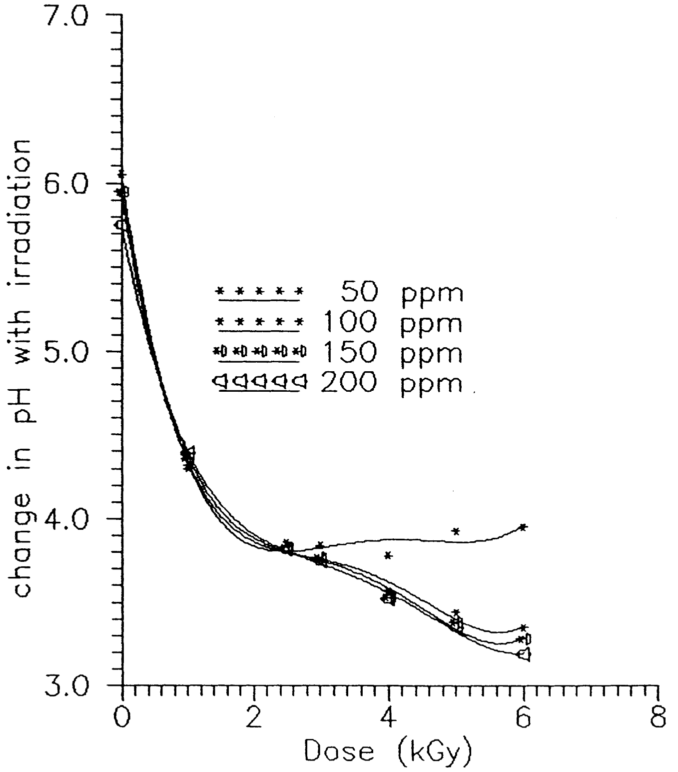

FIG 2. Change in pH with irradiation doses (kGy) of various concentrations (ppm) of Basilen Blue P 5R.

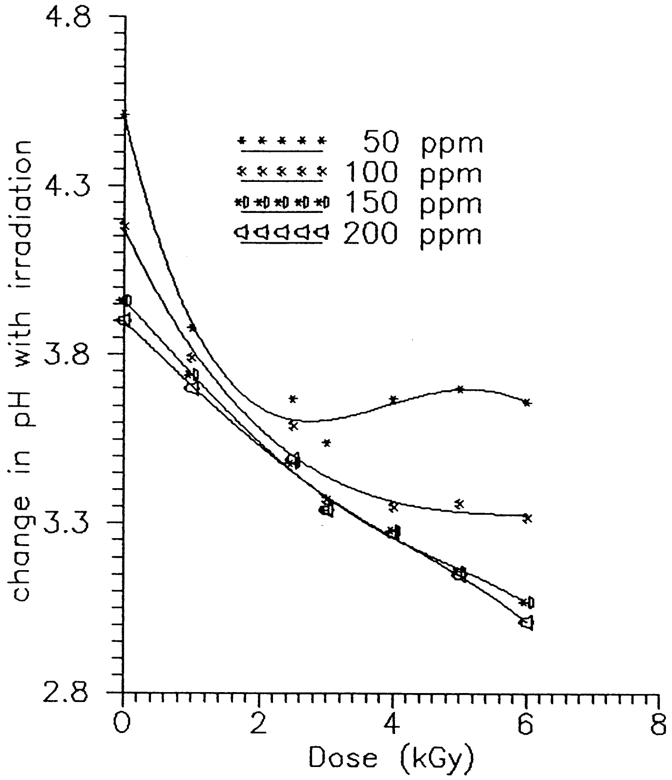

FIG. 3. Change in pH with irradiation doses (kGy) of various concentrations (ppm) of Solidazol Red P RB.

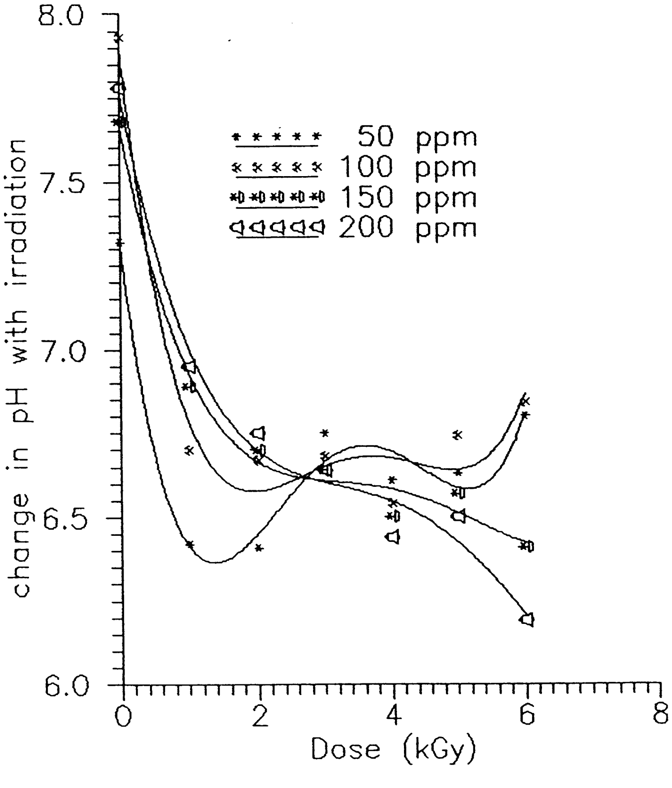

FIG 4. Change in pH with irradiation doses (kGy) of various concentrations (ppm) of Basilen Brown P2R.

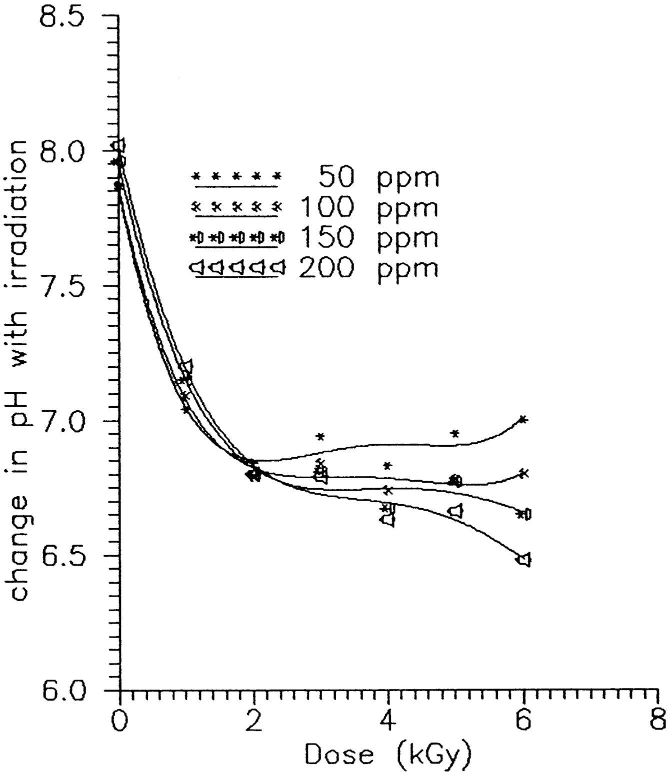

FIG. 5. Change in pH with irradiation doses (kGy) of various concentrations (ppm) of Cibacron Violet 2R.

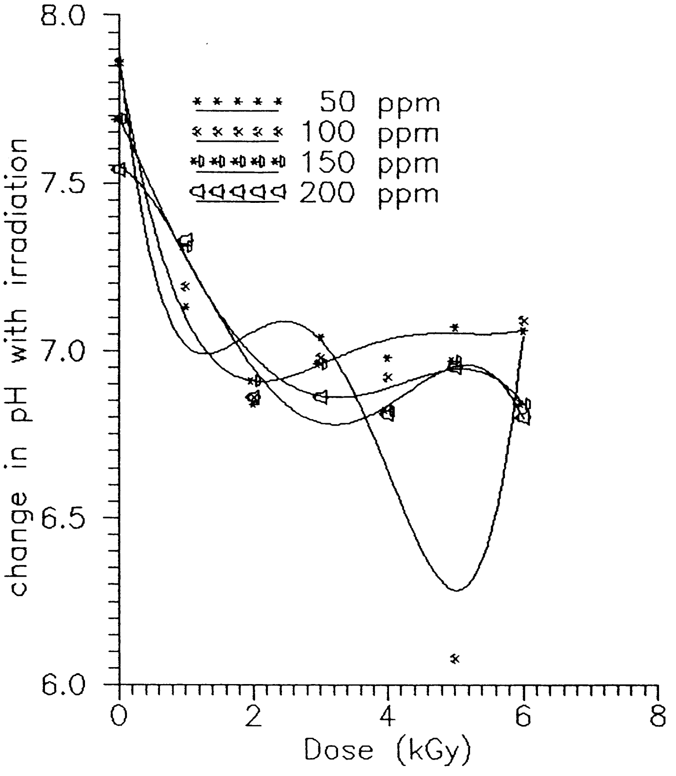

FIG 6. Change in pH with irradiation doses (kGy) of various concentrations (ppm) of Acramin Green FB.

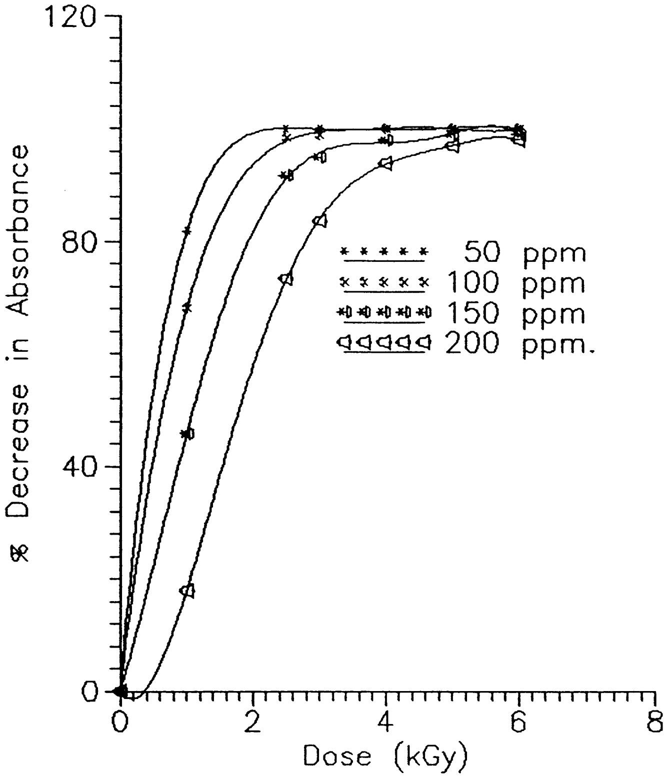

FIG. 7. Degree of decolouration (%) vs. doses (kGy) of various concentrations of Cibacron Yellow 6G.

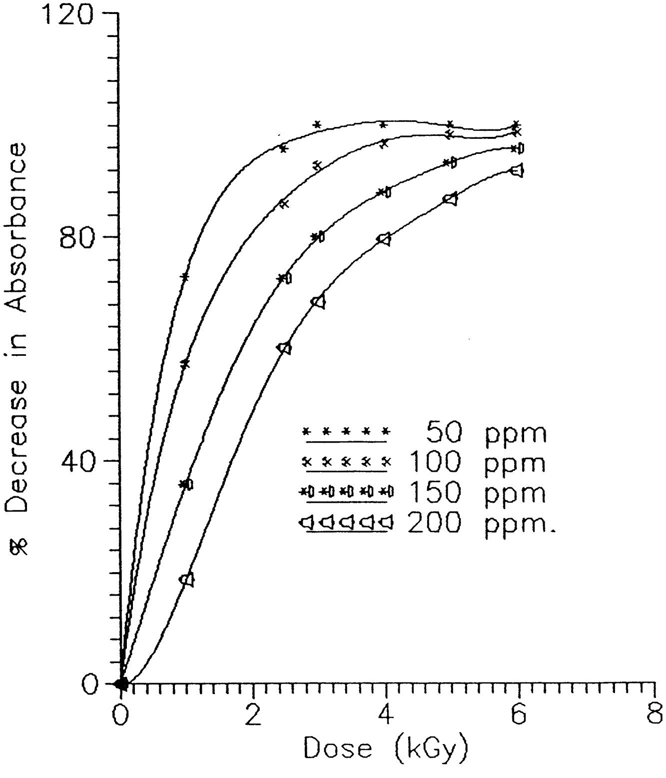

FIG 8. Degree of decolouration (%) vs. doses (kGy) of various concentrations of Basilen Blue P 5R.

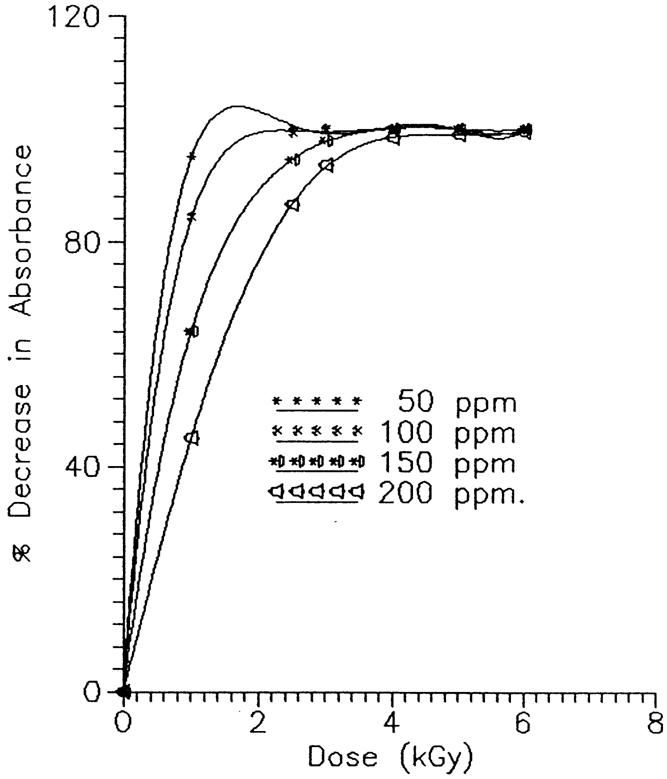

FIG. 9. Degree of decolouration (%) vs. doses (kGy) of various concentrations of Solidazol Red P RB.

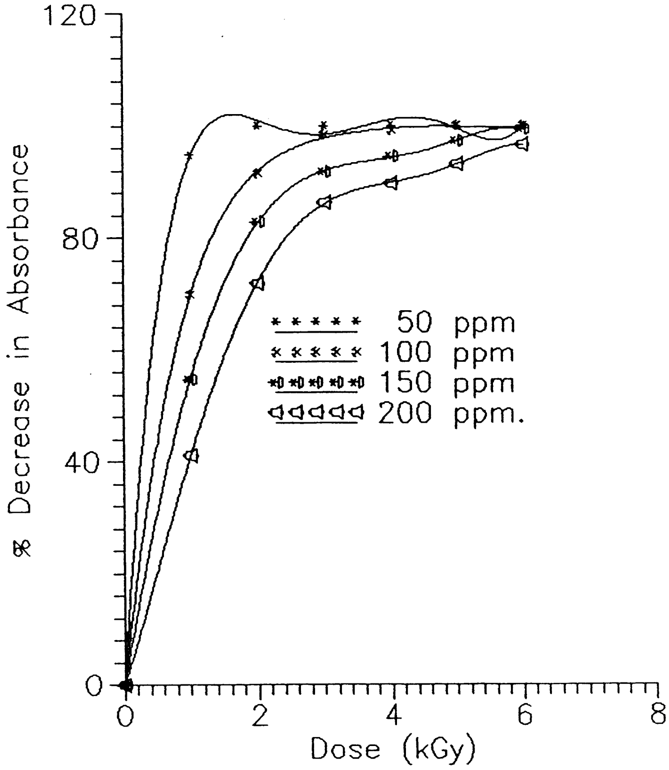

FIG 10. Degree of decolouration (%) vs. doses (kGy) of various concentrations of Basilen Brown P2R.

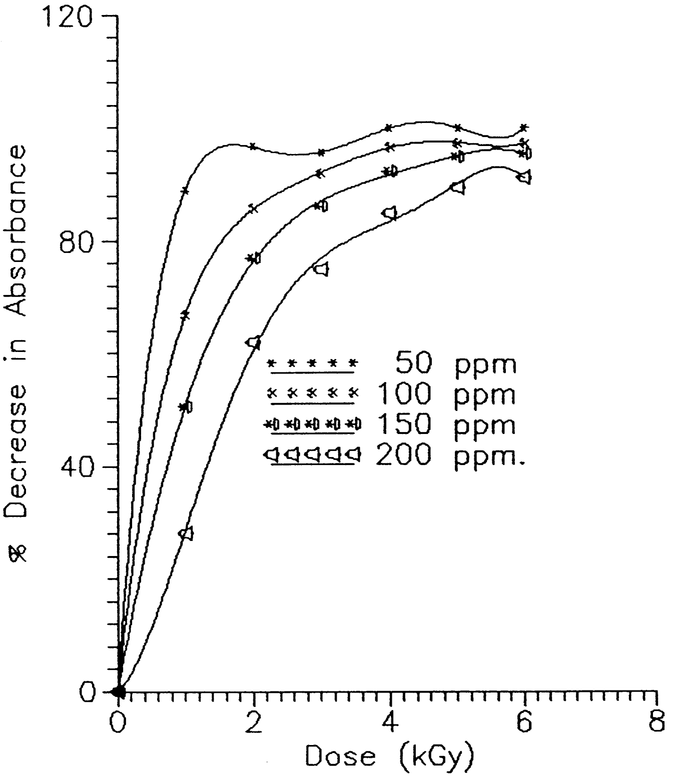

FIG. 11. Degree of decolouration (%) vs. doses (kGy) of various concentrations of Cibacron Violet 2R.

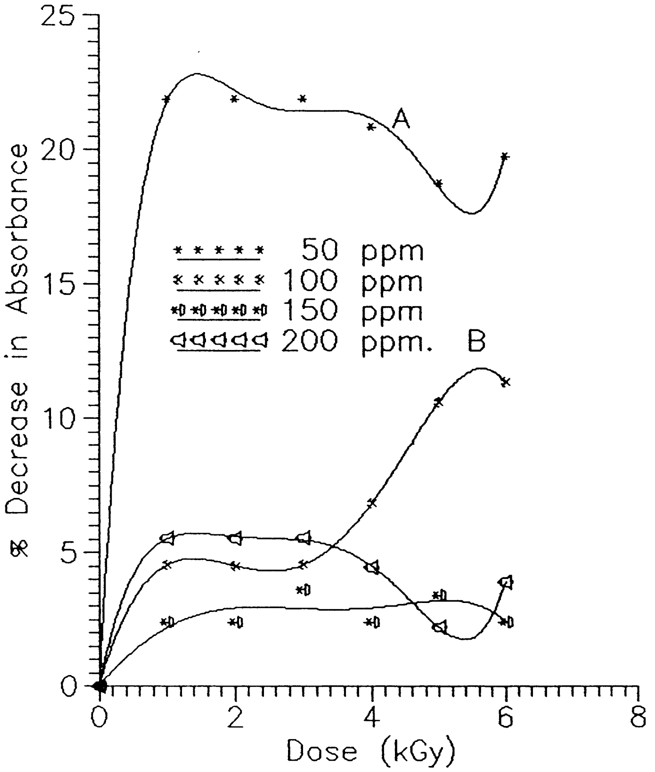

FIG 12. Degree of decolouration (%) vs. doses (kGy) of various concentrations of Acramin Green FB.

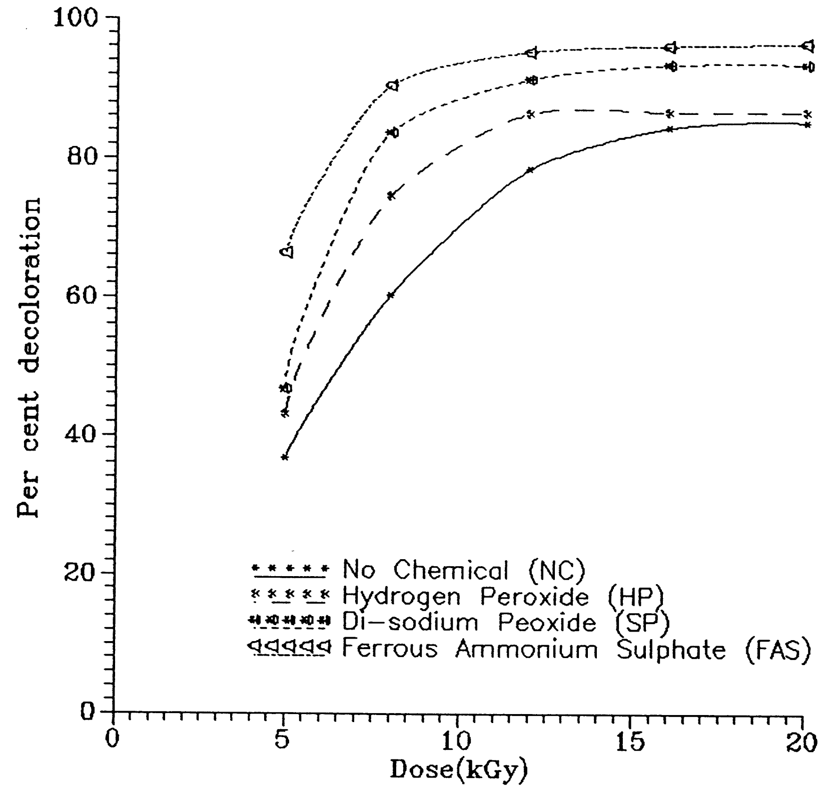

FIG. 13. Percentage decolouration of wastewater (GT.3) treated with irradiation in combination with chemicals.

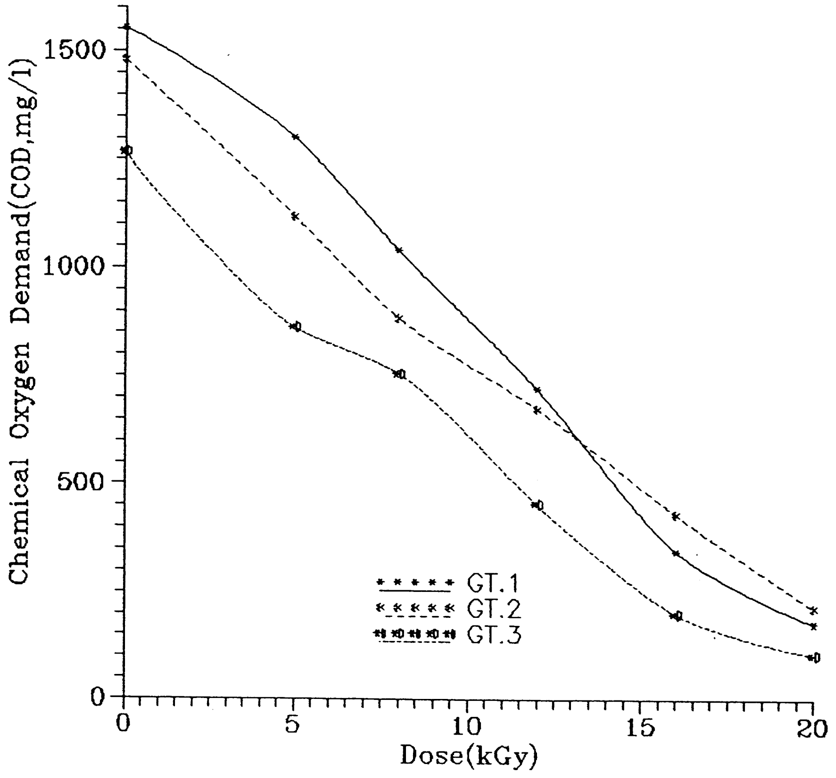

FIG 14. Change in chemical oxygen demand (COD, mg/l) of wastewaters GT. 1, GT. 2,ane GT. 3 with irradiation dose.

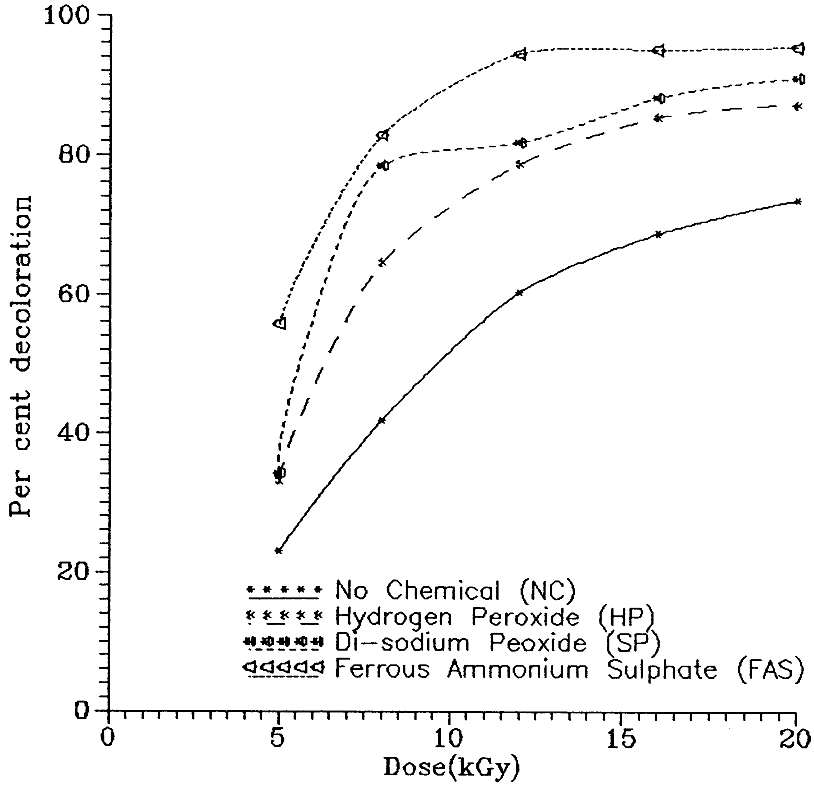

FIG. 15. Percentage decolouration of wastewater (GT.1) treated with irradiation in combination with chemicals.

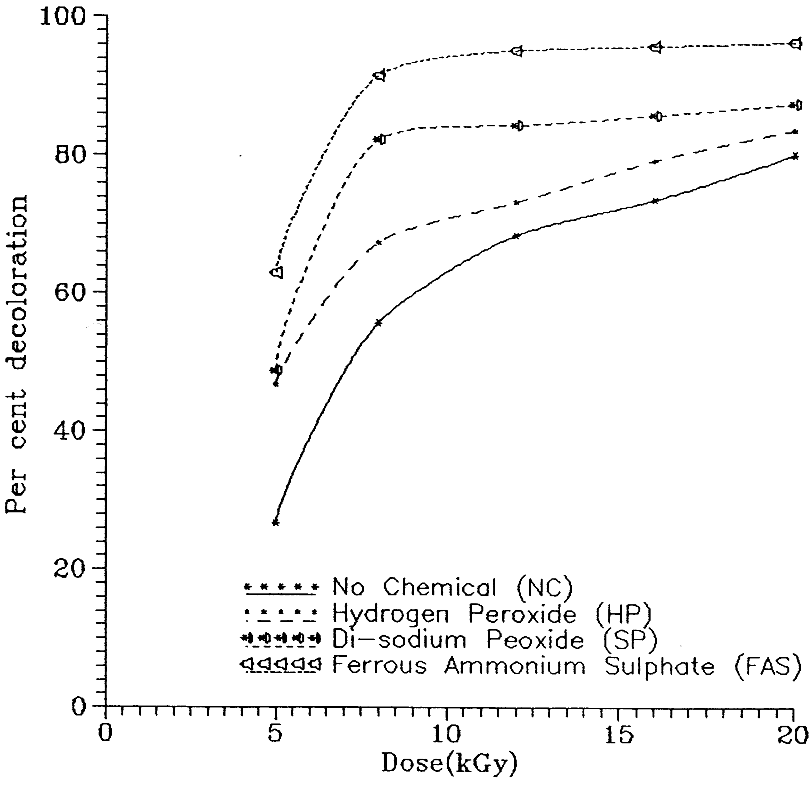

FIG 16. Percentage decolouration of wastewater (GT.2) treated with irradiation in combination with chemicals.

3.2. Effect on pH

In Figs 1–6 are presented changes in pH values with increase in irradiation dose for the dyes and pigment solutions. In all cases the pH decreased sharply after the first irradiation dose of 1 kGy. Thereafter, the pH values changed very slowly or remain constant with increase in irradiation dose. This suggests that organic acid compounds that were initially formed by destruction of the colour forming groups undergo further decomposition to smaller non-acidic molecules with increase in irradiation dose.

3.3. Degree of decolouration

The degree of decolouration of the dyes and pigment solutions with irradiation was estimated as the reduction in optical density at the characteristic wavelength where the absorbency was strongest. The results are presented in Figs 7–12. Decolouration was linear up to about 60 per cent for all the dye solutions. At the same irradiation dose, the lower the concentration of the dye solution, the higher decolouration was. For the pigment, only the solutions that have low concentrations showed some decolouration (Fig. 12). Solutions with high pigment concentration appeared not to be affected by irradiation. The pigment was largely present in the water in a separate phase. For this reason, its reactions with water radiolysis products were suppressed, and the pigment solution was observed to be stable to radiation in this study. Effect of gamma irradiation in combination with hydrogen peroxide, sodium peroxide and ferrous ammonium sulphate, respectively, on the colour of the wastewaters are shown in Figs 13–15. Hydroxyl radicals play very important role in radiation decomposition of organic pollutants in water [3]. In this study, therefore, hydrogen peroxide and sodium peroxide were used to introduce additional OH radicals into the wastewater during irradiation. Improved decolourations of the wastewaters were achieved, as expected, compared to using only irradiation. Disperse dyes and other similar pollutants present in wastewater are in separate phase and will not react with water radiolysis products [6]. To overcome this problem in our study, ferrous ammonium sulphate was added to the wastewaters before irradiation to precipitate any disperse organic pollutant. In this way a much improved decolouration was achieved for all the wastewaters used in this study. It was also observed that high irradiation dose (20 kGy) was involved to achieve 90 per cent decolouration of the wastewaters. This could be attributed to the high concentration of dyes, with some in disperse form, in the wastewater. Besides, it is also possible that other organic pollutants were competing with the water radiolysis products, especially the hydroxyl radicals produced in the wastewater.

3.4. Chemical oxygen demand

The oxidation effect of radiation on organic pollutants in wastewater was determined by measurement of COD values with irradiation. The results are presented in Fig. 16. It was observed that COD values of the wastewaters studied in this work decreased with increased irradiation dose. The decrease in COD values confirms the importance of oxidation in irradiation of wastewaters.

4. CONCLUSION

The potential of gamma irradiation for decolouration and decomposition of textile dyes and similar organic compounds in industrial wastewater in Ghana has been investigated. Complete decolouration of model aqueous solutions of soluble dyes was achieved with irradiation dose of 6 kGy. The irradiation dose required for maximum decolouration depended on the concentration of the solution. Decolouration of aqueous solution of pigment was not achieved by irradiation condition of this study. Improved decolouration of wastewaters from textile industries was achieved by gamma irradiation in combination with hydrogen peroxide, sodium peroxide and ferrous ammonium sulphate, respectively, compared to gamma irradiation alone. Ferrous ammonium sulphate used in combination with irradiation produced the best decolouration at any given irradiation dose. Irradiation promotes oxidation of organic compounds in the wastewaters. The higher the irradiation doses the more the oxidative effect and hence the higher the reduction in COD value of the wastewater.

ACKNOWLEDGEMENTS

The authors wish to thank the following textile industries in Ghana for supplying the dyes used in the preliminary work of this study: Freedom Textile Company Ltd, Akosombo Textile Company Ltd and Ghana Textile Manufacturing Company Ltd. These companies also approved collection of wastewater from their factories. We are also grateful to Messrs. M. Ofori-Appiah and B. Q. Modzinuh for their technical assistance.

REFERENCES

[1] VAN-ESS, A. Water bodies under threat from industrial pollution. Daily Graphic of Ghana No. 147432 (1998) 1 pp.

[2] GETOFF, N., LUTZ, W. Radiation induced decomposition of hydrocarbons in water resources. Radiat. Phys. Chem. **25** (1986) 21 pp.

[3] GETOFF, N., Decomposition of biological resistant pollutants in water by irradiation. Radiat. Phys. Chem. **35** (1990*)* 432 pp.

[4] NAGI, T., SUZUKI, N., Radiation-induced degradation of anthraquinone dyes in aqueous solution. Int. J. Appl. Radiat. Isotopes **27** (1976) 699 pp.

[5] GRAFT, T.E., EICHHOLTZ, G.G., Synergistic treatment of textile dye wastes by irradiation and oxidation. In. J. Appl. Radiat. Isotopes. **25** *(*1997) 543 pp.

[6] PIKAEV, A.K., et al., A combined electron-beam and coagulation method of purification of water from dyes. Mendeleev Commune. (1997) 176 pp.

[7] WOODS R.J., PIKAEV, A.K., Applied Radiation Chemistry: Radiation Processing. New York (1994) Wiley.

[8] Standard Methods for Examination of Water and Wastewater Chemical Oxygen Demand. M. A. H. Franson, 19th edn. American Public Health Association, Washington, DC (1995) 5220.

[9] GILLEN, A.E., STERN, E.S. An Introduction to Electronic Absorption Spectroscopy in Organic Chemistry, Arnold Ltd., Edward, London (1960).

[10] DEYER, J.R. Applications of Absorption Spectroscopy of Organic Compounds, Prentice-Hall, New Jersey, USA (1965).

RADIATION-INDUCED DEGRADATION OF ORGANIC POLLUTANTS IN WASTEWATER

A.N.M. Bagyo, W.A. Lindu, S. Sadjirun, E.K. Winarno,
E. Widayat, Aryanti, H. Winarno
Centre for the Application of Isotopes and Radiation,
National Nuclear Energy Agency,
Jakarta, Indonesia

Abstract. The degradation and decolouration of organic pollutants, i.e. dye stuffs and phenolic compounds, by gamma irradiation have been studied. First, samples from effluent of textile industry were taken to be irradiated at a certain condition. Irradiation was done after dissolving the samples five times with distilled water in laboratory scale, followed by upscaling those samples into 5 litre in volume. Irradiation was done at a dose of 0–25 kGy, aerated and a dose rate of 5 kGy/h. The parameters examined were the change of absorption spectra, COD (Chemical Oxygen Demand), the percentage of the degradation, the change of pH and degradation product using HPLC. It was demonstrated that the dilution of sample enhanced the degradation and decreased the COD values. The degradation product of textile wastewater is mainly oxalic acid.

Second, the effects of radiation on aerated phenolic compounds mixture, i.e. resorcinol, *o*-cresol and *m*-cresol were done. Individual phenol was studied followed by mixture of the phenolic compounds. Irradiation was done in aerated condition with doses of 0–10 kGy, dose rate of 5 kGy/h and pH range from 3 to 12. The initial concentration of resorcinol, *o*-cresol and *m*-cresol were 50 ppm and 60 ppm for phenolic compounds mixture, respectively. Parameters examined were absorption spectrum, pH, and degradation products. The uv-vis absorption of the solution were observed before and after irradiation. HPLC was used to determine the products of degradation. Degradation of resorcinol, *m*-cresol and *o*-cresol could be achieved at dose of 6 kGy at pH 9, while *o*-cresol in acid condition (pH 3). The degree of degradation for resorcinol, *m*-cresol and *o*-cresol at above conditions were 90%, 88% and 45%, respectively. Degradation of phenolic compound mixture occurred at a dose of 7.5 kGy and pH 9', at this condition almost 99% of phenolic compounds degraded. Oxalic acid was the main degradation product.

1. INTRODUCTION

Textile, oil and gas, which give important foreign exchange, are exported from Indonesia. On the other hand the activity of oil production and textile industry causes pollution into the environment. Wastewater released by those industries contains toxic refractory dye stuffs at high concentration. They will go into the environment and contaminate the surface of the water and the water itself. A conventional method was used for decolouration and degradation of such dyes and for removal of phenols, but improvement has not been reached yet since the method is still releasing some amount of sludge [1-2].

Environmental Management Control (EMC) Jakarta reported that decolouration of colouring wastewater was still difficult to be solved, so that the use of another method was necessary.

Some researchers reported that radiation induced decolouration and degradation of disperse, acid and reactive dyes as well as phenolic compounds, so that radiation technology could be an alternative method to solve the problem [3–10]. Investigations were done to at certain conditions, followed by the study of the degradation product using HPLC.

2. EXPERIMENTAL

2.1 Materials

2.1.1. Dyes wastewater

Samples of dyes waste-water were taken from the effluent of the textile industry of PT Unitex, Bogor, Indonesia. Samples were numbered from E to H, and kept in 5 L plastic jars.

2.1.2. Phenolic compounds

Phenols used in this study were standard phenols, i.e. *o*-cresol, *m*-cresol and resorcinol. A study on phenolic compounds was done individually, followed by a mixture of *o*-cresol, *m*-cresol and resorcinol. Others chemical substances used were H_2SO_4, NaOH, and H_3PO_4.

2.2. Sample preparations

2.2.1. Samples E-H

Samples E-H were prepared by dissolving the samples five times with distilled water. The samples were irradiated at a dose of 0–25 kGy with cobalt-60 γ rays at room temperature and placed in 500 mL Pyrex reaction vessel (5 cm dia. and 16 cm height). The dose rate of 5 kGy/h was determined by a Fricke dosimeter. During irradiation air was bubbled. Parameters examined were absorption spectra, COD and percentage of degradation.

2.2.2. Upscaling of samples E and F

Irradiation of samples E and F was done by dissolving the samples five times with distilled water. Irradiation was carried out in a 5 L stainless steel reaction vessel (15 cm dia. and 40 cm height), at a dose of 0–25 kGy and dose rate of 5 kGy/h. Parameters examined were the change of pH and degradation products.

2.2.3. Phenolic compounds

For individual phenol (*o*-cresol, *m*-cresol and resorcinol), irradiation was done at a concentration of 50 ppm with doses of 0, 2, 4, 6, 8 and 10 kGy. The dose rate used in this study was 5 kGy/h, determined by using a Fricke Dosimeter. Irradiation was also done at several pHs (3, 5, 7, 9 and 12) with the same doses as above. During irradiation air was bubbled through the solution. The degree of degradation of individual phenols was measured and the change of spectrum examined.

Degradation studies of the mixture of *o*-cresol, *m*-cresol and resorcinol were done at a concentration of 60 ppm. Irradiation was done at doses of 0, 5, 7.5, 10, 15 and 20 kGy, and various pHs 3, 5, 7, 9 and 11. During irradiation air was bubbled through the solution. Parameters examined were the changes of spectrum and pH, degree of degradation and degradation products. The absorption spectrum was measured with a Hewlett Packard 8453 spectrophotometer. The pH of the solution was measured using Metrohm pH-meter. The degradation product was measured using HPLC using a Shodex RS-pak.

3. RESULTS AND DISCUSSION

3.1. Dye wastewater

Figs 1– 4 show the spectra of samples E, F, G and H, respectively. It is shown that two absorption peaks were detected at uv and visible regions. The absorption band in the uv region is considered to be their substituted aromatic rings and the absorption band in the visible region is considered to be the main absorption assigned to the conjugated system of dye molecules. The peak in the visible region decreased rapidly, but that in the uv region decreased slowly as dose increased. These decreases in intensity are obviously due to the destruction of the conjugated system of dye molecules by attack of OH radicals, just as in the case of water-soluble azo dyes (7). The intensity in the uv region decreased slowly, because substituted aromatic rings has high persistence to radiation. Persistence is obviously due to the π-electrons which are delocalized. In the presence of oxygen during irradiation the oxidative species will be increased. These species will degrade the structure of the dye molecule in wastewater.

The reaction is as follows :

$H^{\bullet} + O_2 \longrightarrow HO_2^{\bullet}$
$e_{aq}^{-} + O_2 \longrightarrow O_2^{\bullet-}$
$O_2^{\bullet-} + H^{+} \longrightarrow HO_2^{\bullet}$
$HO_2^{\bullet} + HO_2^{\bullet} \longrightarrow H_2O_2 + O_2$

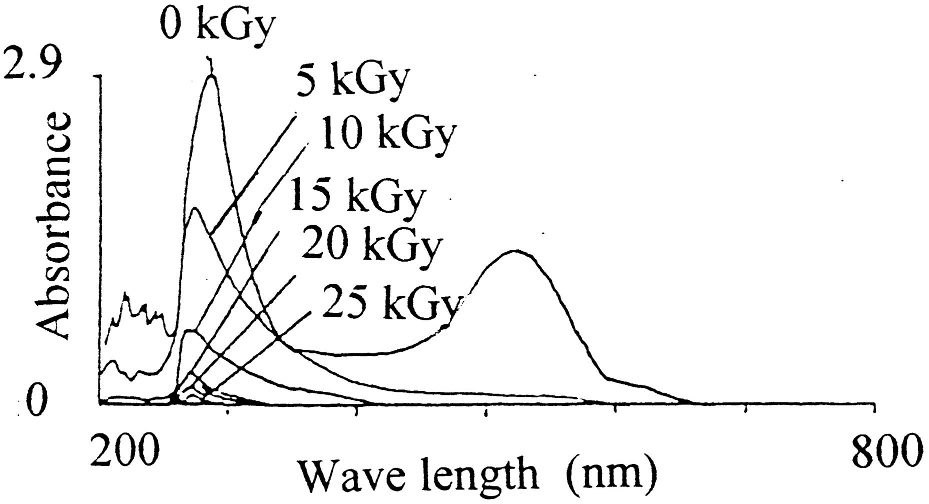

FIG. 1. Spectrum of sample E.

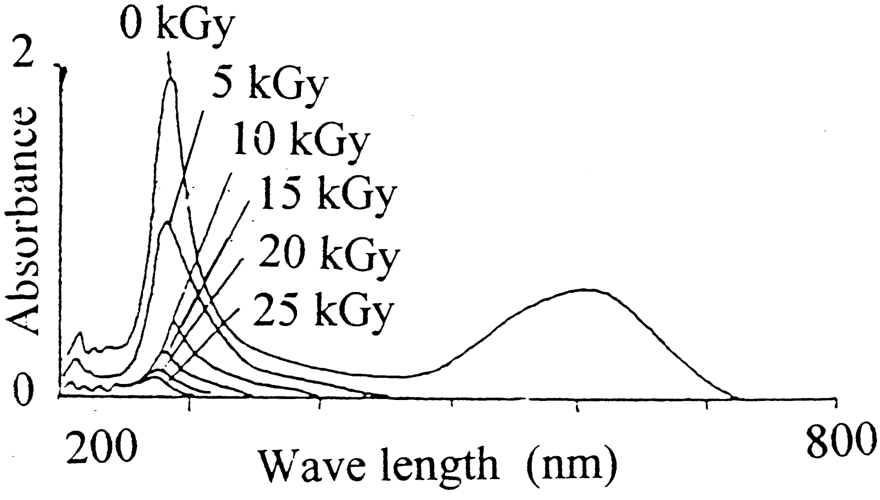

FIG. 2. Spectrum of sample F.

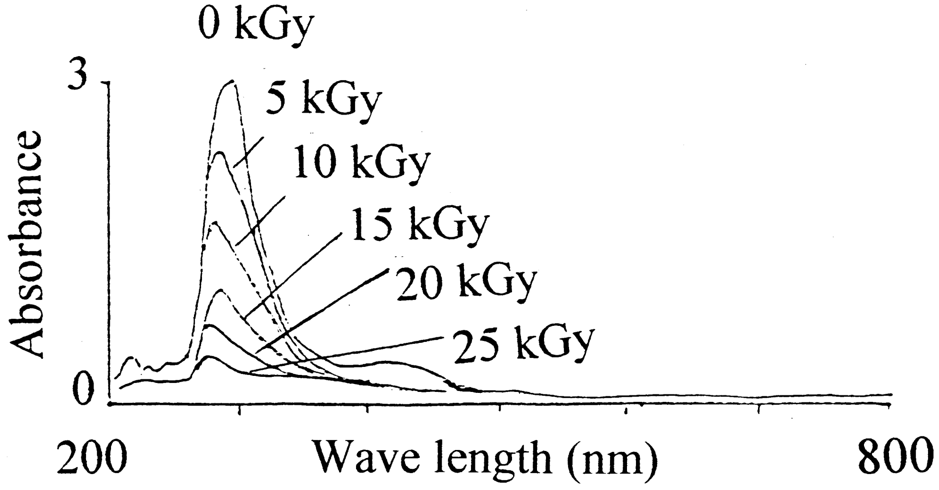

Fig. 3. Spectrum of sample G.

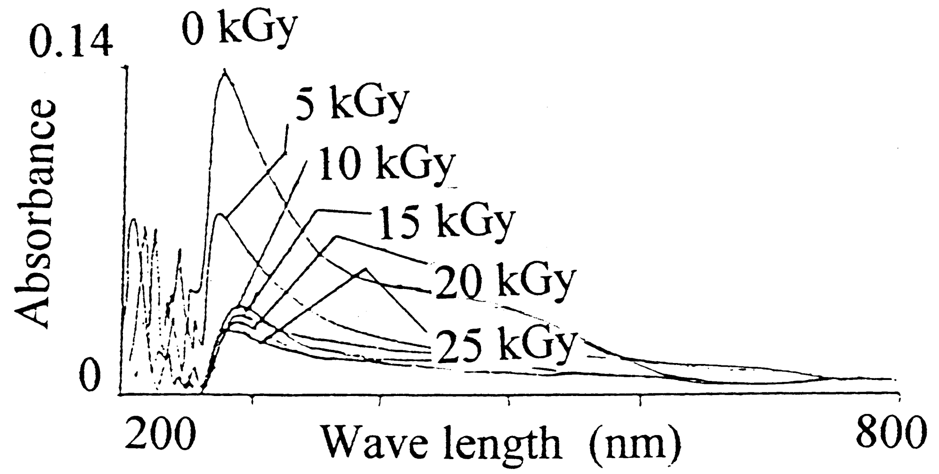

FIG. 4. Spectrum of sample H.

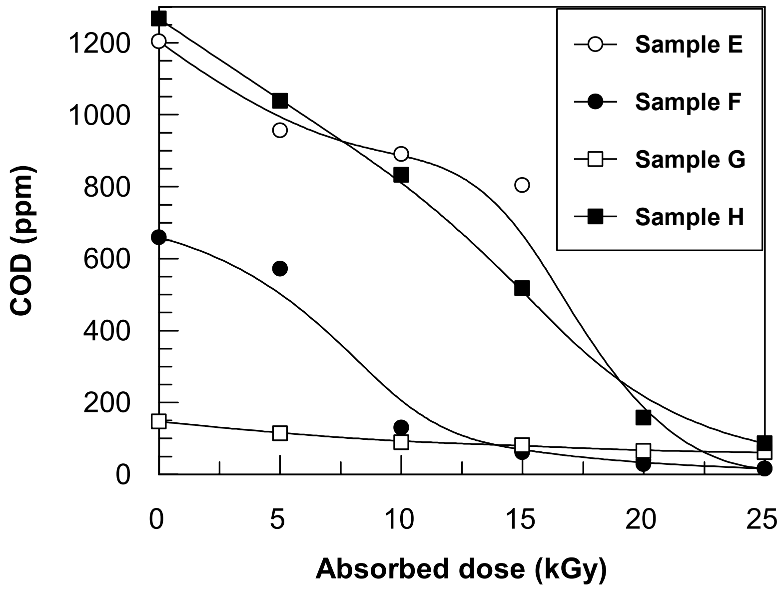

FIG. 5. The COD measurement of samples E-H.

The COD measurement of samples E, F, G and H are shown in Fig. 5, the COD value of sample E, F, G and H decreased after irradiation at a dose of 25 kGy from 1204, 658, 147, 1267 ppm into 16.3, 16.5, 61.2 and 86.9 ppm, respectively. COD measurement is one of the important parameters usually used in wastewater treatment. The decrease of COD upon irradiation indicated that samples have already degraded.

The degree of degradation of samples E-H are shown in Fig. 6. At a dose of 20 kGy, almost all of the samples degraded by more than 80%. It can be estimated from the results that samples have degraded.

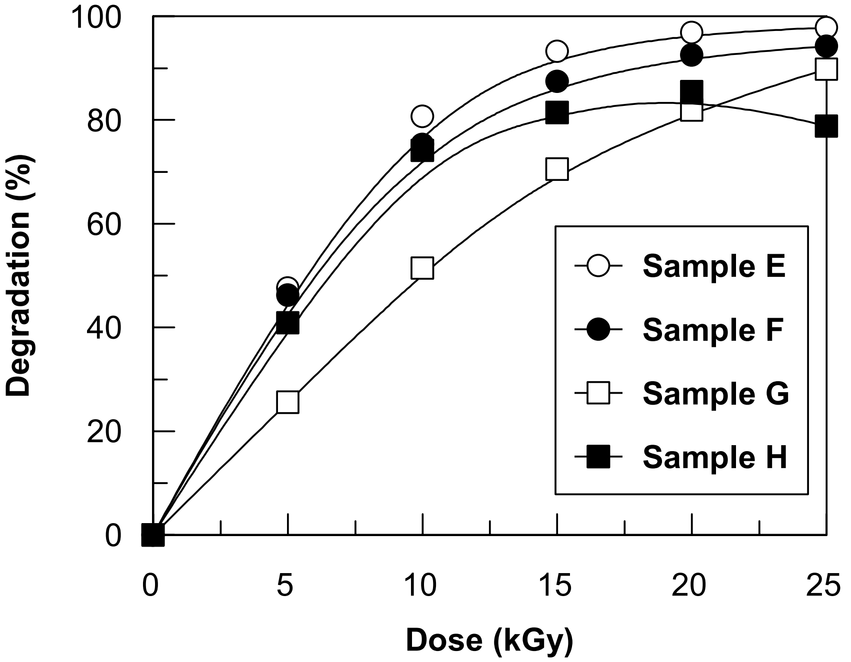

FIG. 6. The degree of degradation of sample E-H.

3.2. The change of pH after irradiation of upscaling of samples E and F

The pH of samples E and F after irradiation are shown in Fig. 7. The pH was slightly decreased; the change in pH indicated that the dye molecules are degraded to lower molecular weight compounds such as organic acids [7].

3.3. Analysis of degradation product of samples E and F

Figures 8 (a) and (b) show the chromatogram of samples E and F after irradiation at a dose of 5 kGy and 20 kGy, respectively. Figure 9 shows the chromatogram of oxalic acid standard. By matching the retention time of the samples with the standard acid it could be seen that the main product of samples E and F is oxalic acid.

The suggested mechanisms of oxalic acid formation proposed by Spadaro et al and Nickelsen et al. in their reports [11, 12], are shown in Figs 10 and 11. Spadaro proposed probable mechanism for benzene formation in the $^{\bullet}$OH mediated degradation of azo dyes. The resulting OH adduct would break down to produce phenildiazene and a phenoxy radical. Phenildiazene is extremely unstable and is further oxidized into benzene as the final compound. The phenoxy radical would be oxidized into CO_2. Nickelsen proposed the oxidation of benzene into carboxilic acids, such as oxalic acid, through the formation of mucondialdehyde.

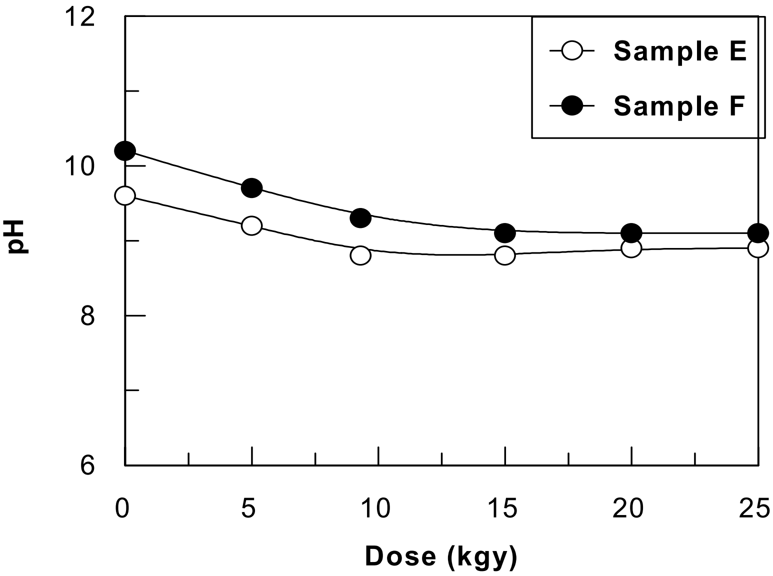

FIG. 7. The change of pH after irradiation of samples E and F.

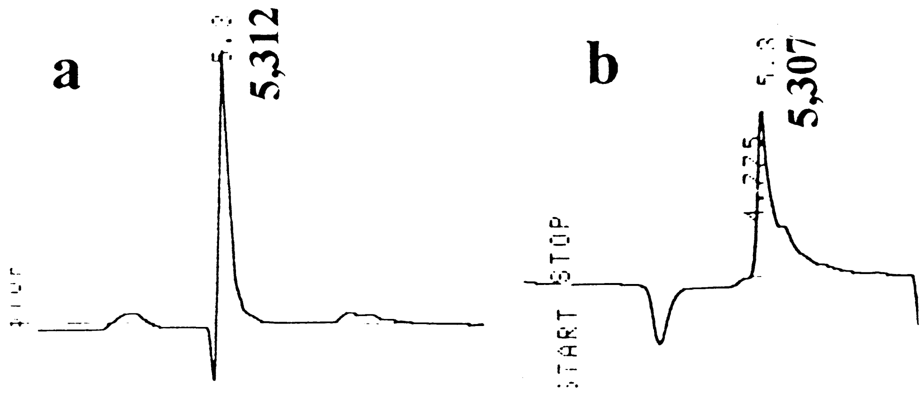

FIG. 8(a). The chromatogram of irradiated sample E (5 kGy);
(b). The chromatogram of irradiated sample F (20 kGy).

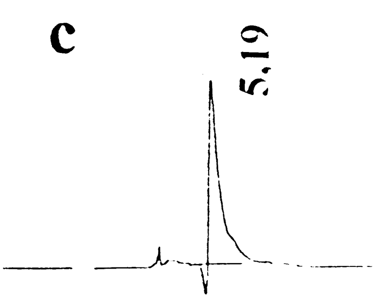

FIG. 9. The chromatogram of oxalic acid standard.

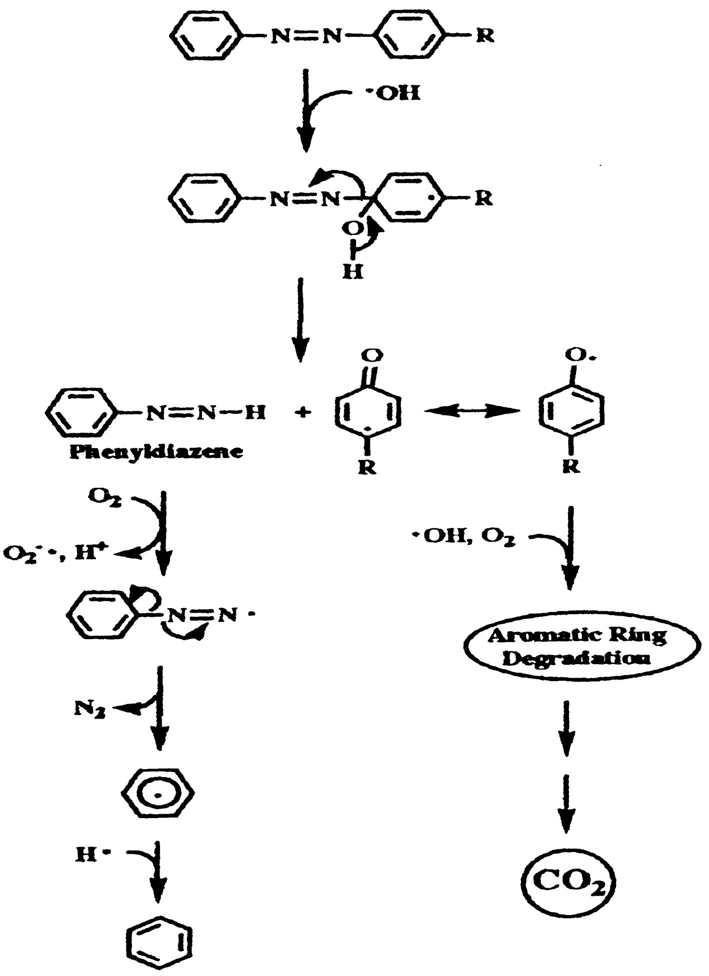

Scheme 1

FIG. 10. The formation of benzene from azo dye.

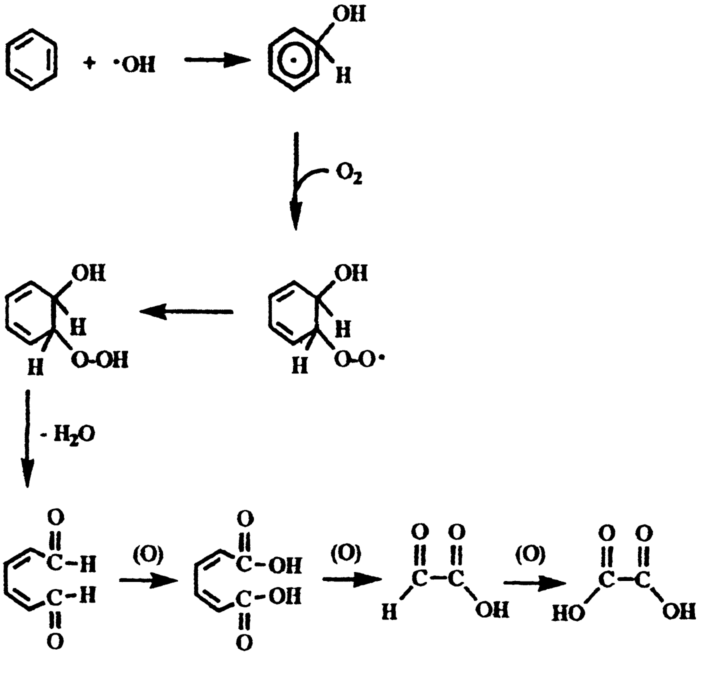

Scheme 2

FIG. 11. The formation of oxalic acid from benzene.

3.4. Measurement of absorption spectra of individual phenol

The absorption spectra of the unirradiated resorcinol, *o*-cresol and *m*-cresol in aerated system showed strong absorption bands in the uv region, namely at 275 nm for resorcinol and 272 nm for *o*- and *m*-cresol. (Figs 12, 13 and 14). It is also shown that the absorption bands of resorcinol, *o*-cresol and *m*-cresol increased at doses of 2 kGy and 4 kGy, respectively, but gradually decreased at higher doses. The results suggested that increase in absorption was caused by the formation of polymer. At low dose, energy is just enough to form polymer molecule structure [8]. The absorption intensity of *o*-cresol decreased by 80% at a dose of 10 kGy. Many factors caused the radiation induced phenol degradation, such as substrate, concentration, applied dose rate, availability of dissolved oxygen, etc. Further investigation on this topic should be done in the future work.

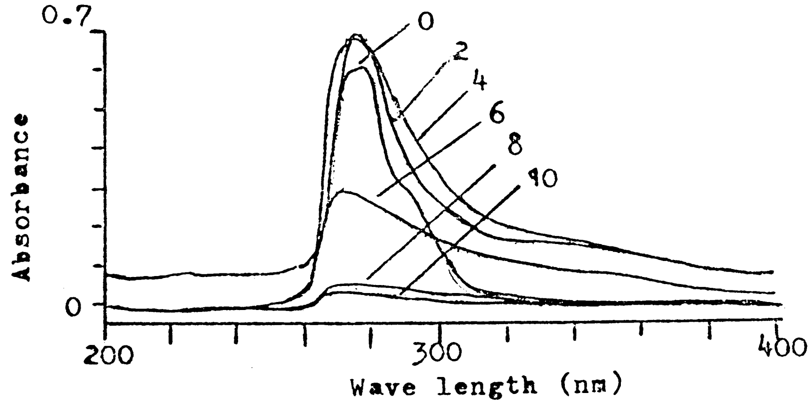

FIG. 12. The spectra changes of aerated resorcinol solution by irradiation. Figures 0, 2, 4, 6, 8 and 10 represent the dose in kGy.

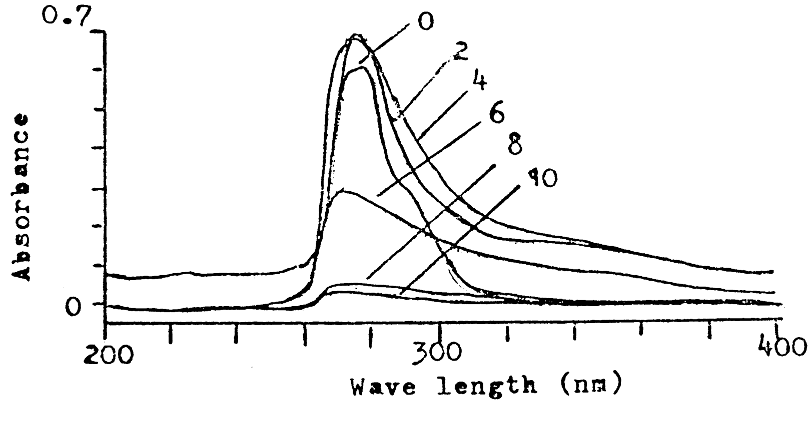

FIG. 13. The spectra changes of aerated o-cresol solution by irradiation. Figures 0, 2, 4, 6, 8 and 10 represent the dose in kGy.

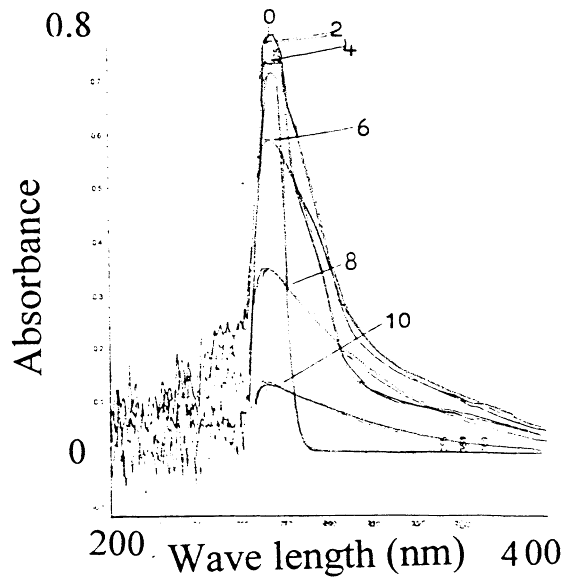

FIG. 14. The spectra changes of aerated m-cresol solution by irradiation. Figures 0, 2, 4, 6, 8 and 10 represent the dose in kGy.

3.5. Effect of pH on the radiolysis of phenolics solution

As shown in Figs 15 (a) and (b), degradation of phenolic compounds increased at various pHs with increasing doses. These increases were obviously due to the high intensity of the primary product that forms from the radiolysis of water, especially the oxidator species. The population of oxidator species increased because air was bubbled through the solution during irradiation. The results showed that resorcinol was the most degradable compound; it is assumed that the structure of the molecule has already changed.

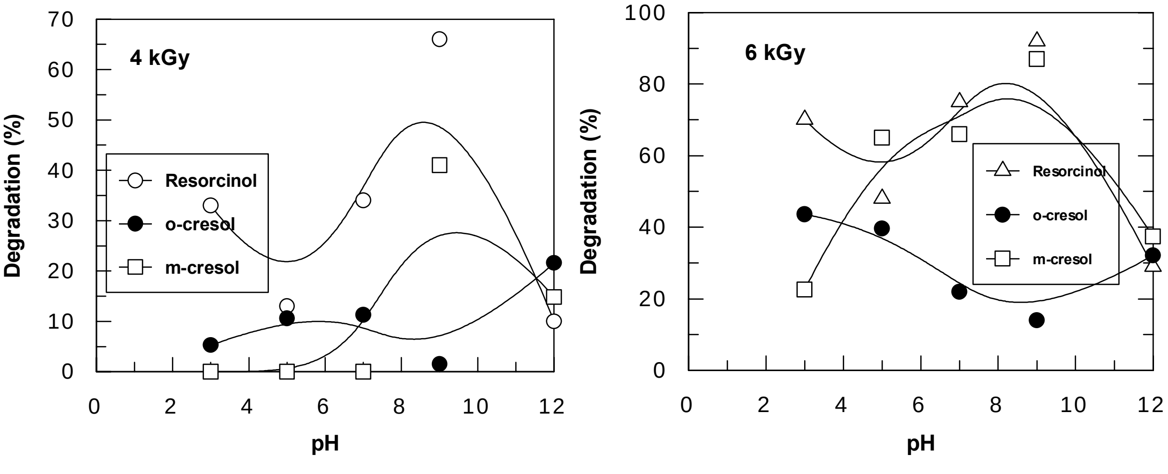

FIG. 15. Effect of pH on the degradation of phenolic compounds; (a) 4 kGy and (b) 6 kGy.

The change of the molecule structure of resorcinol and m-cresol might occur at higher pH and induce less degradable compounds. On the other hand, the pH solution hardly affected the degradation of *o*-cresol.

3.6. Effect of pH on spectrum change of phenolic compounds mixture.

The spectra of phenolic compounds mixture at pH 3, 7 and 11 are shown at Figs 16, 17 and 18, respectively. The phenolic compound mixture at pH 3 and 7 showed strong absorption at 273 nm; in general the spectra at all pHs decreased as dose increased.

At acid condition (pH 3) the spectrum intensity of unirradiated phenolic mixture increased slightly, compared with that at pH 7. It is suggested that hyperchromic effect occurred after the addition of H2SO4 to adjust the pH.

At basic condition (pH 11), the spectrum intensity of unirradiated phenolic mixture increased considerably, and the absorbency shifted from 273 nm to 289 nm. The results suggest that hyperchromic effect and bathochromic shift occurred. The shift of the absorbency indicated a change of the molecule structure of phenolic compound mixture.

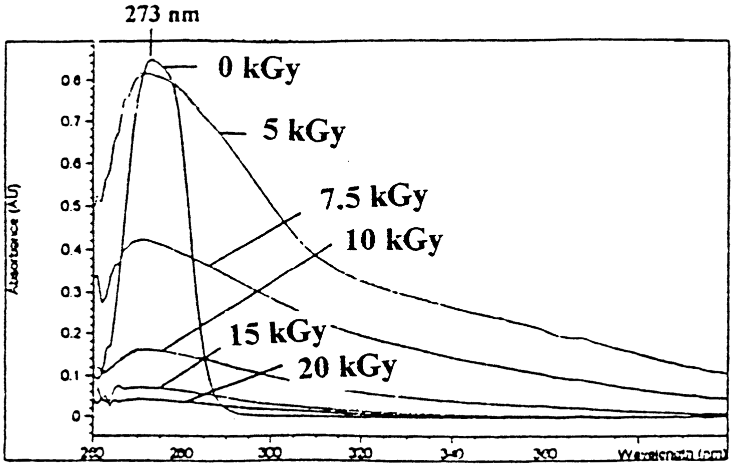

FIG. 16. The spectrum of phenolic compound mixture at pH 3.

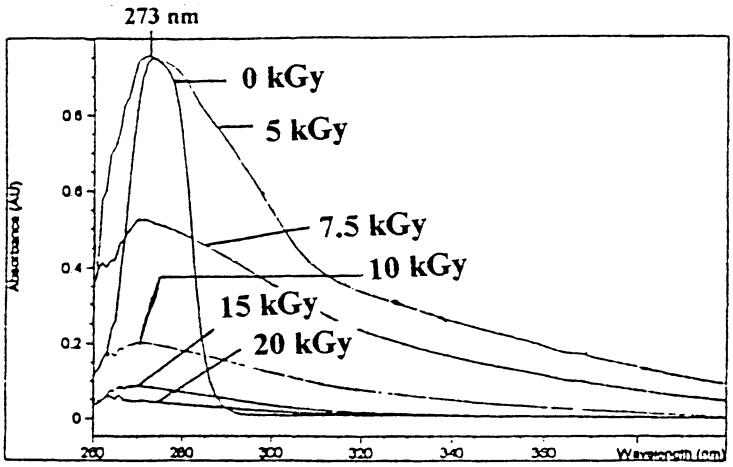

FIG. 17. The spectrum of phenolic compound mixture at pH 7.

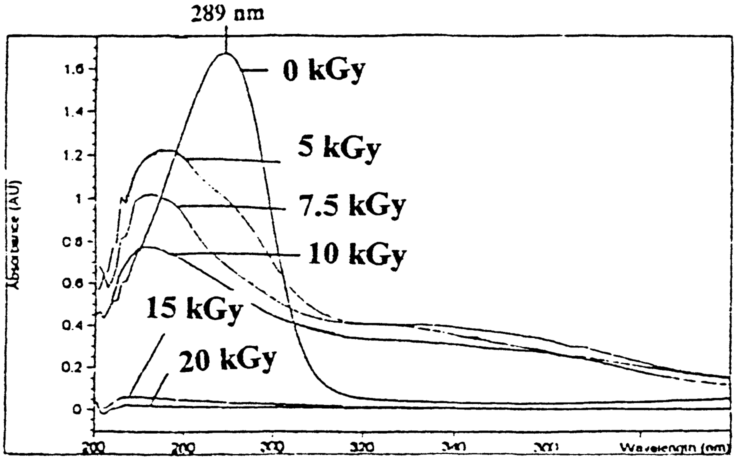

FIG. 18. The spectrum of phenolic compound mixture at pH 11.

3.7. Effect of pH on the radiolysis of phenolic compounds mixture solution

Figure 19 shows the effect of pH on the radiolysis of phenolic compound mixture. The increase of the remaining phenol at pH 3–7 with a dose of 7.5 kGy indicated that the structure of the molecule has already changed thus induced less degradable compounds. The remaining phenol at pH 9 is 0.53 ppm; it means almost 99% of the phenol has degraded. At a high dose (15 kGy) the remaining phenol is only 0.39 ppm; it is indicated that phenolic compounds has degraded completely at that condition.

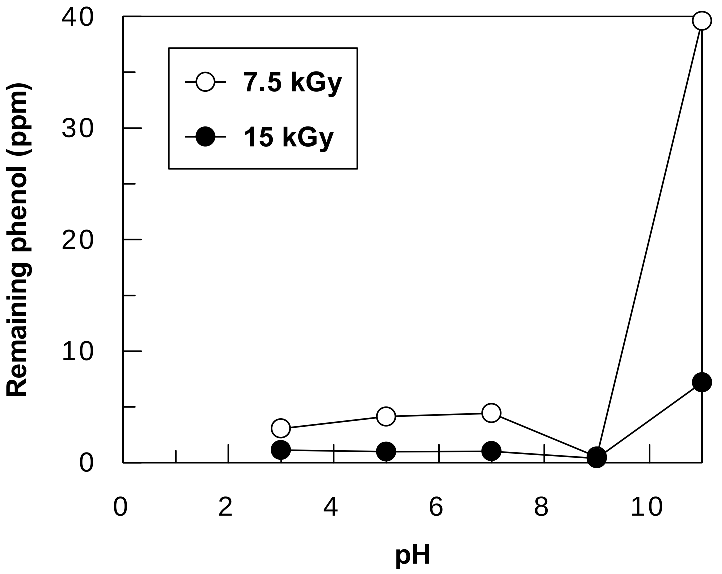

FIG. 19. Effect of pH on radiolysis of phenolic compounds mixture.

3. 8. Change of pH after irradiation

The change of pH after irradiation could be seen in Fig. 20. In the beginning pH lowered steeply at all pHs with the exception of pH 11. The change in pH was caused by the formation of organic acids. The formation of organic acids indicated that the structure of the molecule already degraded into low molecular weight. Degradation of the phenolic molecules is induced by the reaction with oxidative species formed due to water radiolysis.

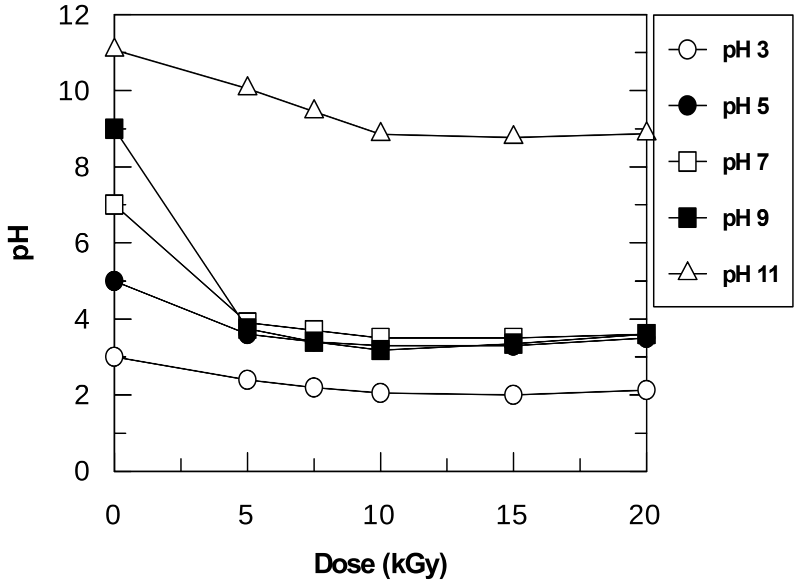

FIG. 20. The change of pH after irradiation.

3. 9. Analysis of degradation products

The degradation products of phenolic mixture compounds were measured using HPLC with Shodex RS-pak column. Determination of acidic compounds were compare with that acidic standard (oxalic acid). The retention time of degradation products of phenolic mixture compounds is exactly the same as the retention time of oxalic acid standard. Figs. 21 (a) and (b) show the spectrum of degradation products of phenolic compounds after irradiation at a dose of 20 kGy and a standard of oxalic acid. It is assumed that the degradation product of phenolic compounds was mainly oxalic acid.

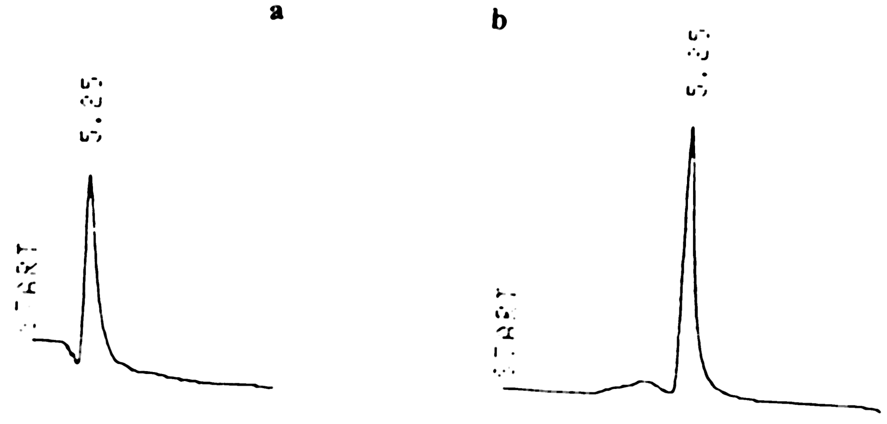

(a) (b)

FIG. 21 (a). Chromatogram of irradiated phenolic mixture compounds at a dose of 20 kGy; (b). Chromatogram of oxalic acid (5,25 min).

4. CONCLUSIONS

Radiation induced decolouration and degradation of textile dyes stuff and phenolic compounds were demonstrated. Degradation of textile dyes stuff could be carried out but the necessary dose varies with the type of waste. In general, irradiation of textile wastewater after dilution can be done. At this condition the COD value, pH and degree of degradation decreased. The main product of degraded wastewater was oxalic acid.

Degradation of resorcinol, o-cresol and m-cresol could be achieved at a dose of 6 kGy at pH 9, while o-cresol is in acid condition (pH 3) and aerated. The degrees of degradation for resorcinol, o- and m-cresol at this condition were 90%, 88% and 45%, respectively.

Radiation degradation of phenolic compound mixture could be carried out in aerated system. The best degradation of phenolic mixture could be achieved at a dose of 7.5 kGy and pH 9; at this condition almost 99% of phenolic compounds was degraded. The main product of degraded phenolic compounds was oxalic acid.

ACKNOWLEDGEMENTS

This work was partly supported by the International Atomic Energy Agency under the research contract grants RC 8801/RO. The authors are grateful to PT Unitex Bogor, Indonesia for their valuable help. Thanks are also due to Ms. Christina T.S., Mr. Armanu, Mr. Syurhubel and Mr. Firdaus for their technical assistance as well as to the members of the irradiation facility of CAIR.

REFERENCES

[1] GETOFF, N., Radiation-Induced Degradation of Water Pollutants-State of the Art., Radiat. Phys. Chem. **47** (1996) 581 pp.

[2] LIN, K., COOPER, W.J., NICKELSEN, M.G., KURUCZ, C.N., WAITE, T.D., Decomposition of aqueous solutions of phenol using high energy electron beam irradiation - a large scale study, Appl. Radiat. Isot. **46** (1995) 1307 pp.

[3] HOSONO, M., ARAI, H., AIZAWA, M., YAMAMOTO. I., SHIMIZU, K., SUGIYAMA, M., Decolouration and degradation of azo dye in aqueous solution, Appl. Radiat. Isot. **44** (1993) 1199 pp.

[4] BAGYO, N.M.A., ANDAYANI, W., SADJIRUN, S., Radiation induced degradation and decolouration of disperse dyes in water, Env. Appl. of Ionizing Radiat. (COOPER, W.J., CURRY, R.D. and O'SHEA, K., Eds.) (1998) 507 pp.

[5] BAGYO, N.M.A., LINDU, W.A., WINARNO, H., WINARNO, E.K., WIDAYAT, E., SOEBIANTO, Y.S., Radiolysis of reactive azo dyes in aqueous solution. (International Symposium on Environmental Engineering, Korea, September, 1997) (to be published).

[6] BAGYO, N.M.A., ARAI, H., MIYATA, T., Radiation induced decolouration and sedimentation of colloidal disperse dyes in water, Appl. Radiat. Isot. **48** (1997) 175 pp.

[7] SUZUKI, N., NAGAI, T., HOTTA, H., WASHINO, M., The radiation induced degradation of azo dyes in aqueous solutions, Int. J. Appl. Radiat. Isot. **26** (1975) 726 pp.

[8] HASHIMOTO, S., MIYATA, T., KAWAKAMI, W., Radiation induced decomposition of phenol in flow system, Radiat. Phys. Chem. **16** (1980) 59 pp.

[9] HASHIMOTO, S., MIYATA, T., WASHINO, M., KAWAKAMI, W., A liquid chromatography study on the radiolysis of phenol in aqueous solution., Env. Sci. Tech, **13** (1979) 71 pp.

[10] TAKEHISA, M., ARAI, H., ARAI, M., MIYATA, T., SAKUMOTO, A., HASHIMOTO, S, NISHIMURA, K., WATANABE, H., KAWAKAMI, W., KURUYAMA, I., Inhibition of Trihalomethane formation in city water by radiation-ozone treatment, Radiat. Phys. Chem. **25** (1985) 63 pp.

[11] SPADARO, J.T., ISABELLE, L., RENGANATHAN, V., Hydroxil radical mediated degradation of azo dyes: evidence for benzene generation, Env. Sci. Tech. **28** (1994) 1389 pp.

[12] NICKELSEN, M.G., COOPER, W.J., Removal of benzene and selected alkyl-substituted benzene from aqueous solution utilizing continuous high energy irradiation, Env. Sci. & Tech. **26** (1992) 144 pp.

RADIATION HYGIENIZATION OF RAW SEWAGE SLUDGE

M.R. Shah, D.S. Lavale, K. P. Rawat, P.G. Benny, A.K. Sharma,
G.R. Dey, V. Bhave
Bhabha Atomic Research Centre,
Isotope Division, Mumbai,
India

Abstract. Radiation treatment of municipal sewage sludge can achieve resource conservation and recovery objectives. The liquid sludge irradiator of Sludge Hygienization Research Irradiator at Baroda (India) was operated for generating data on treatment of raw sludge containing 3-4 % solids. The plant system was modified for irradiating raw sludge without affecting basic irradiator initially designed to treat digested sludge. Hourly samples were analysed for estimation of disinfection dose requirement. Sand separated from the sludge was used as in-situ dosimeter by making use of its thermoluminescence property. Investigations are being carried out for regrowth of Total Coliforms in the sludge samples from this irradiator. Possibility of inadequate treatment due to geometric configuration of irradiator is being checked.

1. INTRODUCTION

Production of municipal wastewater and sludge has reached alarming dimensions with the growth of urban population all over the world. Conventional methods of separation and biological treatment of sludge allow its return to environment by disposal in ocean or landfill. Several technologies such as heat pasteurization, lime application, prolonged storage, composting and curing are recommended to achieve additional inactivation of microorganisms beyond that attainable by conventional sludge stabilization methods [1].

Conventional methods for treatment of wastewater are directed towards removal of pollutants with the least effort. Primary treatment includes screens, grit chambers, gravity sedimentation and chemical precipitation. Secondary treatment is designed to remove colloidal and soluble organics through biological treatment. Aerobic and/or anaerobic digestion processes are carried out in lagoons, trickling filters, activated sludge systems, closed anaerobic digestor tanks and other similarly large equipment [2].

Wastewater and sludge treatment plants use sedimentation and biological stabilization mainly to save energy and running costs. Depending on climatic conditions, problems of growth of algae and aquatic weeds, mosquito breeding, release of obnoxious gases, etc. are associated with the conventional plants. The sludge requires stabilization even after anaerobic digestion. Composting, heat pasteurization or incineration is employed and the inert product is then returned to the environment by way of landfill or ocean dumping.

Municipal sewage sludge is a very rich source of plant nutrients and soil conditioners. Land spreading can become popular in agricultural areas. Nutrient release with sludge is slower than with chemical fertilizers, allowing the nutrient to become available as the crop needs it. The sewage sludge makes an excellent soil conditioner because the humus material provides a good matrix for root growth, while nutrient release is in a right combination for optimal plant growth. Land spreading of sludge requires careful application. Soil microbes will assist in further stabilization of organics. Its reuses are beneficial as energy and nutrients are becoming scarcer [2].

Radiation treatment of sludge reduces pathogenic bacteria to a safe level. It also oxidizes toxic and hazardous organic chemicals [3]. It reduces odour nuisance. The treatment of sludge is achieved in simple, efficient and reliable way with radiation equipment.

Studies undertaken for disinfecting raw sludge with radiation at SHRI Facilities, Baroda would provide useful data as to utilize radiation technology for environmental conservation.

2. SCOPE AND OBJECTIVES OF THE RESEARCH PROJECT

The programme of work under this CRP was specified initially, as follows:

- modification of irradiation plant in order to irradiate raw sludge (3-4 % solid);
- irradiation at different conditions and determination of chemical and microbiological change in sludge;
- analysis and comparison of data with irradiation of digested sludge.

Further research work was assigned in extended projects, as follows:

- collection of more data on the seasonal variations of coliforms to arrive at the required dose for hygienization;
- study of regrowth of bacteria in detail, possibility of inadequate treatment due to geometric configuration of source and attached piping system will be checked;
- post irradiation treatment techniques such as; inoculation of useful bacteria with irradiated sludge and/or irradiation followed by rapid dewatering will be employed;
- combined action of radiation and sensitizers such as oxygen, hydrogen peroxide, heat will be investigated.

The programme goals should be directed to establish the following [4]:

- optimal combination treatment for wastewater and sludges;
- effects of dose rates on decontamination efficiency;
- dosimetric procedures;
- technological and economic parameters.

3. SPECIFICATIONS OF SHRI IRRADIATOR, BARODA (INDIA)

With the aim of demonstrating appropriate radiation technology for treating the entire sludge generated from the 5 MGD (22000 m^3/d or 22 ML/d) conventional municipal treatment plant, the facility was set-up by the Isotope Division of the Bhabha Atomic Research Centre in collaboration with M.S. University of Baroda, Gujarat Water Supply & Sewerage Board and Municipal Corporation of Baroda. The main technical specifications of the SHRI Facility were the following:

— sludge treatment capacity (max.)	110 m^3/d
— maximum ^{60}Co activity	18.5 PBq (500 kCi)
— biological shield capacity	37 PBq (1000 kCi)
— treatment dose	Variable 0.5–5 kGy (50-500 kRad)

Sludge Hygienization Research Irradiator (SHRI) Facility is integrated with the existing conventional plant serving a population of about 0.3 million inhabitants. Since its commissioning in 1990, with an initial charge of 5.5 PBq of ^{60}Co, the plant is continuously in operation and working smoothly. Current ^{60}Co source strength is about 1.76 PBq, which corresponds to the processing rate of approximately 10 m^3/d of sludge.

Sludge Hygienization Research Irradiator (SHRI) Facility is integrated with 5 MGD (22000 m^3/d or 22 ML/d) conventional plant. Since it's commissioning in 1990, it is in daily operation and working smoothly.

4. RAW MATERIAL CHARACTERIZATION

Raw sludge from the primary sedimentation tank of the conventional treatment plant is drawn to SHRI for experiments. The circular conical bottom 150 ft dia tank receives raw sewage after screens and grit chamber. The solid content in the settled sludge drawn from the bottom was found to vary between 2 to 7 % by weight. Non-homogenized fibrous material and other floating particulate matters were also allowed to mix with this sludge. Raw sludge is associated with the presence of foul odour due to high content of volatile gases. Usually this is treated in the anaerobic digestors.

5. MODIFICATIONS IN THE IRRADIATOR SYSTEM

As part of this research project, following modifications in the irradiation plant at Baroda were necessary to irradiate raw sludge directly from the primary settling tank.

(1) Cast iron pipeline of 4” NB size for pumping sludge from primary settling tank to receiving tank of SHRI was commissioned. The connection with a valve was branched off existing pipeline for pumping raw sludge to digestors. By co-ordination with staff of municipal treatment plant, raw sludge is made available to irradiation facility.

(2) A screen made of G.I. wire mesh (25 mm openings) of 3 m height and 2 m width was installed in the receiving tank. Filtering out large sticky objects and fibrous materials has reduced problems in operation of pumps and piping, while filling the irradiation vessel. Frequent cleaning of this screen is carried out manually.

(3) Use of metering silo for sludge is discontinued to decrease pump discharge head. The silo located above the irradiator was used to control volume of sludge to be irradiated in the irradiator vessel. Alternate method of level control by use of nucleonic level gauge as well as visual indication is provided. Difficulties in pumping of raw sludge from underground receiving tank with a self-priming sludge pump were anticipated due to presence of non-homogenized solid and high volatile contents of undigested sludge.

6. DESCRIPTION OF EXPERIMENTAL METHOD

Raw sludge is drawn from the primary settling tank into a 10 m^3 underground receiving tank. For each batch of experiments 3 m^3 of sludge is pumped into an irradiator vessel, which takes about three minutes. Recirculation and aeration are commenced soon after attaining the level in the irradiator vessel. Recirculation rate of 1 m^3/min is achieved by a centrifugal sludge pump. This assures mixing and uniform absorbed dose in sludge and deposition free operation of piping. Aeration within the irradiation zone is provided by compressed air monitored by flowmeter giving 0-100 lit/min of air. Samples for analyses are drawn from recirculation line outside irradiation cell area with the help of stainless steel ball valve arrangement. After completion of batch experiment the treated sludge is drained under gravity to either sand bed for drying or to the facility garden. The process is repeated for the next batch.

7. TL DOSIMETRY FOR SLUDGE IRRADIATION SYSTEM

In our earlier work for dosimetry for the digested sludge disinfection at the SHRI irradiator, it has been shown that sand separated from the sludge can be used as an in situ dosimeter by making use of its thermoluminescence property [5, 6]. The method is usable for estimating dose delivered to the samples in the dose range of 0.25 to 4 kGy.

A minimum of 15 litres of liquid sludge was collected from the receiving tank of SHRI irradiator for calibration. Experimental samples were collected from the same batch of sludge after an interval of two hours. The total irradiation period was six hours. These samples were allowed to settle. The settled portion of the sludge was collected and washed with water repeatedly. Carbonates from the sample were removed by treating with 1N HCl (hydrochloric acid). After cleaning with water, hydrogen peroxide (H_2O_2)(30 %) was added to remove the organic matter. Almost all the organic material could be removed by repeating this process twice or three times. After complete removal of organic material, the sand was separated and cleaned repeatedly with distilled water. The cleaned sample was dried at room temperature.

Magnetic particles and mica were removed from the sample by magnetic and electrostatic separation, respectively. After drying, particles in the size range 75–125 μm were collected using standard test sieves. A part of the above sample was further treated with hydrofluoric acid (40% concentration) in a Teflon beaker for one hour. Immediately after decantation of hydrofluoric acid (HF), concentrated HCl (12 N) was added to the beaker to remove fluorides. Finally, this was cleaned repeatedly with distilled water and quartz was separated.

For calibration, the quartz samples collected from the inlet of the irradiator were irradiated in a dose range of 0.25 kGy to 8 kGy using gamma chamber at a dose rate of 10.01 Gy/min. Care was taken to protect the sand samples from exposure to light (from sun as well as from room lighting) during collection, cleaning, irradiation and TL readout of sludge samples, as they show light-induced TL fading. All the TL measurements (peak height as well as area under the TL glow peaks) on the samples were taken at a heating rate of 10ºC/s, using a Harshaw 3000A TLD reader coupled to a flow chart recorder. For each measurement, 5 mg of sand sample was used.

The absorbed doses in the sludge for three different periods of irradiation were estimated by using 220°C and 370°C TL peaks (differential as well as integral TL methods) of these samples (five readings each) as of 11 June 1997.

The results are summarized in Table I.

TABLE I. ESTIMATION OF DOSE RATE BY TL METHODS

Period of irradiation in hour	Estimated absorbed dose in kGy	
	220°C	370°C
2	0.96 ± 0.04	1.00 ± 0.05
4	2.00 ± 0.06	2.00 ± 0.06
6	3.00 ± 0.04	3.00 ± 0.02

The average dose for two hours of irradiation was estimated to be 0.993 ± 0.03 kGy. This value of dose rate (i.e. 0.5 kGy/h) is considered for current estimation of absorbed dose during irradiation of raw sludge in SHRI irradiator.

8. MICROBIOLOGICAL ANALYSES OF RAW SLUDGE IRRADIATION

Microbiological analyses of raw sludge were carried out for estimating decontamination efficiency of radiation treatment. Hourly samples were taken for analyses. Plate count methods of analysis were employed for determination of colony forming units per ml of Total Coliforms, Total Salmonella-Shigella and Total Bacteria using appropriate agars. The effect of aeration during irradiation was also studied.

Table II shows Total Coliforms data obtained in these experiments. Experiments numbered from 1 to 16 are without aeration batches. Remaining batches are processed using compressed air bubbling in the irradiation vessel during recirculation. The recirculation flowrate during the experiments was observed to be 50 to 70 m^3/hr.

The data for coliform is graphically represented in Fig. 1. Figure 2 is prepared by plotting the average of coliform reductions in respective experiments in log units v/s irradiation time (which is proportional to absorbed dose), which explains the effect of aeration during radiation treatment.

TABLE II. RAW SLUDGE IRRADIATION (PLATE COUNT METHOD) — TOTAL COLIFORMS

Expt No.	Date	Aeration lit/min	% Solids (by wt.)	Total Coliforms in cfu/ml Irradiation Time in hours							
				0	1	2	3	4	5	6	7
1	17/10/96	0	3.50	8300	300	0	30	20	90	370	
2	29/10/96	0	1.10	17600	100	0	0	10	0	0	
3	18/11/96	0	5.00	306000	85	36		13	3	3	5
4	26/12/96	0	2.00	102000	1100	100	2	10	1		
5	03/01/97	0	4.00	207000	18000	3200	560	61	24	15	
6	10/01/97	0	5.00	42000	17600	2600	230	68	51	126	
7	21/01/97	0	3.10	8700	240	40	102	74	87	84	
8	02/04/97	0	0.90	90000				66			
9	17/06/97	0	0.73	212000						50	
10	02/07/97	0	5.04	113000						8	
11	03/07/97	0	1.80	179000						8	
12	02/06/97	0	5.04	680000						8	
13	23/09/97	0	4.50	195000	930	89	56	40	25	17	
14	24/09/97	0	4.37	154000	675	106	64	38	23	7	
15	25/09/97	0		116500	820	96	55	51	27	10	
16	08/10/97	0	2.86	44000	975	189	38	59	13	14	

TABLE II. (cont.)

Expt No.	Date	Aeration lit/min	% Solids (by wt.)	Total Coliforms in cfu/ml Irradiation Time in hours							
				0	1	2	3	4	5	6	7
17	15/10/96	2	2.80	13600	1500	200	32	0	6		
18	24/10/96	2	2.80	29000	0	0	0	0	10	20	
19	22/11/96	2	7.86	98000		5440		0	68	38	124
20	12/12/96	4	3.26	47500		340		12		3	
21	31/12/96	5	6.40	126000	20500	1680		28	18	21	
22	07/01/97	5	3.91	8500	360	4	8	1	5	0	
23	17/01/97	5	5.00	20000	660	90	52	44	28	45	
24	30/01/97	5	2.24	26900	220	10	9	13	24	39	
25	21/02/97	5	2.20	220000				142			
26	26/08/97	7	0.59	2800	106	520	208	12			
27	02/09/97	7	3.04	72000	1410		28	8	6	6	
28	04/09/97	7	3.82	93000	142	100	36	8	8	18	
29	28/11/96	8	3.60	32000	200	20	20	0	10	27	19
30	28/08/97	9	3.93	90000	1500	116	40	22	8	4	
31	04/04/97	10	1.43	720000		152				50	
32	06/05/97	10	2.21	160000						34	
33	07/05/97	10	1.07	101000						14	
34	15/05/97	10	0.95	2580						10	
35	19/05/97	10	4.56	65000						24	
36	10/06/97	10	1.86	233000						34	
37	26/06/97	12	0.80	3200						24	
38	25/06/97	14	1.42	57000						38	
39	18/06/97	18	0.71	38000						6	
40	30/09/97	100	3.33	155000	300	108	45	39	72	91	
41	01/10/97	100		35000	36	22	25	22	10	29	
42	09/10/97	100	3.02	18800	320	49	62	102	139	230	
43	16/10/97	6	3.68	520000	216	89	151	69	97	70	
44	23/10/97	4	3.55	24950	164	127	95	129	119	81	
45	5/12/97	10		2195	202	60	31	8	110	18	
46	26/12/97	7		17150	26				7		
47	2/1/98	6		3300	78	56	20	12	37	18	
48	20/1/98	8		42000	60	29	19	14	12	10	
49	23/1/98	12	1.64	10750	88	57	34	10	14	11	
50	28/1/98	18	1.89	43500	64	17	10		16	9	
51	3/2/98	8	1.56	120500	343	148	15	13	9	10	
52	10/2/98	12	0.92	121000	112	26	16	10	24	17	
53	13/2/98	12		171500	180	110	4	28	87	273	

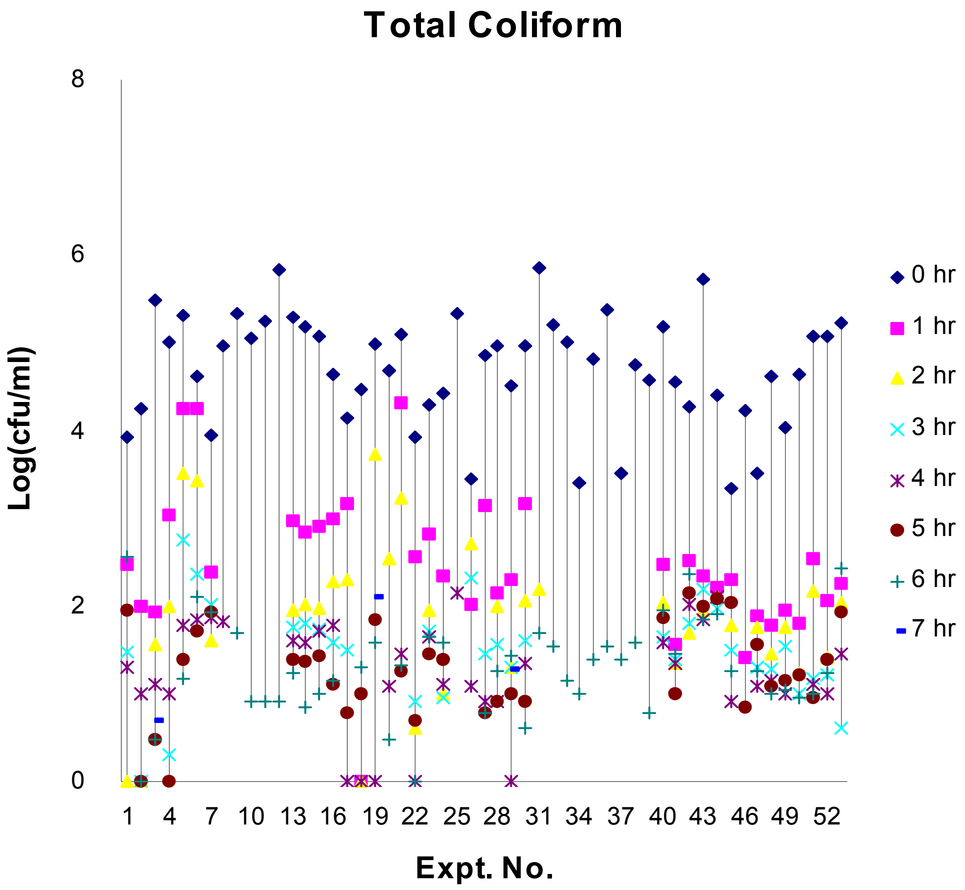

FIG. 1. Analyses of irradiated raw sludge-total coliforms.

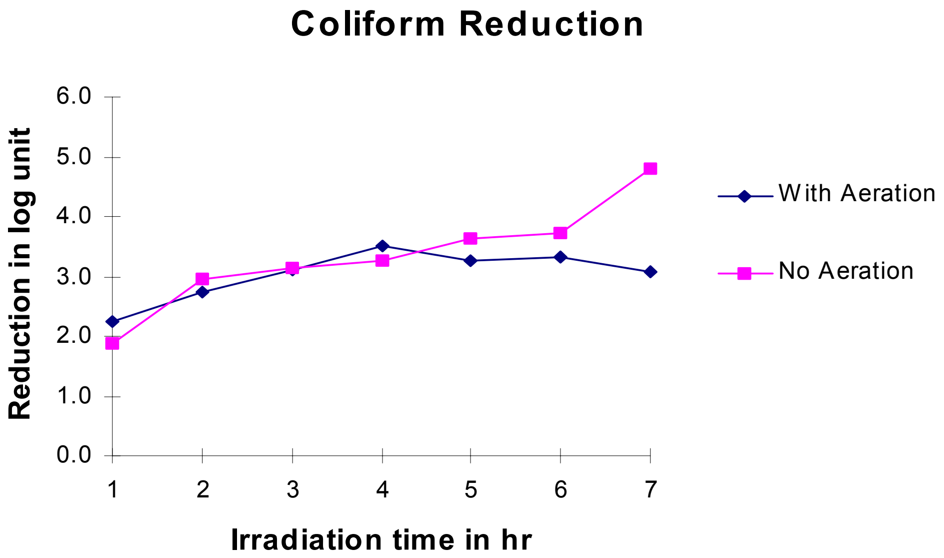

FIG. 2. Effect of aeration-total coliforms.

Analyses were also carried out to estimate reductions in Total Bacteria for some of the above experimental batches. Table III shows data for the same. Charts were prepared similarly as for Total Coliforms and presented as Figs 3 and 4.

TABLE III. RAW SLUDGE IRRADIATION (PLATE COUNT METHOD)-TOTAL BACTERIA

Expt No.	Date	Aeration lit/min	% Solids	Total Bacteria in 100 x cfu/ml Irradiation Time in hours							
			(by wt.)	0	1	2	3	4	5	6	7
1	17/10/96	0	3.50	29000	120	100	40	48	36	50	
2	29/10/96	0	1.10	16000	140	150	68	55	65	68	
3	18/11/96	0	5.00	32700	1100	264		149	116	130	107
4	26/12/96	0	2.00	38500	13	100	140	90	90		
5	03/01/97	0	4.00	88000	920	470	160	162	165	120	
6	10/01/97	0	5.00	3700	650	85	21	14	11	10	
7	21/01/97	0	3.10	25000	700	200	197	146	156	182	
8	02/04/97	0	0.90	20600				870			
9	17/06/97	0	0.73	280000						19600	
10	02/07/97	0	5.04	140000						6800	
11	03/07/97	0	1.80	70000						3400	
12	02/06/97	0	5.04	140000						6800	
13	23/09/97	0	4.50	14800	4800	4200	3800	3100	2900	1100	
14	24/09/97	0	4.37	35500	4250	2650	3550	2200	785	540	
15	25/09/97	0		53000	4550	3200	2800	1275	825	320	
16	08/10/97	0	2.86	20300	1745	880	585	440	220	133	
17	24/10/96	2	2.80	8800	156	170	109	65	25	32	
18	22/11/96	2	7.86	75000	26000	1170		182	130	88	117
19	12/12/96	4	3.26	24700		360		28		212	
20	31/12/96	5	6.40	20800	1200	250		275	180	180	
21	07/01/97	5	3.91	3000		230	300	92	163		
22	17/01/97	5	5.00	1600	1000	130	140	136	220	109	
23	30/01/97	5	2.24	1400	600	232	116	74	75	38	
24	02/09/97	7	3.04	14400	670	580	570	410	350	275	
25	04/09/97	7	3.82	34500	900	850	645	510	660	645	
26	28/11/96	8	3.60	98000	3100	1170	500	109	78	57	54
27	28/08/97	9	3.93	40000	970	790	680	540	345	290	
28	04/04/97	10	1.43	16200		640				64	
29	06/05/97	10	2.21	126000						96	
30	07/05/97	10	1.07	27900						76	
31	15/05/97	10	0.95	13200						250	
32	10/06/97	10	1.86	56000						380	
33	26/06/97	12	0.80	7800						890	
34	25/06/97	14	1.42	59000						1250	
35	18/06/97	18	0.71	9300						104	
36	30/09/97	100	3.33	73000	3850	2250	1500	405	300	590	
37	01/10/97	100		35000	16000	566	480	525	360	330	
38	09/10/97	100	3.02	9850	735	460	345	300	196	167	
39	16/10/97	6	3.68	3300	815	605	730	715	151	115	
40	21/10/97	6	6.81	237000	19000	11900	7900	7300	5200	4300	
41	23/10/97	4	3.55	1435	93	81	62	105	91	69	
42	5/12/97	10		6050	1050	245	360	142			
43	26/12/97	7		6000	3500						
44	2/1/98	6		9400	805	425	320	260	365	68	
45	23/1/98	12	1.64	161	130	114	66	57	42	41	
46	28/1/98	18	1.89	4850	640	560	240		74	39	
47	3/2/98	8	1.56	3850	1500	1150	570	345	215	100	
48	10/2/98	12	0.92	2140	445	265	230	78	51	15	
49	13/2/98	12		5250	1490	800	470	425	345	164	

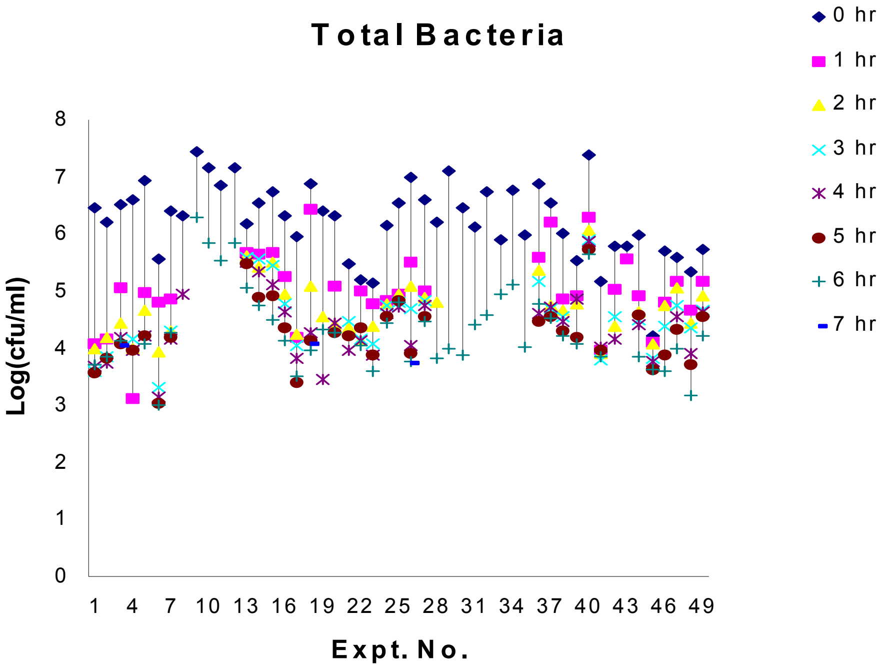

FIG. 3. Analyses of irradiated raw sludge-total bacteria.

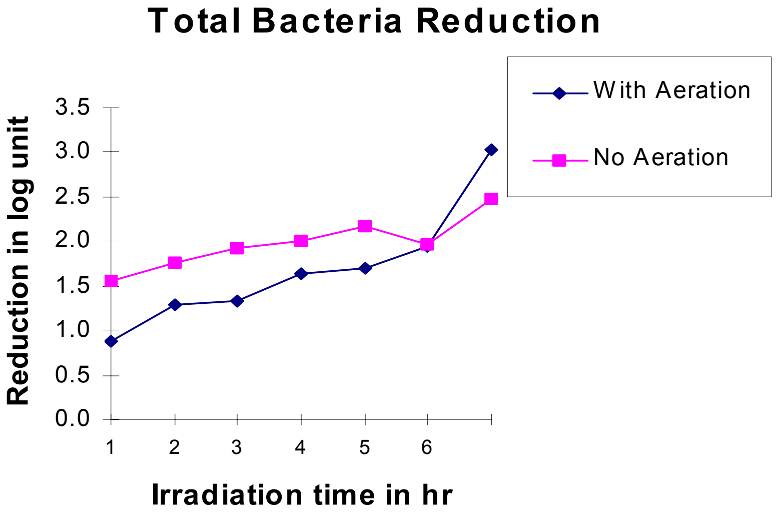

FIG. 4. Effect of aeration-total bacteria.

Total Salmonella-Shigella are considered to be pathogenic bacteria. Similar data for some of the above batches were collected. Table IV represents data for Total Salmonella-Shigella. Figs 5 and 6 are constructed from the same data.

TABLE IV. RAW SLUDGE IRRADIATION (PLATE COUNT METHOD) – TOTAL SALMONELLA-SHIGELLA

Expt No.	Date	Aeration lit/min	% Solids (by wt.)	Total Salmonella-Shigella in cfu/ml Irradiation Time in hours							
				0	1	2	3	4	5	6	7
1	17/10/96	0	3.50	5400	0	0	10	10	20	90	
2	29/10/96	0	1.10	185000	100	0	10	10	90	10	
3	18/11/96	0	5.00	2400	20	3		4	0	1	0
4	26/12/96	0	2.00	4600	100	0	7	3	0		
5	03/01/97	0	4.00	172000	1520	100	19	2	6	4	
6	10/01/97	0	5.00	30000	1940	240	23	11	11	9	
7	21/01/97	0	3.10	5600	30	4	11	8	6	15	
8	24/09/97	0	4.37	1350	42	32	18	6	5	1	
9	25/09/97	0		1210	47	24	19	12	7	1	
10	08/10/97	0	2.86	750	510	18	15	9	4	7	
11	24/10/96	2	2.80	16000	0	0	0	0	10	10	
12	31/12/96	5	6.40	13200	1100	3		1	1	0	
13	07/01/97	5	3.91	13000	220	50	5	6	5	1	
14	17/01/97	5	5.00	22000	80	20	4	10	5	8	
15	30/01/97	5	2.24	7600	120	12	15	2	11	19	
16	02/09/97	7	3.04	4150		55		0	0	0	
17	04/09/97	7	3.82	5400	16	4	4	0	0	2	
18	28/11/96	8	3.60	15000	0	0	0	4	4	4	5
19	30/09/97	100	3.33	16600	30	4	3	6	3	8	
20	01/10/97	100		7270	9	12	6	8	17	7	
21	09/10/97	100	3.02	1025	18	13	2	8	29	15	
22	16/10/97	6	3.68	140	22	13	7	2	5	12	
23	21/10/97	6	6.81	16600	1870	1550	446	375	199	111	
24	23/10/97	4	3.55	930	215	145	95	70	56	42	
25	5/12/97	10		365						6	
26	2/1/98	6		1000	28					0	

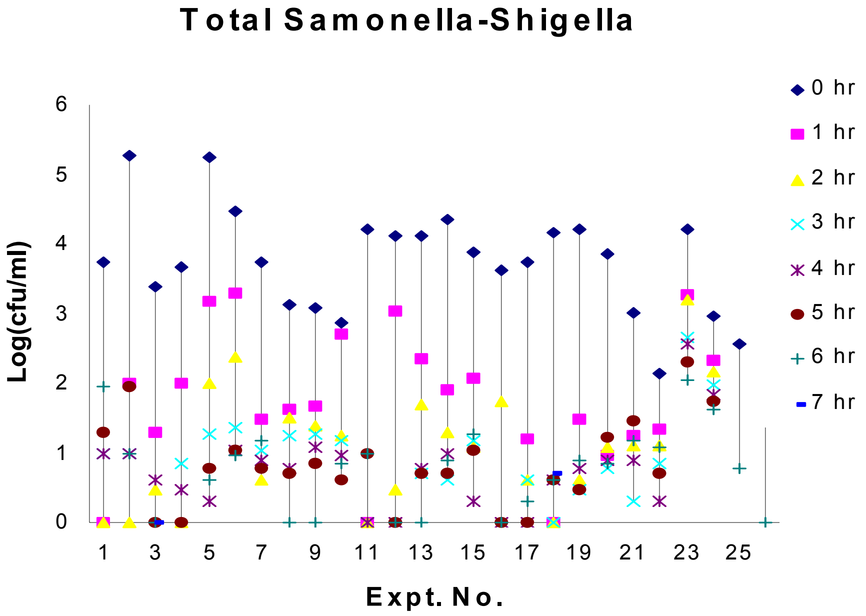

FIG. 5. Analyses of irradiated raw sludge-total Salmonella-Shigella.

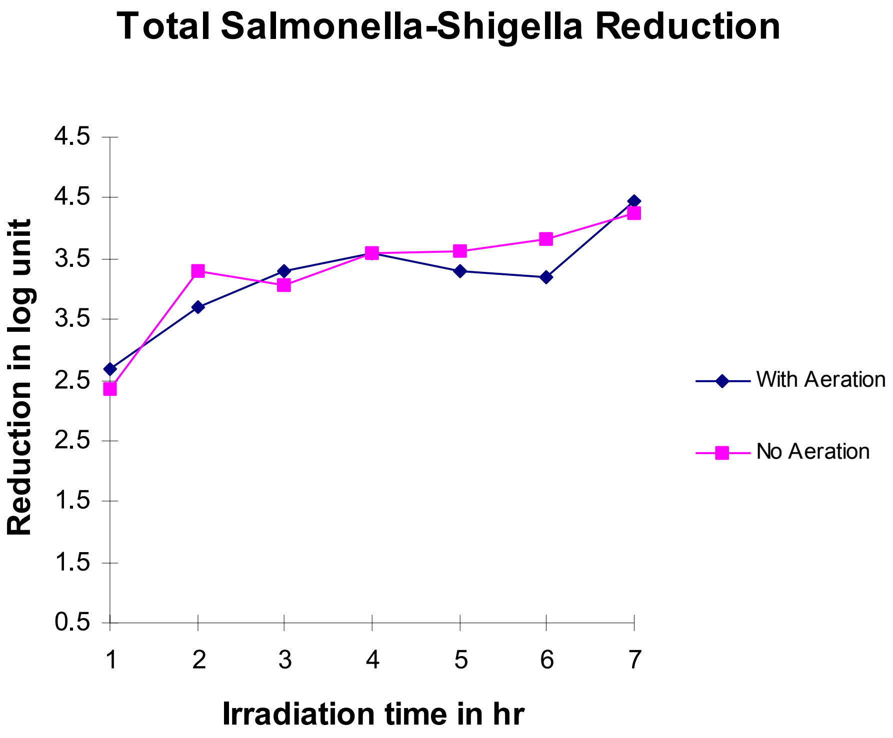

FIG. 6. Effect of aeration – total Salmonella-Shigella.

9. REGROWTH STUDIES

Regrowth of Total Coliforms were observed after 7–8 hours of treatment in the liquid sludge samples irradiated in this irradiator. As drying in the sand bed may take more than 7–8 hours, this may cause problems of recontamination with pathogenic bacteria.

Hence, this aspect was taken up for study in detail. Efforts were directed to investigate the possibility of inadequate treatment due to geometric configuration of the radioactive sources, irradiator vessel dimensions and shape, piping system and liquid sludge flow. Radiotracer study of SHRI irradiator and study of dose distribution by TL dosimetry technique are carried out.

Post irradiation inoculation with some agriculturally useful bacteria were carried out at BARC. The bacteria used for inoculation were phosphate solubilizer Enterobacter esburae and symbiotic nitrogen fixer Rhizobium leguminosarum. Both showed good growth in radiation sterilized sewage sludge. Their ability to grow in the presence of residual microflora is under investigation.

In another set of experiments, reduced volume of sludge 400 litres) was irradiated in the SHRI irradiator. It was felt that at present low source activity and large sludge volume dose rate are very low. It may result in recontamination of sludge during irradiation. As the other configuration of the irradiator could not be modified, volume of the batch was reduced. The experiments show improved results in terms of regrowth. They would be continued for further confirmation.

In an investigation by an external laboratory at Baroda, it was opined after confirmatory tests of about 8 samples of irradiated sludge, that the regrowth bacteria are not all coliform and/or salmonella-shigella. But these tests have to be further confirmed. Materials and methods adopted were as follows.

TESTS FOR THE CONFIRMATION OF COLIFORMS, SHIGELLA/SALMONELLA

Medium	Positive reaction	Possible interference
MacConkey Agar	+ ve (Pink colonies)	Coliforms
	– ve (Colourless colonies)	Salmonella /Shigella
EMB Agar	Metallic sheen	E. coli
Catalase test	+ ve (effervescence)	E.coli / Salmonella
	– ve (No effervescence)	Shigella

- EMB-Eosin Methylene Blue Agar for confirmation of Escherichia coli
- Catalase and Triple Sugar Iron Agar are for determining presence of E. Coli, Shigella and Salmonella group of organisms.

TRIPLE SUGAR IRON AGAR TEST

Reaction	Name of organism		
Colour change	Sh. Flexneri	Sh. Sonnei	Sh. Dysentriae
Slant	Acid	Acid	Acid
Butt	Alkaline	Acid	Acid
H_2S & Gas	+ ve / – ve	– ve / – ve	– ve / – ve
Colour change	S. typhi	S. Paratyphi A	S. Paratyphi B
Slant	Alkaline	Acidic	Alkaline
Butt	Acidic	Acidic	Alkaline
H_2S & Gas	– ve / – ve	– ve / + ve	+ ve / + ve

10. RADIOTRACER STUDY OF SHRI IRRADIATOR

Bromine-82 as aqueous ammonium bromide solution was used as a radiotracer to study the flow characteristics in the irradiator. The direction of sludge flow was varied from its designed direction of downward flow in irradiator. Study for once through instead of closed-loop recirculation was also carried out. Data on dead volumes, mixing time and residence time were generated. These parameters can be used to optimize the plant operation.

11. DOSE DISTRIBUTION BY TL DOSIMETRY

Experiments were carried out for examining the inadequacy of treatment in terms of uniformity of absorbed dose using dosimetry technique. As mentioned in the earlier CRP report, Thermoluminescence properties of sand give very good estimation of absorbed dose in the liquid sludge. Batch of sludge was irradiated in the irradiator for four hours. Twenty-eight samples (15 litres each) of sludge were collected after irradiation. Sand was separated from these samples for measurement of their TL. Five readings were recorded for each sample.

From a total of 145 sample readings, maximum value of TL (in arbitrary units per mass) of 10.00 and minimum value of 7.02 were recorded. The mean value of 8.66 with standard deviation of .55 were worked out.

Frequency distribution curve for the samples is plotted against normal distribution for comparison in Fig. 7.

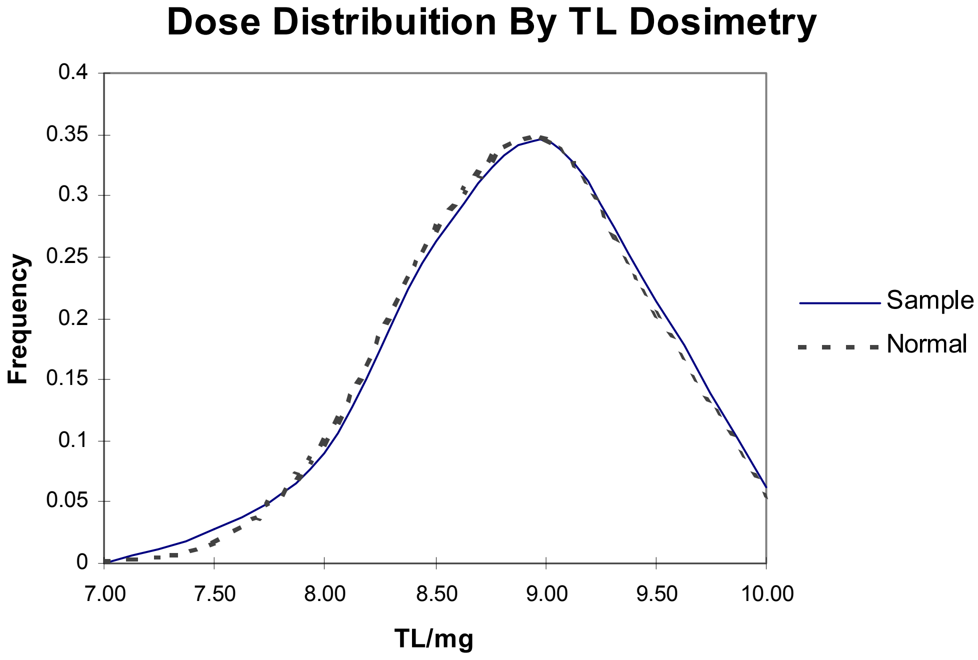

FIG. 7. Distribution of dose in SHRI irradiator.

TABLE V. DOSE DISTRIBUTION BY TL DOSIMETRY

Sample No.	TL (Arbitrary Unit) per mg Readings				
	1	2	3	4	5
1	9.79	9.32	8.89	8.51	8.85
2	9.43	8.49	9.02	8.43	9.06
3	8.18	7.92	8.44	7.45	8.60
4	8.55	8.89	9.18	8.30	9.02
5	8.73	8.80	8.36	9.06	8.33
6	9.17	9.36	10.00	9.78	8.72
7	8.52	9.02	9.57	9.35	9.18
8	9.06	8.97	8.21	8.16	8.25
9	8.57	8.24	8.21	8.57	8.44
10	8.93	9.07	8.91	8.25	8.45
11	10.00	9.27	9.47	9.51	9.06
11a	9.30	9.07	8.81	9.25	9.00
12	7.91	8.25	9.09	8.60	8.75
13	7.88	9.05	8.05	8.41	8.33
14	7.92	8.75	8.63	8.26	8.18
15	8.26	9.00	8.72	8.70	8.84
16	8.60	8.75	8.60	8.75	8.81
17	9.76	8.50	9.15	8.37	9.41
18	8.18	8.60	8.52	8.44	9.00
19	8.60	8.62	8.96	9.07	8.67
20	8.72	8.65	8.81	8.67	9.52
21	8.51	8.44	9.50	9.15	8.91
22	9.07	7.84	9.07	8.22	8.00
23	8.29	7.91	7.67	8.18	7.08
24	7.36	7.91	8.13	8.22	7.95
25	8.78	8.18	7.92	7.02	7.83
26	8.51	9.11	8.84	8.57	8.89
27	8.57	8.22	9.27	8.75	9.79
28	8.18	7.62	8.33	8.37	8.22

12. CONCLUSIONS

(1) A dose of about 2 kGy is found to be adequate for hygienizing the raw sewage sludge. Total Coliforms and salmonella-shigella counts are reduced below 100 cfu/ml. The dose of 2.7 kGy was observed for similar disinfection for digested sludge in earlier studies at SHRI Facility [7]. Average log unit reduction in Total Coliforms, Total Bacteria and Total Salmonella-Shigella in raw sludge was 3.6, 1.9 and 3.5, respectively, after four hour radiation treatment (absorbed dose 2 kGy) along with aeration.

(2) The variations in initial counts of bacteria are attributed to variations in the solid contents of the sludge. The functioning of primary settling tank of the conventional sewage treatment plant affects the raw sludge characteristics. Seasonal and climatic conditions affect the operation of the conventional treatment plant. But, the radiation hygienization are less affected due to these reasons. The reduced final counts(<100 cfu/ml coliform) are achieved irrespective of the initial counts (generally less than 10^6 cfu/ml of Total Coliforms) after 2 kGy dose.

(3) Aeration does not seem to reduce dose requirement significantly as observed in the case of digested sludge. However, average log unit reduction in case of Total Coliforms and Total Salmonella-Shigella was more in combination treatment than that in radiation treatment without aeration. Besides, aeration seems to reduce bad odour from the sludge under processing as well as from treated sludge.

(4) A few chemical analyses have shown reduction in BOD, COD, volatile solid, ammonia content and sulphide.

(5) Sand separated from the sludge was used as an in situ dosimeter by making use of its thermoluminescence property. Average dose for two hours of irradiation was estimated to be 0.993 ± 0.03 kGy. This value of dose rate (i.e. 0.5 kGy/h) was considered for dose estimation.

(6) Dose distribution study with the help of measurement of TL of sand obtained from sludge has shown that the uniform dose was received by the sludge on recirculation for four hours. Mean value of TL was 8.66 with standard deviation of .55 for 145 observations.

(7) As the irradiator is operating at low source strength, microbiological investigations for reduced volume irradiation treatment are carried out. There is improvement in the results in respect of regrowth of bacteria.

13. PROPOSED STUDIES

— Further investigation on regrowth of bacteria is very essential. Experiments using reduced volumes of sludge will be carried out.

— The irradiated sludge can be mixed with some natural chemicals having antibacterial and antifungal activity. They will be selected in view of economic viability.

— Centrifugal decantation of sludge will dry the sludge in very short period of time. Sludge dried with this method can be studied for its regrowth potential.

— Toxic chemical and odour removal will be studied in detail.

— Treatment after replenishment of radioactive sources are planned to observe the effect of increased dose rate. Also, it is planned to reduce the irradiator vessel volume.

ACKNOWLEDGEMENTS

The authors wish to thank Dr. D. D. Sood, former Director, Radiochemistry and Isotope Group and Dr. S. M. Rao, Head, Isotope Division, BARC for their encouragement and interest in this work. We wish to acknowledge with respect the active guidance provided by Dr. B.C. Bhatt, Radiological Physics Division, BARC in the TL dosimetry work. We thank Mr. H.J. Pant and Mr. P. Walinjkar for their work in the Radiotracer study of the SHRI irradiator. We also thank SHRI staff personnel for their work in this programme.

REFERENCES

[1] LAVALE, D.S., SHAH, M.R., RAWAT, K.P., GEORGE J.R., “Sewage Sludge Irradiators-Batch And Continuous Flow”, Radiation Technology for Conservation of the Environment (Proc. International Symp. Poland, 1997).

[2] PERRY’S CHEMICAL ENGINEERS’ HANDBOOK, sixth edition, 26-47.

[3] SWINWOOD, J.F., WAITE, T.D., KRUGER, P., RAO, S.M., “Radiation technologies for liquid and solid waste treatment: an international perspective”, IAEA Bulletin **36** (1994) 11 pp.

[4] Report of the First RCM of the IAEA CRP on Irradiation Treatment Of Waste, Wastewater And Sludges (1996).

[5] BENNY, P.G., BHATT, B.C., Appl. Radiat. Isot. **47** (1996) 115 pp.

[6] BENNY, P.G., BHATT, B.C., SHAH, M.R., Radiat. Phys. Chem. **49** (1997) 377 pp.

[7] SHAH, M.R., “Disinfection of sewage sludge at SHRI, Baroda” (Proc. NAARI Annual Conf., 1997) 71 pp.

RADIATION TECHNOLOGY FOR SEWAGE SLUDGE TREATMENT: THE ARGENTINE PROJECT

J.G. GRAIÑO
Comisión Nacional de Energía Atómica,
Buenos Aires, Argentina

Abstract. Within the environmental applications of ionizing radiation, disinfection of wastewaters or sewage sludges is one of the most best known. Argentina based the project of a full scale irradiation plant on the gamma irradiation application, utilizing Argentine made Cobalt-60 sources. The design characteristics, process descriptions and costs are included.

The research project developed information about the irradiation effects on the sludges with respect to plant performance. For the purpose of oxi-irradiation experiments, a lab-scale pool irradiator was constructed and is described.

1. INTRODUCTION

There are many examples of commercial on-line irradiation plants as well as laboratory experiments [1], when irradiation technology is used to solve problems in water contamination, wastewaters and sludge, using radioactive sources of Co-60 or electron beam accelerators with energy above 1.5 Mev. Decontamination, degradation and reuse of material must be analysed bearing in mind not only technological aspects. Public acceptance, environmental laws, engineering, replacement and operation costs must be considered for the final balance of every project.

The Project in Argentina, conducted by PIBA, was created using nuclear technology to solve environmental problems associated with the treatment and final disposal of sewage sludge. Therefore radiation application is used for biological and physicochemical modifications in semisolid material obtained by conventional treatment of wastewaters.

In all big cities the demographic pressure creates distortions and environmental problems, one of them the effluent and waste treatment, which must be solved by closed cycles that allow maximum degradation and re-utilization and then, minimum loss of energy and investment. In the case of sewage sludges reused in agriculture, for example, the organic material may be degraded in soil by natural oxidation cycles, and the nutrients reutilized by the plants [2]. But control for human health risks avoiding pathogen microorganisms back into the food chain by means of the contaminated crops or agriculture workers is required [3].

Ionizing radiation of radioactive sources or accelerators causes alteration in cell membranes and then destroy bacteria, fungi, viruses, etc. as well as breaks chemical chains in some organic toxic substances like pesticides, herbicides, PCBs, etc., included in the sludge contents.

The design parameters and main features of a full scale gamma irradiation plant projected for the treatment of sewage sludges of a populated city (Tucumán: 600,000 inhabitants) in the Northwest Argentina, and some research about irradiation effects on the sludges are described. Also shown are the design and construction of an experimental irradiator of a hundred litres to be used for irradiation experiments in sludges, wastewaters or effluents.

2. PRELIMINARY CALCULATIONS

After a review of previous work [5,6] the Argentine project was based on the batch process type, with anaerobically digested sludges, 5% to 8% solids concentration. The Wastewater Treatment Plant at Tucumán, which the irradiation plant was designed for, accomplishes primary treatment processes on the wastewaters (grids, sand exclusion, clarifiers, and chlorination before being dumped into the river) and anaerobic digestion on the thickened sludges. According to the reported data summarized in the table below, it is assumed that the quantity of anaerobically digested sludges is 0.35 lt/day.inh (Table 1) [7].

TABLE 1. SLUDGE AMOUNT PRODUCED BY DIFFERENT TREATMENTS

Treatment	Dried Sludge g/inh.day	Dried Sludge %	Sludge Amount L/inh.day
Primary Raw Sludge	54	5	1.08
Primary Digested Sludge	34	10	0.34
Secondary Raw Sludge	74	5	1.48
Secondary Digested Sludge	48	8	0.60
Biological Treatment Raw Sludge	85	4.5	1.87
Biological Treatment Digested Sludge	55	7	0.79

The facility was designed for a population of 100,000 to 400,000 inhabitants served, and therefore the maximum processing capacity should be 140 m^3/day. It was already concluded that the required dose for satisfactory decontamination is 3 kGy without oxygen addition, and 2 kGy with oxygenation [8]. Then, it is possible to calculate the required energy and also the radioactive charge of the irradiation plant to accomplish the process.

2.1. Plant power and activity calculation

The total activity of an irradiation plant is proportional to the annual volume of treated material and to the required radiation dose as follows:

$$P(kw) = \frac{D\,(kGy) \times M\,(kg/h)}{\mu\ \times 3600\,(s/h)}$$

$$13\,(kw) = \frac{3\ (kGy) \times 6270\,(kg/h)}{0.4 \times\ 3600\,(s/h)}$$

where

P is source power,
D is absorbed dose required,
M is mass to be treated by hour in 8150 h/operational year,
µ is energy transference yield.

The expression represents the rate of absorbed energy in the required treatment by the available energy in the radioactive sources.

Now, Co-60 disintegration produces two photons with isotopic yield of 100%; the total released energy is the sum of: 1.17 MeV + 1.33 MeV = 2.5 MeV.

Then, the source activity is:

$$2.5\text{MeV/dis} \times 1.6 \times 10^{-13}\ \text{w.seg/MeV} \times 3.7 \times 10^{10}\ \text{dis/seg.Ci} = 14.8 \times 10^{-3}\ \text{w/Ci}$$

$$\frac{13 \times 10^{3}\, w}{14.8 \times 10^{-3}\ w/Ci} = 0.878\ MCi$$

For Co-60 sources the attenuation in water may be calculated by the expression:

$$D = Do \times B \times (e^{-0.063.x})$$

being $Do = A(Ci) \times Kr(1.34\ R.m^2/h.Ci)$

$B = B\ f(u.x)$

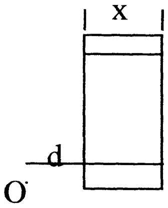

where

μ is attenuation coefficient 0.063 (cm^{-1}),
A is source activity,
Kr is gamma radiation specific constant,
d is distance from the source to the object point,
B is multiplication factor,
X is shielding thickness: 30 cm.

The attenuation in 20 cm water results are greater than 70%. This is conditioning for the tank diameter not to be exceeding 1.6 m if the irradiator is composed with the source distribution in a circular shape, like it is shown in the Fig. 1a/1b.

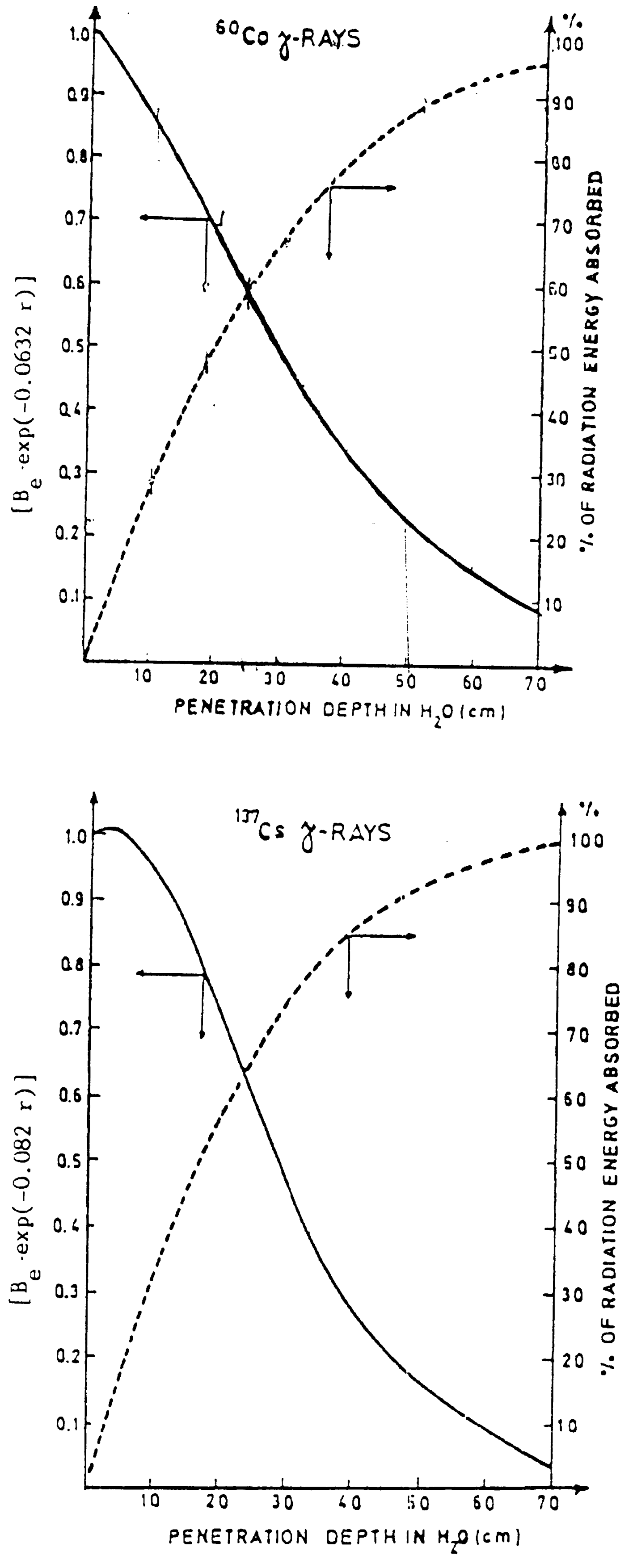

FIG. 1a-1b. Relation between the attenuation radiation and the energy absorbed at various water thickness.

3. CHARACTERISTICS OF DESIGN AND OPERATION

The plant core is the cylindric irradiator tank surrounded by shielding concrete; the other tanks, intake and outlet tanks, are conveniently located within the installations which cover an area of about 200 m^2 [9] Fig. 2.

The irradiator has 304 L capacity, two concentric stainless steel of 1m and 1.60 m, respectively. The interior tank lodges the radioactive sources, keeping them separated from the sludges; it has also a chamber containing deionized water for refrigeration and control of the cobalt-60 sources.

The refrigeration system recycles the water and allows any possible radioactivity coming from any source to be measured in case of eventual failure or original weakness. The permanent and continuous control of the refrigeration water is automatically made and watched from the computer video display at the control desk.

The digested sludges are previously pumped to the intake tank and are discharged by gravity into the irradiator tank as soon as a 10 inch electromechanical valve is opened, and in very short time (less than 1 minute). The intake way is by the central tube and simultaneously by the periferic distributor tube; in this way the sludges could best receive radiation coming from the cylindric distributed sources, see Fig. 2. Once the opening valve is closed a pump 240 m3/h is activated to make the sludges recirculate during the necessary time to achieve the required disinfection dose (about 30 minutes). Once the irradiation time is over and 20 recirculation cycles are accomplished, the recirculation pump is automatically stopped and the sludges are discharged into the outlet tank. This cycle might be modified for the complete operation during 24 hour a day.

For the source charges and redistribution, a transference well five meters deep is available next to the irradiation room and connected by a channel. The container with new source material enters the pool of the transference well using a crane 10 t maximum charge.

Source movements, for recharge as redistribution, are made under protection of a five meter water column, guaranteeing the required biological shielding; these operations are made only when the radioactive charge is not enough to carry out the total available amount of sludges processed.

The system software automatically determines what activity of the source is needed in case of increasing the sludge amount to be processed, and, on the other hand, controls and tests the sludge levels in the three tanks, opening and close of the valves, warning to the operator every possible failure that might be happening.

The entire installation is located within the Wastewater Treatment Plant; the sludges are directly pumped from the digesters to the Irradiation Plant, and the charge cycle is automatically controlled. Once the sludges are sufficiently irradiated, they are spread unto drying beds, or are eventually applied in liquid form.

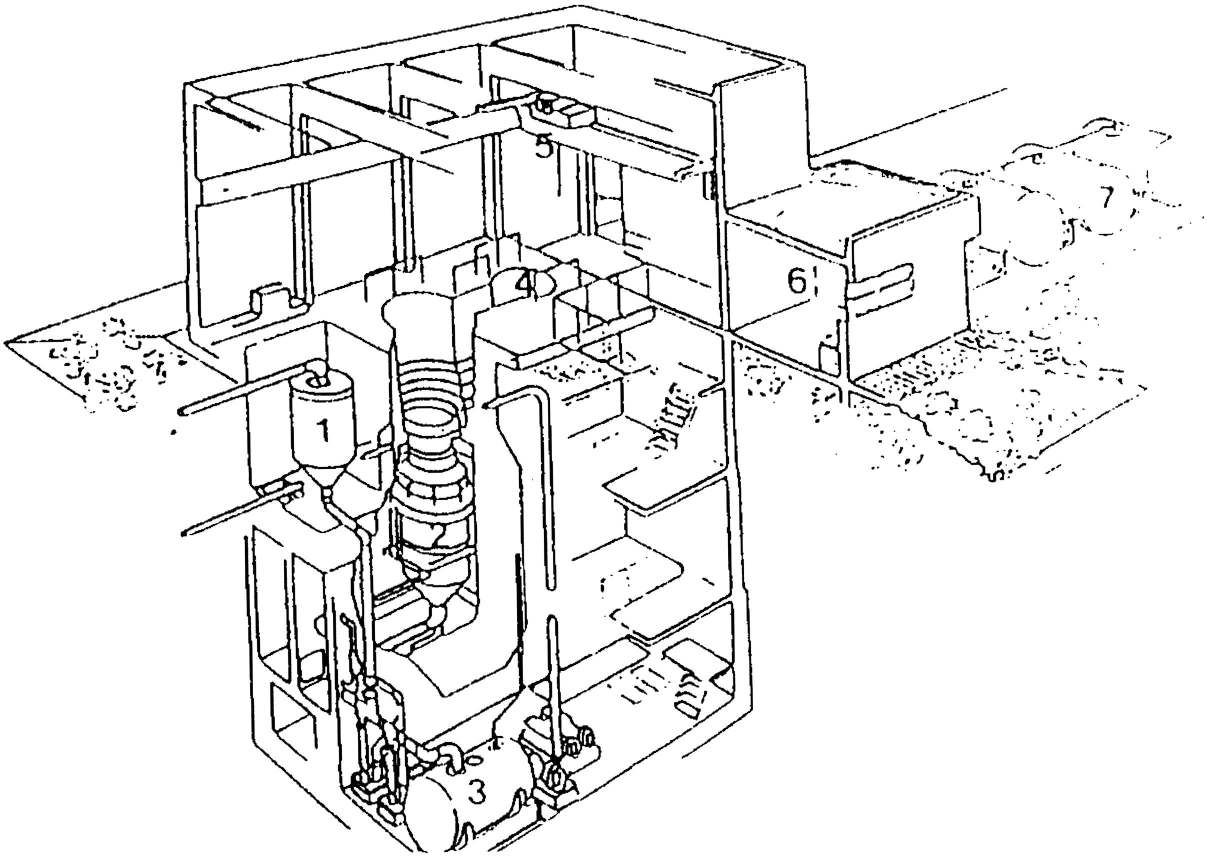

FIG. 2. Drawing of the installations. 1- Intake tank. 2- Irradiation tank. 3- Outlet Tank. 4- Transference well. 5- Grantry crane. 6- Repair work and lab. 7- Storage tanks of deionized water.

3.1. Details of the source loading tank

The concentric source loading tank, located inside the irradiation tank, is a separate unit, thus allowing any repair, if necessary, Fig. 3. This unit has 32 locations, where a specially designed support lodges nine sources in vertical position. These are industrial Co-60 sources, model FIS 60-05 with an averaged activity of 7,000 to 10,000 Ci each.

As the maximum radioactivity capacity is 700,000 Ci, it would be necessary to have 70 sources of maximum activity which would initially occupy eight locations; then, approximately 24 positions would be free for new charges or arrangements. Thus, the total amount and homogeneity of activity is conserved for more than 20 years, without the necessity of taking off exhausted sources. The ensemble is refrigerated by demineralized water circulation, as mentioned before.

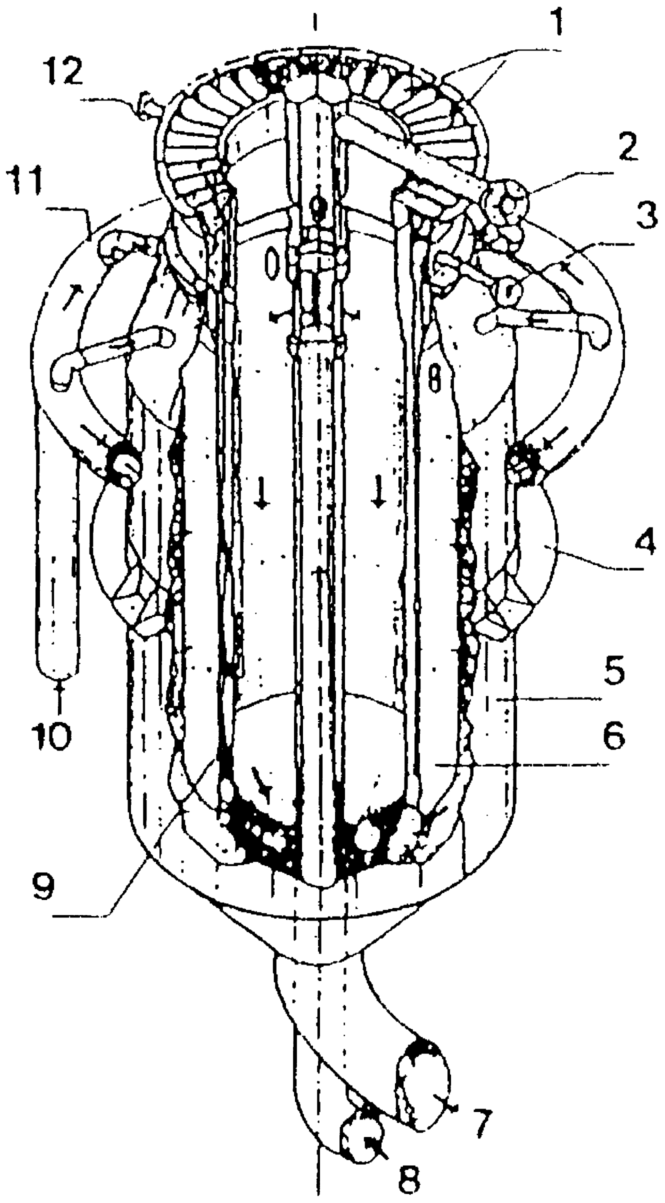

FIG. 3. Irradiation Tank. 1- Source lodging rail. 2- Ventilation. 3- Refrigeration water intake. 4- Support. 5- Tank. 6- Source holder. 7- Sludge outlet. 8- Sludge intake. 9- Sources. 10- Sludge intake. 11- Distribution pipe. 12- Refrigeration water outlet.

3.2. Auxiliary installations

The installations include several other facilities and systems like electromechanical work, chemical laboratory, radioactive dose testing systems, gas ventilation systems, oxygenation system, flood system, alarms and warnings systems.

The existence of auxiliary installations makes this plant to be autonomous but more expensive; this plant was designed as a prototype but future ones would be constructed with lower costs.

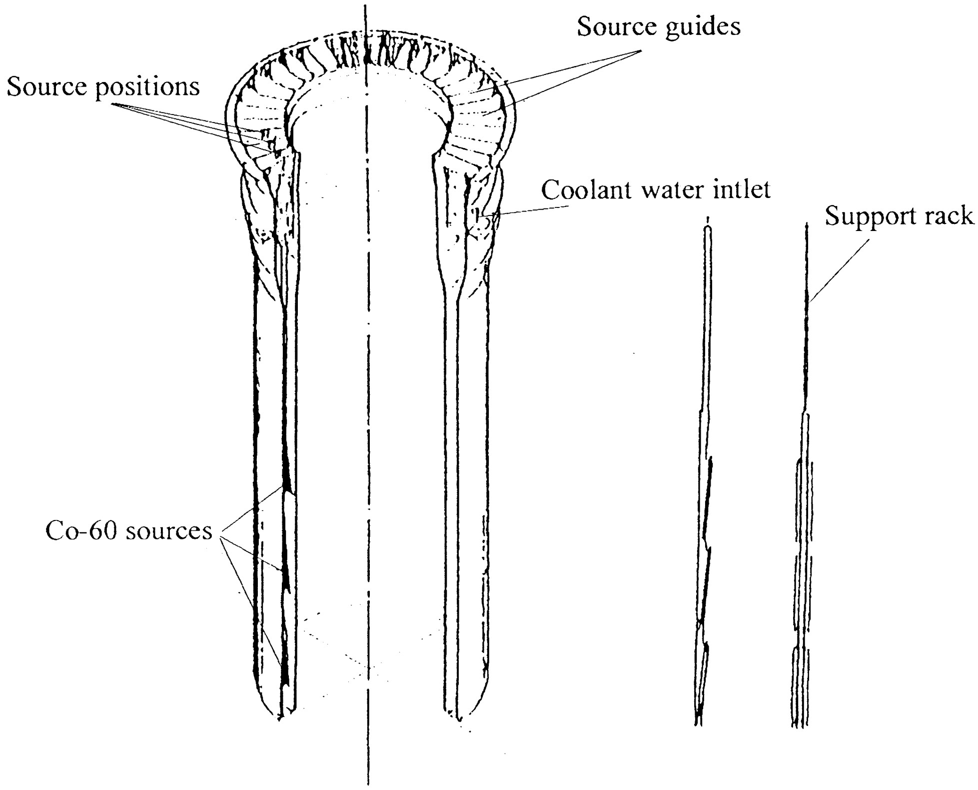

FIG. 4. Internal loading tank.

DESIGN PARAMETERS

Served population	100,000 to 400,000 inhabitants
Amount of produced sludges	0.35 l/inh.day
Annual volume treated	47,500 m^3
Annual operational time	8,150 h
Maximum radioactive capacity	700,000 Ci
FIS 60 type source activity	7,000 to 9,000 Ci
Irradiation time	30 min
Absorbed dose without oxygenation	3 kGy
Absorbed dose with oxygenation	2 kGy
Batch volume	6 m^3
Volume of treated sludge	140 m^3/day
Annual amount of sludge (dry weight)	4,750 tn
Energy transference yield	40%
Tank diameter	1.60 m
Amount of Source lodging	32
Recirculation Rate	240 m^3/h

4. COSTS

The construction of the first full-scale Sewage Irradiation Plant was bided at auction, both the civil work and the electromechanical installations. As result of the auction process, the following amounts were estimated (in US $):

Investment:

Civil works	900,000
Electromechanical works	1,600,000
Subtotal	2,500,000
Co-60 sources (700,000 Ci)	700,000
Total	3,200,000

Operational costs:

Personnel	70,000
Co-60 recharge (average)	50,000
Maintenance and repair	28,000
Electric power	25,000
Sludge transport	50,000
Oxygen	10,000
Subtotal	233,000
Unforeseen (5%)	11,000
	244,000
Amortization (25 years 5%)	225,000
Total	469,000

Annual cost by inh. (400,000 inh)U$S	1.17
Cost by dry ton (4,750 ton)	99
Cost by wet ton	9.9
Sludges amendment	3,400 kg /ha
Total capacity of use	1,400 ha /year
Cost by hectare	US $ 336

The resulting cost by hectare is also high, but again it must be considered that this is a case of a demonstrative project; some systems that are redundant should be omitted in further constructions. It is estimated that the cost of a new plant might be decreased by approximately 30%.

5. IRRADIATION EFFECTS

5.1. Pathogen elimination

The main purpose of the radiation technology treatment on the sewage sludge is to inactivate the pathogenic microorganisms and then to allow the reuse in agriculture without any sanitary risk. Several research programmes have already determined the effective absorbed dose for the elimination of the most known pathogenics. The effectiveness in the faecal or hydric transmission of pathogenic agents was verified in the Argentine project. Bacteria, fungi and parasite ova were inactivated by an absorbed gamma irradiation dose of 2 kGy [10].

The Argentine environmental regulations are still not complete and the limitations for the reuse of sludges in agriculture have not been pronounced, but the project is following foreigner regulations such as the USEPA or the European Community regulations. For example, survival of faecal coliform bacteria after irradiation treatment is still less than the maximum of 1000 MPN/g of the EPA regulations.

However, the recommended absorbed dose is 3 kGy because of the virus inactivation requirement. Enteric pathogenic viruses, like all viruses in general are more radioresistant, and some of them are surviving on land for a long time. One of the topics of the project was the investigation of this type of pathogen control.

Some technical difficulties were solved first about the isolation of the virus species, after that, the species identified were tested after irradiation of maximum 3 kGy abs. dose. A positive result was found in only one of the six tests on the main types of enteric viruses, i.e. Cocksakie virus, Echovirus, etc. It is still necessary to confirm the minimum dose to guarantee virus inactivation below the acceptable limits.

5.2. Detoxification effects

Aqueous solutions of organic toxic compounds are destroyed by ionizing radiation because of the decomposition secondary effects due to irradiation. There are many examples in literature about organochlorinated pesticides, phenols, etc. Purely domestic sludges should not have significant concentration of these substances but the existence of them in the sewage sludges is known, increased by the industrial effluents dumped sometimes into the sewerage.

Some organochlorinated pesticides were detected in low concentration in the sludges at Tucumán where the project will be located: Chlorpyrifos, Heptachlor, etc. Experimental irradiations were carried out to measure decomposition, and this was really proved. But the identification of by-products of the modified compound and their toxicity is still to be accomplished according to the plan for future steps.

5.3. Physicochemical effects

It is known that ionizing radiation may cause some changes in the physicochemical characteristics of the sludges. The project has determined the decrease in the viscosity with dose level surrounding the recommended dose for the project [11].

The simple tests of sedimentation velocity have demonstrated the effect of irradiation, more evidently in diluted samples of the irradiated sludges than in the pure ones.

Also, the test of "filtration specific resistance: r" has been carried out to evaluate the possible changes of the material due to irradiation. The decrease of r value as the dose is increasing is evident up to 3 kGy of absorbed dose, reaching a difference of 60% less than the non-irradiated sludge. This was tested in three different sludges, and the results are shown in Fig. 5.

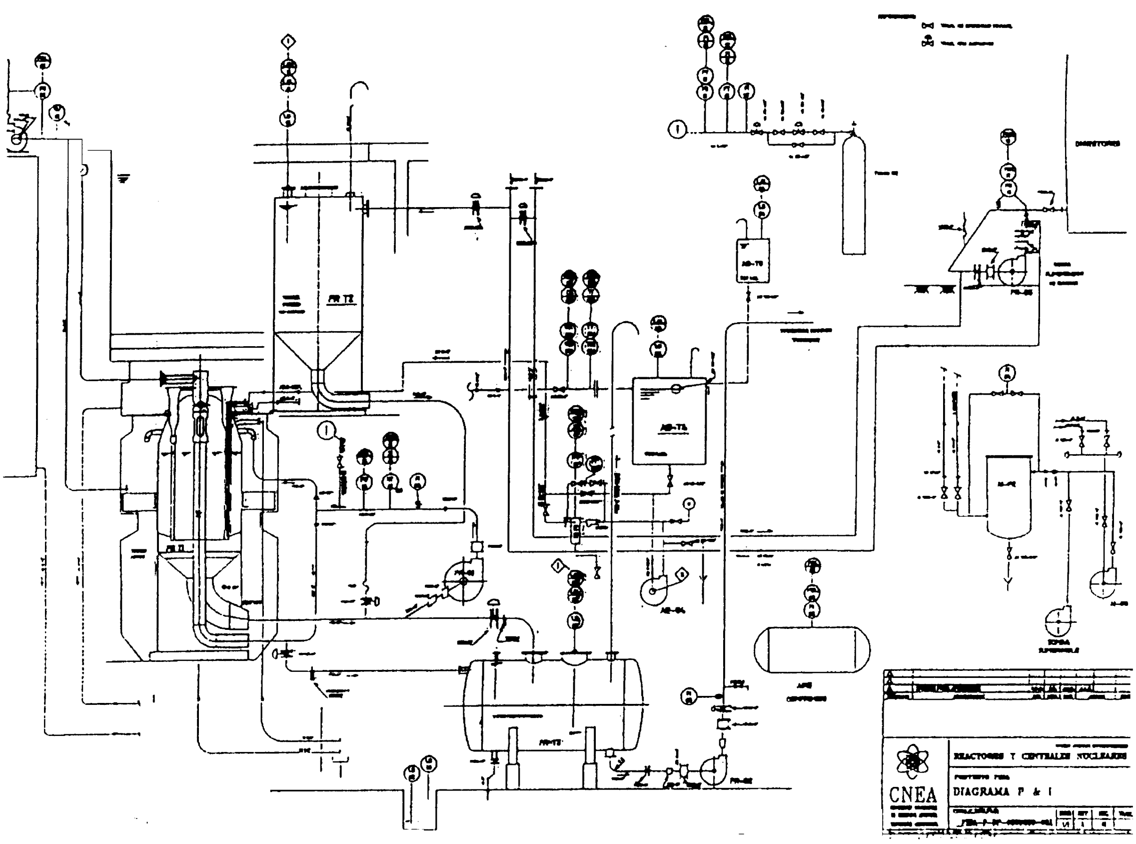

FIG. 5. Flowsheet.

These changes on the physicochemical characteristics of the sludges can be important in connection with the sludge movement into the mechanical systems of the plant. Even if they are not enough to improve the sludge sliding, they are, on a positive sense, for the sludge managing.

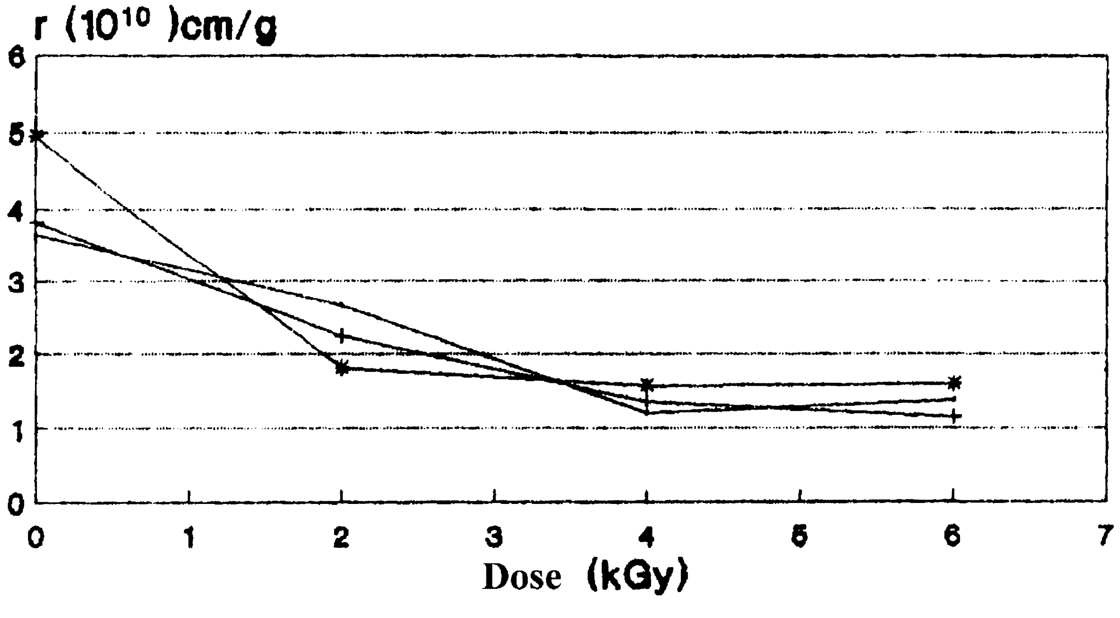

FIG. 6. Filtration Specific Resistance In Irradiated Sewage Sludges.

6. IP-100 EXPERIMENTAL IRRADIATOR

The Pool Irradiator, 100 L capacity (IP-100) is an irradiation facility for the purpose of the study about the irradiation effect on several liquid materials. The main feature is that the radioactive sources are included in the liquid core with the benefit of:

- minimum loss of energy
- high dose homogeneity due to recirculation systems
- addition of other fluids (oxygen, gases, etc.)
- possibility of heating for technical effects
- easy accessibility for cleaning and repair.

The IP-100 was created for experimental purposes concerning the oxi-irradiation of sewage sludges; however, is might also be used for dyes, pesticides solutions, hydrocarbons, latex, liquid industrial effluents in general; and it may be adapted and dimensioned for semi industrial purposes.

The IP-100 consists in a stainless steel cylindric tank, with a centrifuge pump that recirculates the liquid volume from the bottom to the third upper part. The radioactive elements are in tubes, and these are fixed to the stopper. The gases or additions may be injected by a connecting tube with a valve and a second valve on the upper side of the tank for ventilation [12].

For operation it is submerged in a pool no more than five m deep. The water column makes the needed shielding. The movements for the sources charge and discharge are carried out under water at the bottom of the pool, with direct vision and illumination. Usually there are pools in simple nuclear research installations for storage or replacement of sources that may be used for the IP-100 operation, avoiding the construction of expensive concrete shielding.

Main design parameters are:

Irradiation volume:	100 lt
External diameter:	450 mm
Thickness:	2.5 mm
Material:	AISI 304 lt
Recirculation pump:	0.6 kw
Recirculation volume:	120 lt/min
Maximum radioactive capacity:	40,000 Ci (Co-60)
Verification to the interior pressure:	P max: 20 N/cm^2
Verification to the external pressure:	P max: 10.5 N/cm^2

6.1. Laboratory tests

The IP-100 was tested on hydraulic resistance and leakproof, under pressure already mentioned during 1 h, without watching any change or alteration. For control of homogeneity and death zones existence, a radioactive solution of I-131 was used. The tracer was detected by INa-Tl scintillator on the entrance of the pump, and the recorded data were graphed. The mixing time resulted to be very low as compared to the total expected irradiation time, so as to have high dose homogeneity.

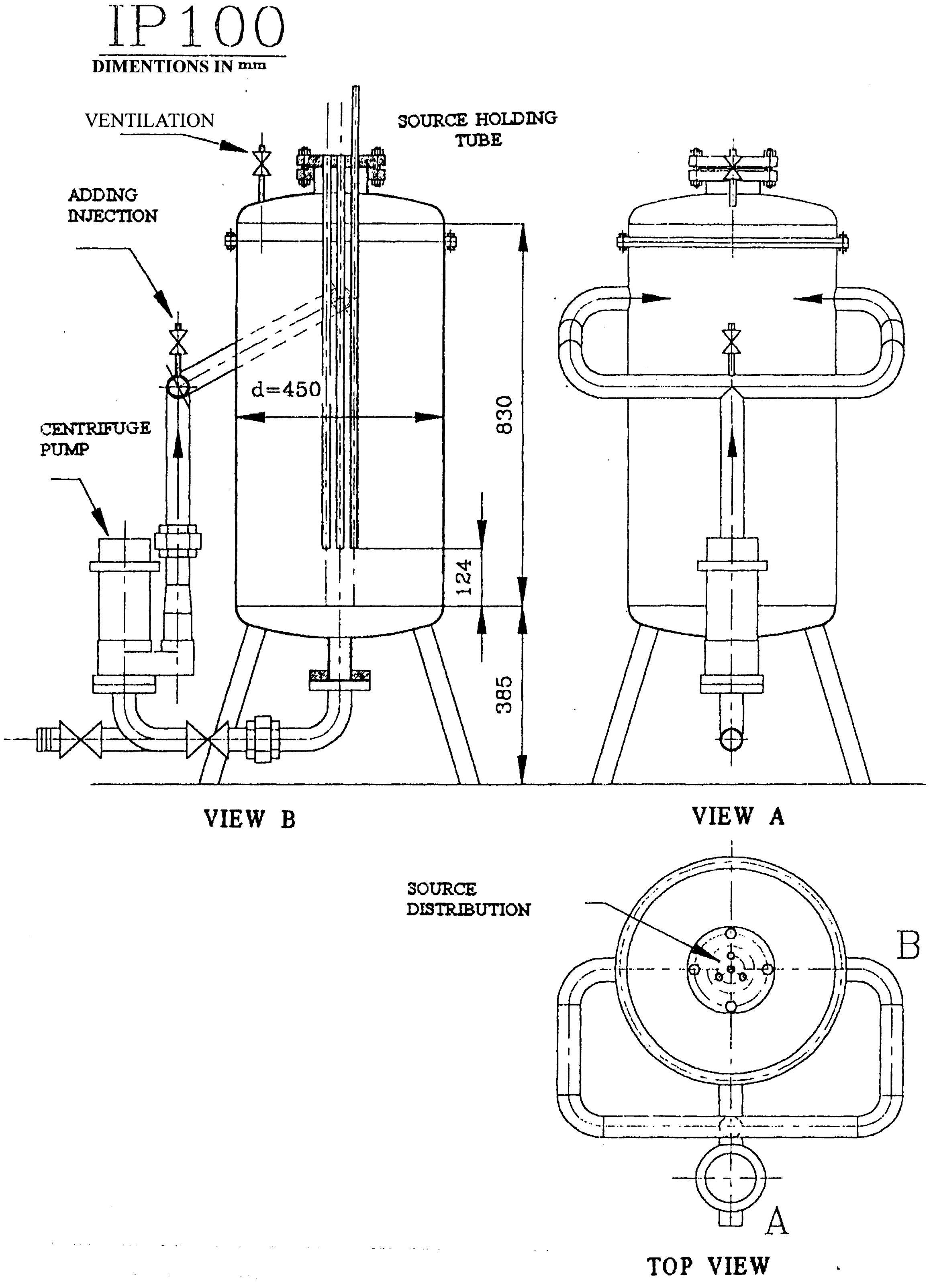

FIG. 7. Irradiator schematic diagram.

7. CONCLUSIONS

The basic concepts of irradiation facilities have been reported in the last decades; at the present, the aim of radiation processing development is the optimization of the rate: cost over absorbed energy. For this purpose, the factors that may participate are: the design improvements and the combination with other processes (heat, oxygenation, etc.). Mathematical or physics models in lab-scale facilities like the IP-100, will lead to find out the best irradiation conditions. In this sense, and based on the 20 years German experience, the Sewage Sludge Irradiation Project is being developed.

As the project has been planned as full-scale plant, to treat the sludges coming from a big city and to reuse them for Agriculture, many topics has to be considered. The first of them is the protection of the Public Health, and life quality improvement, taking into account the pathogen elimination, toxic decontamination and agronomic value of the use on land. These factors imply also a benefit and they have to be taken into account whenever a project is evaluated.

ACKNOWLEDGEMENTS

Dr. Cecilia Magnavacca in the conduction of research about the irradiated sludges, and all the personnel of CNEA involved in different aspects of the project. The Tucumán City, the National University of Tucumán, the Agro Industrial Experimental Station O. Colombres, professionals and colleagues. The IAEA, by means of the Co-ordinated Research Programme and Technical Co-operation Assistance.

REFERENCES

[1] IAEA – TEC-DOC-1062, Environmental Application of Ionizing Radiation (Proc. Symp. Zakopane, Poland, 1997) Vienna (1998).

[2] LABRADOR MORENO, J., La materia orgánica en los ecosistemas. Ministerio de Agricultura, Pesca y Alimentación. Madrid (1996) 174 pp.

[3] PAGE, A., LOGAN, T., RYAN, J., Land application of sludge: food chain implications, Lewis Publishers, Michigan (1987) 151 pp.

[4] KURUCZ, CH., WAITE, T., COOPER, W., NICKELSEN, M., Empirical models for estimating the destruction of toxic organic compounds utilizing electron beam irradiation at full scale, Radiat. Phys. Chem. **45** (1995) 805 pp.

[5] IAEA-TECDOC-971, Sewage sludge and wastewater for use in agriculture, Vienna (1997).

[6] RESEARCH OF DEPARTMENT OF RADIATION RESEARCH FOR ENVIRONMENT AND RESOURCES, Sludges pasteurization and upgrading by radiation, JAERI, Japan (1995) 171 pp.

[7] HERNÁNDEZ MUÑOZ, A., Depuración de aguas residuales. (Paraninfo, Ed.) Madrid (1992) 926 pp.

[8] LESSEL, T., Disinfection of sewage sludges by gamma irradiation and alternative methods", IAEA TEC-DOC-454, Vienna (1986).

[9] GRAIÑO, J., MAGNAVACCA, C., "Sewage sludge irradiation plant in Argentina", Environmental Applications of Ionizing Radiation (Cooper, W., Curry, R., O'Shea, K., Ed.) J.Wiley & Sons, Inc., New York (1998) 699 pp.

[10] MAGNAVACCA, C., GRAIÑO, J.G., BERRETTONI, J.L., GUTIERREZ, O., LANZETTA, D., “Desinfección por irradiación de barros cloacales para uso en Agricultura. XVIII Reunion Argentina de Ecología. Buenos Aires (1997).

[11] MAGNAVACCA, C., GRAIÑO, J.G., Efectos fisicoquímicos de la irradiación de barros cloacales para uso en Agricultura. XXIV Congreso Interamericano de Ingeniería Sanitaria y Ambiental, Buenos Aires (1994).

[12] GRAIÑO, J.G., “Diseño y construcción del Oxi-Irradiador experimental de pileta: IP-100”, in press.

LIST OF PARTICIPANTS

Bagyo, A.N.M.	Centre for the Application of Isotopes and Radiation, National Atomic Energy Agency, P.O. Box 7002 JKSKL, Jakarta 12070, Indonesia
Cooper, W.J.	Department of Chemistry, University of North Carolina at Wilmington, 601 South College Road, Wilmington, North Carolina 28403-3297, USA
Dogbe, S.A.	National Nuclear Research Institute, Ghana Atomic Energy Commission, Department of Chemistry, P.O. Box 80 Legon, Accra, Ghana
Emara, A.G.	Atomic Energy Authority, 7 Nasr Ahmed Zakir Street, Nasr City, Cairo, Egypt
Gehringer, P.	Austrian Research Centre Seibersdorf, A-2444 Seibersdorf, Austria
Graiño, J.G.	Comisión Nacional de Energía Atómica, Centro Atomico Ezeiza, Proyecto Irradiacion, 1842 Agencia Minipost Ezeiza, Buenos Aires, Argentina
Güven, O.	International Atomic Energy Agency, Wagramer Strasse 5, P.O. Box 100, A-1400, Vienna, Austria
Han, B.	Central Research Institute, Samsung Heavy Industries Co., Ltd., P.O. Box 43, Daeduk Science Town, Taejon 305-600, Republic of Korea
He, Yongke	Department of Technical Physics, Beijing University, Beijing 100871, People’s Republic of China
Pikaev, A.K.	Institute of Physical Chemistry of the Russian Academy of Sciences, Leninsky Prospect, 31, 117915 Moscow, Russian Federation
Sampa, M.H.O.	Instituto de Pesquisas Energeticas e Nucleares, Commissão Nacional de Energía Nuclear do Brasil, P.O. Box 11049 - Pinheiros, 05499-970 São Paulo, Brazil
Shah, M.R.	Isotope Division, Bhabha Atomic Research Centre, Mumbai 400 085, India